

SCHOOL OF AERONAUTICS (NEEMRANA)

UNIT-1 NOTES

FACULTY NAME: D.SUKUMAR.

CLASS: B.Tech AERONAUTICAL

SUBJECT CODE: 6AN5

SEMESTER: VI

SUBJECT NAME: AIRCRAFT DESIGN

Preliminaries:

Aircraft Design Requirements, specifications, role of users. Aerodynamic and Structural Consideration, Importance of weight. Airworthiness requirements and standards. Classifications of airplanes. Special features of modern airplane.

Air Loads in Flight: Symmetrical measuring loads in flight, Basic flight loading conditions, Load factor, Velocity - Load factor diagram, gust load and its estimation, Structural limits.

INTRODUCTION:

The process of design of a device or a vehicle, in general involves the use of knowledge in diverse fields to arrive at a product that will satisfy requirements regarding functional aspects, operational safety and cost. The design of an airplane, which is being dealt in this course, involves synthesizing knowledge in areas like aerodynamics, structures, propulsion, systems and manufacturing techniques. The aim is to arrive at the configuration of an airplane, which will satisfy aforesaid requirements.

The design of an airplane is a complex engineering task. It generally involves the following.

- a) Obtaining the specifications of the airplane, selecting the type and determining the geometric parameters.
- b) Selection of the power plant.
- c) Structural design and working out details of construction.
- d) Fabrication of prototype.
- e) Determination of airplane performance, stability, and structural integrity from flight tests.

STAGES IN AIRPLANE DESIGN:

The design process can be divided into the following three stages.

- a) Project feasibility study.
- b) Preliminary design.
- c) Design project

Project Feasibility Studies:

The aim of this study is to evolve a complete set of specifications for the airplane. It involves the following steps.

- 1) Comprehensive market survey to assess the number of airplanes needed.

2) Study of the operating conditions for the proposed airplane. These conditions include (a) landing field length, (b) type of landing field, (c) weather conditions in flight and near landing sites and (d) visibility.

3) Study of the relevant design requirements as laid down by the civil and military regulating agencies. Some of the regulating agency for civil airplanes are : FAA (Federal Aviation Administration) in USA; EASA (European Aviation Safety Agency) in Europe; DGCA (Director General of Civil Aviation) in India.

The military airplanes are governed by more stringent regulations called MIL specifications in USA.

4) Evaluation of existing designs of similar airplanes and possibility of incorporating new concepts.

5) Collection of data on relevant power plants.

6) Laying down preliminary specifications which may consist of the following.

a) Performance: Maximum speed, maximum rate of climb, range, endurance, rate of turn, radius of turn, take-off and landing field lengths.

b) Payload.

c) Operating conditions at the destinations.

d) Maneuverability.

Preliminary design

This stage of design process aims at producing a brochure containing preliminary drawings and stating the estimated operational capabilities of the airplane. This is used for seeking approval of the manufacturer or the customer. This stage includes the following steps.

(i) Preliminary weight estimate.

(ii) Selection of geometrical parameters of main components based on design criteria.

(iii) Selection of power plant.

(iv) Arrangement of equipment, and control systems.

(v) Aerodynamic and stability calculations.

(vi) Preliminary structural design of main components.

(vii) Revised weight estimation and c.g. travel.

(viii) Preparation of 3-view drawing.

(ix) Performance estimation.

(x) Preparation of brochure. Section 10.3 deals with the items included in the brochure. It is also called aircraft type specification.

Design project

After the preliminary design has been approved by the manufacturer / customer. The detailed design studies are carried out. These include the following stages.

1) Wind tunnel and structural testing on models of airplane configuration arrived after preliminary design stage. These tests serve as a check on the correctness of the estimated characteristics and assessment of the new concepts proposed in the design.

2) Mock-up: This is a full scale model of the airplane or its important sections. This helps in (a) efficient lay-out of structural components and equipments, (b) checking the clearances, firing angles of guns, visibility etc.

Currently this stage is avoided by the use of CAD(Computer Aided Design) packages which provide detailed drawings of various components and subassemblies.

3) Complete wind tunnel testing of the approved configuration. Currently CFD (Computational Fluid Dynamics) plays an important role in reducing the number of tests to be carried-out. In CFD, the equations governing the fluid flow are solved numerically. The results provide flow patterns, drag coefficient, lift coefficient, moment coefficient, pressure distribution etc. Through the results may not be very accurate at high angles of attack, they are generally accurate near the design point. Further, they provide information on the effects of small changes in the geometric parameters, on the flow field and permit parametric studies.

4) Preparation of detailed drawings.

5) Final selection of power plant.

6) Calculations of (a) c.g. shift (b) performance and (c) stability.

7) Fabrication of prototypes. These are the first batch of full scale airplane. Generally six prototypes are constructed. Some of them are used for verifying structural integrity and functioning of various systems. Others are used for flight testing to evaluate performance and stability.

Classification of airplanes

At this stage, it is helpful, to know about the different types of airplanes.

The classification is generally based on

- (a) The purpose of the airplane,
- (b) The configuration and
- (c) Design Mach number (e.g. subsonic, supersonic and hypersonic).

Classification of airplanes according to function

There are two main types of airplanes viz.

- i) Civil aircraft and
- ii) Military aircraft.

The civil airplanes are categorised as

- a) Passenger,
- b) Cargo,
- c) Agricultural,
- d) Sports and
- e) Ambulance.

The military airplanes are categorised as

- a) Fighter,
- b) Bomber,
- c) Interceptor,
- d) Reconnaissance, and
- e) Airplanes for logistic support like troop-carriers and rescue airplane.

The military aircraft are often designed to cater to more than one role e.g. fighter-bomber or interceptor-fighter.

Influence of the function of airplane on specifications/design requirements

The specifications or design requirements of an airplane are decided by its function. It can be mentioned that a passenger airplane should have:

- (a) High level of safety in operation,
- (b) Adequate payload carrying capacity,
- (c) Economy in operation,
- (d) Comfort level depending on range and cruising altitude,
- (e) Ability to fly in weather conditions normally encountered on chosen routes and
- (f) Ability to use airfields of intended destinations.

A bomber airplane should have:

- (a) Range corresponding to the mission,
- (b) Capacity to carry and deploy intended bomb load,
- (c) High values of speed, endurance, and ceiling
- (d) Adequate protection against accidental fire.

An interceptor airplane should have:

- (a) Adequate thrust to give high
 - (i) Rate of climb,
 - (ii) Maximum flight speed and
 - (iii) Maneuverability
- (b) Ceiling 3 to 4 km above that of contemporary bombers
- (c) Ability to fly in adverse weather conditions and
- (d) Appropriate armament.

Civil & Fighter Aircraft



Classification by Configuration

Airplanes can be classified in accordance with their shape and structural layout, which in turn will contribute to their aerodynamic, tactical and operational characteristics. It can be done by classification of the following:

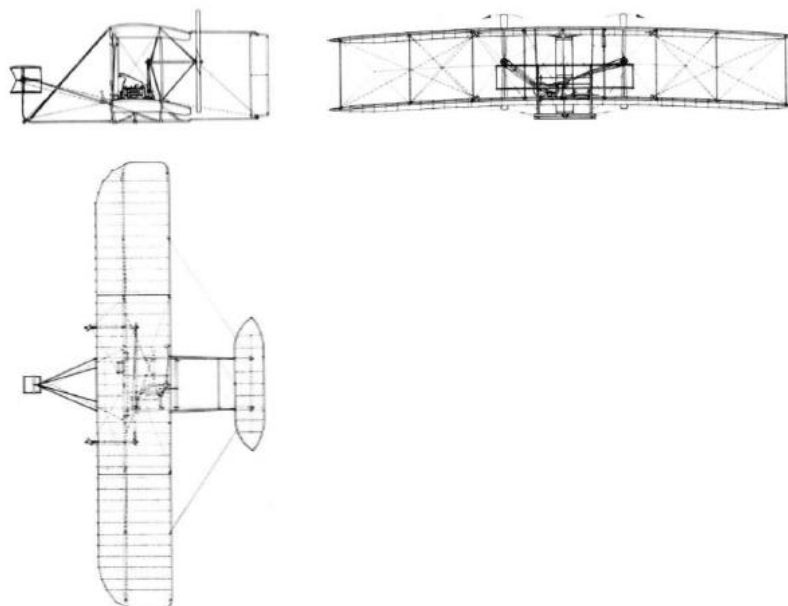
- (a) Shape and position of the wing
- (b) Type of fuselage
- (c) Location of horizontal tail surfaces
- (d) Type of landing gear
- (e) Location and number of engines.

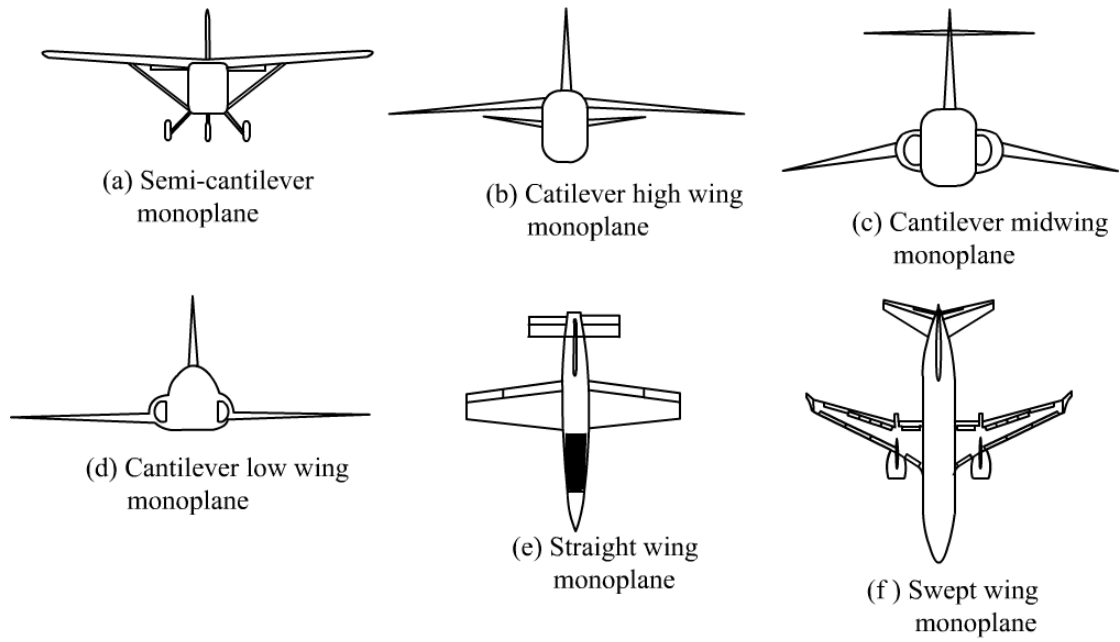
Classification of airplanes based on wing configuration

Early airplanes had two or more wings e.g. the Wright airplane had two wings braced with wires. Presently only single wing is used. These airplanes are called monoplanes. When the wing is supported by struts the airplane is called semi cantilever monoplane. Depending on the location of the wing on the fuselage, the airplane is called high wing, mid-wing and low wing configuration. Further, if the wing has no sweep the configuration is called straight wing monoplane. The swept wing and delta wing configurations are shown in Figs.

(a) Shape and Position of the Wing

- (1) Braced airplane – D.H. Tigermoth
- (2) Braced sesquiplane – An- 2
- (3) Semi-Cantilever monoplane, Pushpak, Piper Cub,
- (4) Semi-cantilever parasol monoplanes...Baby Ace
- (5) Cantilever low-wing monoplane DC-3, HJT-16, IL-18, DH Comet
- (6) Cantilever mid-wing monoplane ...Hawker Hunter, Canberra
- (7) Cantilever high-wing monoplane...An-22, Breguet 941, Fokker friendship
- (8) Straight wing monoplane... F-104 A....
- (9) Swept-wing monoplane... F-24, MIG-21, Lightning
- (10) Delta-monoplane with small ARAvro-707, B-58 Hustler, Avro Vulcan.





Types of Wings



Straight Wing



Swept Wing



Forward Swept Wing



Oblique Wing

Types of Wings



Variable Sweep Wing



Delta Wing



Biplane



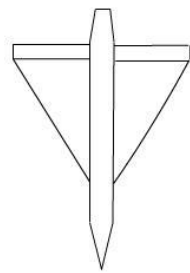
Triplane

Classification of airplanes based on fuselage

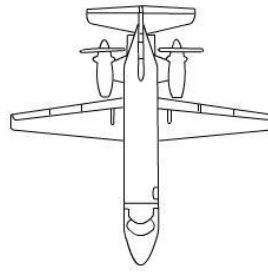
Generally airplanes have a single fuselage with wing and tail surfaces mounted on the fuselage. In some cases the fuselage is in the form of a pod. In such a case, the horizontal tail is placed between two booms emanating from the wings. These airplanes generally have two vertical tails located on the booms. The booms provide required tail arm for the tail surfaces. Some airplanes with twin fuselage had been designed in the past. However, these configurations are not currently favoured.

(b) Type of fuselage

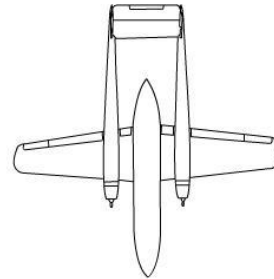
- (1) Conventional single-fuselage HT-2, Boeing 707,
- (2) Twin-fuselage design
- (3) Pod and Boom construction. Fairchild Packet, Vampire



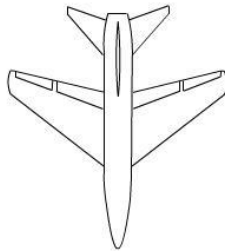
(g) Cropped delta wing monoplane



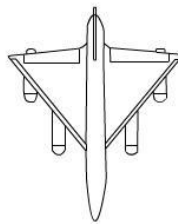
(h) Conventional single fuselage



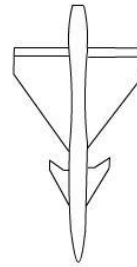
(i) Pod and boom configuration



(j) Conventional configuration (tail behind wing)



(k) Tailless configuration



(l) Canard configuration

Classification of airplanes based on horizontal stabilizer

In a conventional configuration, the horizontal stabilizer is located behind the wing. In some airplanes there is no horizontal stabilizer and the configuration is called tailless design. In these airplanes, the functions of elevator and aileron are performed by ailerons located near the wing tips.

When both ailerons (on left and right wings) move in the same direction, they function as elevators and when the two ailerons move in opposite direction, they function as ailerons. In some airplanes, the control in pitch is obtained by a surface located ahead of the wing. This configuration is called canard configuration

Types of Tails



T Tail



Twin Fin



Horizontal Tailless



Vertical Tailless

(c) Location of horizontal tail surface

- (1) Conventional design with horizontal tail located behind the wing Krishak, Avro-748,
- (2) Tail-less design with no horizontal tail ... Mirage IV, B-58 Hustler, Concorde
- (3) Canard design with horizontal tail located ahead of the wing... (XB-70-A ...)

(d) Type of landing gear

- (1) Retractable landing gear... DC-9, TU-114, SAAB-35
- (2) Non-retractable landing gear... Pushpak, An-14, Fuji KM-2



Fixed type of landing gear



Retractable type of landing gear

Classification of airplanes based on number of engines and their location

Airplanes with one, two, three or four engines have been designed. In rare cases, higher number of engines are also used. The engine, when located in the fuselage, could be in the nose or in the rear portion of the fuselage. When located outside the fuselage the engines are enclosed in nacelles, which could be located on the wings or on the rear fuselage. In case of airplanes with engine-propeller combination, there are two configurations – tractor propeller and pusher propeller. In pusher configuration the propeller is behind the engine. In tractor configuration the propeller is ahead of the engine.

(e) Classification by Power Plants

a. Types of engines

Piston engines – Krishak, Dakota, Super Constellation, etc. Turboprop engines – Viscount, Fokker Friendship, An-12, etc.

Turbo-jet engines – Turbo-fan, By-pass engines – HJT-16 (Kiran), Boeing 707, MIG-21, etc.

Ram-jet engines

Rocket engines – Liquid propellant – Solid propellant – X-15A

b. Number of engines

Single-engine – HJT-16, DH Chipmunk, Hawker Hunter, etc.

Twin-engine – HF-24, DC-3, Canberra, etc.

Multi-engine – An-22, Boeing 707, Belfast etc.

c. Engine Located

Propeller single engine located in fuselage nose (HT-2, YAK-9, BEAGLE A-109).

“Pusher”-engine located in the rear fuselage (Bede x BD-2)

Engines (jet) submerged in the wing

(a) At the root – DH-Comet, TU-104, Tu-16

(b) Along the span – Canberra, U-2, YF-12A

Jet engines in nacelles suspended under the wing by “POD” mountings - Boeing 747, Airbus, Boeing 707, DC-8, Convair 880,

Boom and Pod construction - Fairchild Packet, Vampire Engines (jet) located on the rear fuselage – Trident, VC-10, IL-62, Caravelle

Jet engines located within the rear fuselage – HF-24 (Marut), Lightning, MIG-19,...

Engine Arrangement



Factors affecting the configuration

The configuration of an airplane is finalized after giving consideration to the following factors.

- (I) Aerodynamics
- (II) Low structural weight
- (III) Lay-out peculiarities
- (IV) Manufacturing procedures
- (V) Cost and operational economics
- (VI) Interaction between various features

(I) Aerodynamic considerations – drag, lift and interference effects

The aerodynamic considerations in the design process involve the following.

(A) Drag

The drag of the entire configuration must be as small as possible. This requires (a) thin wings, (b) slender fuselage, (c) smooth surface conditions, and (d) proper values of aspect ratio (A) and sweep (Λ).

(B) Lift

The airplane must be able to develop sufficient lift under various flight conditions including maneuvers. The maximum lift coefficient also decides the landing speed. These considerations require proper choice of (a) aerofoil, (b) means to prevent flow separation and (c) high lift devices.

(C) Interference effects

In aerodynamics the flows past various components like the wing, the fuselage and the tail are usually studied individually. However, in an airplane these components are in proximity of each other and the flow past one component affects the flow past the others (components). The changes in aerodynamic forces and moments due to this proximity are called interference effects. The lay-out of the airplane should be such that increase in drag and decrease in lift due to interference effects are minimized. These can be achieved in subsonic airplanes by proper fillets at the joints between

- (a) Wing and fuselage,
- (b) Tail and fuselage and
- (c) Wing and engine pods.

(II) Low structural weight

The weight of the aircraft must be as low as possible.

This implies use of

- (a) High strength to weight ratio material,
- (b) Aerofoil with high thickness ratio
- (c) Wing with low aspect ratio
- (d) Relieving loads (e.g. wing mounted engines) etc..

The airplane structure must be strong enough, to take all permissible flight loads and stiff enough to avoid instabilities like, divergence, aileron reversal and flutter.

(III) Layout peculiarities

The specific function of the airplane often decides its shape e.g. the fuselage of a cargo airplane generally has a rectangular cross section and a large cargo door. The height of fuselage floor should be appropriate for quick loading and unloading



(Source:www.flickr.com)
(a) General view



(Source:www.img525.imageshack.uscom)
(b) Cargo being loaded

(IV) Manufacturing processes

During the detail design stage, attention must be paid to the manufacturing processes. The cost of manufacture and quality control also must be kept in mind.

(V) Cost and operational economics – Direct operating cost (DOC) and Indirect operating cost (IOC)

The total operating cost of an airplane is the sum of the direct operating cost (DOC) and the indirect operating cost (IOC). The DOC relates to the cost of hourly operation of the airplane viz. cost of fuel, lubricants, maintenance, overhaul, replacement of parts for airframe and engine. IOC relates to crew cost, insurance cost, depreciation of airplane and ground equipment, hangar rental, landing charges and overheads. Thus, for a personal plane lower initial cost of the airplane may be more important whereas, for a long range passenger airplane lower cost of fuel may be the primary consideration.

(VI) Interaction of various factors

Some of the considerations mentioned above may lead to conflicting requirements. For example, a wing with an airfoil of relatively higher thickness ratio, has lower structural weight but, at the same time has higher drag. In such situations, optimization techniques are employed to arrive at the best compromise.

Primary requirements for Civil Aircraft

Passenger Aircraft

- High Safety level
- High payload carrying capacity
- Economy in operation
- Comforts
- Ability to fly in any Weather (All-weather flying) aerodromes
- Ability to use aerodromes of respective classes

Cargo Aircraft

- High payload carrying capacity
- Economy in operation
- Ability to fly in any Weather
- Suitable for civil aerodromes

Primary requirements for Military Aircraft

Strategic

- Long range (over 6000 km)
- High load carrying capacity - (2000-4000 kg)
- High speed
- High endurance
- High ceiling
- Adequate fire protection

Tactical

- Long range 3000-5000 km)
- High load carrying capacity (above 6000 kg)
- High speed
- High ceiling

- High endurance
- All-weather flying
- Ability to use field aerodromes

Primary requirements for Military Aircraft – FIGHTERS-Tactical

- High speed (300-400 kmph- more than contemporary bomber speeds)
- High ceiling (2-4 km than bomber more than contemporary bomber ceilings)
- Maneuverability
- Sufficient endurance
- High rate of climb
- Ability to launch repeat- ed attacks
- All-weather flying
- Ability to use field aerodromes
- Ease of dismantling and assembling

Primary requirements for Military Aircraft – FIGHTERS- Interceptor

- High rate of climb
- High ceiling (3-4 km contemporary ceilings)
- High speed (500-600 kmph more than contemporary bomber speeds)
- High Maneuverability
- All-weather flying
- Ability to fire powerful single volley at target
- Ease of dismantling and assembling

Primary requirements of bomber

- Long range,
- High load carrying capacity,
- High speed ,
- High endurance,
- High ceiling and
- Adequate fire protection.

Primary requirements of interceptor

- High rate of climb,
- High ceiling (3 to 4 km above contemporary bombers),
- High speed ,
- High Maneuverability,
- Ability to fly in any weather and
- Appropriate armament.

Tailless and Flying Wing Design

A flying wing is a tailless fixed-wing aircraft which has no definite fuselage, with most of the crew, payload and equipment being housed inside the main wing structure.

Advantages of tailless and flying wing design

- Small drag-reduction of the number of non lifting surfaces and minimizing the interference effects lead to much lower CD.

- Smaller structural weight. In this design the horizontal tail and that part of the fuselage carrying the tail is eliminated. The bending moment is less
- Large thickness at the root of the wing .The structure can therefore be made lighter due to the increased rigidity of the wing section

Disadvantages

- Restricted c.g travel due to the absence of horizontal stabilizer
- The wing tips are wash-out. This causes a negative lift at wing tips and hence a larger wing area is required to develop the same overall lift.
- Poor directional stability
- Use of high lift devices results in large diving moments.
- Reversal of panel stresses at wing tips-Due to the negative lift at the tips of flying wing some of the wing panels have to be designed for both tensile and compressive loads

Canard design

In this special type of design the horizontal tail surfaces are located ahead of the main plane. In the major part of the flight the canard tail assists the wing in sharing the weight. The horizontal tail is effective as it is not in the downwash of the wing surface.

Advantages

- The forces acting on the horizontal tail is upwards and supplements the lift developed by the wing. Hence for the same CL the wing area is reduced, and there is a decrease in drag.
- The wing weight is lesser than the conventional aircraft wing
- At low speeds the horizontal tail stalls first, and automatically sets the airplane to a smaller angle of attack. Wing stall is difficult.
- After reaching the critical mach number the lifting stabilizer permits compensation of the growing wing diving moment
- When the Mach number increases, the static stability of the canard also increases.

Disadvantages

- Shock stall may occur on the horizontal stabilizer before occurs in the wing
- At supersonic speeds the longitudinal stability is more difficult in the canard the canard type than conventional airplane.
- The elevator power required for landing is very high.
- The landing characteristics are very poor.

The advantages of high wing design

- Increased lateral stability
- The possibility of engine failure due to suction of hard particles from the ground is 4 times less than in a low wing design.
- In passenger aircraft there is passenger comfort. The down view of the passenger is undisturbed by the wing
- In cargo aircraft, loading and unloading are easier, on account of the lower position of fuselage.

- The interference drag is lower as compared to low wing airplane.

Disadvantages of high wing design

- The area of the vertical stabilizer is 20-22% of the wing area as compared to 10-12 % in low wing design. This increases weight and drag.
- The weight of the fuselage is increased as lower fuselage is to be reinforced for protection in emergency landing.
- The weight of the fuselage structure is increased by the heavy frames needed for the attachment of the landing gear to the fuselage. Landing gear weight also very high.
- If the bogies are attached to the fuselage the treads are narrow, which leads to poor stability on the ground.
- Maintenance and inspection of engines are difficult

Location of engines

- Engine under pylons
- Inside the root portion of the wing
- Outside the rear fuselage
- Advantages in engine under pylon
- The weight of wing structure decreases by 15-20 % as the wing is relieved by the weight of the engines
- The space inside the wing is utilized for fuel storage, maintenance, inspection and replacements are facilitated
- The wing structure is free from the heat from the engines, and better fire safety can be achieved.

Disadvantages

- Failure of outboard engine create a large yawing moment. This moment has to be counted by rudder deflection which results in higher drag.
- Smaller ground clearance increases the possibility of foreign particles entering the engines.
- The noise level in the cabin is 5 db higher as compared to airplanes having engines on the rear fuselage.

Engines located in the wing root

Advantages

- There is very little increase in frontal area due to installation of power plants.
- Almost the entire wing span can be used for ailerons and high lift devices

Disadvantages.

- The weight of the wing is high due to the cut portion in the wing spars to accommodate engine
- The weight of the power plant is high due to the long air ducts.
- The intake is located at a place where the air flow is not clear.
- The space in the root cannot be used for fuel accommodation

Engine located on the rear fuselage

Advantages

- There is less noise in the cabin and the fuselage
- The entire wing can be used for fuel storage
- The whole wing space can be used for high lift devices and ailerons
- Fire hazard is minimum.
- The actual wing does not deviate from the design profile and the wing is clean.

Disadvantages

- The fuel is located far from the engines, therefore the length of the pipe line is increased and special fuel pumps should be provided.
- Due to power plant weight at the tail, longer fuselage is provided ahead of the wing which requires larger vertical and horizontal stabilizers.

AIRCRAFT LOADS

A general understanding of the various types of airframe loads, their generation and application during the design process, the transfer processes from "external loads" into "structural loads", loads qualification during ground and flight testing is therefore of equal importance to the process of usage monitoring and derivation of usage factors from the different fatigue tests or the set-up of structural inspection programs.

When life of aircrafts are discussed, often the flight hours or number of flights are still considered the governing factor, sometimes adapted with factors on "damage hours" or "usage", while from a structural engineering viewpoint the operational stress spectrum and therefore the life on the different aircraft components are not only a matter of flight hours and spectrum ratio but also driven by modification status, structural weight status and role equipment.

This paper describes loads- analysis and verification activities during the major phases of the life of an airframe, where structural loads and their influences on the airframe condition are vital to the structural integrity and the economic usage of the weapon system:

- The structural loads during design and Qualification of A/C structures
- Loads monitoring during usage
- Impacts due to aircraft modification and role changes.

Trends with respect to the increased usage of theoretical modelling are also discussed.

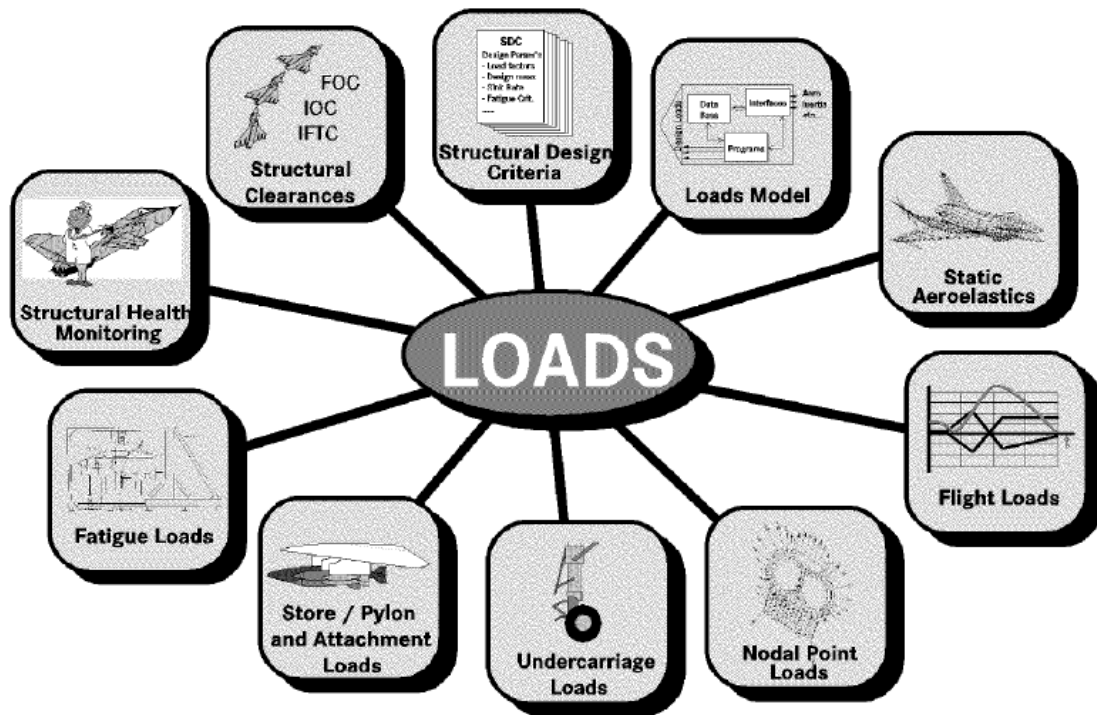
1. STRUCTURAL LOADS DURING THE DESIGN AND QUALIFICATION OF AIRCRAFT STRUCTURES

Loads are accompanying an aircraft's life from "the cradle to the grave". Although the overall type and magnitude of major load sets remain the same, there is no "fixed" loadset that is applied to one aircraft model throughout the life and often identical airframes serving different roles within a fleet over time will be subjected to very different loads.

To include as much as possible (or specified) of these loading scenarios in the early process of designing a new type of aircraft is the responsibility of the loads engineering department, while ensuring that these loads can be safely endured throughout the specified life is the task of the design and stress engineers. "New" load sets, developed later during usage of the

aircraft are common tasks and handled similar as the "initial design loads" by the design authority with the constrictions, that now the airframe is already build and deployed and the focus is on minimising changes through structural modifications to qualify the structure for its new environment either through analysis and / or test.

In short, every major change in the aircraft's role, payloads or usage in principle influences the loads acting on the airframe or at least some components. Figure below gives an idea how loads are initially generated and how they are used throughout the design-, qualification- and usage process.



Loads and Fatigue

The determination of loads together with the qualification for static strength and fatigue by calculation and test for all important structural components is a main prerequisite for successful design and safe operation of any aircraft.

Whereas for transport aircraft with their rather limited range of operational manoeuvres and high number of flight hours / cycles fatigue is the main design driver for the airframe, fighter aircraft are predominantly designed to (static) limit load cases for the "corners" of the envisaged flight envelope, which in general cover a lot of strength required for fatigue of their comparatively short life.

But this is only true as long as fighter life does not exceed the originally planned lifetime and the roles, missions etc. Are compatible with the design criteria at the beginning.

Aging aircraft in both cases does not only mean that an aircraft is getting older in terms of flight hours and flight cycles, it also means that some of the reference data for the basic design criteria have changed during time, i.e.:

- airframe and equipment mass growth
- enhancement of systems performance, especially engine thrust
- new configurations (stores)

- update of flight control systems (FCS) (electronically or hardware changes like added slats or enlarged ailerons)
- mission profiles and additional/changed roles
- actual usage spectrum

Most of these changes have an immediate impact on aircraft load scenarios, others will not change load levels but may change underlying statistic, e.g. fatigue spectra. Assessment of external loads is therefore a basic task throughout the life of a fleet.

Admittedly in many cases there is no simple one to one relationship between "external" loads and local internal stresses, which after all are the basis for the assessment of "life consumption" or "remaining life" of structural components. But providing loads are known for a special structural interface or component, reliable conclusions can be drawn regarding local stresses relating the manifold of load cases from experience, measurement and detailed FE analysis during design, qualification and test phases in many cases.

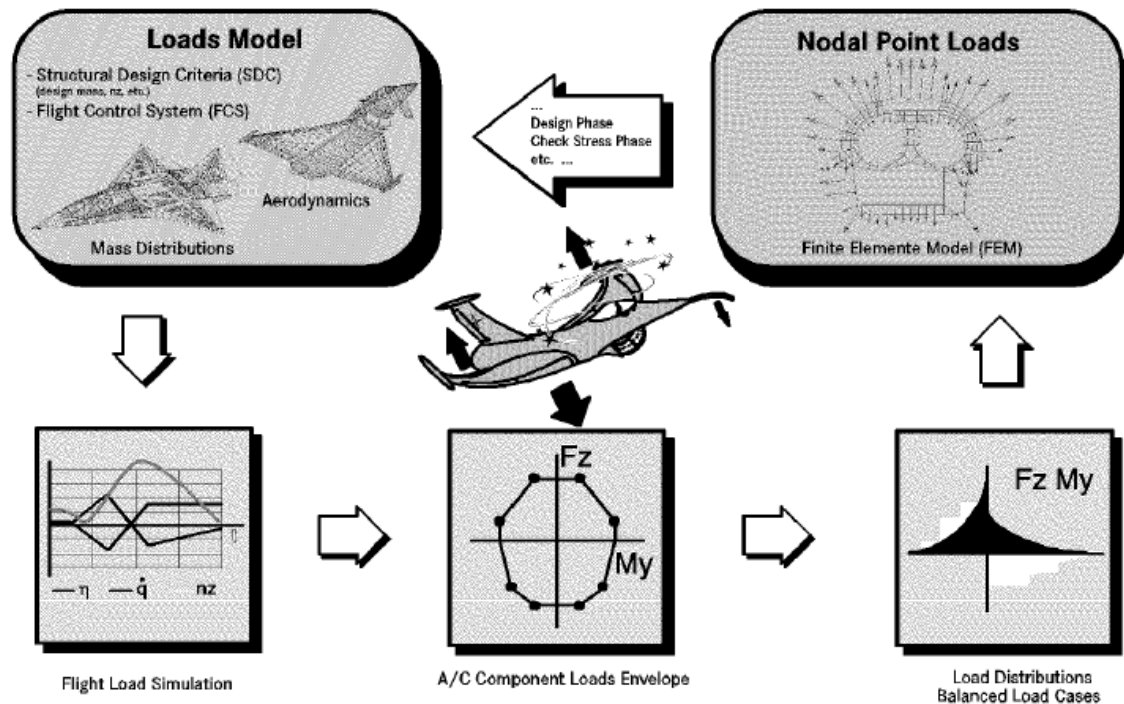
In addition the comparison of load spectra alone may already be suitable for drawing conclusions without recourse to detail stress calculations of specific locations for components with limited load case variations i.e. landing gears.

The Determination of Design Loads

Design loads, better "Initial Design Loads" are the first step in the loads history of an airframe that influences the detail design of a component (i.e. wing or fuselage structure) or, at a later stage in the design process, a part (i.e. wing spar cap or fuselage skin panel) in many details. Since not every load is determining these design tasks, establishment and identification of the "design loadcases" is important. The following is a summary on the methods how design loadcases are determined, with special attention to points where an immediate context with fatigue calculations exists.

Fig. below shows a typical "loads loop" which usually is repeated several times in the different phases of the aircraft design.

First of all the Structural Design Criteria (SDC) are prepared as a basis for design, specifying the basic performance and flight parameters, then a Loads Model (LM) is built, based on the SDC's, the aerodynamic, flight mechanic and weight and balance data of the aircraft.



LOADS LOOP

The loads module ensures that load cases selected for design are analysed for an overall balanced aircraft (mass, inertia and aerodynamic forces) for all manoeuvres and the loads analysis is performed in a time history sequence, thus providing load information on structural interfaces for every time step of the chosen manoeuvre. Results of the loads module is either continues external load distribution for any component (i.e. bending, torque and shear force distribution along fuselage stations for all load cases or a) distribution of loads on the Finite Element (FE) grid nodal points for subsequent "global FEAnalysis".

Thus, starting with the SDC the load loop ends with the preparation of external loads for stress analysis of components.

Usually an improved or changed data basis results in an update of the LM and consequently in more accurate and more detailed design load cases. Typical improvements are a better aerodynamic data basis (i.e. via extensive wind tunnel testing) or a refined FE-model because of an advanced design status. Modifications in the mass and balance status, control laws etc. may also result in substantial changes of the loads model, especially in advanced computer controlled flight vehicles.

The importance of the link between knowledge of external loads and structural stress distributions for the assessment of fatigue life cannot be underestimated. Whereas in the past the available computer resource was rather poor and strong software tools were scarce goods, leading to a strong selection of load cases to be analysed in detail, today there are virtually no limits, from this side. Computers power do play an important part with respect to better and refined results in the assessment of loads, however the correct selection of the critical manoeuvres for the fatigue spectrum and their loads analysis still influences the fatigue performance of a structure during the design phase.

Most of today's ageing aircraft fleets of the NATO air forces were designed and flight tested by the end of the sixties or the beginning seventies, like the Tornado, Harrier, F-16, F-18,

Mirage 2000 etc. An aircraft like the F-4 Phantom even dates back to the fifties and is still in service in some air forces of the alliance.

When comparing design environments of the a.m. models it should be pointed out that in the meantime the circumstances and requirements for aircraft design and analysis have changed in many ways, in detail:

- much better tools, soft- and hardware, and with that a very intensive investigation to calculate and control limit and fatigue loads (including a substantial increase in the number of component load monitoring stations)

	Tornado IDS	Future Europ.Fighter
Basic Loads Cases (BLC) Flight and Ground Handling Loads	33	105
Unit Loads Cases (ULC) Hammershock, Engine Thrust, Airbrake etc.	12	16
Combined Load Cases Superposition of scaled ULCs to BLCs	~ 100	590

- More accurate loads databases in terms of
 - ❖ Advances in "Carefree Handling"- Flight Control Systems (FCS)
 - ❖ Aircraft mass distributions predictions
 - ❖ Aircraft aerodynamics calculated with mature CFD (Computational Fluid Dynamics) methods and verified earlier and more reliable in wind tunnel tests.
 - ❖ coupling of structural models and aerodynamic models for aeroelastic effects available
 - ❖ Finite Element modelling of the structure with interfaces to the Loads Model
- extensive flight testing, especially dedicated flight load surveys
- extensive structural ground tests

Basically this means that the static design of "old" aircraft usually is rather conservative and on the safe side.

With respect to fatigue the situation is often less satisfying, i.e. without powerful tools like a balanced Loads Model, one procedure was balancing loads over the aircraft artificially in those days, and design load cases therefore were generated for parts of the structure like aft or forward fuselage or tail plane only, the effect of these loads on other areas of the structure remained unknown and components, not immediately under survey were not analysed for this load case, therefore the effect of changes to these load cases later remained also unknown.

Structural Design Criteria (SDC)

Aircraft loads are determined according to requirements and regulations collected in a systems specification document called Structural Design Criteria, the major reference for loads and structural analysis engineers during the design phase.

Many of the SDC requirements come from the customer; others are prepared in co-operation between customer and original equipment manufacturer (OEM), usually the principal design contractor. The SDC are also subject to revisions during the design process.

Some of the more important items regarding loads and structures are:

Design masses are defined for different flight conditions to cover the whole mass and centre of gravity (C.G.) range, i.e.:

- Basic flight design mass
- Landing design mass
- Maximum take off mass

Total mass and mass distribution not only affect loads on wing as is sometimes believed but loads on most parts of the aircraft's structure. Design mass is one of the most important criteria for structural design. For example the basic flight design mass is coupled to the max/min allowed vertical load factor N_z , for increased masses through the rule: $N_z \cdot \text{Weight} = \text{const.}$ to avoid overloads or assessing the effects of over-g.

V-n DIAGRAM

A V-n diagram shows the flight load factors that are used for the structural design as a function of the air speed. These represent the maximum expected loads that the aircraft will experience. These load factors are called as limit load factors. These diagrams are used primarily in the determination of combinations of flight condition and load factors to which the airplane structure must be designed.

For purposes of structural sizing, analysis is performed at four extreme loading conditions on the V-n diagram. The Positive High Angle of Attack (PHAA) is the loading condition represented by the intersection between the positive operational load limit line and the positive maximum lift curve. The Positive Low Angle of Attack (PLAA) is at the intersection between the positive operational load limit line and the dive speed. The Negative High Angle of Attack (NHAA) and Negative Low Angle of Attack (NLAA) are defined similarly except are for the negative loads. Should the gust envelope extend beyond the manoeuvring envelope in any of these four locations, the load factor of the gust envelope is instead used for the extreme loading condition. The high angle of attack conditions are characterized by a high coefficient of lift and high drag. The low angle of attack conditions are characterized by a high lift force. Designing to accommodate these four extreme loading conditions will guarantee that the wing will not undergo structural damage so long as operational load limits are not exceeded.

The control of weight in aircraft design is of extreme importance. Increase in weight requires stronger structures to support them, which in turn lead to further increase in weight & so on. Excess of structural weight means lesser amounts of payload, affecting the economic viability of the aircraft. Therefore there is need to reduce aircraft's weight to the minimum compatible with safety. Thus to ensure general minimum standards of strength & safety, airworthiness regulations lay down several factors which the primary structures of the aircraft must satisfy. These are,

- ❖ **LIMIT LOAD:** the maximum load that the aircraft is expected to experience in normal operation.

- ❖ **PROOF LOAD:** product of the limit load and proof factor
- ❖ **ULTIMATE LOAD :** product of limit load and ultimate factor

There are two types of V-n diagram:

- ✚ The V-n maneuver diagram
- ✚ The V-n gust diagram

STALL SPEED AND MINIMUM SPEEDS:

The so-called 1-g stall speed of an airplane is defined by:

$$V_S = \sqrt{\frac{2W}{\rho C_{L_{max_{trim}}} S}}$$

Where

$C_{L_{max_{trim}}}$ is the maximum trimmed lift coefficient of the airplane.

The minimum speed at which an airplane is controllable is defined by:

$$V_S = \sqrt{\frac{2W}{\rho C_{L_{max_{controllable}}} S}}$$

Where

$C_{L_{max_{controllable}}}$ is the maximum trimmed lift coefficient at which the airplane is controllable.

The load factor encountered by an airplane in flight is defined by:

$$n = \frac{L}{W}$$

Clearly, in level flight, $n=1$. Most flight tests close to stall encounter a load factor of about $n=0.9$. Therefore, an effective stall lift coefficient may be computed from:

$$C_{L_{max_{controllable}}} = \frac{C_{L_{max}}(n = 1)}{n}$$

The V-n diagram for the aircraft is drawn for the two cases namely:

- ✚ Intentional maneuver(pilot induced maneuver)
- ✚ Unintentional maneuver(gusts)

Maneuvering Envelope:

In accelerated flight, the lift becomes much more compared to the weight of the aircraft. This implies a net force contributing to the acceleration. This force causes stresses on the aircraft structure. The ratio of the lift experienced to the weight at any instant is defined as the Load Factor (n).

$$n = \frac{\frac{1}{2} \rho_{\infty} V_{\infty}^2 C_{Lmax}}{W/S}$$

Using the above formula, we infer that load factor has a quadratic variation with velocity. However, this is true only up to a certain velocity. This velocity is determined by simultaneously imposing limiting conditions aerodynamically ($(C_L)_{max}$) as well as structurally (n_{max}). This velocity is called the Corner Velocity, and is determined using the following formula,

$$V_A = V_{Corner} = \sqrt{\left(2 \frac{n_{max} W}{C_{Lmax} S}\right)}$$

V-n diagram is used primarily in the determination of combination of flight conditions and load factors to which the airplane structure must be designed. V-n diagram precisely gives the structural (maximum load factor) and aerodynamic (maximum C_L) boundaries for a particular flight condition.

Calculation:

The main velocities that are plotted in the V-n diagram are:

- 1-g Stall Velocity
- Design Manoeuvring Velocity
- Design Cruise Velocity
- Design Dive Velocity 1-g Stall Velocity, V_s :

$$V_s = \sqrt{\frac{2W_{FDWG}}{\rho C_{N_{max(rollable)}} S}}$$

Where,

ρ = Density at the sea altitude (1.225kg/m³)

(W_{FDWG} / S) = Wing Loading

$$= 29770 \cdot 9.81 / 44.3$$

$$= 6592.40 \text{ kg/m}^2$$

$$C_{N_{max(rollable)}} = \sqrt{\left(C_{L_{max(rollable)}}\right)^2 + \left(C_{D_{at C_{L_{max(rollable)}}}\right)^2}$$

Where, $C_{Lmax} = 2$
 $\therefore C_N = 1.1 * C_{Lmax}$
 $= 2.2$

1-g Stall Velocity, $V_s = 69.94 \text{ m/s}$.

DESIGN LIMIT LOAD FACTORS n_{limpos} and n_{limneg} :

The positive design limit load factor, n_{limpos} , must be selected by the designer, but must meet the following condition

$$n_{limpos} \geq 2.1 + \frac{24,000}{W_{FDGW} + 10,000}$$

$$\geq 2.1 + (24000 / (29770+10000))$$

$$\geq \mathbf{2.705}$$

Hence our design satisfied the above condition.

The negative design limit load factor n_{limneg} , must be selected by the designer, but must meet the following condition:

$n_{limneg} \geq 0.4n_{limpos}$ for normal and for utility category airplanes. Therefore,

$$n_{limneg} \geq 0.4 \times 2.705$$

$$\therefore 1.52 \geq 1.082$$

Hence our design satisfied the above condition.

DESIGN MANEUVERING SPEED V_A :

The design manoeuvring speed V_A , must be selected by the designer, but must satisfy the following relationship:

$$V_A \geq V_S \sqrt{(n_{limpos})}$$

$$V_A \geq 69.94 \sqrt{2.705}$$

$$V_A \geq \mathbf{114.986 \text{ ms}^{-1}}$$

DESIGN CRUISE SPEED V_C :

The design cruise speed V_C , must be selected by the designer, but must satisfy the following relationship:

$$V_C \geq k_c \sqrt{(W_{FDGW})/S}$$

$k_c = 36$ for acrobatic aircraft

$$V_C \geq 36 \times \sqrt{672.00}$$

$$V_C \geq \mathbf{933.23 \text{ ms}^{-1}}$$

DESIGN DIVING SPEED V_D

The design diving speed must satisfy the following relationship:

$$VD \geq 1.25 VC$$

$$VD \geq 1.25 * 933.23$$

$$VD = 1166.541 \text{ms}^{-1}$$

Construction of V-n Diagram

Maximum Load Factor,

$$n_{max} = \left(\frac{L}{D}\right)_{max} \times \left(\frac{T}{W}\right)_{max}$$

$$n_{max} = \frac{1}{2} \rho_{\infty} V_{\infty}^2 \frac{C_{Lmax}}{\left(\frac{W}{S}\right)}$$

Curve AC:

AC is a line limiting the maximum amount of load that can be withstood by the weakest structure of the aircraft.

$$V_C = \sqrt{\frac{\left[\frac{T}{W} \times \frac{W}{S}\right] - \sqrt{\left[\frac{W}{S} \times \left(\frac{T}{W}\right)_{max}^2 - (4 k C_{D,0})\right]}}{\rho C_{D,0}}}$$

Along CD:

The velocity at point D is given by,

A straight line is used to join the points C and D. This VD is the dive velocity or the maximum permissible EAS in which the aircraft is at the verge of structural damage due to high dynamic pressure.

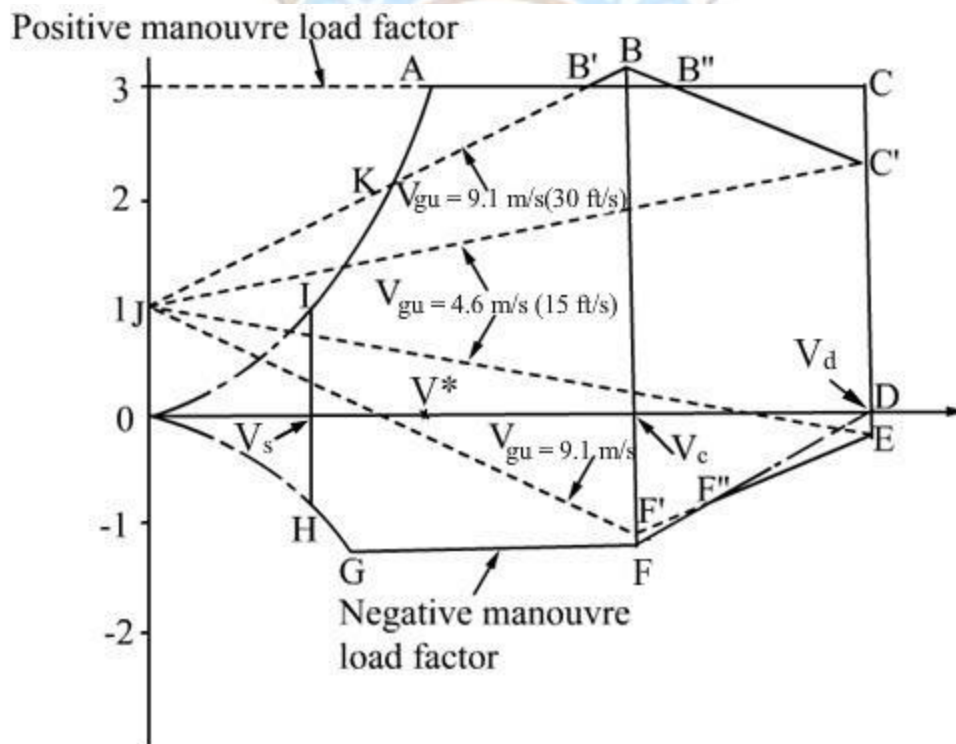
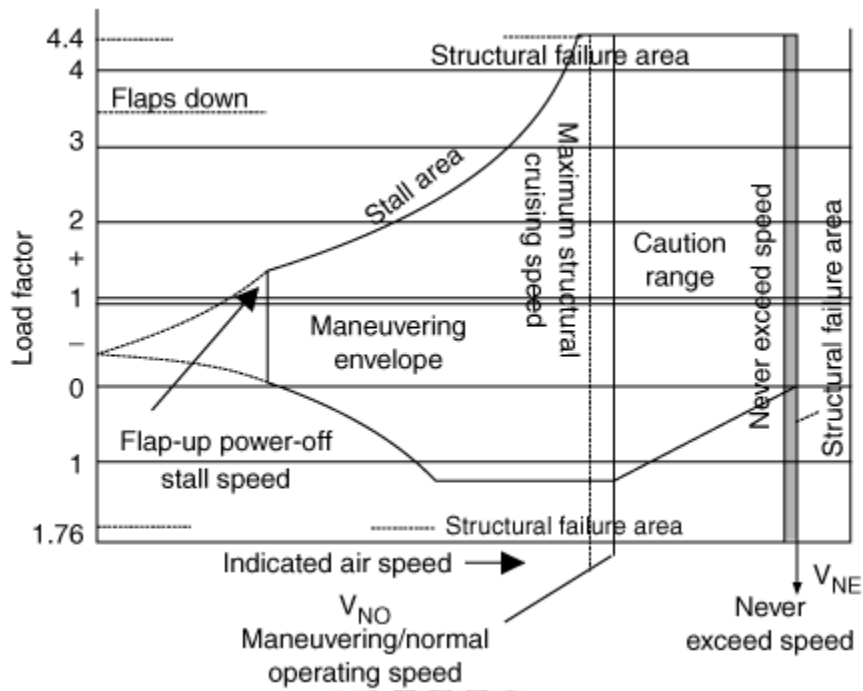
Along DE:

E corresponds to zero load factor point i.e. $n = 0$

Curve OG:

Along GF:

Also $n_G = n_F$ Finally join GF by using a straight line



The load factor (n) has already been defined as the ratio of lift and weight i.e. $n = L / W$. In level flight $n = 1$. However, the value of ' n ' during a manoeuvre is greater than one. Hence, the structure of the airplane must be designed to withstand the permissible load factor. Further, when an airplane encounters a gust of velocity V_{gu} the angle of attack of the airplane

would increase by $\Delta\alpha = V_{gu} / V$. This increase in angle of attack, would increase the lift by ΔL , given by :

$$\begin{aligned}\Delta L &= \frac{1}{2} \rho V^2 S C_{L\alpha} \Delta\alpha = \frac{1}{2} \rho V^2 S C_{L\alpha} V_{gu} / V \\ &= \frac{1}{2} \rho V S C_{L\alpha} V_{gu}\end{aligned}$$

$$\text{Hence, } \Delta n = \Delta L / W = \frac{1}{2} \rho V S C_{L\alpha} V_{gu} / W$$

From Eqs above, ΔL increases with V_{gu} . Further, for a given V_{gu} , the values of ΔL & Δn increase with flight velocity. An airplane must be designed to withstand the gust loads also.

In aeronautical engineering practice, the load factors due to manoeuvre and gust are indicated by a diagram called 'Velocity-load factor diagram or V-n diagram'. A typical V-n diagram is shown in Figure above. This diagram can be explained as follows.

(i) Curves OIA and OHG: The lift (L) produced by an airplane is given by

$$L = \frac{1}{2} \rho V^2 S C_L$$

It should be noted that

- (i) $C_L \leq C_{Lmax}$ and
- (ii) at stalling speed (V_s),
 $L = W$ and $n = 1$.

However, if the airplane is flown with $C_L = C_{Lmax}$ at speeds higher than V_s , then

- (a) L will be more than W and
- (b) L or n would be proportional to V^2 .

This variation is a parabola and is shown by curve OIA in

Figure above, In an inverted flight the load factor will be negative and the V vs n curve in such a flight is indicated by the curve OHG in Fig. It may be mentioned that an airplane can fly only at $V \geq V_s$ and hence the portions OI and OH in Fig are shown by chain lines.

(ii) Positive and negative manoeuvre load factors:

An airplane is designed to withstand a certain permissible load factor. Higher the permissible load factor, heavier will be the weight of airplane structure. Hence, for actual airplanes the manoeuvre load factor is limited depending on its intended use. Federal Aviation Administration (FAA) in USA and similar agencies in other countries, prescribe the values of permissible manoeuvre limit load factors ($n_{positive}$ and $n_{negative}$) for different categories of airplanes.

Type of airplane	$n_{positive}$	$n_{negative}$
General aviation-non aerobatic	2.5 to 3.8	-1
Transport	3 to 4	-1
Fighter	6 to 9	-3

A limit load is obtained by multiplying the limit load factor with the weight (W). The airplane structure is designed such that it can withstand the limit load without yielding. The ultimate load factor, in aeronautical practice, is 1.5 times the limit load factor. The ultimate load is obtained by multiplying the ultimate load factor with the weight (W). The airplane structure is designed such that it can withstand the ultimate load without failing, though there may be permanent damage to the structure.

In Figure, $n_{\text{positive}} = 3$ and $n_{\text{negative}} = -1.2$ have been chosen; the actual values depend on the weight of the airplane and its category.

(iii) Lines AC, GF and FD: The positive manoeuvre load factor is prescribed to be constant upto the design diving speed (V_d); line AC in Fig. The design diving speed could be 40 to 50% higher than the cruising speed (V_c) for subsonic airplanes. For supersonic airplanes, the Mach number corresponding to V_d could be 0.2 faster than the maximum level flight Mach number. The negative manoeuvre load factor is prescribed to be constant upto design cruising speed (line GF in Fig) and then increases linearly to zero at $V = V_d$ (line FD in Fig).

(iv) Manoeuvre load diagram: The diagram obtained by joining the points OACDFGO is called 'Manoeuvre load diagram'.

(v) Manoeuvre point and Corner speed: The point 'A' in Figure is called 'Manoeuvre point'. The flight speed at this point is denoted by V^* and is called 'Corner speed'. At point 'A' the lift coefficient equals $C_{L_{\text{max}}}$ and the load factor equals n_{positive} . This combination would result in the maximum instantaneous turn rate at the speed V^* . See subsection 9.3.6 for definition of instantaneous turn rate.

(vi) Positive and negative gust load factors: From Equation it is observed that the gust load factor varies linearly with velocity. The regulating agencies like FAA prescribe that an airplane should be able to withstand load factors corresponding to $V_{\text{gu}} = 30$ ft/s (9.1 m/s) upto cruising speed (V_c) and $V_{\text{gu}} = 15$ ft/s (4.6 m/s) upto design diving speed (V_d). Lines JB and JF' in Figure show the gust lines corresponding to $V_{\text{gu}} = 30$ ft/s (9.1 m/s) and Lines JC' and JE in the same figure show the gust lines corresponding to $V_{\text{gu}} = 15$ ft/s (4.6 m/s).

It may be pointed out that a gust in real situation is not a sharp edged gust and the velocity V_{gu} is attained in a gradual manner. This causes reduction in the gust load factor. To take care of this reduction the gust load factor is multiplied by a quantity called 'Gust alleviation factor'.

(vii) Gust load diagram: The diagram obtained by joining the points JBC'EF'J is called 'Gust load diagram'.

(vi) Final V-n diagram: For its safe operation, an airplane must be designed to withstand load factors occurring at all points of the gust and manoeuvre load diagrams. Hence, the final V-n diagram is obtained by joining the parts of these two diagrams representing the higher of the manoeuvre and gust load factors.

The final V-n diagram in the case presented in Figure, is given by the solid curve obtained by joining the points IAB'BB''CEF''FGHI.

It may be pointed out that the gust load line JB' is above the curve IA in the region IK. However, along the curve IK the airplane is already operating at $C_{L_{\text{max}}}$ and any increase in angle of attack due to gust cannot increase C_L beyond $C_{L_{\text{max}}}$.

Hence, the portion JK of the line JB is not included in the final V-n diagram.

It may also be pointed out that the angles of attack of the airplane are different at various points of the V-n diagram. Consequently, the components of the resultant aerodynamic force along and perpendicular to the chord of the wing would be different at different angles of attack. The structural analysis needs to take this into account. For example, the angle of attack is positive and high at point A and it is positive and low at point C. At points G and E the angles of attack are negative. Books on Airplane structures may be consulted for details.

Developments of Aircraft upto 1960's

Important developments upto 1960's are summarized in this section.

- (a) First successful flight in Europe was by Voisin on March 30, 1907.
- (b) Louis Bleriot's airplane, flown in 1907, appears to be the first airplane to have ailerons.
- (c) A. Verdon Roe's airplane, flown in 1911, was a tractor airplane with engine ahead of wing and with horizontal stabilizer at rear.
- (d) Prior to the First World War, the airplanes were developed for military use, namely reconnaissance and for guiding artillery fire and later for throwing grenades and bombs.
- (e) During the First World War (1914 – 1918), the airplanes were developed as bombers and fighters. Passenger flights appeared later and by 1925 a variety of airplanes were being designed and used.
- (f) By 1930's the following developments had been achieved.
 - (i) Streamlining of the airplane shape by features like retractable landing gear, engine cowling, fairing at wing-fuselage joints.
 - (ii) More powerful and reliable piston engines.
 - (iii) New aluminum alloys with higher strength to weight ratio and
 - (iv) Better instrumentation for control of airplane.

These developments brought about bigger airplanes, with improved performance namely higher speed, longer range and higher ceiling as compared to the earlier airplanes.

- (g) The speed of the airplanes increased sharply with the availability of jet engines in 1940's.
- (h) Supersonic flight was possible in 1950's due to the developments in aerodynamics. The problems associated with changes in lift & drag in the transonic range were tackled. Features like swept back wings, delta wing, fuselage with pointed nose were introduced.

For example, for the fighter airplanes the maximum speed increased from 150 kmph in 1914 to about 3500 kmph in 1970. The engine power increased from about 60 kW to a thrust of 30,000 kgf and the weight of the airplane increased from about 600 kgf to about 50,000 kgf.

Some of the subsequent developments

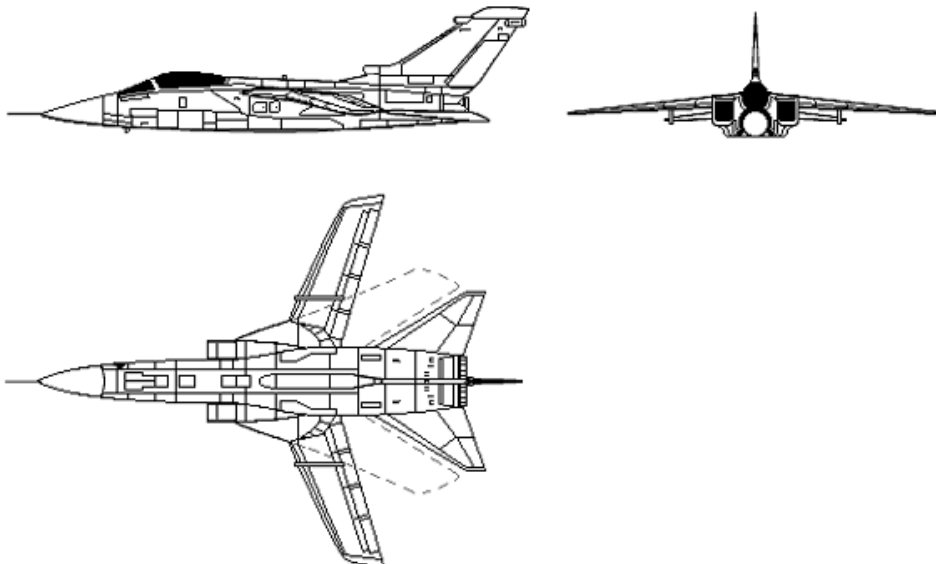
Some of the important subsequent developments are as follows.

- (a). Supersonic passenger airplane – Anglo-French Concorde in 1971 (Fig.1.6). Another example in this category is the Russian TU-144.



Concorde in flight

(b). Variable sweep military airplane - low sweep at low speed & high sweep at high speed



Variable sweep airplane – Tornado

(c). Passenger airplanes with upto 450 seats and range of 12000 km were available in early 1970's



Boeing 747

Currently the seating capacity of 650 passengers is available on Airbus A380



Airbus A380

- (d). Supercritical airfoils with higher critical Mach number were available in 1970's.
- (e). Automatic Landing system was introduced in 1960's.
- (f). Fly - by -wire control was introduced in 1984. In this case, the movements of the control stick or pedals by the pilot are transmitted to a digital computer. The input to the computer is processed along with the characteristics of the airplane and the actuators of the controls are operated, so as to give optimum performance. Presently fibre optics is used for communication of signals and the system is called Fly-by-light (FBL).
- (g). Bypass engine whose developments started in 1950's has become high bypass ratio engine; a bypass ratio of 17 has been achieved.
- (h). Winglet at wing tips which were studied in 1970's are now found on most of the new jet airplanes and are also being retrofitted on older airplanes.



Airplane with winglets – Boeing 737-800

- (i). The use of FRP (Fiber Reinforced Plastics) has increased and components like wings are also being made of FRP (for example LCA –Tejas made by HAL, Bangalore,India).
- (j). Low Radar cross-section – stealth technology was introduced in late 1980's



B2 Stealth bomber

Features of some special airplanes:

1. Largest Airplane: Airbus A380-800F (Fig.1.8b)

Wing span - 79.75 m

4 engines each 355 kN thrust.

Maximum take-off Weight - 590 tons

2. Airplane with advanced technologies:

X-29A airplane (Fig.1.11) has, according to Ref.1.22:

Digital flight control

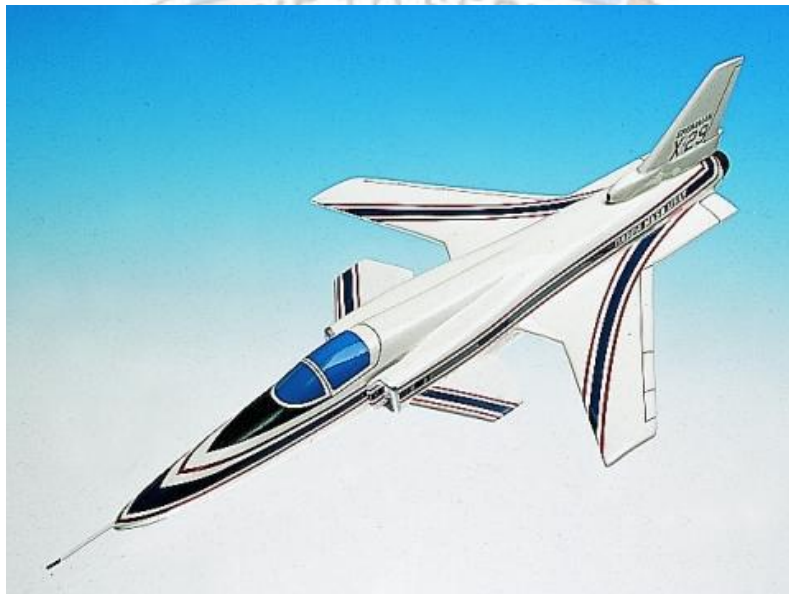
Negative longitudinal static stability (relaxed stability)

Closely coupled canard.

Forward swept wing

Aero- elastically tailored composite wing.

Thin supercritical wing with discrete variable camber.



X-29A

Modern fighter:

Lockheed YF-22 Advanced tactical fighter. Presently it is called F-22 Raptor.

Span: 13.1 m;

Length: 19.6 m;

Height: 5.4 m;
Wing Area: 77.1 m²;
Basic Empty weight: 15441 kgf.



Lockheed YF-22 Advanced tactical fighter

Reusable vehicle:

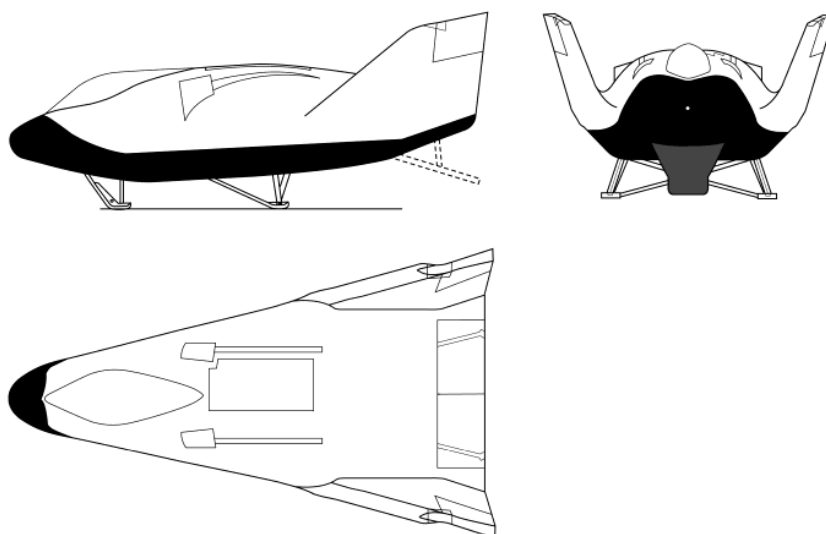
X-38 (Fig 1.13)

Length: 8.7 m

Wingspan: 4.4 m

Empty weight: 7260 kgf.

It may be added that the project was abandoned in 2002.



Reusable vehicle

AIRPLANE DATA SHEET

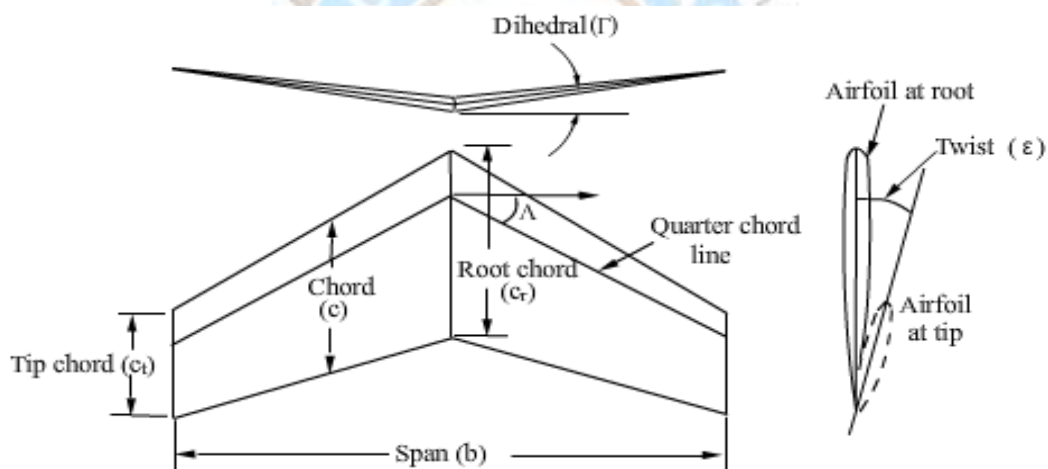
1. General description of airplane

- i) Name of the airplane:
- ii) Type of airplane *:
- iii) Name of manufacturer and country of origin:

2. Power Plant

- i) Type of power plant*:
- ii) Name:
- iii) Engine rating*:
- iv) Specific fuel consumption:
- v) Oil consumption :
- vi) Weight of power plant:
- vii) Overall dimensions of engine:
 - a. Diameter (m):
 - b. Length (m):
- viii) Engine centre of gravity:
- ix) Special accessories and controls:
- x) No. of engines and their locations:
- xi) Intake/propeller details

3. Wing: Planform shape



- i) Airfoil section:
- ii) Span (m):
- iii) Root chord (m):
- iv) Tip chord (m):
- v) Area (S) (m^2):
- vi) Mean chord* (m):
- vii) Mean aerodynamic chord* (m):
- viii) Sweep (Λ):
- ix) Dihedral. (Γ):
- x) Twist (ϵ)*:
- xi) Incidence (i)*:
- xii) Flap area (m^2):

- xiii) Aileron area (m^2):
- xiv) Type of high-lift devices:
- xv) Location of spars:
- xvi) Taper ratio (λ)*:
- xvii) Aspect ratio (A)*:
- xviii) Flap area/wing area: or S_{flap}/S
- xix) Aileron area/wing area or $S_{aileron}/S$:
- xx) Flap chord/ wing chord or C_{flap}/C_{wing} :
- xxi) Aileron chord/wing chord or $C_{aileron}/C_{wing}$:
- xxii) Location of wing on fuselage (high wing/mid wing/low wing):
- xxiii) Construction and other details:

4. Horizontal tail surface

- i) Type of horizontal tail *:
- ii) Platform shape:
- iii) Airfoil:
- iv) Span (m):
- v) Root chord (m) :
- vi) Tip chord (m):
- vii) Area (m^2):
- viii) Sweep:
- ix) Incidence (i)*:
- x) Elevator area (m^2):
- xi) Tab area (m^2):
- xii) Aspect ratio:
- xiii) Taper ratio:
- xiv) Elevator area / Tail area:
- xv) Tab area / elevator area:
- xvi) Tail area(S_{ht}) / wing area(S):
- xvii) Elevator chord / tail chord:
- xviii) Location of H.tail:
- xix) Type of control and aerodynamic balancing*:
- xx) Construction and other details:

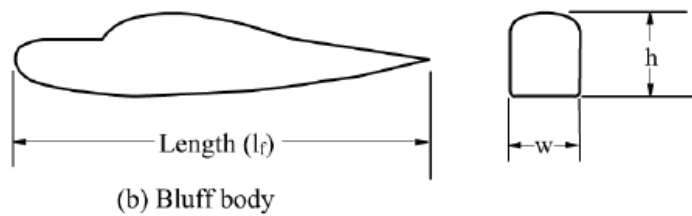
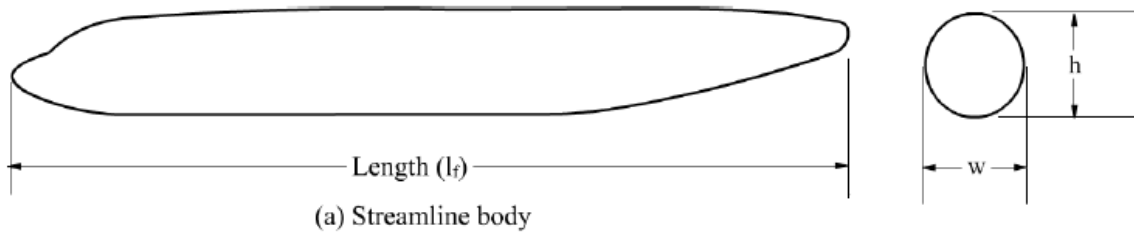


5. Vertical tail surface

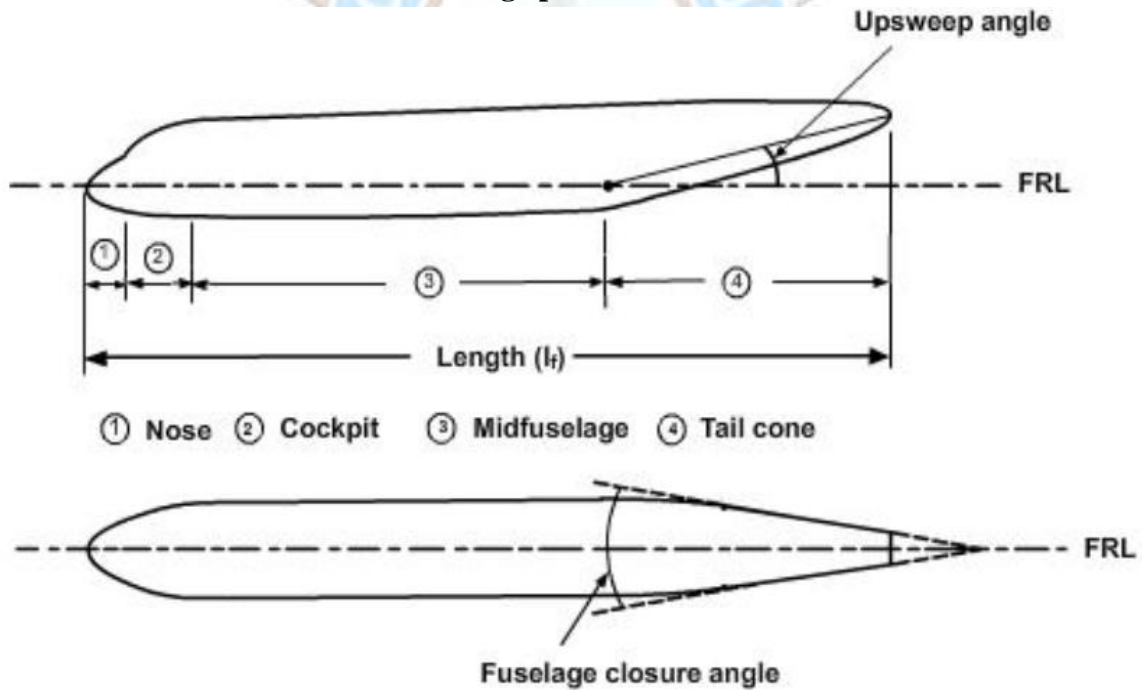
- i) Type of vertical tail *
- ii) Airfoil:
- iii) Height (m):
- iv) Root chord (m):
- v) Tip chord (m):
- vi) Area (m^2):
- vii) Sweep:
- viii) Off-set angle*:
- ix) Rudder area (m^2):
- x) Tab area (m^2):

- xi) Aspect ratio (A_v)*:
- xii) Taper ratio:
- xiii) Rudder area/tail area:
- xiv) Tab area / rudder area:

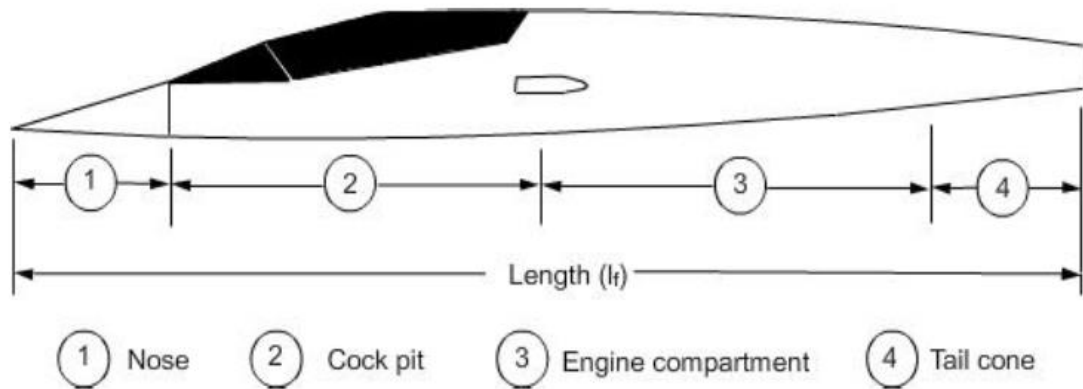
6. Fuselage



Fuselage parameters



Typical segments of a passenger airplane fuselage



Typical segments of a military airplane fuselage

- i) Length (m):
- ii) Length of nose (l_{nose}):
- iii) Length of cockpit ($l_{cockpit}$):
- iv) Length of tail cone ($l_{tailcone}$):
- v) Length of payload compartment:
- vi) Length of midfuselage:
- vii) Upsweep angle
- viii) Fuselage closure angle
- ix) Shape and size of cabin:
- x) Arrangement of payload and auxiliary equipment:
- xi) Cockpit:
- xii) Number and arrangement of seats:
- xiii) Cockpit instruments:
- xiv) Vision (angle):
- xv) Construction and other details:
- xvi) Length(l_f)/wingspan(b):
- xvii) l_{nose}/l_f :
- xviii) $l_{cockpit}/l_f$:
- xix) $l_{tailcone}/l_f$:

7. Landing gear

- i) Type of landing gear*:
- ii) Number and size of wheels:
- iii) Tyre pressure:
- iv) Wheel base* (m):
- v) Wheel tread* (m):
- vi) Location of landing gears:
- vii) Means to reduce landing run and other details:

8. Overall dimensions of airplane:

- i) Length (m):
- ii) Wing span (m):
- iii) Height (m):
- iv) Landing gear wheel tread (m):

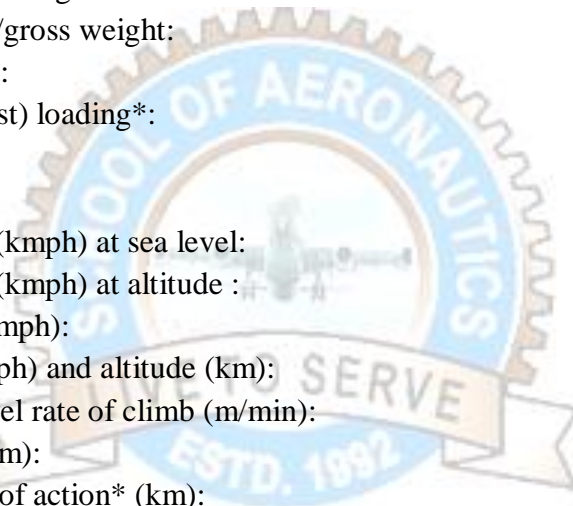
- v) Landing gear wheel base(m):
- vi) Length/span:
- vii) Height/span:
- viii) Tread/span:

9. Weights

- i) Pay load* (kgf):
- ii) Empty weight* (kgf):
- iii) Fuel weight (kgf):
- iv) Structural weight (kgf):
- v) Disposable load* (kgf):
- vi) Landing weight (kgf):
- vii) Normal gross weight (kgf):
- viii) Maximum gross weight (kgf):
- ix) Payload/gross weight:
- x) Empty weight/gross weight:
- xi) Fuel weight/gross weight:
- xii) Structural weight/gross weight:
- xiii) Wing loading*:
- xiv) Power (or thrust) loading*:

10. Performance

- i) Maximum speed (kmph) at sea level:
- ii) Maximum speed (kmph) at altitude :
- iii) Landing speed (kmph):
- iv) Cruise speed (kmph) and altitude (km):
- v) Maximum sea level rate of climb (m/min):
- vi) Service ceiling (km):
- vii) Range* or radius of action* (km):
- viii) Endurance* (hours):
- ix) Take-off run* (m):
- x) Landing run* (m):



SCHOOL OF AERONAUTICS (NEEMRANA)

UNIT-II NOTES

FACULTY NAME: D.SUKUMAR.

CLASS: B.Tech AERONAUTICAL

SUBJECT CODE: 6AN5

SEMESTER: VI

SUBJECT NAME: AIRCRAFT DESIGN

AIRPLANE WEIGHT ESTIMATION:

Weight estimation based on type of airplane, trends in wing loading, weight estimation based on mission requirements, iterative approach.

BASIC WING DESIGN:

Selection of airfoil selection, influencing factors. Span wise load distribution and planform shapes of airplane wing. Stalling take off and landing considerations. Wing drags estimation. High lift devices.

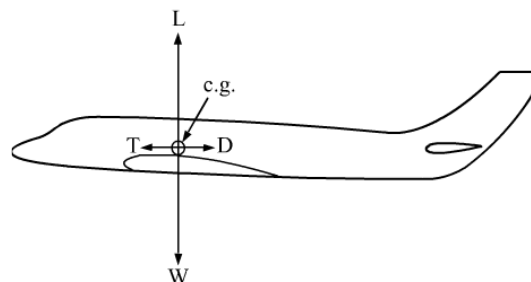
STRUCTURAL DESIGN:

Cockpit and aircraft passenger cabin layout for different categories, types of associated structure, features of light airplanes using advanced composite materials. Structural aspects of design of airplane, Bending moment and shear force diagram. Design principles of all metal stressed skin wing for civil and military applications.

DEPENDENCE OF AIRPLANE PERFORMANCE ON AIRPLANE PARAMETERS AND ATMOSPHERIC CHARACTERISTICS

The airplane performance parameters like maximum speed, maximum rate of climb, ceiling, range, endurance, rate of turn, take-off distance and landing distance, depend on weight of airplane (W) wing area (S), drag polar, thrust / power available, fuel weight etc. This dependence is examined in the following subsections.

Steady level flight – maximum flight speed (V_{max})



Steady level flight

Figure above shows the forces acting on an airplane and the velocity vector in the steady level flight. The equations of motion, in standard notations, for this flight are:

$$T - D = 0$$

$$L - W = 0$$

Noting that, $L = 1/2 (\rho V^2 S C_L)$, and $D = 1/2 (\rho V^2 S C_D)$,

The thrust required $= T_r = D = W (C_D / C_L)$

Further, if the drag polar is parabolic i.e. $C_D = C_{D0} + K C_L^2$, then :

$$T_r = D = (1/2) \rho V^2 S C_D = (1/2) \rho V^2 S (C_{D0} + K C_L^2) \quad (3.1)$$

$$\text{Or } T_r = \frac{1}{2} \rho V^2 S \left[C_{D0} + K \left(\frac{W}{\frac{1}{2} \rho V^2 S} \right)^2 \right] = \frac{1}{2} \rho V^2 S C_{D0} + \frac{2KW^2}{\rho S V^2} \quad (3.2)$$

$$\text{The power required} = P_r = \frac{T_r V}{1000} = \frac{1}{2000} \rho V^3 S C_{D0} + \frac{K W^2}{500 \rho V S} \quad (3.2a)$$

Thus, T_r or P_r depends on W/S , ρ and the drag polar which is characterised by C_{D0} and K . Equations (3.2) and (3.2a) can be expressed as

T_r or $P_r = f (W/S, \rho, \text{drag polar})$.

Further, at maximum speed (V_{max}), (a) the thrust required (T_r) equals, the thrust available (T_a) and (b) the power required (P_r) equals the power available (P_a), Hence, V_{max} of a jet airplane is dependent on W , T/W , ρ and drag polar i.e.

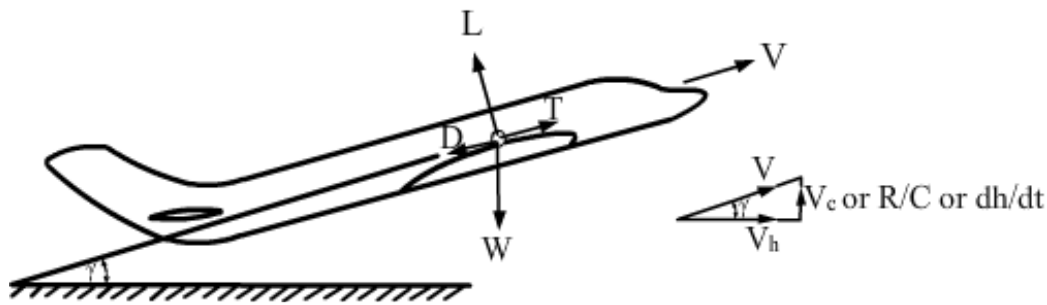
$$V_{max} = f \{W, W/S, T_a/W, \rho, \text{drag polar}\}; (T_a/W) \text{ is the thrust loading} \quad (3.3)$$

The V_{max} of an airplane with engine-propeller combination is dependent on W , W/P , ρ and drag polar i.e.

$$V_{max} = f \{W, W/S, W/P_a, \rho, \text{drag polar}\}; (W/P_a) \text{ is the power loading} \quad (3.3a)$$

Steady Climb – maximum rate of climb $(R/C)_{max}$

Figure below shows the forces on an airplane and the velocity vector in a steady climb.



Steady Climb

The equations of motion are :

$$T - D - W \sin \gamma = 0$$

$$L - W \cos \gamma = 0$$

Hence,

$$R / C = V \sin \gamma = V (T - D) / W$$

If the drag in climb is approximated as equal to drag in level flight (D_L), then

$$R / C = (TV - D_L V) / W = 1000(P_a - P_{rL}) / W \quad (3.4)$$

Where, P_{rL} is the power required in level flight at a flight velocity V and P_a is the power available at the same speed.

Hence, R/C is proportional to excess power. For a piston engined airplane, $V_{(R/C)_{max}}$ is approximately equal to V_{mp} ; where V_{mp} is the speed corresponding to minimum power in level flight. For a jet airplane, the ratio of $V_{(R/C)_{max}}$ to V_{md} is greater than unity and depends on the thrust to weight ratio (T/W); V_{md} is the speed corresponding to the minimum drag in level flight.

The expressions for D_L and P_{rL} are given in the previous subsection. Further, $(R/C)_{max}$ is generally prescribed at sea level and hence ρ in Eq.(3.2) and (3.2a) is equal to that at sea level. Keeping these factors in view the dependence of $(R/C)_{max}$ for a jet airplane can be expressed as :

$$(R/C)_{max} = f(W, W/S, T_a/W, \text{drag polar}) \quad (3.5)$$

For an airplane with engine propeller combination

$$\text{The expression is } (R/C)_{max} = f(W, W/S, W/P_a, \text{drag polar}) \quad (3.5a)$$

Absolute ceiling (H_{max}):

From the engine characteristics, it is known that the thrust horse power available (THP_a) and the thrust available (T_a) decrease with altitude. Further, at a chosen altitude the thrust horse power required (THP_r) and the thrust required (T_r) are minimum at flight speeds which are decided by the drag polar of the airplane. Keeping these in view it can be stated that (i) for an airplane with engine propeller combination, at absolute ceiling or H_{max} , the power available (THP_a) equals the minimum power required in level flight (P_{min}) and (ii) for an airplane with jet engine, at H_{max} , the thrust available (T_a) equals the minimum thrust required (T_{rmin}) in level flight. i.e.

$$\text{At } H_{max}, \quad (THP_a) = (P_r)_{min} \text{ or } (T_a) = (T_r)_{min}$$

From performance analysis, (sections 5.6 and 5.7 of Ref. 3.3), it is known that,

$(T_r)_{min}$ and $(P_r)_{min}$ in level flight occur respectively at C_L corresponding to C_{Lmd} and C_{Lmp} . If the drag polar is parabolic, i.e. $C_D = C_{D0} + KC_L^2$, then:

$$C_{Lmd} = (C_{D0} / K)^{1/2}, \quad C_{Dmd} = 2C_{D0} \text{ and } (C_D / C_L)_{min} = 2\sqrt{C_{D0}K}$$

$$C_{Lmp} = (3C_{D0} / K)^{1/2}, \quad C_{Dmp} = 4C_{D0} \text{ and } (C_D / C_L^{3/2})_{min} = \left(\frac{256}{27} C_{D0} K^3 \right)^{1/4}$$

Hence,

$$T_{min} = W (C_D / C_L)_{min} = 2W \sqrt{C_{D0}K} \quad (3.6)$$

$$P_{min} = \frac{1}{1000} \left(\frac{2W^3}{\rho S} \right)^{1/2} \left(\frac{256}{27} C_{D0} K^3 \right)^{1/4} \quad (3.7)$$

Hence, H_{max} depends on the drag polar, W / S and variation of engine output with altitude.

Range and endurance for airplanes with engine-propeller combination and with jet engine

Based on the performance analysis the Breguet formulae for range and endurance for airplanes with engine-propeller combination or jet engine, in standard notation, are given below. The range is in km and the endurance is in hours.

(a) For an airplane with engine-propeller combination the range (R_{EP}) and endurance (E_{EP}) are:

$$R_{EP} = \frac{8289.3}{BSFC} \frac{\eta_p}{C_D / C_L} \log_{10}(W_1 / W_2) \quad (3.8)$$

$$E_{EP} = \frac{1565.2 \eta_p}{BSFC(C_D / C_L^{3/2})} \left(\frac{\sigma S}{W_1} \right)^{1/2} \left[\left(\frac{W_1}{W_2} \right)^{1/2} - 1 \right] \quad (3.9)$$

where , η_p = propeller efficiency; BSFC = specific fuel consumption is N/kW -hour with BHP in kW; σ = density ratio = $(\rho/\rho_{sealevel})$; W_1 and W_2 are respectively the weights of the airplane at the start and the end of the cruise.

(b) For a Jet-engined airplane the range (R_{jet}) and the endurance (E_{jet}) are given by:

$$R_{jet} = \frac{9.2}{TSFC (C_D / C_L^{1/2})} \left(\frac{W_1}{\sigma S} \right)^{1/2} \left[1 - \left(\frac{W_2}{W_1} \right)^{1/2} \right] \quad (3.10)$$

$$E_{jet} = \frac{2.303}{TSFC (C_D / C_L)} \log_{10} \left(\frac{W_1}{W_2} \right) \quad (3.11)$$

where, TSFC = Specific fuel consumption in N/N -hr or hr^{-1} .

From Eqs.(3.8) to (3.11) it can be concluded that :

$$R_{EP} = f \left\{ BSFC, \eta_p, (C_L / C_D)_{max}, \frac{W_1}{W_2} \right\} \quad (3.12)$$

$$R_{jet} = f \left\{ TSFC, (C_L^{1/2} / C_D)_{max}, \frac{W}{S}, \sigma, \frac{W_1}{W_2} \right\} \quad (3.13)$$

$$E_{EP} = f \left\{ BSFC, \eta_p, (C_L^{3/2} / C_D)_{max}, \frac{W}{S}, \sigma, \frac{W_1}{W_2} \right\} \quad (3.14)$$

$$E_{jet} = f \left\{ TSFC, (C_L / C_D)_{max}, \frac{W_1}{W_2} \right\} \quad (3.15)$$

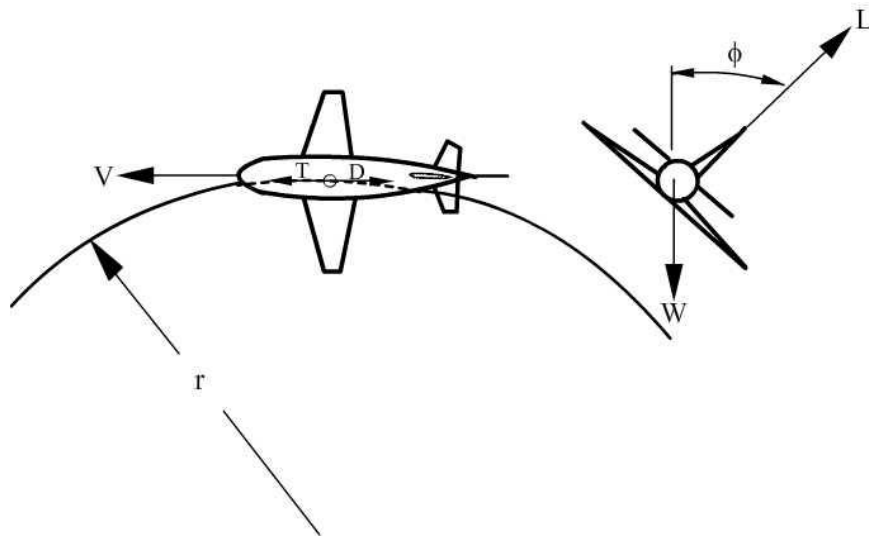
Turning – minimum radius of turn (r_{min}) and maximum rate of turn (Ψ_{max})

Figure below shows the forces on an airplane and the velocity vector in a turn.

The Equations of motion in a steady, level, co-ordinated-turn is:

$$T-D=0$$

$$L \cos\phi = W$$



Turning flight

$$L \sin \phi = (W/g) (V^2/r)$$

where, ϕ = angle of bank and r = radius of turn

Hence,

$$r = V^2 / (g \tan \phi) \text{ and} \tag{3.16}$$

$$\text{rate of turn} = \dot{\psi} = (g \tan \phi) / V \tag{3.17}$$

From the above equations it may be noted that (a) the lift required in turn is greater than the lift required in level flight ($L_{\text{turn}} > L_{\text{level}}$) (b) the thrust required in turn is greater than that required in level flight ($T_{\text{turn}} > T_{\text{level}}$) and (c) the load factor ($n = L / W$) is more than unity. We note that an airplane (a) is designed for a prescribed value of n_{max} , (b) has a value of $C_{L\text{max}}$ depending on its wing design and (c) has a certain value of $(\text{THP}_a)_{\text{max}}$ or $(T_a)_{\text{max}}$ depending on the engine installed. Thus, a turn is limited by $C_{L\text{max}}$, n_{max} and the available thrust or power.

Consequently, for a jet airplane,

$$\dot{\psi} = f(T_a/W, n_{\text{max}}, \text{drag polar}, C_{L\text{max}}) \tag{3.18}$$

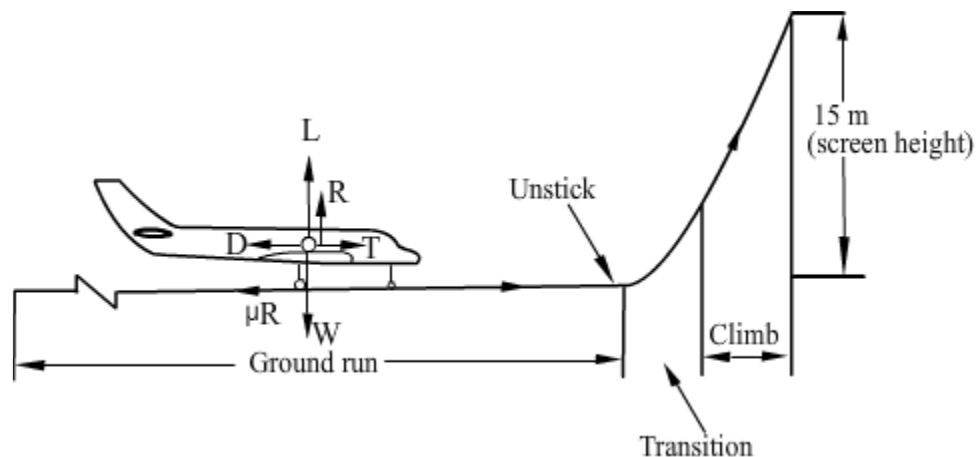
$$r_{\text{min}} = f(T_a/W, n_{\text{max}}, \text{drag polar}, C_{L\text{max}}) \tag{3.19}$$

For an airplane with engine-propeller combination

$$\dot{\psi}_{\text{max}} = f(W/\text{THP}_a, n_{\text{max}}, \text{drag polar}, C_{L\text{max}}) \tag{3.18a}$$

$$r_{\text{min}} = f(W/\text{THP}_a, n_{\text{max}}, \text{drag polar}, C_{L\text{max}}) \tag{3.19a}$$

Take off distance (s_{t0})



Phases of take-off flight

Figure above shows the phases of take-off flight. It also shows the forces on the airplane during the ground run.

The equation of motion during the ground run is:

$$T - D - \mu R = (W / g) a$$

Ground reaction = $R = W - L$, where ' μ ' is the coefficient of friction between the ground and the tyres and ' a ' is the acceleration.

Hence,

$$\text{ground run} = s_1 = \int_0^{V_{t.o}} \frac{V dV}{a} = \frac{W}{g} \int_0^{V_{t.o}} \frac{V dV}{T - D - \mu(W - L)} \quad (3.20)$$

$$V_{t.o} = k \sqrt{\frac{2W}{\rho S C_{Lmax}}}$$

where, $k = 1.1$ to 1.3 . Hence, higher the value of $V_{t.o}$, longer is the take off run.

Consequently, for reducing the take off run, low W/S , high C_{Lmax} and high T/W (or P/W) are required. The take-off distance (s_{t0}) is proportional to take-off run (s_1).

Hence, for a jet airplane,

$$s_{t0} = f(T_a/W, C_{Lmax}, \text{polar}, W/S, \mu) \quad (3.21)$$

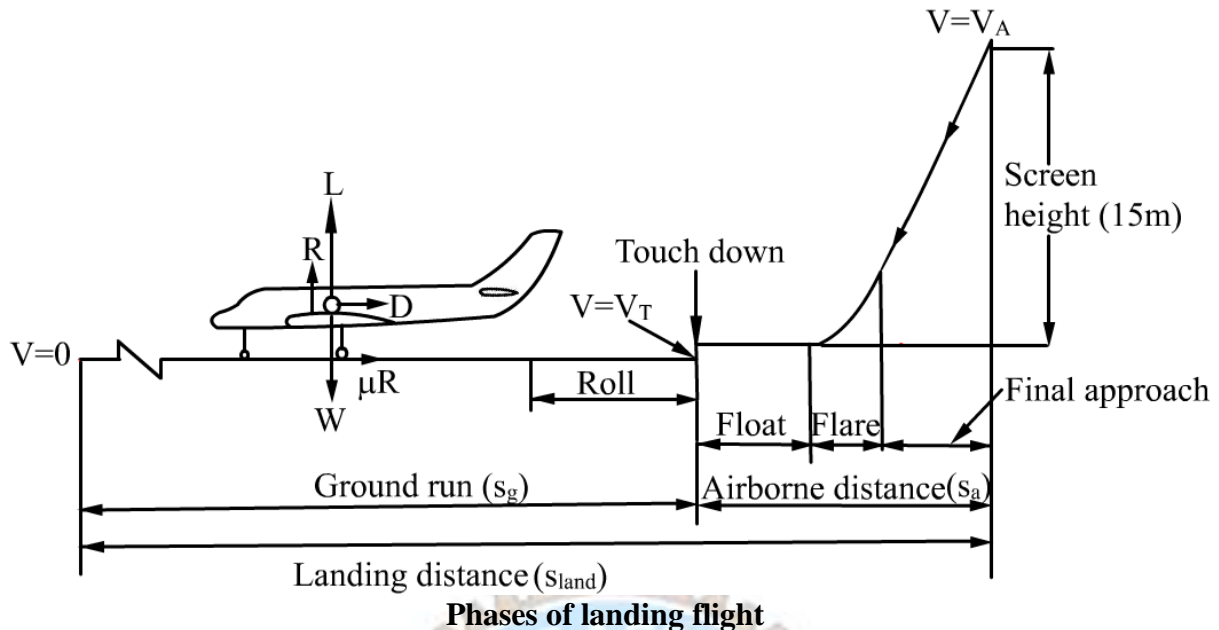
For an airplane with engine-propeller combination,

$$s_{t0} = f(W/P_a, C_{Lmax}, \text{polar}, W/S, \mu) \quad (3.21a)$$

It may be noted that the take-off distance is generally prescribed at sea level and hence ' ρ ' is not included in Eqs (3.21) and (3.21a).

Landing distance (s_{land})

Figure below shows the phases of landing flight. The estimation of landing distance (s_{land}) is more complicated than that of s_{t0} . However, it depends on the square of stalling speed in landing configuration (V_s) and the type of braking system.



The stalling speed is given by :

$$V_s^2 = \frac{2W}{\rho S C_{Lmax}}$$

Thus, for reducing the landing distance requires (a) low wing loading (W/S), (b) high value C_{Lmax} and (c) good braking system i.e.

$$s_{land} = f(C_{Lmax}, W/S, \text{braking system}) \quad (3.22)$$

Weight Estimation – outline of approach

A good estimate of the gross weight (W_0) is necessary for further progress in the design process.

The gross weight (W_0) is expressed as the sum of

- (a) The weight of the crew (W_{crew}),
- (b) The weight of payload ($W_{payload}$),
- (c) The weight of fuel required for the mission (W_f) and
- (d) The empty weight (W_e) i.e

$$W_0 = W_{crew} + W_{payload} + W_f + W_e \quad (3.23)$$

(i)The payload is the weight for which the airplane is designed. For a passenger airplane $W_{payload}$ would be the weight of the passengers plus the baggage. For a cargo airplane $W_{payload}$ would be the weight of the intended cargo. For a trainer airplane $W_{payload}$ would be the weight of the trainee plus the instructor. For special purpose airplanes like agricultural airplane $W_{payload}$ would be the weight of the fertilizer etc. For a fighter airplane $W_{payload}$ would be the

weight of the missiles, guns and ammunition. For a bomber airplane W_{payload} would be the weight of bombs and associated equipment.

(ii) The crew members are: (a) the flight crew, (b) cabin crew in passenger airplanes and special crew in airplanes like reconnaissance/patrol or for scientific measurements.

(iii) In passenger airplanes the number of cabin crew is: (a) one cabin crew for about 30 passengers in economy class and (b) one cabin crew for about 15 passengers in first class. Presently the number of flight crew would be two for commercial airplanes. On long range airplanes this number could be more to provide rest period for the pilot.

(iv) As regards the weights of the passengers and baggage are concerned, a value of 110 kgf per passenger can be taken for long range airplanes (82 kgf for passengers plus the cabin baggage and 28 kgf for the check-in baggage). The value of 16 kgf for check-in baggage can be taken for short and medium range airplanes.

(v) For long range airplanes the weight of flight and cabin crew can be taken as 110 kgf. For short range airplanes it could be 85 kgf.

(vi) The weight of the trainee and the instructor in trainer airplanes can be taken as 80 kgf. In combat airplanes the weight of the pilot could be 100 kgf due to the additional weight of protection gear.

(vii) In the approach, the empty weight is the gross weight of the airplane minus the weight of crew, payload and fuel.

In some other approaches, in passenger airplanes, the weights of operational items like food, water etc., are not included in the empty weight of the airplane.

Thus, W_{crew} & W_{payload} are known from the design specifications.

W_f & W_e depend on gross weight (W_0).

Hence, Eq.(3.23) is rewritten as:

$$W_0 = W_{\text{crew}} + W_{\text{pay}} + \left(\frac{W_f}{W_0}\right)W_0 + \left(\frac{W_e}{W_0}\right)W_0$$

$$\text{Or } W_0 = \frac{W_{\text{crew}} + W_{\text{pay}}}{1 - \left(\frac{W_f}{W_0}\right) - \left(\frac{W_e}{W_0}\right)} \quad (3.24)$$

The next two sections deal with the determination of W_e/W_0 and W_f/W_0 .

Estimation of empty-weight fraction (W_e/W_0)

From the data collection of the various aircraft, the data on empty weights of different types of airplanes. When the data are plotted as (W_e / W_0) vs $\log_{10}(W_0)$ the resulting curves are roughly straight lines. This suggests that these curves can be approximated by an equation of the type:

$$\frac{W_e}{W_0} = A W_0^c \quad (3.25)$$

Where, W_0 = Take-off gross weight in kgf. The quantities A and c depend on the type of the airplane.

The values of A and c are presented in Table below. The last column refers to the range of W_0 over which Eq.(3.25) can be used.

Type of airplane	A (W_0 in kgf)	c	Range of validity (W_0 in kgf)
Sailplane-unpowered	0.83	-0.05	150-700
Sailplane-powered	0.88	-0.05	200-1100
Homebuilt-metal/wood	1.11	-0.09	250-1800
Homebuilt-composite	1.07	-0.09	200-900
General aviation-single engine	2.05	-0.18	750-2300
General aviation-Twin engine	1.40	-0.10	1800-4000
Agricultural aircraft	0.72	-0.03	1300-7000
Twin turboprop	0.92	-0.05	3000-26000
Flying boat	1.05	-0.05	1200-9500
Jet Trainer	1.47	-0.10	2400-7400
Jet fighter*	2.11	-0.13	8200-58000
Military cargo/bomber*	0.88	-0.07	10000-400,000
Jet Transport	0.97	-0.06	10000-450000

Estimation of fuel fraction (W_f/W_0)

The weight of fuel needed depends on the following.

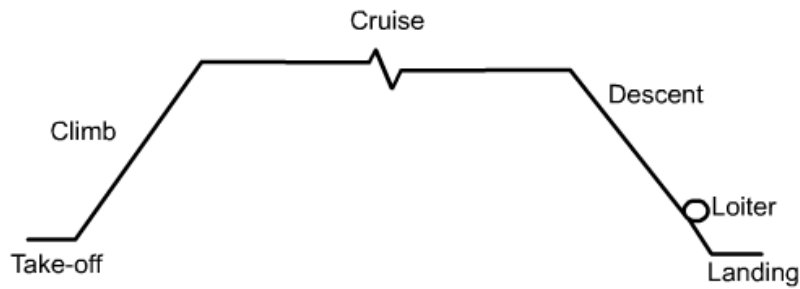
- I. Fuel required for mission.
- II. Fuel required as reserve.
- III. Trapped fuel which cannot be pumped out.

The fuel required for the mission depends on the following factors.

- a) Mission to be flown.
- b) Aerodynamics of the airplane viz. (L / D) ratio.
- c) SFC of the engine.

Mission profile

- a) **Simple mission:** For a transport airplane the mission profile would generally consist of (a) warm up and take off, (b) climb, (c) cruise, (d) descent, (e) loiter and (f) landing (Fig. below). Sometimes the airplane may be required to go to alternate airport if the permission to land is refused. Allowance also has to be made for head winds encountered en-route.



Typical mission profile of a transport airplane

(i) For a military airplane the flight profile could consist of (a) warm up and take-off, (b) climb, (c) cruise to target area, (d) performing mission in the target area, (e) cruise back towards the base, (f) descent, (g) loiter and (h) land. In the target area the airplane may carry out reconnaissance, or drop bombs or engage in combat.

As additional examples of the mission profiles, the following three cases can be cited.

(a) A trainer airplane, after reaching the specified area, may perform various maneuvers and return to the base.

(b) An airplane on a humanitarian mission may go to the desired destination, drop food and relief supplies and return to the base.

(c) In some countries the doctors from cities fly to the remote areas, examine the patients and fly back.

ii) The various segments of the mission can be grouped into the following five categories.

(a) Warm up, taxiing and take-off.

(b) Climb to cruise altitude.

(c) Cruise according to a specified flight plan. This item is covered under the topic of "Range" in "Performance analysis".

(d) Loiter over a certain area for a specified period of time. This item is covered under the topic "Endurance" in "Performance analysis".

(e) Descent and landing.

Weight fractions for various segments of mission

The fuel required in a particular phase of the mission depends on (a) the weight of the airplane at the start of that phase and (b) the distance covered or the duration of time for the phase. Keeping these in view, the approach to estimate fuel fraction for chosen mission profile is, as follows.

i) Let the mission consist of 'n' phases.

ii) The fuel fractions for the phase 'i' is denoted as W_i / W_{i-1} .

iii) Let W_0 be the weight at the start of the flight (say warm up) and W_n be the weight at the end of last phase (say landing). Then, W_n/W_0 is expressed as:

$$\frac{W_n}{W_0} = \frac{W_1}{W_0} \times \frac{W_2}{W_1} \times \dots \times \frac{W_{n-1}}{W_{n-2}} \times \frac{W_n}{W_{n-1}} \quad (3.26)$$

iv) The fuel fractions (W_i/W_{i-1}) for all phases are estimated and (W_n/W_0) is calculated from Eq.(3.26).

Subsequently, the fuel fraction (W_f/W_0) is deduced as:

$$\frac{W_f}{W_0} = K_{tf} \left(1 - \frac{W_n}{W_0} \right); \text{ where } K_{tf} \text{ is factor allowing for trapped fuel.} \quad (3.26a)$$

Fuel fraction for warm up, taxiing and take-off (W_1 / W_0)

From the various data analysis of different aircrafts, it was found that Fuel fraction for warm up, taxiing and take-off (W_1 / W_0) is given as,

For home built and single engine piston airplanes W_1/W_0 is 0.99. For twin engine turboprops, jet transports (both civil and military), flying boats and supersonic airplanes W_1/W_0 is 0.98. For military trainers and fighters W_1/W_0 is 0.97.

Fuel fraction for climb (W_2 / W_1)

From the various data analysis of different aircrafts, it was found that Fuel fraction for climb (W_2 / W_1) is given as,

The low speed airplanes including the twin-engine airplanes and flying boat cruise at moderate altitude (say 4 to 6 km) and hence (W_2 / W_1) is taken as 0.99. The military and civil transport jets cruise around 11 km altitude and W_2/W_1 is taken as 0.98. The fighter airplanes have very powerful engines and attain supersonic Mach number at the end of the climb. In this case, (W_2 / W_1) is between 0.9 to 0.96. Similarly, the supersonic transport airplanes which cruise at high altitudes (15 to 18 km), W_2/W_1 is around 0.9.

Fuel fraction during cruise – outline of approach

Equations (3.8) and (3.10) present the Breguet formulae for range of airplanes with engine-propeller combination and with jet engine respectively.

However, it may be pointed out that while deriving these formulae it is assumed that the following quantities remain constant during the flight.

- (a) Lift coefficient.
- (b) Specific fuel consumption (BSFC or TSFC).
- (c) Propeller efficiency for airplanes with engine-propeller combination and
- (d) Flight altitude.

Equations for range can also be derived when the flight velocity remains constant instead of the lift coefficient.

The derivation is as follows.

In a flight at velocity V (in m/s), the distance dR (in km) covered when a quantity of fuel dW_f (in N) is consumed in time dt , is given as :

$$dR = dW_f \times (\text{km} / \text{N of fuel}) \quad (3.27)$$

Now, in a time interval dt , the distance covered in km is $3.6 V dt$, where V is the flight speed in m/s; the factor 3.6 is to convert velocity to kmph. Note dt is in hrs.

Further, for jet engined airplanes the fuel consumed, dW_f , in the time interval ' dt ' is :

$$dW_f = \text{TSFC} \times T \times dt$$

where T is in N, TSFC is $\text{N}/\text{N-hr}$ or hr^{-1} and dt is in hrs.

$$\text{Hence, (km / N of fuel)} = \frac{3.6V \times dt}{\text{TFSC} \times T \times dt}$$

Substituting this in Eq. (3.27) gives :

$$dR = dW_f \frac{3.6V \times dt}{\text{TFSC} \times T \times dt} = \frac{3.6V}{\text{TFSC} \times T} dW_f \quad (3.28)$$

Noting that, $T = W \frac{C_D}{C_L} = \frac{W}{(L/D)}$ and $dW_f = -dW$, gives :

$$dR = \frac{-3.6 \times V \times (L/D)}{\text{TFSC} \times W} dW \quad (3.29)$$

Assuming V , TSFC and (L/D) to be constant and taking W_{i-1} and W_i as the weights of the airplane at the beginning and the end of the cruise, and integrating Eq.(3.29), yields :

$$R = \frac{-3.6 \times V \times (L/D)}{\text{TFSC}} \ln \left(\frac{W_{i-1}}{W_i} \right) \quad (3.30)$$

$$\text{Or } \frac{W_i}{W_{i-1}} = \exp \left\{ \frac{-R \times \text{TSFC}}{3.6 \times V \times (L/D)} \right\}; \quad V \text{ in m/s.} \quad (3.31)$$

For an airplane with engine-propeller combination, the fuel consumed in the time interval 'dt' is :

$$\text{BSFC} \times \text{BHP} \times dt = \text{BSFC} \times \frac{\text{THP}}{\eta_p} \times dt = \frac{\text{BSFC} \times T \times V \times dt}{\eta_p \times 1000}$$

$$\text{Hence, (km / N of fuel)} = \frac{3.6 \times V \times dt}{\text{BSFC} \times \frac{TV}{\eta_p \times 1000} \times dt}$$

Substituting this in Eq.(3.27) yields:

$$dR = \frac{3.6 \times V \times dt \times dW_f}{\text{BSFC} \times \frac{TV}{\eta_p \times 1000} \times dt} = \frac{3600 \times \eta_p}{\text{BSFC} \times T} dW_f \quad (3.32)$$

Noting that, $T = W \frac{C_D}{C_L} = \frac{W}{L/D}$ and $dW_f = -dW$ yields:

$$dR = \frac{-3600 \times \eta_p \times (L/D)}{\text{BSFC}} \frac{dW}{W} \quad (3.33)$$

Assuming η_p , BSFC and L/D to be constant and integrating Eq.(3.33) gives:

$$R = -\frac{3600 \times \eta_p}{\text{BSFC}} (L/D) \ln\left(\frac{W_i}{W_{i-1}}\right)$$

$$\text{Or } \frac{W_i}{W_{i-1}} = \exp\left\{\frac{-R \times \text{BSFC}}{3600\eta_p(L/D)}\right\} \quad (3.34)$$

i) While deriving Eq.(3.30) both V and C_L are assumed to be constant, during cruise. However, weight of the airplane decreases during the flight and to satisfy $L = W = (1/2)\rho V^2 S C_L$ the values of ρ should decrease as weight decreases. The consequence is, the altitude of the airplane should increase as the flight progresses. This is called 'Cruise climb'. However, the change in the altitude is small and the flight can be regarded as level flight.

ii) To evaluate the fuel fraction using Eq.(3.31) requires values of TSFC, V and (L/D) . When Eq.(3.34) is used, the values of BSFC, (L/D) and η_p are needed.

iii) The following may be pointed out.

(a) For airplanes with engine-propeller combination, Eq.(3.34) shows that the fuel required would be minimum when the flight takes place at a C_L corresponding to $(L/D)_{\max}$.

(b) For jet engined airplanes, Eq.(3.31) shows that for minimizing the fuel required, the product $V(C_L/C_D)$ should be maximum. Since, V is proportional to $1/(C_L^{1/2})$, the quantity (VC_L/C_D) is maximised when C_L corresponds to

$(C_L^{1/2}/C_D)_{\max}$. Assuming parabolic polar i.e. $C_D = C_{D0} + KC_L^2$, it is shown that the value of C_L corresponding to $(C_L^{1/2}/C_D)_{\max}$ is $\sqrt{C_{D0}/3K}$. The value of (L/D) for this value of C_L is $0.866 (L/D)_{\max}$.

Fuel fraction during loiter – outline of approach

Equations (3.9) and (3.11) present the Breguet formulae for endurance of airplanes with engine-propeller combination and with jet engine, respectively. As mentioned earlier, the derivations of these formulae assume that the following quantities remain constant during the flight.

- (a) Lift coefficient
- (b) Specific fuel consumption (BSFC or TSFC)
- (c) Propeller efficiency for airplanes with engine-propeller combination and
- (d) Flight altitude.

Equation for endurance can also be derived when the flight velocity remains constant instead of the lift coefficient.

In a flight at velocity V , the time elapse dE (in hr) when a quantity of fuel dW_f (in N) is consumed is given by :

$$dE = dW_f \times \left(\frac{\text{hr}}{N \text{ of fuel}} \right) = \left(\frac{dW_f}{N \text{ of fuel/hr.}} \right)$$

For a jet engined airplane, $(N \text{ of fuel/hr}) = \text{TSFC} \times T$

$$\text{Hence, } dE = \frac{dW_f}{\text{TSFC} \times T}$$

Noting that, $T = W(C_D/C_L) = W/(L/D)$ and $dW_f = -dW$ gives:

$$dE = -dW \left(\frac{(L/D)}{\text{TSFC} \times W} \right) \quad (3.35)$$

Let (a) (L/D) and TSFC be assumed to remain constant during the flight,

(b) W_{i-1} and W_i the weights of the airplane at the beginning and end of flight.

On integrating Eq.(3.35), gives

$$E = \left(\frac{L/D}{\text{TSFC}} \right) \ln \left(\frac{W_{i-1}}{W_i} \right) \quad (3.36)$$

$$\text{Or } \frac{W_i}{W_{i-1}} = \exp \left\{ \frac{-E \times \text{TSFC}}{(L/D)} \right\} \quad (3.37)$$

For an airplane with engine-propeller combination, the quantity $(N \text{ of fuel/hr})$ is :

$$(N \text{ of fuel/hr}) = \text{BSFC} \times \text{BHP} = \text{BSFC} \times \frac{T \times V}{1000 \times \eta_p}$$

$$\begin{aligned} \text{Consequently, } dE &= \frac{dW_f}{\text{BSFC} \times \frac{TV}{1000\eta_p}} = \frac{dW_f \times 1000 \times \eta_p}{\text{BSFC} \times W \times \frac{C_D}{C_L} \times V} \\ &= \frac{-1000 \times \eta_p \times (L/D) dW}{\text{BSFC} \times V \times W} \end{aligned} \quad (3.38)$$

Assuming η_p , BSFC , (L/D) and V to be constant during flight and integrating Eq.(3.38) yields:

$$E = \frac{-1000 \times \eta_p (L/D)}{\text{BSFC} \times V} \ln \left(\frac{W_i}{W_{i-1}} \right) \quad (3.39)$$

$$\text{Or } \frac{W_{i-1}}{W_i} = \exp \left\{ \frac{-E \times \text{BSFC} \times V}{1000 \times \eta_p \times (L/D)} \right\} \quad (3.40)$$

(i) As mentioned earlier, in a flight with both (L/D) and V as constant, the flight altitude of airplane would increase as the weight of airplane decreases due to consumption, of fuel. This is called cruise-climb. However, change in flight altitude is small and flight can be regarded as level flight.

(ii) To evaluate the fuel fraction for loiter of specified duration, the values of BSFC, V , η_p and (L/D) are required for airplanes with engine-propeller combination and those of TSFC and (L/D) for the jet airplanes.

(iii) Equation (3.37) shows that for a jet airplane the fuel required for a specified endurance, would be minimum when the flight takes place at C_L corresponding to $(L/D)_{\max}$.

Equation (3.40) shows that for an airplane with engine-propeller combination, the fuel required for given endurance would be minimum, when $V/(L/D)$ is minimum. Since, V is proportional to $1/(C_L^{1/2})$, this implies that $(C_D / C_L^{3/2})$ should be minimum or $(C_L^{3/2} / C_D)$ should be maximum, for fuel required to be minimum. For a parabolic polar ($C_D = C_{D0} + KC_L^2$), it can be shown that value of C_L corresponding to $(C_L^{3/2} / C_D)_{\max}$ is $(3C_{D0}/K)^{1/2}$. The value of (L/D) corresponding to this value or C_L is $0.866 (L/D)_{\max}$.

Estimation of $(L/D)_{\max}$ – outline of approach

$(L/D)_{\max}$ for a chosen type of airplane depends on the wetted aspect ratio (A_{wet}) defined as :

$$A_{\text{wet}} = \frac{b^2}{S_{\text{wet}}} \quad (3.41)$$

Where, b = wing span and S_{wet} = wetted area of the airplane. Further S_{wet} , for a chosen type of airplane, is a multiple of S the wing area.

However, keeping in view the need for drag polar for optimization of wing loading, the expressions for drag polar ($C_D = C_{D0} + KC_L^2$) are deduced which appear to be adequate at this stage of preliminary design. The general expressions for C_{D0} and K obtained general expression for C_{D0} and K for both subsonic and supersonic airplanes; here the attention is focussed on subsonic airplanes.

The following expressions for C_{D0} and K for subsonic airplanes with wings of moderate to high aspect ratio ($A > 5$).

$$C_{D0} = 0.005 \tau R_w T_f S^{-0.1} \left(1 - \frac{2C_{if}}{R_w} \right) \times \left[1 - 0.2M + 0.12 \left\{ \frac{M(\cos \Lambda_{1/4})^{1/2}}{A_f - (t/c)} \right\}^{20} \right] \quad (3.42)$$

$$K = \left\{ \frac{1}{\pi A} (1 + 0.12M^6) \right\} \left[1 + \frac{0.142 + f(\lambda) A \left(10 \frac{t}{c} \right)^{0.33}}{\left(\cos \Lambda_{1/4} \right)^2} \right] + \frac{0.1(3N_e + 1)}{(4 + A)^{0.8}} \quad (3.43)$$

where, A = wing aspect ratio

M = Mach number

S = wing area

t/c = wing thickness ratio

λ = taper ratio of wing

$\Lambda_{1/4}$ = quarter chord sweep of wing

N_e = number of engines, if any, located on top surface of wing

A_f = airfoil factor. A value of 0.93 is suggested for special airfoils and 0.75 for older (NACA) airfoils.

C_{if} = function of airfoil chord over which the flow is laminar.

$R_w = S_{wet} / S$

T_f = a factor which is unity for a very streamlined shape and takes into account the increase in C_D due to departure from streamlined shape.

τ = A factor which gives correction for wing thickness ratio and is given by :

$$\tau = \left[\left(\frac{R_w - 2}{R_w} \right) + \frac{1.9}{R_w} \left\{ 1 + 0.526 \left(\frac{t/c}{0.25} \right)^3 \right\} \right] \quad (3.44)$$

$f(\lambda)$ = factor which takes into account effect of wing taper ratio.

$$= 0.005 [1 + 1.5(\lambda - 0.6)^2] \quad (3.45)$$

Once C_{D0} and K are obtained, $(L/D)_{max}$ is given by :

$$(L/D)_{max} = \frac{1}{2\sqrt{C_{D0} K}} \quad (3.46)$$

Three typical cases viz. a high subsonic jet airplane, a turboprop airplane and a low speed piston-engined airplane are considered. Based on Eqs.(3.42) and (3.43) drag polars are deduced for these three cases. Suggestions are also given to obtain drag polars of similar airplanes.

Drag polar of typical high subsonic jet airplane

A typical high subsonic jet has the following features:

- (a) $M = 0.8$, (b) $A = 9$, (c) an advanced supercritical airfoil with t/c of 0.14 ,
 (d) taper ratio of 0.25, (e) sweep ($\Lambda_{1/4}$) of 30° , (f) $N_e = 0$, (g) due to high Reynolds number the flow can be treated as turbulent almost from the leading edge or $C_{if} = 0$.

Hence, in the present case, with the above chosen parameters, the following values are obtained.

$$(I) 1 - \frac{2C_{if}}{R_w} = 1.0 .$$

$$(II) A_f - (t/c) = 0.93 - 0.14 = 0.79 .$$

$$(III) \tau = \left(\frac{5.5-2}{5.5} \right) + \frac{1.9}{5.5} \left\{ 1 + 0.526 \left(\frac{0.14}{0.25} \right)^3 \right\} = 1.013 .$$

For this category of airplanes the effect of t/c on τ can be obtained by substituting different values of (t/c) in Eq.(3.44). The following values for τ are obtained.

t/c	0.1	0.14	0.18
τ	0.9926	1.013	1.049

$$(IV) f(\lambda) = 0.005 [1 + 1.5(0.25 - 0.6)^2] = 0.00592 .$$

$$(V) \left[\frac{M(\cos \Lambda_{1/4})^{1/2}}{A_f - (t/c)} \right]^{20} = \left[\frac{0.8 \times (0.866)^{1/2}}{0.93 - 0.14} \right]^{20} = 0.305 .$$

$$(VI) 1 - 0.2M + 0.12 \left[\frac{M(\cos \Lambda_{1/4})^{1/2}}{A_f - (t/c)} \right]^{20} = 1 - 0.2 \times 0.8 + 0.12 \times 0.305 = 0.8766 .$$

Consequently,

$$\begin{aligned} C_{D0} &= 0.005 \times \tau \times 5.5 \times 1.1 \times 1 \times 0.8766 S^{-0.1} \\ &= 0.02652 \tau S^{-0.1} \end{aligned} \quad (3.47)$$

The effect of swept angle on C_{D0} is of secondary nature. However, it is observed that C_{D0} should be reduced by about 0.4% for each increase in sweep by 1° . The effect of aspect ratio on C_{D0} is negligible.

Thus, for $\Lambda_{\frac{1}{4}} = 30^\circ$, $A = 9$ and $t/c = 0.14$

$$C_{D0} = 0.02686 S^{-0.1} \quad (3.48)$$

From Eq.(3.48) the variation of C_{D0} with S is as follows.

$S(m^2)$	50	100	500
C_{D0}	0.0182	0.0169	0.0144

EXAMPLE:

For Boeing 747 with $S = 511 \text{ m}^2$, and $\Lambda_{1/4}=38.5$ these parameters would give C_{D0} of 0.014. This value is close to the actual value for the airplane.

Value of K :

The terms in Eq.(3.43) are now evaluated for typical high subsonic jet airplane with features mentioned under items (a) to (g) at the beginning of this subsection.

The following quantities are obtained.

$$(I) 1+0.12 M^6 = 1 + 0.12 (0.80)^6 = 1.0315$$

$$(II) \frac{1+0.142+f(\lambda)A\left(10\frac{t}{c}\right)^{0.33}}{\cos^2 \Lambda_{1/4}} = 1 + \frac{0.142+0.0592 \times 9 \times (1.4)^{0.33}}{\cos^2 30^\circ}$$

$$= 1 + \frac{0.2015}{\cos^2 30^\circ} = 1.2687$$

$$(III) \frac{0.1(3N_e+1)}{(4+A)^{0.8}} = \frac{0.1(0+1)}{(4+9)^{0.8}} = 0.0128$$

Hence, Eq.(3.43) yields:

$$K = \frac{1}{\pi \times 9} \{1.0315 \times (1.2678 + 0.0128)\} = 0.0468$$

$$\text{Expressing } K = \frac{1}{\pi A e}, \text{ gives } e = 0.757$$

NOTE:

(i) Angle of sweep does have significant effect on K . For $M = 0.8$, $t/c = 0.14$, $\lambda = 0.25$, $N_e = 0$ and $C_{if} = 0$, Eq.(3.43) gives:

$$K = \frac{1.0315}{\pi A} \left\{ 1 + \frac{0.2015}{\cos^2 \Lambda_{1/4}} + 0.0128 \right\} = \frac{1}{\pi A} \left\{ 1.0447 + \frac{0.2078}{\cos^2 \Lambda_{1/4}} \right\} \quad (3.49)$$

For an airplane with $S = 100 \text{ m}^2$, $\Lambda_{1/4} = 30^\circ$, Eqs.(3.48) and (3.49) give the following drag polar.

$$C_D = 0.0169 + 0.0468 C_L^2$$

$$\text{Hence, } (L/D)_{\max} = \frac{1}{2\sqrt{C_{D0}K}} = \frac{1}{\sqrt{0.0169 \times 0.0468}} = 17.8$$

i) Boeing 787-Dreamliner being produced by Boeing has very smooth surface, $(t/c)_{\text{average}} = 11\%$, $\Lambda_{1/4} = 32^\circ$, $S = 331 \text{ m}^2$ and aspect ratio of 10.4 with winglets at wing tips. It is estimated to have a C_{D0} of 0.0128 and K of 0.04 resulting in $(L/D)_{\max}$ of 22.

It may be added that the effect of winglets on reducing induced drag can be estimated approximately by adding half the height of winglet to the wingspan

Drag polar of a typical turboprop airplane.

Typical values of the parameters, which influence the drag polar of such airplanes, could be (a) $A = 12$, (b) $\lambda = 0.4$, (c) $\Lambda_{1/4} = 0$, (d) $t/c = 18\%$ (conventional airfoil), (e) $M = 0.5$, and (f) $C_{if} = 0$.

The values of R_w , T_f and A_f for this type of airplanes are:

$$R_w = 5, T_f = 1.4, A_f = 0.75,$$

The other quantities in Eq. (3.42) are evaluated below.

$$(I) \left(1 - \frac{2C_{it}}{R_w} \right) = 1.0$$

$$(II) \tau = \left[\left(\frac{R_w - 2}{R_w} \right) + \frac{1.9}{R_w} \left\{ 1 + 0.526 \left(\frac{t/c}{0.25} \right)^3 \right\} \right]$$

$$= \left(\frac{5-2}{5} \right) + \frac{1.9}{5} \left\{ 1 + 0.526 \left(\frac{0.18}{0.25} \right)^3 \right\} = 1.0546$$

$$(III) 1 - 0.2M + 0.12 \left[\frac{M \times \cos^{1/2} \Lambda_{1/4}}{A_f - (t/c)} \right]^{20}$$

$$= 1 - 0.2 \times 0.5 + 0.12 \left\{ \frac{0.5 \times 1}{0.75 - 0.18} \right\}^{20} = 0.9087$$

Consequently, for this category of airplanes,

$$C_{D0} = 0.005 \times 1.0546 \times 5 \times 1.4 \times 1 \times 0.9087 S^{-0.1}$$

$$= 0.03354 S^{-0.1}$$

(3.50)

Example:

Drag polar of Fokker F-27. This airplane has $S = 70 \text{ m}^2$ and $A = 12$. From the figures in the aforesaid reference, it is observed that for this airplane $C_{D0} = 0.022$ and $(L/D)_{\max}$ of 17.6. These two values indicate a value of 0.0359 for K .

From Eq.(3.50) a value of $S = 70 \text{ m}^2$ would give C_{D0} of 0.02192, which is almost same as the actual value of 0.022.

Further in this case,

$$f(\lambda) = 0.005 \{1 + 1.5(0.4 - 0.6)^2\} = 0.0053$$

$$\text{Hence, } f(\lambda) \times A \times (10t/c)^{0.33} = 0.0053 \times 12 \times (10 \times 0.18)^{0.33} = 0.07721$$

Consequently,

$$1 + \frac{0.142 + f(\lambda)A(10t/c)^{0.33}}{\cos^2 \Lambda_{1/4}} = 1 + \frac{0.142 + 0.07721}{1} = 1.2192$$

$$\text{Further, } \frac{0.1(3N_e + 1)}{(4 + A)^{0.8}} = \frac{0.1(0 + 1)}{(4 + 12)^{0.8}} = 0.01088 \text{ and}$$

$$1 + 0.12 M^6 = 1 + 0.12(0.5)^6 = 1.002$$

From Eq.(3.43), the value of K for this category of airplanes, is :

$$\begin{aligned} K &= \frac{1}{\pi \times A} [1.002 \{1.2192 + 0.01088\}] \\ &= \frac{1.2325}{\pi \times A}; \end{aligned} \quad (3.51)$$

with $A = 12$, $K = 0.0327$.

Drag polar of a typical low subsonic general aviation airplane with fixed landing gear

In this case the typical values of airplane parameters can be taken as:

$$M = 0.2, A = 6, \lambda = 1, \Lambda_{1/4} = 0, t/c = 0.15 \text{ (conventional airfoil), } C_{lf} = 0$$

$$R_w = 4, T_f = 2.0, A_f = 0.75$$

In this case the other values would be:

$$\left(1 - \frac{2C_{lf}}{R_w}\right) = 1.0$$

$$1 - 0.2M + 0.12 \left\{ \frac{M(\cos \Lambda_{1/4})^{1/2}}{A_f - (t/c)} \right\}^{20}$$

$$= 1 - 0.2 \times 0.2 + 0.12 \left\{ \frac{0.2 \times 1}{0.75 - 0.15} \right\}^{20} = 0.96$$

$$\tau = \left[\frac{4-2}{4} + \frac{1.9}{4} \left\{ 1 + 0.526 \left(\frac{0.15}{0.25} \right)^3 \right\} \right] = 1.029$$

Consequently,

$$C_{D0} = 0.005 \times 1 \times 1.029 \times 0.96 \times 4 \times 2S^{-0.1} = 0.03951S^{-0.1} \quad (3.54)$$

For a typical value of $S = 15 \text{ m}^2$,

$$C_{D0} = 0.03951 \times 15^{-0.1} = 0.0301$$

Estimation of K

In this case the following values are obtained.

$$1 + 0.12 M^6 = 1$$

$$f(\lambda) = 0.005 \left[1 + 1.5(1 - 0.6)^2 \right] = 0.0062,$$

$$1 + \frac{0.142 + f(\lambda) A \left(10 \frac{t}{c} \right)^{0.33}}{(\cos \Lambda_{1/4})^2}$$

$$= 1 + \frac{0.142 + 0.0062 \times 6 \times (10 \times 0.15)^{0.33}}{1} = 1.1845, \text{ and}$$

$$\frac{0.1(3N_e + 1)}{(4 + A)^{0.8}} = \frac{0.1 \times 1}{(4 + 6)^{0.8}} = 0.01585$$

$$\text{Hence, } K = \frac{1}{\pi A} \left[1 \times \{1.1845 + 0.01585\} \right] = \frac{1.2003}{\pi A} \text{ or } e = 0.833$$

$$K = \frac{1.333}{\pi A} \quad (3.55)$$

Thus, typical drag polar of this category of airplanes can be written as:

$$C_D = 0.03951S^{-0.1} + \frac{1.333}{\pi A} C_L^2 \quad (3.56)$$

For $A = 6$ and $S = 15 \text{ m}^2$, Eq.(3.56) gives :

$$\text{From this } C_D = 0.0301 + 0.0708 C_L^2$$

These values of C_{D0} and K would give:

$$(L/D)_{\max} = \frac{1}{2\sqrt{0.0301 \times 0.0708}} = 10.83$$

The value of C_{D0} could be lower by about 10% for airplanes made of FRP with very smooth surface.

General remarks on drag polar :

At this stage of preliminary design, from data collection, the first estimates of the wing area (S), the aspect ratio (A) and wing quarter chord sweep ($\Lambda_{1/4}$) are known. Based on this information C_{D0} and K can be obtained from the following formulae.

(A) High subsonic speed jet airplanes:

$$C_D = 0.02686 S^{-0.1} + \frac{1}{\pi A} \left\{ 1.0447 + \frac{0.2078}{\cos^2 \Lambda_{1/4}} \right\} C_L^2 \quad (3.57)$$

The value of 0.02686 in Eq.(3.56) is for $\Lambda_{1/4} = 30^\circ$. For $25^\circ \leq \Lambda_{1/4} \leq 35^\circ$ decrease this value by 0.4% for each 1° increase in $\Lambda_{1/4}$ or increase it by 0.4% for each 1° decrease in $\Lambda_{1/4}$.

(B) For airplanes with turboprop engine:

$$C_D = 0.03354S^{-0.1} + \frac{1.356}{\pi A} C_L^2 \quad (3.58)$$

This expression in Eq.(3.58) is for fuselage shape typical of passenger airplanes. For cargo airplanes with rectangular fuselage, increase C_{D0} by about 20% and K by about 5%. The basis for increasing C_{D0} is that the contribution of fuselage to

C_{D0} is about 40% in passenger airplanes and this contribution would go up by about 50% for a rectangular fuselage. The change in the value of 'K' due to the change in fuselage cross section is small.

C) Airplanes with piston engine:

$$C_D = 0.03951S^{-0.1} + \frac{1.333}{\pi A} C_L^2 \quad (3.59)$$

Using the above expressions for C_{DO} & K the drag polar is obtained. Then the value of $(L/D)_{max}$, which is needed for obtaining the fuel fraction is given by Eq.(3.46) as :

$$(L/D)_{max} = \frac{1}{2\sqrt{C_{DO} K}}$$

Introduction to estimation of BSFC, η_p and TSFC

As mentioned earlier, here the attention is confined to subsonic airplanes. The piston engines are used in low subsonic airplanes ($M \leq 0.3$), the turboprop engines are used in the range of flight Mach numbers from 0.4 to 0.7 and the turbofan engines are used in the flight Mach number range of 0.7 to about 0.9. The details regarding the propellers and the engines are given in chapter 4. Here, the values of propeller efficiency and BSFC/TSFC are presented. These can be used as guidelines at this stage of design process.

BSFC and η_p of typical piston engine airplanes

The propeller efficiency (η_p) depends on the pitch setting (β),

engine r.p.m, power output and the advance ratio ($J = V/nd$, where V is the flight velocity in m/s, n is the revolutions per second of the propeller and d is the propeller diameter). These airplanes may have (i) a fixed pitch propeller whose pitch setting could generally be chosen to give best efficiency in cruise or (ii) a propeller with two or three pitch setting and would give good efficiency both during take-off and cruise.

The BSFC of a piston engine depends on the r.p.m and power output. Generally the BSFC is higher at lower power settings. The power setting and flight velocity are lower in loiter than in cruise. At this stage of design, the following values of η_p and BSFC are suggested as ballpark values for calculations of fuel fraction.

(a)Fixed pitch propeller :

$$\text{Loiter: } \eta_p \approx 0.6, \text{BSFC} \approx 3.0 \text{ N/kW - hr} \quad (3.60)$$

$$\text{Cruise: } \eta_p \approx 0.8, \text{BSFC} \approx 2.7 \text{ N/kW - hr} \quad (3.61)$$

(b)Variable pitch propeller :

$$\text{Loiter: } \eta_p \approx 0.7, \text{BSFC} \approx 3.0 \text{ N/kW - hr} \quad (3.62)$$

$$\text{Cruise: } \eta_p \approx 0.8, \text{BSFC} \approx 2.7 \text{ N/kW - hr} \quad (3.63)$$

BSFC and η_p of a typical turboprop powered airplanes

Keeping these aspects in mind the following values of η_p and BSFC are suggested as ballpark values for calculation of fuel fraction at this stage of design.

$$\text{Loiter: } (M \approx 0.3 \text{ at s.l.}): \eta_p \approx 0.75, \text{BSFC} \approx 2.85 \text{ N/kW-hr} \quad (3.64)$$

$$\text{Cruise: } (M \approx 0.5 \text{ at } h \approx 5 \text{ km}): \eta_p \approx 0.85, \text{BSFC} \approx 2.7 \text{ N/kW-hr} \quad (3.65)$$

TSFC of a typical turbofan engine:

The turbofan engines have lower TSFC at lower altitudes and lower Mach numbers. Besides, the flight altitude and Mach number, the TSFC also depends on the bypass ratio (μ) of the engine. This ratio is the ratio of the air mass that passes through the bypass duct to the mass of air that passes through the gas generator.

$$\text{TSFC} = c \{1 - 0.15 \mu^{0.65}\} [1 + 0.28 (1 + 0.063 \mu^2) M] \sigma^{0.08} \quad (3.66)$$

where, $c = 0.7$, μ = bypass ratio, σ = density ratio = $\rho/\rho_{\text{sealevel}}$.

Note : Equation (3.66) is valid for $h < 11$ km. At $h > 11$ km TSFC is same as that at $h = 11$ km.

Taking typical values of $M = 0.8$ and $h = 11$ km, the following variation of TSFC with by-pass ratio is obtained.

Bypass ratio (μ)	5	8	10
TSFC (hr^{-1})	0.574	0.569	0.552

Typical variation of TSFC with bypass ratio μ ; $h = 11$ km, $M = 0.8$.

Consider loiter at sea level and $M = 0.3$, Then Eq.(3.66) gives the following variation of TSFC with bypass ratio.

Bypass ratio (μ)	5	8	10
TSFC (hr^{-1})	0.488	0.419	0.373

Typical variation of TSFC with bypass ratio (μ); $h = \text{sea level}$, $M = 0.3$.

Fuel fraction for descent, landing and taxiing:

The homebuilt, low speed single engine and agricultural airplanes generally fly close to the ground and the value of fuel fraction, for this phase of flight, of 0.99 is suggested. For other types of airplanes, except supersonic cruise airplane, the suggested value is 0.98. For supersonic cruise airplanes, the descent phase would be longer and consequently the suggested value is 0.937.

Fuel fraction for the mission:

After calculating the fuel fractions in various phases of the mission, the weight of the airplane at the end of the mission is given by:

$$\frac{W_n}{W_0} = \frac{W_1}{W_0} \times \frac{W_2}{W_1} \times \dots \times \frac{W_{n-1}}{W_{n-2}} \times \frac{W_n}{W_{n-1}} \quad (3.67)$$

Consequently, the mission fuel fraction is :

$$1 - (W_n/W_0) \quad (3.68)$$

Generally an allowance of 6 % is provided for trapped fuel. Thus,

$$\frac{W_f}{W_0} = 1.06 \left[1 - \frac{W_n}{W_0} \right] \quad (3.69)$$

WING DESIGN

In the context of wing design the following aspects need consideration.

- I) Wing area (S): This is calculated from the wing loading and gross weight which have been already decided i.e. $S = W / (W / S)$
- II) Location of the wing on fuselage: High-, low- or mid-wing
- III) Aerofoil: Thickness ratio, camber and shape
- IV) Sweep (Λ): Whether swept forward, swept backward, angle of sweep, cranked wing, variable sweep.
- V) Aspect ratio (A): High or low, winglets
- VI) Taper ratio (λ): Straight taper or variable taper.
- VII) Twist (ϵ): Amount and distribution
- VIII) Wing incidence or setting (i_w)
- IX) High lift devices: Type of flaps and slats; values of C_{Lmax} , S_{flap}/S
- X) Ailerons and spoilers: Values of $S_{aileron}/S$; $S_{spoiler}/S$
- XI) Leading edge strakes if any.
- XII) Dihedral angle (Γ).
- XIII) Other aspects: Variable camber, planform tailoring, area ruling, braced wing, aerodynamic coupling (intentionally adding a coupling lifting surface like canard).

The above parameters are dealt with in the following order.

- i) Airfoil selection
- ii) Aspect ratio
- iii) Sweep
- iv) Taper ratio
- v) Twist
- vi) Incidence
- vii) Dihedral
- viii) Vertical location
- ix) Wing tips
- x) Other aspects

Airfoil selection

Large airplane companies like Boeing and Airbus may design their own airfoils. However, during the preliminary design stage, the usual practice is to choose the airfoil from the large number of airfoils whose geometric and aerodynamic characteristics are available in the aeronautical literature. To enable such a selection it is helpful to know the aerodynamic and geometrical characteristics of airfoils and their nomenclature. These topics are covered in the next three subsections.

Presentation of aerodynamic characteristics of airfoils

Figure below shows typical experimental characteristics of an aerofoil. The features of the three plots in this figure can be briefly described as follows.

(I) Lift coefficient (C_L) vs angle of attack (α). This curve, shown in Fig. below, has four important features viz. (a) angle of zero lift (α_{0l}), (b) slope of the lift curve denoted by $dC_L / d\alpha$ or a_0 or $C_{L\alpha}$, (c) maximum lift coefficient (C_{Lmax}) and (d) angle of attack (α_{stall}) corresponding to C_{Lmax} .

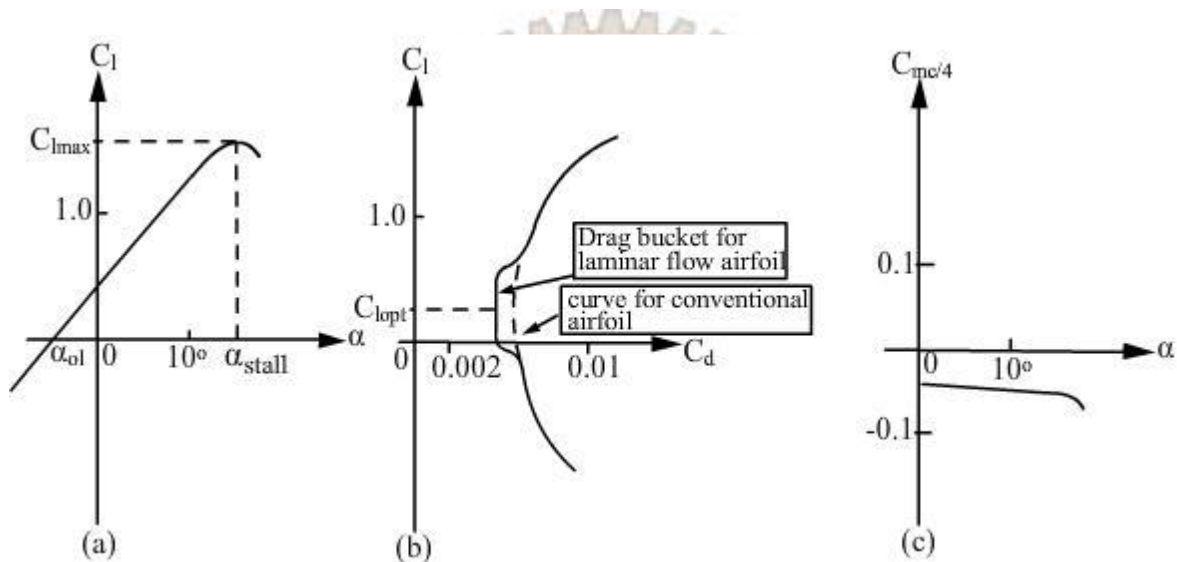


Fig 5.1a Aerodynamic characteristics of an airfoil

(II) Drag coefficient (C_d) vs C_l . This curve, shown in Fig.5.1b, has two important features viz. (a) minimum drag coefficient (C_{dmin}) and (b) lift coefficient (C_{lopt}) corresponding to C_{dmin} . In some airfoils, called laminar flow airfoils or low-drag airfoils, the minimum drag coefficient extends over a range of lift coefficients (Fig.5.1b). This feature is called 'Drag bucket'. The extent of the drag bucket and the lift coefficient at the middle of this region are also characteristic features of the airfoil. It may be added that the camber decides C_{lopt} and thickness ratio decides the extent of the drag bucket.

(III) Pitching moment coefficient about quarter-chord $C_{mc/4}$ vs α . This curve is shown in Fig.5.1c. Sometimes this curve is also plotted as $C_{mc/4}$ vs C_l . From this curve, the location of the aerodynamic center (a.c.) and the moment about it (C_{mac}) can be worked out. It may be recalled that a.c. is the point on the chord about which the moment coefficient is independent of C_l .

(IV) Stall pattern : Variation of the lift coefficient with angle of attack near the stall is an indication of the stall pattern. A gradual pattern as shown in Fig.5.1a is a desirable feature. Some airfoils display abrupt decrease in C_l after stall. This behaviour is undesirable as pilot does not get adequate warning regarding impending loss of lift. Airfoils with thickness ratio (t/c) between 6 – 10% generally display abrupt stall while those with t/c more than 14% display a gradual stall. It may be added that the stall patterns on the wing and on the airfoil are directly related only for high aspect ratio ($A > 6$) unswept wings. For low aspect ratio highly swept wings three-dimensional effects may dominate.

Geometrical characteristics of airfoils

To describe the geometrical characteristics of airfoils, the procedure given in chapter 6 of Ref.5.1 is followed. In this procedure, the camber line or the mean line is the basic line for definition of the aerofoil shape (Fig.5.2a). The line joining the extremities of the camber line is the chord. The leading and trailing edges are defined as the forward and rearward extremities, respectively, of the mean line.

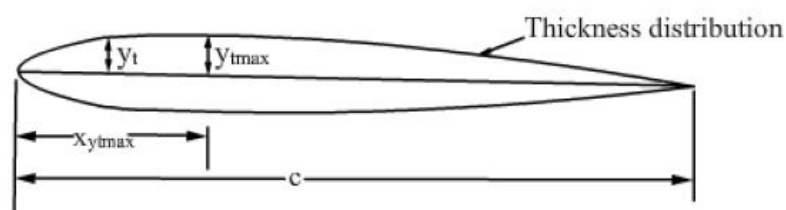
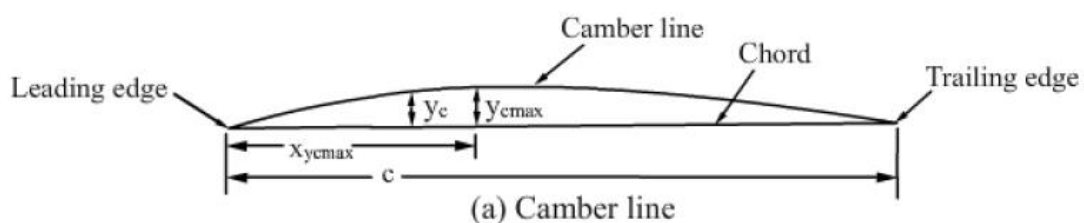
Various camber line shapes have been suggested and they characterize various families of airfoils. The maximum camber as a fraction of the chord length (y_{cmax}/c) and its location as a fraction of chord (x_{ycmax}/c) are the important parameters of the camber line.

Various thickness distributions have been suggested and they characterize different families of airfoils Fig.5.2b. The maximum ordinate of the thickness distribution as fraction of chord (y_{tmax}/c) and its location as fraction of chord (x_{ytmax}/c) are the important parameters of the thickness distribution.

Airfoil shape and ordinates

The aerofoil shape (Fig.5.2c) is obtained by combining the camber line and the thickness distribution in the following manner.

- a) Draw the camber line shape and draw lines perpendicular to it at various locations along the chord (Fig.5.2c).
- b) Lay off the thickness distribution along the lines drawn perpendicular to the mean line (Fig.5.2c).
- c) The coordinates of the upper surface (x_u, y_u) and lower surface (x_l, y_l) of the airfoil are given by the four equations presented in Eq.(5.1) :



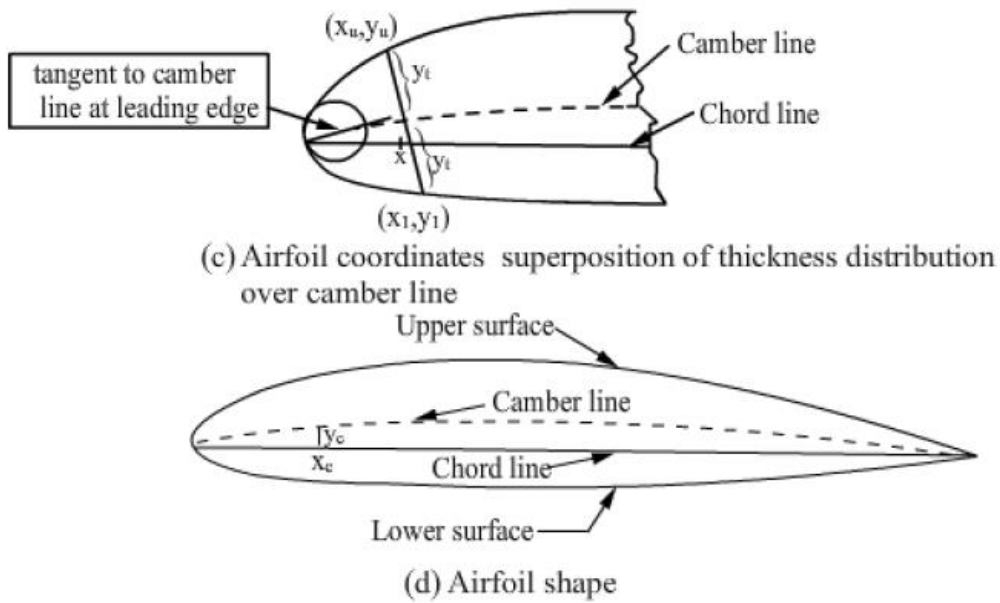


Fig.5.2 Airfoil geometry

$$\left. \begin{aligned} x_u &= x - y_t \sin\theta \\ y_u &= y_c + y_t \cos\theta \\ x_l &= x + y_t \sin\theta \\ y_l &= y_c - y_t \cos\theta \end{aligned} \right\} \text{-----} \quad (5.1)$$

where y_c and y_t are the ordinates, at location x , of the camber line and the thickness distribution respectively; $\tan \theta$ is the slope of the camber line at location x (see also Fig.5.2c and d).

d)The leading edge radius is also prescribed for the aerofoil. The center of the leading edge radius is located along the tangent to the mean line at the leading edge (Fig.5.2c).

e)Depending on the thickness distribution, the trailing edge angle may be zero or have a finite value. In some cases, thickness may be non-zero at the trailing edge.

Airfoil nomenclature/designation

Early airfoils were designed by trial and error. Royal Aircraft Establishment (RAE), UK and Gottingen laboratory of the German establishment which is now called DLR (Deutsches Zentrum für Luft-und Raumfahrt – German Centre for Aviation and Space Flight) were the pioneers in airfoil design. Clark Y airfoil

shown in Fig.5.3a is an example of a 12% thick airfoil with almost flat bottom surface which has been used on propeller blades.

Taking advantage of the developments in airfoil theory and boundary layer theory, NACA (National Advisory Committee for Aeronautics) of USA systematically designed and tested a large number of airfoils in 1930's. These are designated as NACA airfoils. In 1958 NACA was superseded by NASA (National Aeronautic and Space Administration). This organization has developed airfoils for special purposes. These are designated as NASA airfoils.

The NACA 4 Digit Series

- ▶ The NACA four-digit wing sections define the profile by:
- ▶ One digit describing maximum camber as percentage of the chord.
- ▶ One digit describing the distance of maximum camber from the airfoil leading edge in tens of percents of the chord.
- ▶ Two digits describing maximum thickness of the airfoil as percent of the chord.
- ▶ For example, the NACA 2412 airfoil has a maximum camber of 2% located 40% (0.4 chords) from the leading edge with a maximum thickness of 12% of the chord. Four-digit series airfoils by default have maximum thickness at 30% of the chord (0.3 chords) from the leading edge.

The NACA 0015 airfoil is symmetrical, the 00 indicating that it has no camber. The 15 indicates that the airfoil has a 15% thickness to chord length ratio: it is 15% as thick as it is long.

The NACA 5 Digit Series

- ▶ The NACA five-digit series describes more complex airfoil shapes:
- ▶ The first digit, when multiplied by 0.15, gives the designed coefficient of lift (C_L).
- ▶ Second and third digits, when divided by 2, give p , the distance of maximum camber from the leading edge (as per cent of chord).
- ▶ Fourth and fifth digits give the maximum thickness of the airfoil (as per cent of the chord).
- ▶ For example, the NACA 12018 airfoil would give an airfoil with maximum thickness of 18% chord, maximum camber located at 10% chord, with a lift coefficient of 0.15

The NACA 6 Digit Series

- ▶ 6 - Stands for the family number.
- ▶ 3 - Stands for the chord-wise position of the minimum pressure in tenths, which is 0.3 or 30% for this example.
- ▶ 2 - Stands for the lift coefficient range in tenths above and below the design lift coefficient where a favourable pressure gradient exists on both surfaces of the wing, which for this example is a lift coefficient range of 0.2 - 0.6.
- ▶ 4 - Stands for the design lift coefficient in tenths, which is 0.4 for this example.
- ▶ 30 - Stands for the maximum section thickness as a percentage of the chord length.

The Lift and Drag of Wings

The study of airfoils in Chapter 3 gave insight into how wings generate lift, but it did not tell the whole story. The flow over a wing near the wingtips is very different from the two-dimensional flow around an airfoil. The differences have profound effects on the lift and drag generated by a wing. Understanding these effects is crucial to the aircraft designer who must shape an aircraft's wing to optimize its performance.

Whole Aircraft Lift Curve

Other components besides the wing contribute to an aircraft's lift. The lift contributions of the aircraft's fuselage, control surfaces, high-lift devices, strakes, etc. must all be considered in order to accurately predict an aircraft's lifting capability. The aircraft's maximum lift coefficient is one of the governing factors in an aircraft's instantaneous turn capability, landing speed and distance, and takeoff speed and distance.

Whole Aircraft Drag Polar

The drag of all aircraft components must also be included when estimating whole aircraft drag. The variation of an aircraft's drag coefficient with its lift coefficient is called the aircraft's **drag polar**. The drag polar is the key information about an aircraft needed to estimate most types of aircraft performance. Aircraft maximum speed, rate and angle of climb, range, and endurance depend so heavily on an aircraft's drag polar that a 1% change in drag can make a huge difference in a jet fighter's combat effectiveness or an airliner's profit potential.

4.2 WINGS

The Language

Figure 4.1 illustrates a view of a wing planform with some of the important dimensions, angles and parameters used to describe the shape of an aircraft wing. The wing span, b , is measured from **wing tip** to wing tip. The symbol c is used for the chord length of an airfoil at any point along the wing span. The subscript r indicates the chord length at the wing **root** or the aircraft centerline. The subscript t denotes the wing tip chord. The overbar denotes an average value of chord length for the entire wing. The symbol AR is used for a parameter called **aspect ratio**. Aspect ratio indicates how short and stubby or long and skinny the wing is. The symbol Λ is used for wing **sweep angle** with the subscript LE denoting the wing leading edge. The subscript 25 denotes the line connecting the 25% chord positions on each airfoil of the wing. The symbol τ is used for the wing **taper ratio**, or ratio of tip chord to root chord.

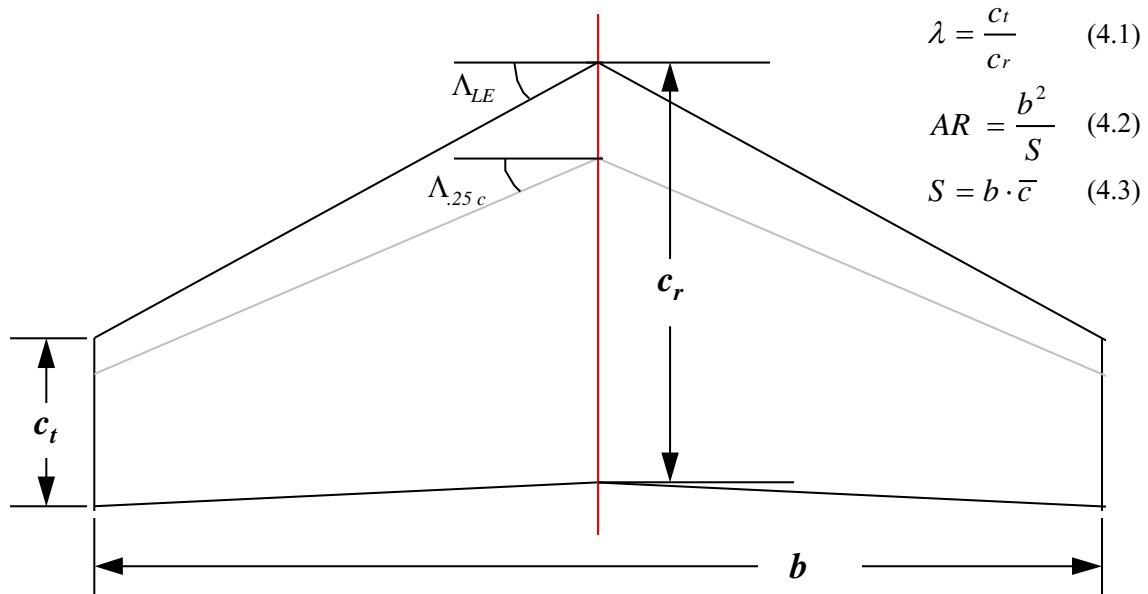


Figure 4.1 Finite Wing Geometry Definitions

Figure 4.2 shows a side view of the wing to illustrate the **angle of twist**. Wings which are twisted so that the wing tip airfoil is at a lower angle of attack than the wing root airfoil are said to have **washout**. Wing twist in the opposite sense from washout is **washin**. Wing twist of this sort is also called **geometric twist**. An effective twist of the wing can also be achieved by changing the airfoil shape along the wing span. If the airfoil at the wingtip has less camber than the airfoil at the root, this has much the same affect on the wing lift as if the airfoils were the same but the wingtip airfoil was at a lower angle of attack than the root. Changing airfoils along the wing span in this way is called **aerodynamic twist**.

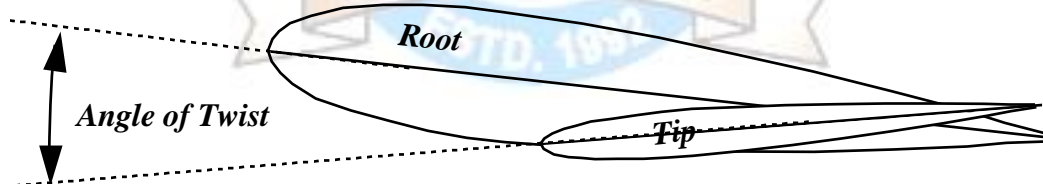


Figure 4.2 Wing Twist

Wingtip Vortices

The flow around a wing section which spans the test section of a wind tunnel approximates the flow around a wing with an infinite span, no twist, and a constant chord length along its span. In Chapter 3, this type of flow was labeled two-dimensional, because flow properties did not vary in the direction. The flowfield around a **finite wing**, or wing with a finite span is not two-dimensional. The majority of differences between the flow around a finite wing and that around an infinite wing result from flow phenomena which occur at the wingtips. Figure 4.3 shows a front view of the flowfield around a finite wing. Note that the differences between the pressures above and below the wing which produce lift also produce a strong flow around the wing tip. The arrows in Figure 4.3 are intended to illustrate a front view of flow streamlines in the plane of the 50% chord point on the wing.

The lengths of the tails of the arrows do not indicate the magnitude of the velocity vectors. Of course, the actual magnitudes of the velocity vectors must be such that there is no flow through the surface of the wing.

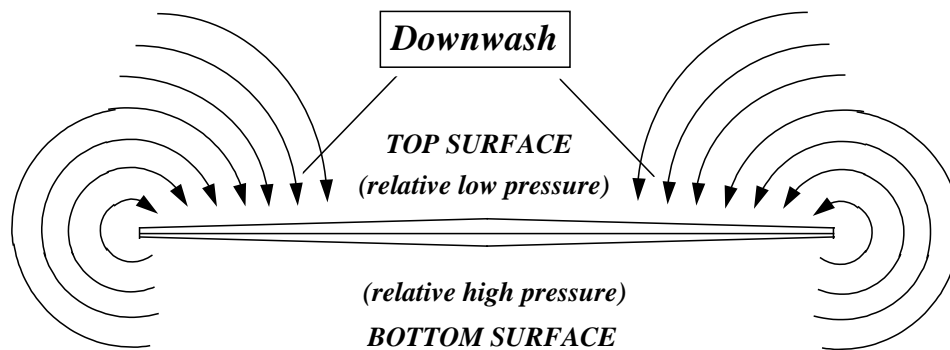


Figure 4.3 Front View of Wing with Flow around the Wing Tips

As shown in Figure 4.4, these circular flow patterns around the wing tips become concentrated into very strong tornado-like swirling flows known as **wingtip vortices** or **trailing vortices**. The trailing vortices generated by large aircraft persist for many miles behind them and can pose serious hazards to smaller aircraft which encounter them. Air traffic controllers must allow sufficient spacing between aircraft so that the action of air viscosity and turbulence can dissipate a preceding plane's trailing vortices before the arrival of the next one. This spacing requirement to allow vortex dissipation is the limiting factor on traffic density at most commercial airports.

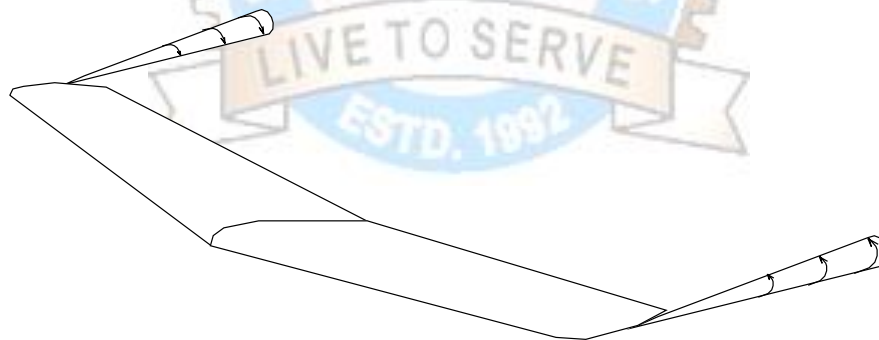


Figure 4.4 Trailing Vortices

Downwash

Also note in Figure 4.3 that the circular flow pattern around the wingtips results in a downward component to the flow over the wing. This downward flow component is called **downwash**. Figure 4.5 shows that downwash adds vectorially to the freestream velocity to change the direction of the flow velocity. Note that the resulting total velocity vector still results in flow parallel to the wing surface, but the orientation of the effective free stream velocity direction relative to the airfoil is altered.

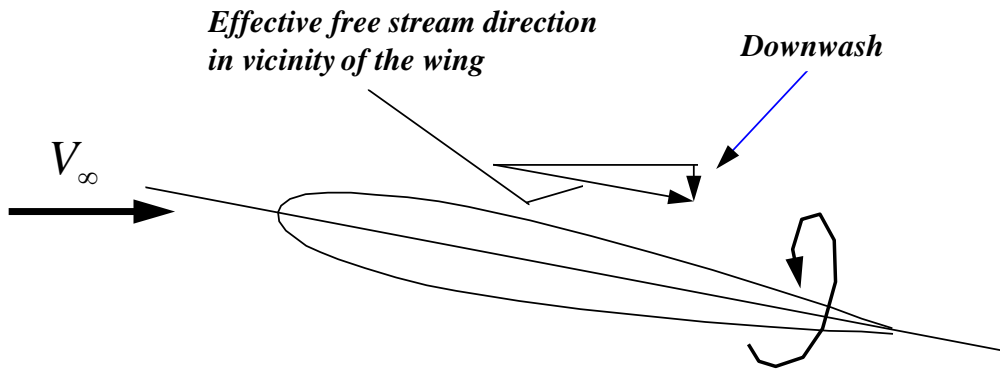


Figure 4.5 Downwash

The change in flow direction due to downwash is called the **downwash angle**, and is given the symbol ϵ . The angle between the airfoil chord line and the local flow velocity vector is called the effective angle of attack, α_{eff} . Each individual wing section's lift, drag, and angle of attack vary with the airfoil's orientation to this local flow direction, but the whole wing's lift, drag and angle of attack must still be defined relative to the free stream direction. Figure 4.6 reveals that, as a consequence of the change in effective flow direction caused by the downwash, the effective angle of attack of the airfoil is reduced, and the lift generated by each airfoil has a component in the wing's drag direction. This component of lift in the drag direction is called **induced drag**. The reduction in effective angle of attack due to the downwash causes the wing to produce less lift than it would if there were no downwash.

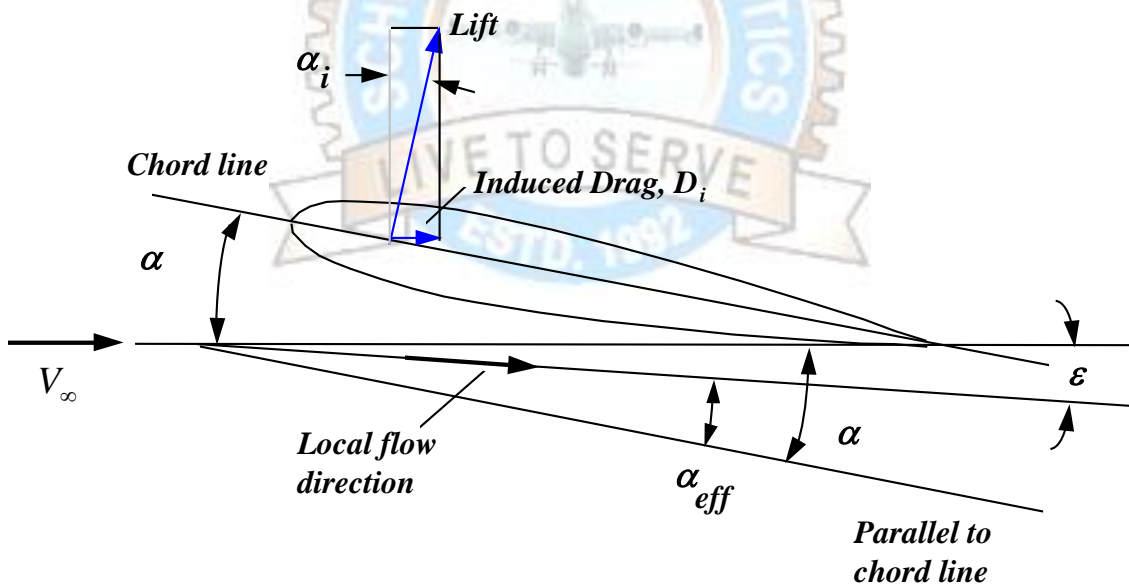


Figure 4.6 Downwash Angle and Induced Drag

Figure 4.7 illustrates lift coefficient curves for an airfoil and for a finite wing with the same airfoil section shape. Note that c_l denotes two-dimensional airfoil lift coefficient while:

$$C_L = L / qS \quad (4.4)$$

is used for the three-dimensional finite wing lift coefficient. This same convention will be followed for c_d and:

$$C_D = D / qS \quad (4.5)$$

The reduction in effective angle of attack due to downwash decreases lift at any given α and delays stall to higher values of α . As in Chapter 3, slopes of the lift curves are defined as:

$$c_{l_\alpha} \equiv \frac{\partial c_l}{\partial \alpha} \quad \text{and} \quad C_{L_\alpha} \equiv \frac{\partial C_L}{\partial \alpha} \quad (4.6)$$

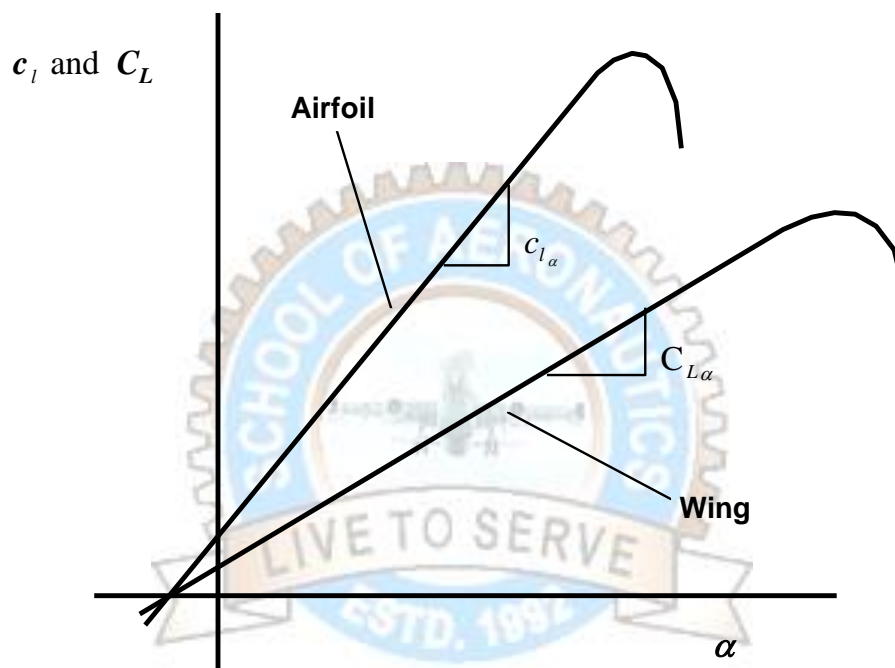


Figure 4.7 Two-Dimensional and Three-Dimensional Lift Coefficient Curves

Span wise Lift Distribution

Unlike the two-dimensional flow around an airfoil in a wind tunnel, the flow around a finite wing varies in the spanwise direction. This spanwise variation is primarily due to the inability of the wing to support a pressure difference at its tips (the cause of trailing vortices). It may be influenced by wing taper, wing twist, or even differences in airfoil shape at different spanwise positions on the wing. Spanwise variation of airfoil shape is called **aerodynamic twist**. But even an untapered, untwisted, unswept wing still has span wise variation of the flow field around it. This is because the trailing vortices on such a wing have a stronger effect and produce more downwash near the wing tips than they do far from the tips. As a result, even though the wing is not twisted, increasing downwash reduces effective angle of attack and therefore lift near the wing tips. Tapering the wing or giving it wash out can help reduce this effect. In fact, a wing which is tapered and/or twisted to give an elliptical spanwise distribution of lift will have a constant downwash at every spanwise position. Figure 4.8 shows an elliptical spanwise lift distribution. An untwisted wing with

an elliptical planform will have an elliptical lift distribution. As shown in Figure 4.9, the famous Supermarine Spitfire and Republic P-47 Thunderbolt fighter aircraft of World War II both used elliptical wing planforms. Such wings are relatively complex and expensive to build, so straight-tapered wings are much more common.

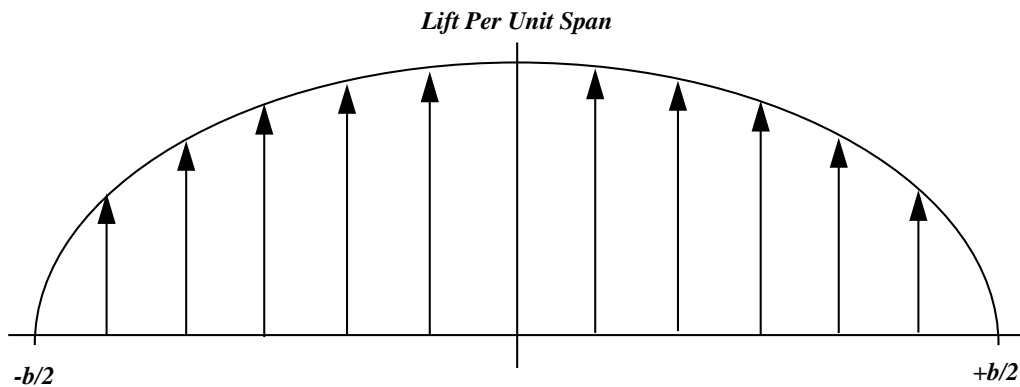


Figure 4.8 Elliptical Lift Distribution

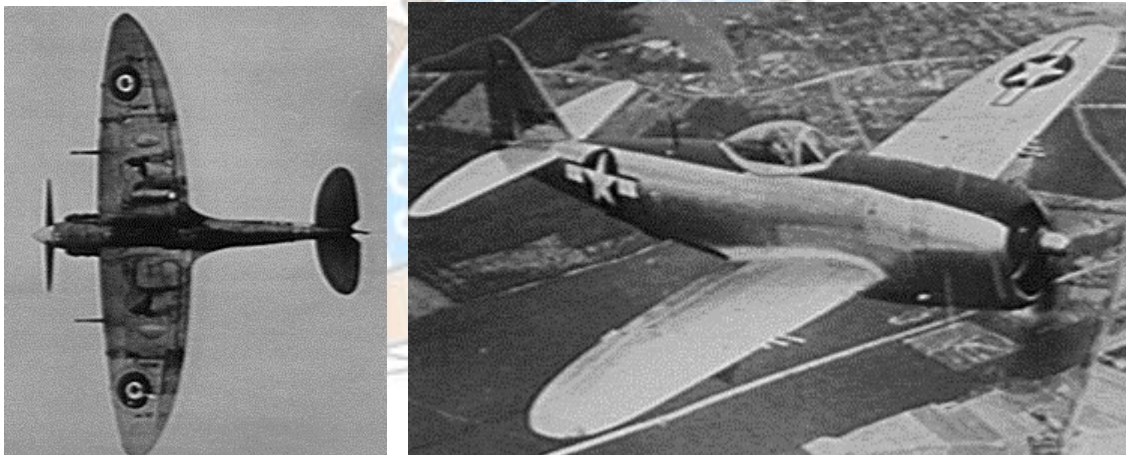


Figure 4.9 The Supermarine Spitfire and Republic P-47 Thunderbolt Fighter Aircraft of World War II Both Had Elliptical Wing Planforms (Photos Courtesy National Air and Space Museum)

Finite Wing Induced Drag

Figure 4.6 shows that induced drag is a component of the three-dimensional lift in the drag direction:

$$D_i = L \sin \varepsilon \quad \text{or} \quad C_{D_i} = C_L \sin \varepsilon \quad (4.7)$$

It can be shown that the induced angle of attack everywhere along the span of wings with elliptical lift distributions is given by:

$$\varepsilon = \frac{C_L}{\pi AR} \text{ radians} = \frac{57.3 C_L}{\pi AR} \text{ degrees}$$

For α small, $\sin \alpha \approx \alpha$ (in radians) and :

$$C_{D_i} = C_L \varepsilon = C_L \frac{C_L}{\pi AR} = \frac{C_L^2}{\pi AR} \quad (4.8)$$

Span Efficiency Factor

Equation (4.8) applies only to wings with elliptical lift distributions. However, it is possible to modify (4.8) slightly to make it apply to any wing by using a **span efficiency factor**, e , such that:

$$C_{D_i} = \frac{C_L^2}{\pi e AR} \quad (4.9)$$

The value of e is 1 for elliptical wings and between .5 and 1 for most common wing shapes.

Finite Wing Total Drag

The total drag of the wing is the sum of profile drag and induced drag:

$$C_D = c_d + \frac{C_L^2}{\pi e AR} \quad (4.10)$$

Recall, however, from Chapter 3 that profile drag is composed of skin friction drag and pressure drag. Figure 4.10 illustrates the variation of each type of drag with lift coefficient.

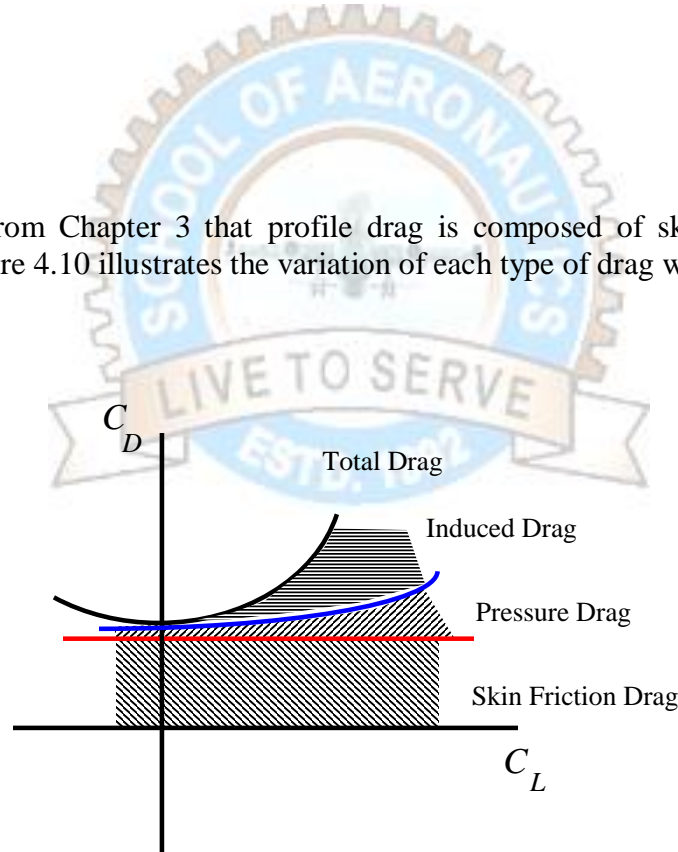
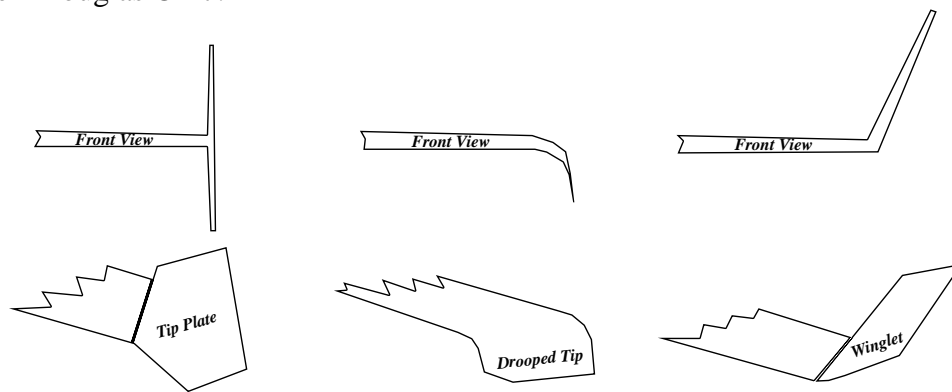


Figure 4.10 Finite Wing Total Drag

Winglets and Tip Plates

A variety of devices have been used on aircraft to reduce induced drag. Figure 4.11(a) shows three such devices. Of the three, the winglet is the most effective and most widely used. In addition, jet fighter aircraft which carry fuel tanks or air-to-air missiles on

their wingtips experience a small reduction in induced drag when such wingtip stores are in place. All of these devices inhibit the formation of the wingtip vortices and therefore reduce downwash and induced drag. Figure 4.11(b) shows a winglet on the wingtip of a McDonnell-Douglas C-17.



(a) Three Induced-Drag-Reducing Wingtip Devices



(b) Winglets on a C-17 (USAF Photo)

Figure 4.11 Wingtip Devices for Reducing Induced Drag

Of course, just extending the wing to increase its span and aspect ratio will have a similar effect. However, the increased lift far out at the end of the wing will increase the bending moment at the wing root and create greater loads on the wing root structure. The winglet increases wing span only slightly. It is preferred because it achieves an effective increase in aspect ratio without significantly increasing wing root structural loads.

Finite Wing Lift

Since the induced angle of attack for a wing with an elliptical lift distribution is constant everywhere along the span, it is relatively easy to determine the lift of such a wing. If the wing has an elliptical planform and no geometric or aerodynamic twist, it will have an elliptical lift distribution for a wide range of angles of attack. A twisted rectangular or tapered wing will normally achieve a true elliptical lift distribution at only one angle of attack. The elliptical planform wing's zero-lift angle of attack will be the same as for its airfoil section. At an arbitrary positive angle of attack below stall, an elliptical wing's effective angle of attack will be given by:

$$\alpha_{eff} = \alpha - \varepsilon = \alpha - \frac{57.3 C_L}{\pi AR} \quad (4.11)$$

As shown in Figure 4.7, the airfoil and finite wing lift curve slopes may be represented as:

$$c_{l_\alpha} = \frac{c_l}{(\alpha - \alpha_{l=0})} \quad C_{L_\alpha} = \frac{C_L}{(\alpha - \alpha_{L=0})} \quad (4.12)$$

where α is any arbitrary angle of attack in the linear range of the lift curves. C_L and c_l are the lift coefficients at that arbitrary value of α and $\alpha_{l=0}$. From Figure 4.7 we recognize that:

$$C_L = C_{L_\alpha} (\alpha - \alpha_{L=0}) = c_{l_\alpha} (\alpha_{eff} - \alpha_{L=0}) = c_{l_\alpha} \left(\alpha - \frac{57.3 C_L}{\pi AR} - \alpha_{L=0} \right) \quad (4.13)$$

Combining (4.12) and (4.13), the expression for C_{L_α} becomes:

$$C_{L_\alpha} = \frac{c_{l_\alpha}}{1 + \frac{57.3 c_{l_\alpha}}{\pi AR}}$$

Following the same convention as in (4.7) for non-elliptical wings, the expression can be written:

$$C_{L_\alpha} = \frac{c_{l_\alpha}}{1 + \frac{57.3 c_{l_\alpha}}{\pi e AR}} \quad (4.14)$$

Note that in general for a given wing, the value of e required for (4.14) is not the same as that required for (4.7). The two values are typically quite close to each other, however.

HIGH-LIFT DEVICES

Relatively thin airfoils with low camber generally give low drag at high speeds. Unfortunately, these airfoils also typically have relatively low values of maximum lift coefficient. Most aircraft are equipped with devices which can be used to increase lift when needed, at the expense of additional drag. These devices are of several types.

Trailing-Edge Flaps

Moveable surfaces on the rear portion of the wing which can be deflected downward to increase the wing's camber are called **trailing-edge flaps** or simply flaps. Figure 4.12 shows four different types of flaps. The plain flap changes camber to increase lift, but its effect is limited by additional flow separation which occurs when it is deflected. The

additional separation occurs because the upper surface of the deflected flap experiences a stronger adverse pressure gradient. The split flap deflects only the underside of the trailing edge so that, while it creates a great deal of pressure drag, it avoids the strong adverse pressure gradient on its upper surface and therefore keeps the flow attached slightly longer. This gives the split flap slightly greater lift.

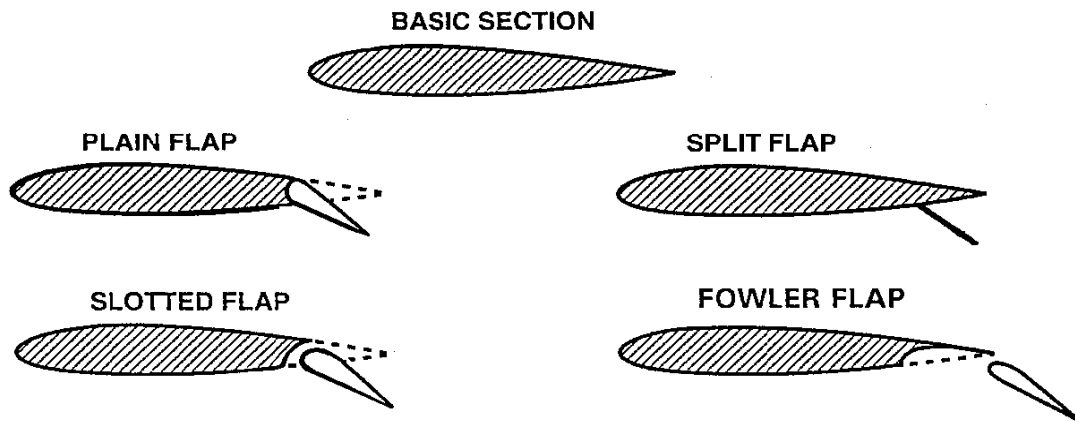


Figure 4.12 Trailing-Edge Flaps (Adapted from Reference 1)

Slotted flaps have a gap or **slot** in them to allow faster-moving air from the lower surface to flow over the upper surface. The higher-energy air from the slot gives the boundary layer more energy to fight the adverse pressure gradient and delay separation. A single-slotted flap creates the slot by moving away from the wing slightly when it is deflected. Double- and triple-slotted flaps are also used. Each slot admits more high-energy air onto the upper surface to further delay separation and increase lift. The **Fowler flap** moves aft to increase the wing area before deflecting downward to increase camber. Fowler flaps usually have one or more slots to increase their effectiveness.

Figure 4.13 shows airfoil lift and drag coefficient curves for a typical trailing-edge flap. Note that in general the effect of flaps is to increase camber, moving the lift curve up and to the left. For flaps other than Fowler flaps the lift curve slope is unchanged. The angle of attack for zero lift is made more negative. With the flap extended, the wing generates more lift at all angles of attack below stall. The maximum lift coefficient is greater, but it occurs at a lower angle of attack. The amount of this shift in $\alpha_{l=0}$ and increase in C_{Lmax} is different for each type of flap. Slots in flaps help delay the stall to higher angles of attack and higher values of C_{Lmax} . The lift curve slope increases when Fowler flaps are used. This is because Fowler flaps increase the actual lifting area of the wing when they are extended, but the lift coefficient is defined using the same reference planform area as when the flaps are retracted.

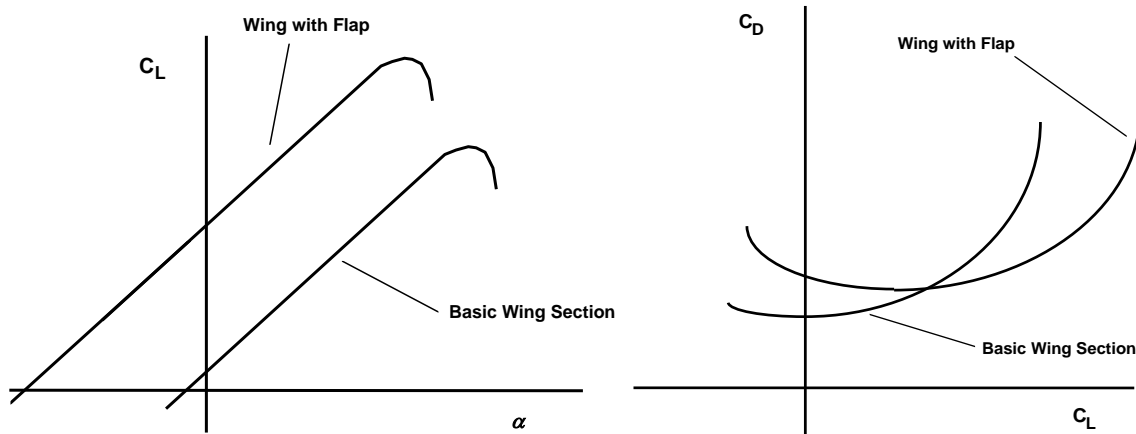


Figure 4.13 Lift and Drag Coefficient Curves for Wings with Flaps

Strakes and Leading-Edge Extensions

Figure 4.14 shows a **strake** on an F-16. A similar device on the F-18 is referred to as a **leading edge extension (LEX)**. The strake has a sharp leading edge. When the aircraft operates at high angles of attack, the flow cannot stay attached as it flows over the sharp strake leading edge, and it separates. Because the leading edge of the strake is highly swept, the separated flow does not break down into turbulence, but instead rolls up into a tornado-like **vortex**. The vortex generates an intense low pressure field which, since it is on the upper surface of the strake and wing, increases lift. The presence of the vortex gives the rest of the wing a more favorable pressure gradient, so that stall is delayed. The strake also increases the total lifting area, but it is usually not included in the reference planform area. Therefore, the strake increases lift coefficient curve slope even at low angles of attack when the vortex does not form. Figure 4.15 shows lift and drag coefficient curves for a wing with and without strakes. Note that at relatively high angles of attack, the lift curve for the wing with strakes is actually above the dotted line which is an extension of the linear region of the curve. It is at these angles of attack where strakes are most effective.

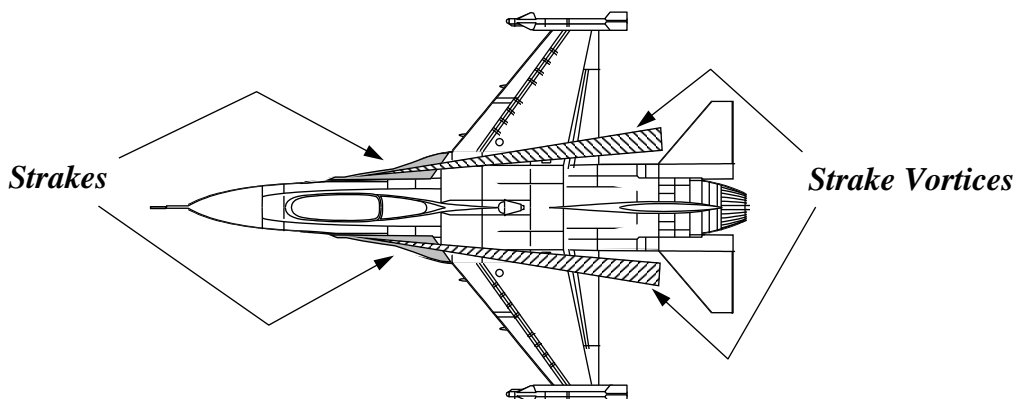


Figure 4.14 F-16 Strakes

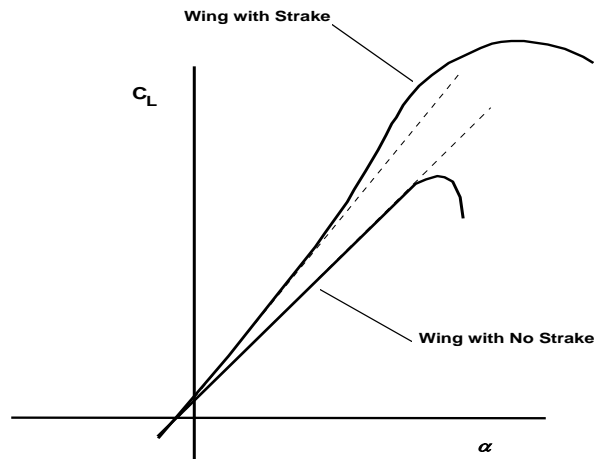


Figure 4.15 Lift Coefficient Curves for Wing Alone and Wing with Strake

Leading-Edge Flaps, and Slats

Figure 4.16 shows several devices which are used on wings to increase lift. Plain **leading edge flaps** deflect to increase wing camber and move the point of minimum pressure further aft on the upper surface of the airfoil at high angles of attack. The aft movement of the point of minimum pressure extends the region of favorable pressure gradient and delays separation. A fixed **slot** may be used to admit higher-speed air onto the upper wing surface to re-energize the boundary layer and delay separation. A **slat** is a leading edge flap which, when it is extended, opens up a slot as well. All three leading-edge devices delay stall and extend the lift curve to higher angles of attack and higher maximum lift coefficients. Because angle of attack is defined using the chord line of the airfoil with no high-lift devices extended, extending a leading-edge device may actually decrease the lift coefficient at a particular angle of attack. Some slats increase the lifting area when they are deployed, so they increase the lift curve slope like Fowler flaps. Figure 4.17 illustrates lift coefficient curves for a wing with and without a typical leading-edge slot, slat, or flap. The magnitude of the increase in maximum lift coefficient and stall angle of attack is different for each type of leading-edge device.

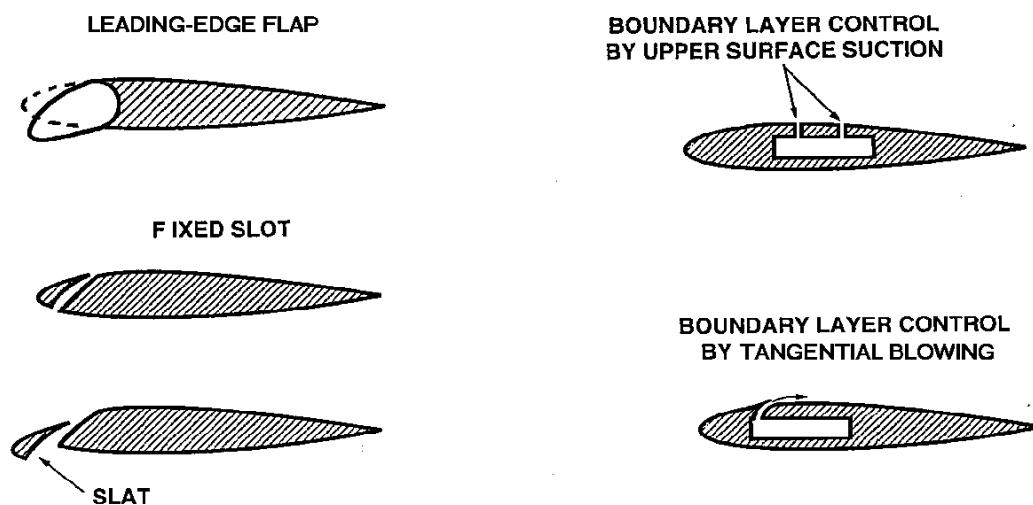


Figure 4.16 Leading-Edge Flaps and Boundary Layer Control Devices (Adapted from Reference 1)

Boundary Layer Control

Since flow separation and stall are caused by depletion of flow velocity in the boundary layer, several methods may be used to remove or re-energize this low-energy air and delay separation. One method is to drill thousands of tiny holes in the wing surface and use **suction** to pull the low-energy air inside the wing. Another method is to use **blowing** of high-velocity air tangent to the wing surface to re-energize the boundary layer and delay separation. Air for tangential blowing is normally obtained as **bleed air** from a jet engine's compressor. Both of these boundary layer control devices delay separation and stall to higher angles of attack. Their lift curves look similar to those for leading-edge devices shown in Figure 4.17. Examples of boundary layer suction and blowing are illustrated in Figure 4.16.

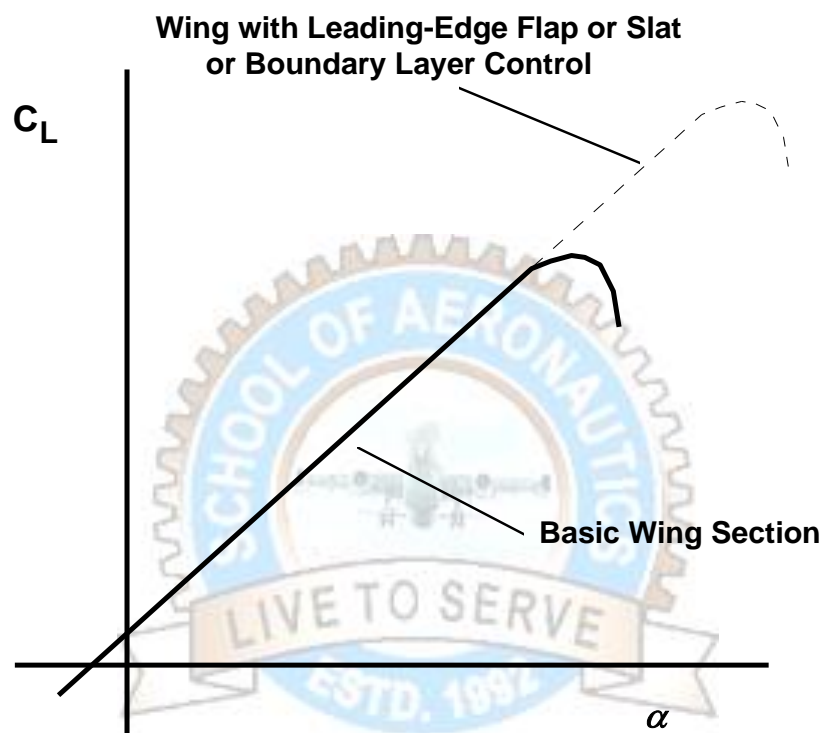


Figure 4.17 Effects of Leading-Edge Flaps and Boundary Layer Control on Lift Coefficient Curves

Powered Lift and Vectored Thrust

An **internally blown flap** or **jet flap** has bleed air directed onto its leading edge and upper surface from the rear of the wing. The high-velocity air delays separation and increases lift. Figure 4.18(a) shows a typical internally blown flap configuration. Engine exhaust may also be used to increase or assist lift. Figure 4.18 shows three ways this may be done. The exhaust may be directed at the leading edge of a flap as on the McDonnell-Douglas C-17, or at the wing and flap's upper surface, as on the Boeing YC-14. In either case, the vastly increased airflow over the flap increases lift. The engine nozzle may also be moveable to redirect or **vector** the engine exhaust downward. This re-orientes the engine thrust vector so that it has a component in the lift direction to assist the lift generated by the wing. Also note in Figure 4.18 the multiple slots in each Fowler flap. Several high-lift devices are often used together on an aircraft. Each device adds to the total C_{Lmax} . In some

cases the devices complement each other so that the total increase in C_{Lmax} for several devices used together is greater than the sum of the C_{Lmax} increments for each device used alone.

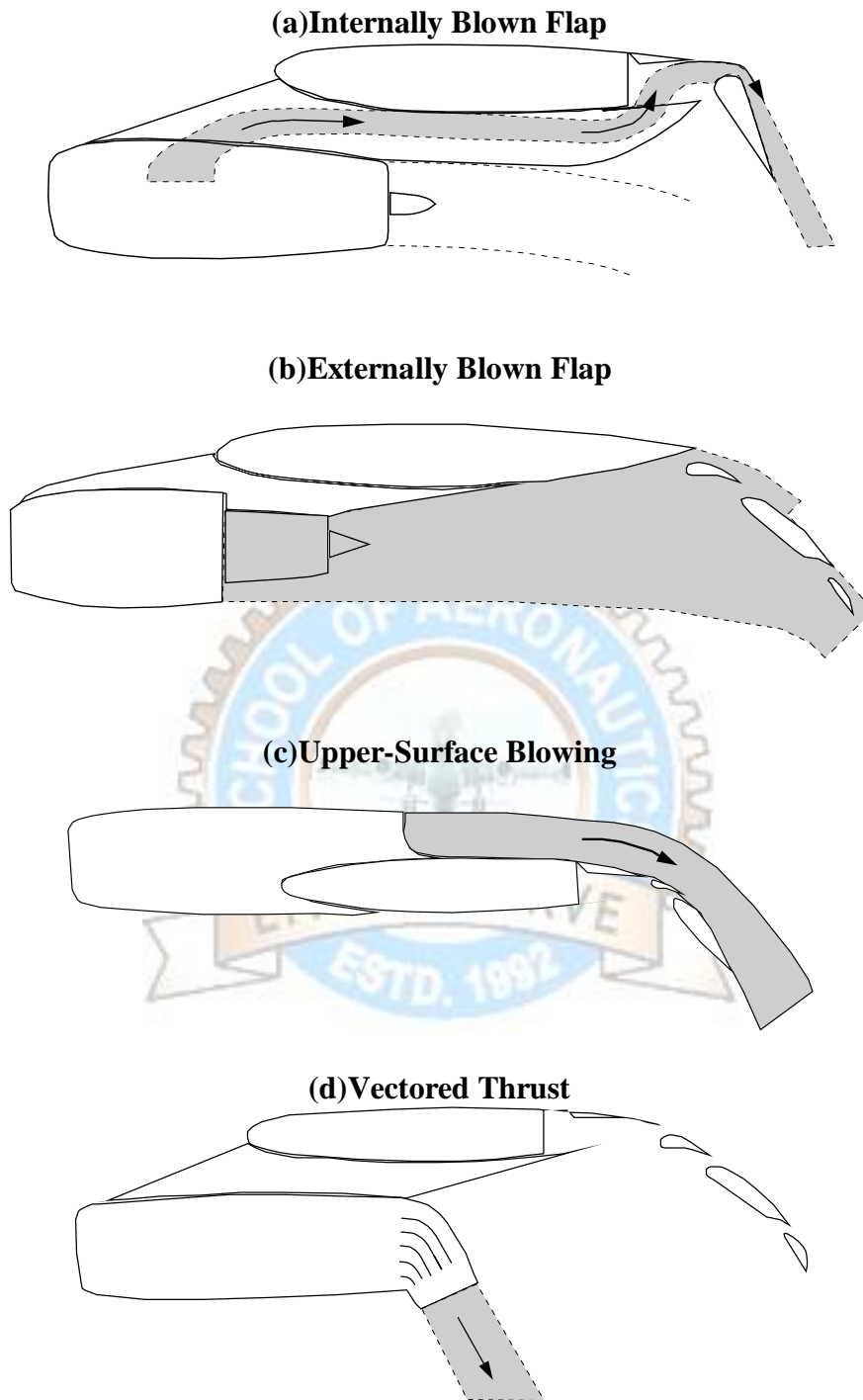


Figure 4.18 Four Powered Lift Configurations (Adapted from Reference 1)

WHOLE AIRCRAFT DRAG

The drag polar for the complete aircraft is written somewhat differently than that for a wing alone. For the whole aircraft, drag is identified as either **parasite drag** or **drag due to lift**. The parasite drag is all drag on the aircraft when it is not generating lift. This includes both skin friction and pressure drag, as well as several additional types of zero-lift drag which are associated with the complete aircraft configuration. The drag due to lift includes all types of drag which depend on the amount of lift the aircraft is producing. These include induced drag due to downwash, the pressure drag which increases with lift due to forward movement of the separation point, induced and pressure drag from canards and horizontal tails, and addition drag such as vortex drag due to the leading-edge vortices on strakes and highly swept wings. All of these types of drag may be approximated by the following simple expression for drag coefficient:

$$C_D = C_{D_o} + k_1 C_L^2 + k_2 C_L \quad (4.26)$$

where:

$$k_1 = 1/(\pi e_o AR) \quad (4.27)$$

and k_2 is chosen to allow modeling of wings with airfoils which generate minimum drag at some non-zero value of lift. C_{D_o} is called the parasite drag coefficient. It represents all drag generated by the aircraft when it is not generating lift (hence the 'o' subscript). The variable e_o in the expression for k_1 is called the **Oswald's efficiency factor**. It is not the same as the span efficiency factor, e , used in Equations (4.9), (4.14) and (4.15), because it includes all the other types of drag due to lift*.

For relatively straight wing ($\Lambda_{LE} < 30$ deg):

$$e_o = 1.78(1 - 0.045AR^{0.68}) - 0.64$$

For relatively swept wing ($\Lambda_{LE} > 30$ deg):

$$e_o = 4.61(1 - 0.045AR^{0.68})(\cos \Lambda_{LE})^{0.15} - 3.1$$

In order to model the common situation where minimum drag occurs at a positive value of lift coefficient, k_2 must be negative. This has the effect of shifting the entire C_D vs C_L curve to the right. Figure 4.24 illustrates this effect. The C_L for which C_D is a minimum is called C_{LminD} .

* Although confusing, it is common to refer to the $k_1 C_L^2$ term in (4.26) as induced drag, though it is significantly different from the induced drag in (4.9)

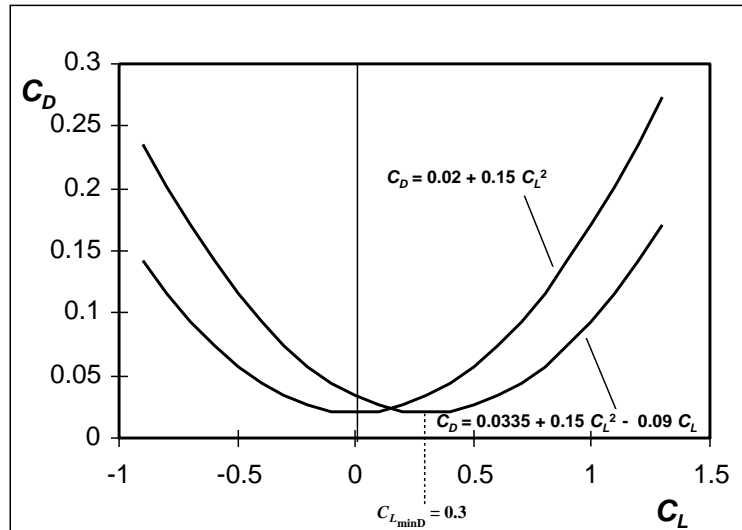


Figure 4.24 Example of Drag Polar with Minimum Drag Coefficient at Non-Zero Lift Coefficient

Parasite Drag

Just as lift predictions for the early stages of conceptual design rely heavily on the results of wind tunnel testing of similar configurations, so drag predictions rely heavily on drag data for similar types of aircraft. In later design stages, it is necessary to make very precise predictions of the aircraft's drag, since just a 1% difference in the drag at cruise conditions, for instance, can make the difference between success and failure of a design. The methods used in making these precise predictions go far beyond the scope of this textbook and require details of the design which are generally not available early in the conceptual design phase. It is important, however, to understand in a qualitative sense where the drag on an aircraft comes from.

Skin friction drag on a complete aircraft configuration is generally much greater than that on the wing alone, because the **wetted area**, S_{wet} , is greater. Wetted area of an aircraft is all the surface area over which air flows, and therefore to which the flowing air imparts shear stress. Pressure drag for the complete aircraft includes drag due to separation of the airflow around the aircraft fuselage, control surfaces, etc., in addition to the wing. **Interference drag** results from flow interactions between the various components of an aircraft which cause them to have more drag when assembled together than the sum of their drags when tested in a wind tunnel separately. Miscellaneous drags include drag due to cooling air flowing through heat exchangers, air which leaks through doors and fairings which don't fit perfectly and around moveable surfaces, plus the profile drag of antennae, gun barrels, sensors, etc. which protrude from the aircraft. The total of all these drags is the profile drag of the complete aircraft. To this must be added wave drag if the aircraft flies at or near the speed of sound. Wave drag will be discussed in a later section.

A very good initial estimate of subsonic parasite drag may be made from drag data for similar aircraft using the concept of an **equivalent skin friction drag coefficient**, C_{fe} , which is defined as follows:

$$C_{fe} = C_{D_o} \frac{S}{S_{wet}} \quad (4.28)$$

Table 4.1 lists average C_{fe} values for several classes of aircraft. These values are based on historical data^{4,5} for large numbers of each type of aircraft. C_{fe} is a function of such diverse factors as aircraft skin materials and shape; paint; typical flight Reynolds numbers; number of additional air scoops for ventilation; type, size, number, and location of engine air inlets; and attention to detail in sealing doors, control surface gaps, etc. Naturally, these details vary significantly from aircraft to aircraft, but the data in Reference 5 suggest that there is enough similarity among aircraft of a given class that useful average C_{fe} values can be established. Table 4.1 lists the most commonly used values of C_{fe} ^{4,5}.

Table 4.1 Common C_{fe} Values

Type	C_{fe}
Jet Bomber and Civil Transport	0.0030
Military Jet Transport	0.0035
Air Force Jet Fighter	0.0035
Carrier-Based Navy Jet Fighter	0.0040
Supersonic Cruise Aircraft	0.0025
Light Single Propeller Aircraft	0.0055
Light Twin Propeller Aircraft	0.0045
Propeller Seaplane	0.0065
Jet Seaplane	0.0040

Using C_{fe} to predict C_{D_o} for an aircraft which generates minimum drag when it is generating zero lift only requires selecting a C_{fe} for the appropriate category of aircraft and estimating the total wetted area of the aircraft concept. The value of C_{D_o} is then obtained by solving (4.28):

$$C_{D_o} = C_{fe} \frac{S_{wet}}{S} \quad (4.29)$$

Drag Due to Lift

Predicting drag due to lift must begin with predicting Oswald's efficiency factor, e_o . This is done with a curve fit of wind tunnel data² for a variety of wing and wing-body combinations. The equation for this curve fit is:

$$e_o = 4.61(1 - 0.045AR^{0.68})(\cos \Lambda_{LE})^{0.15} - 3.1 \quad (4.30)$$

Note that increasing wing sweep tends to decrease the value of e_o . Also note that increasing AR will tend to decrease e_o . This is due to the fact that for high-aspect-ratio wings, that part of the airfoil profile drag which varies with lift is a larger part of the total drag due to lift which e_o must model.

Effect of Camber

There are a number of reasons why an aircraft may generate its minimum drag at a positive (non-zero) value of lift coefficient. As one example, the profile drag on cambered airfoils is typically at a minimum at some small positive value of lift coefficient. As another example, the shape and orientation of an aircraft's fuselage may cause it to generate the least amount of drag at other than the zero-lift condition. Equation (4.26) has an additional term, the $k_2 C_L$ term, to model this effect. If, for instance, the minimum drag coefficient for an aircraft occurs at a lift coefficient signified by the symbol C_{LminD} , then the necessary value of k_2 is given by:

$$k_2 = -2k_1 C_{LminD} \quad (4.31)$$

The value of C_{LminD} is determined by plotting the drag polar for the wing using actual airfoil data and (4.3). If actual airfoil data is not available, as a crude approximation assume that the airfoil generates minimum drag when it is at zero angle of attack, and that the effect of induced drag is to move C_{LminD} to a value halfway between zero and the value of C_L when $C_D = 0$. The value of C_L when $C_D = 0$ is given by:

$$C_{L\alpha=0} = C_{L\alpha}(\alpha_a) = C_{L\alpha}(-\alpha_{L=0}) \text{ since } \alpha_a = \alpha - \alpha_{L=0} \text{ and } C_D = 0 \quad (4.32)$$

and:

$$C_{LminD} = C_{L\alpha} \left(\frac{-\alpha_{L=0}}{2} \right) \quad (4.33)$$

This value of C_{LminD} is then used for the entire aircraft. This is done because it is assumed that the aircraft designer will design the fuselage, strakes, etc. so that they also have their minimum drag at the angle of attack that puts the wing at its C_{LminD} . When this is done, the minimum value of C_D , which is given the symbol C_{Dmin} , must not be any lower than the C_{Do} predicted by (4.28). Recall that C_{Do} is the aircraft's zero-lift drag coefficient. For aircraft with minimum drag at non-zero lift this leads to the following revised predictions:

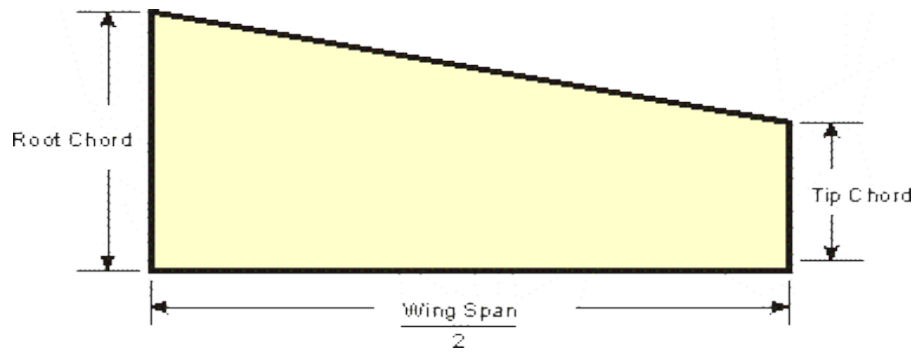
$$C_{Dmin} = C_{fe} \frac{S_{wet}}{S} \quad (4.34)$$

$$C_{Do} = C_{Dmin} + k_1 C_{LminD}^2 \quad (4.35)$$

Wing area

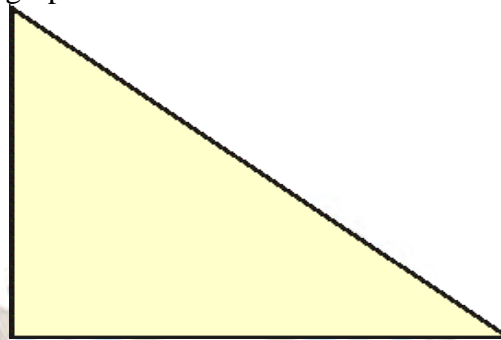
a) Trapezoidal wing

- ▶ Average Chord = (Root Chord + Tip Chord) ÷ 2
- ▶ Wing Area = Wing Span x Average Chord



b) Delta wing

Wing Area = $1/2 \times \text{Wing Span} \times \text{Root Chord}$



c) Elliptical wing

Aspect ratio

$$C_{L\alpha} = \frac{2\pi A}{2 + \sqrt{4 + \frac{A^2 \beta^2}{\eta^2} \left(1 + \frac{\tan^2 \Lambda_{\frac{1}{2}}}{\beta^2} \right)}}$$

where $\beta^2 = 1 - M^2$, $\eta = C_{l\alpha} / (2\pi)$, $\Lambda_{\frac{1}{2}}$ = sweep of the half chord line

In this section, the selection of aspect ratio (A), sweep (Λ) and taper ratio (λ) are considered.

$$C_{L\alpha W} = \frac{2\pi A}{2 + \sqrt{\frac{A^2 \beta^2}{\kappa^2} \left(1 + \frac{\tan^2 \Lambda_{\frac{1}{2}}}{\beta^2} \right) + 4}}$$

$C_{L\alpha W}$ = slope of lift curve of wing in radians

A = aspect ratio of wing

R = a factor which depends on (a) Reynolds number based on leading edge radius, (b) leading edge sweep (Λ_{LE}), (c) Mach number (M), (d) wing aspect ratio (A) and (e) taper ratio (λ).

$$\beta = \sqrt{1-M^2}$$

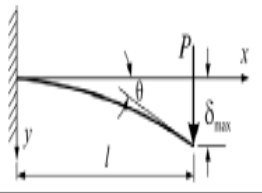
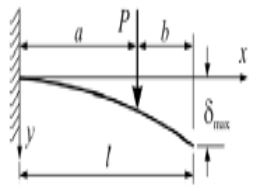
$\Lambda_{1/2}$ = sweep of semi-chord line

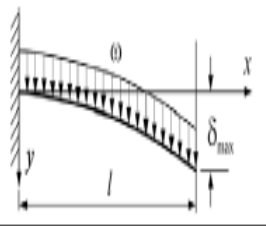
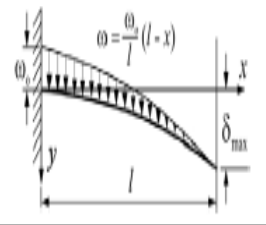
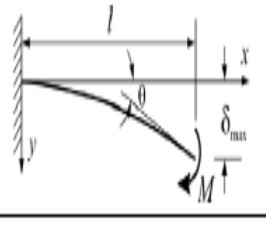
κ = ratio of the slope of lift curve of the airfoil used on wing divided by 2π .

It is generally taken as unity.

BENDING MOMENT

BEAM DEFLECTION FORMULAE

BEAM TYPE	SLOPE AT FREE END	DEFLECTION AT ANY SECTION IN TERMS OF x	MAXIMUM DEFLECTION
1. Cantilever Beam - Concentrated load P at the free end			
	$\theta = \frac{Pl^2}{2EI}$	$y = \frac{Px^2}{6EI}(3l-x)$	$\delta_{\max} = \frac{Pl^3}{3EI}$
2. Cantilever Beam - Concentrated load P at any point			
	$\theta = \frac{Pa^2}{2EI}$	$y = \frac{Px^2}{6EI}(3a-x)$ for $0 < x < a$ $y = \frac{Pa^2}{6EI}(3x-a)$ for $a < x < l$	$\delta_{\max} = \frac{Pa^2}{6EI}(3l-a)$

3. Cantilever Beam – Uniformly distributed load ω (N/m)			
	$\theta = \frac{\omega l^3}{6EI}$	$y = \frac{\omega x^2}{24EI} (x^2 + 6l^2 - 4lx)$	$\delta_{\max} = \frac{\omega l^4}{8EI}$
4. Cantilever Beam – Uniformly varying load: Maximum intensity ω_0 (N/m)			
	$\theta = \frac{\omega_0 l^3}{24EI}$	$y = \frac{\omega_0 x^2}{120EI} (10l^3 - 10l^2x + 5lx^2 - x^3)$	$\delta_{\max} = \frac{\omega_0 l^4}{30EI}$
5. Cantilever Beam – Couple moment M at the free end			
	$\theta = \frac{Ml}{EI}$	$y = \frac{Mx^2}{2EI}$	$\delta_{\max} = \frac{Ml^2}{2EI}$

Wing vertical location

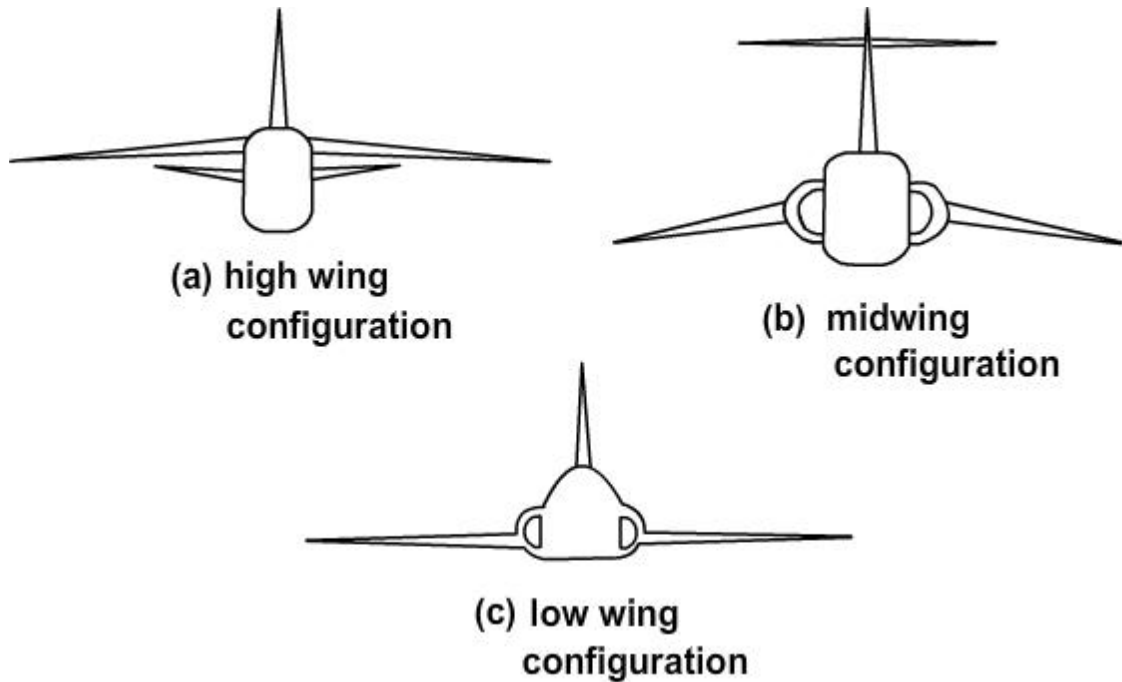
There are three choices for the location of the wing on the fuselage namely, high-, mid- and low- wing. Figure below shows three military airplanes with these locations for the wing.

The advantages and disadvantages of the three configurations are as follows.

High Wing configuration

Advantages:

- i) Allows placing fuselage closer to ground, thus allowing loading and unloading without special ground handling equipment.
- ii) Jet engines & propeller have sufficient ground clearance without excessive landing gear length leading to lower landing gear weight.
- iii) For low speed airplanes, weight saving can be effected by strut braced wing
- iv) For short take off and landing (STOL) airplanes, the high wing configuration has the following specific advantages.
 - (a) Large wing flaps can be used.
 - (b) Engines are away from the ground and hence ingestion of debris rising from unprepared runways is avoided.
 - (c) Prevents floating of wing due to ground effect which may occur for low wing configuration.



High wing, mid wing and low wing configurations

Disadvantages

- i) Fuselage generally houses the landing gear in special pods leading to higher weight and drag.
- ii) Pilot's visibility may be blocked during a turning flight.

Mid wing configuration

Advantages:

- i) Lower drag.
- ii) Advantages of ground clearance as in the case of high wing configuration.
- iii) No blockage of visibility. Hence, used on some military airplanes.

Disadvantages:

Wing root structure passing through the fuselage is not possible, which leads to higher weight. However, in HFB Hansa airplane, a swept forward mid-wing is located behind the passenger cabin. This permits wing root structure passing through the fuselage.

Low-wing configuration

Advantages:

- i) Landing gear can be located in the wing thereby avoiding pods on the fuselage and hence lower drag. However, to provide adequate ground clearance, the fuselage has to be at a higher level as compared to the high wing configuration.
- ii) Wing structure can be through the fuselage.

Disadvantages:

- (i) Low ground clearance.
- (ii) A low-wing configuration has unstable contribution to the longitudinal and lateral static stability. In addition Ref.1.18, chapter 4, mentions that for low-wing airplanes

the dihedral angle may be decided by need to avoid wing tip hitting the ground during a bad landing. A wing with high value of dihedral may require higher vertical tail area to prevent tendency to Dutch roll.

Fuselage sizing

The primary purpose of the fuselage is to house the payload. The payload is the part of useful load from which the revenue is derived or for which the airplane is designed. In transport airplanes the payload includes the passengers, their luggage and cargo. In military airplanes it is the ammunition and /or special equipment.

In addition to the payload, the fuselage accommodates the following.

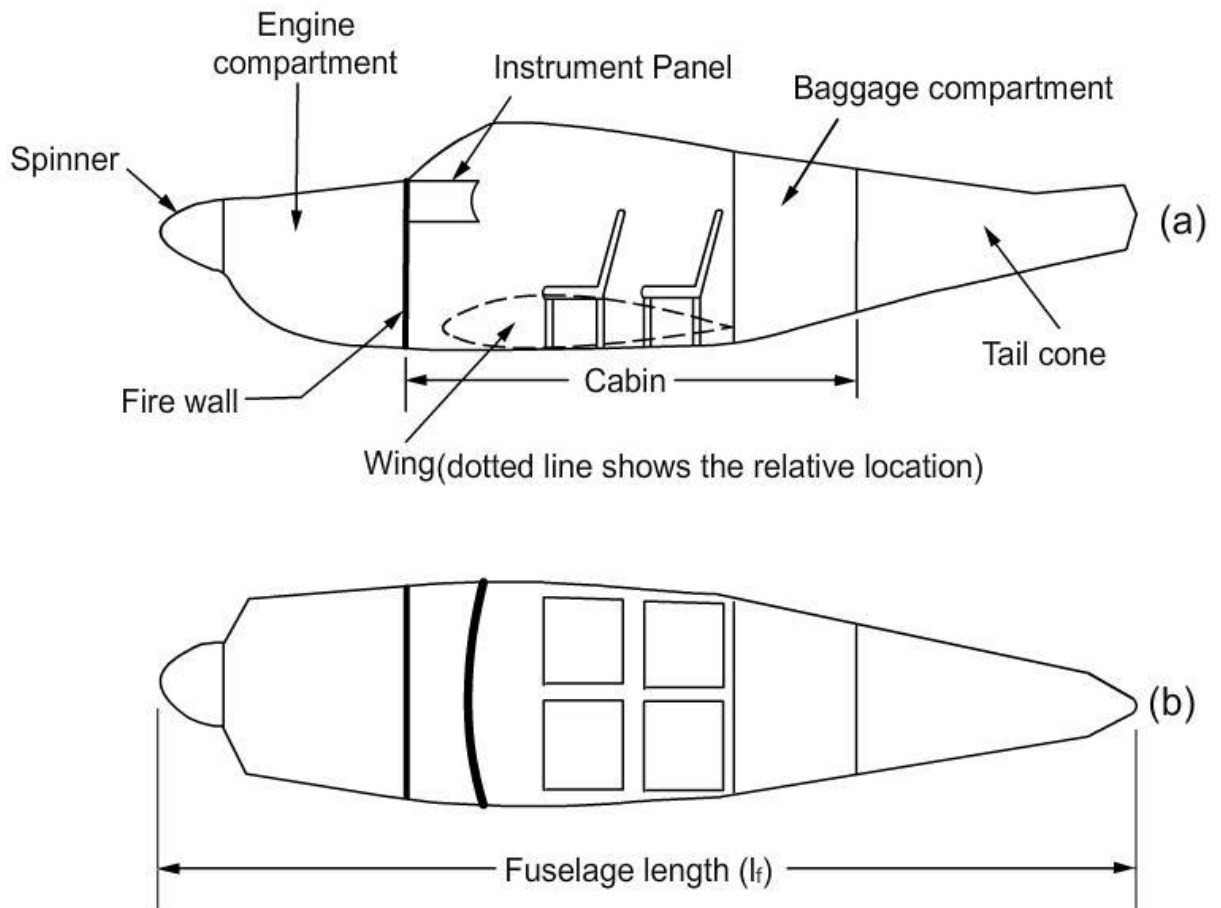
- (a) The flight crew and the cabin crew in the transport airplane and the specialist crew members in airplanes used for reconnaissance, patrol and remote sensing.
- (b) Fuel, engine and landing gear when they are housed inside the fuselage.
- (c) Systems like air-conditioning system, pressurization system, hydraulic system, electrical system, pneumatic system, electronic systems, emergency oxygen, floatation vests and auxiliary power unit.

Features of the fuselage of a general aviation aircraft

Figure below shows the schematic side view and plan view of the fuselage of a four seater general aviation aircraft with low wing and tractor propeller.

It is observed from Fig below that the propeller is located ahead of the fuselage. A spinner is located just ahead of the propeller. It is a streamlined fairing over the propeller hub and enables smooth entry of air flow in the propeller. The length of the spinner is roughly 20% of the diameter of the propeller.

The engine is located inside the engine compartment. The engine is attached to the fuselage by an engine mounting. The length of the engine compartment is approximately 1.5 times the length of the engine. The width of the engine compartment is approximately 1.2 times the width of the engine. The rest of airplane is separated from the engine compartment by a fire- wall which is a fire-resistant sheet attached to a bulk head. When the airplane has a nose wheel type landing gear, the nose wheel strut is attached to the frame inside the engine compartment.



Schematic side view and plan view of the fuselage of a four seater general aviation aircraft with low wing and tractor propeller (a) Side view (b) Plan view

The cabin is the portion of fuselage that extends from the firewall to the end of the baggage compartment. This definition of cabin appears to be the practice followed by Cessna aircraft company. The cabin consists of (a) the portion of fuselage including rudder pedals and instrument panel (b) the seats of pilot and passengers and (c) the baggage compartment. Some companies consider the cabin as the portion of fuselage between the instrument panel and the end of baggage compartment. The distance between the firewall and the instrument panel is approximately 0.7 m.

The cabin accommodates the pilot and the passengers. Its internal dimensions are decided by human factors. The passengers must be comfortable and the pilot should be able to fly the airplane efficiently without undue strain. Ergonomics is the branch of science dealing with the topics like human behaviour, dimensions of the parts of human body and the range of their movements.

The former reference (Ref.1.12), shows dimensions of cabins of single seater, two seater (with side by side or tandem seating), four seater and six seater airplanes propelled by single piston engine propeller combination.

The gap between the instrument panel and the front seat is between 0.69 to 0.84 m. The seat pitch (distance between back of one seat to the back of next seat) is between 0.71 to 0.84 m. The minimum width of cabin for a two seater airplane with side by side seating arrangement is between 1.04 to 1.13 m. The maximum height of the cabin for such an airplane is between 1.13 to 1.25 m. For a single seater airplane or a two seater airplane with tandem seating, the

width would be between 0.58 m to 0.7 m. The thickness of the cabin wall is between 6 cm to 10 cm.

The baggage compartment is located behind the passenger seats. The volume of the baggage compartment for such airplanes is between 0.17 to 0.23 m³ per occupant (passenger / pilot).

In this type of airplane, the tail cone is the portion of the fuselage aft of the baggage compartment. The length of the tail cone is obtained as a compromise between the aerodynamic, structural and stability considerations.

The aerodynamic consideration, for this type of airplane, requires that the drag of the fuselage should be minimum.

In this context, instead of the length of the fuselage, the fineness ratio of the fuselage (A_f) is used as the parameter. It is defined as:

$$A_f = l_f / d_e$$

where, l_f = length of fuselage

d_e = equivalent diameter of fuselage

$$\frac{\pi}{4} d_e^2 = \text{area of the maximum cross section of the fuselage}$$

Passenger cabin layout

Two major geometrical parameters that specify the passenger cabin are cabin diameter and cabin length. These are in turn decided by more specific details like number of seats, seat width, seating arrangement (number abreast), seat pitch, aisle width and number of aisles.

Cabin cross section

The shape of the fuselage cross section is dictated by the structural requirements for pressurization. A circular shell resists the internal pressure loads by hoop tension. This makes the circular section efficient and therefore lowest in structural weight. However, a fully circular section may result in too much unusable volume above or below the cabin space. This problem is overcome by the use of several interconnecting circular sections to form the cross-sectional layout. The parameters for the currently designed airplane are arrived at by considering similar airplanes (Table A).

A circular cross section for the fuselage is chosen here. The overall size must be kept small to reduce aircraft weight and drag, yet the resulting shape must provide a comfortable and flexible cabin interior which will appeal to the customer airlines. The main decision to be taken is the number of seats abreast and the aisle arrangement. The number of seats across will fix the number of rows in the cabin and thereby the fuselage length. Design of the cabin cross section is further complicated by the need to provide different classes like first class, business class, economy class etc.

Cabin length

Following the trend displayed by current airplanes, a two class seating arrangement is chosen viz economy class and business class. The total number of seats (150) is distributed as 138 seats in the economy class and 12 seats in the business class.

Cabin parameters are chosen based on standards for similar airplanes. The various parameters chosen are as follows.

Parameter	Economy class	Business class
Seat / pitch (in inches)	32	38
Seat width (in inches)	20	22
Aisle width (in inches)	22	24
Seats abreast	6	4
Number of aisles	1	1
Max. height (in m)	2.2	2.2

Since, the business class has a 4 abreast seating arrangement, the number of rows required is 3 and the economy class has 23 rows. The cabin length is found out by using the seat pitch for each of the classes.

Cabin diameter:

Using the number of seats abreast, seat width, aisle width the internal diameter of the cabin is calculated as:

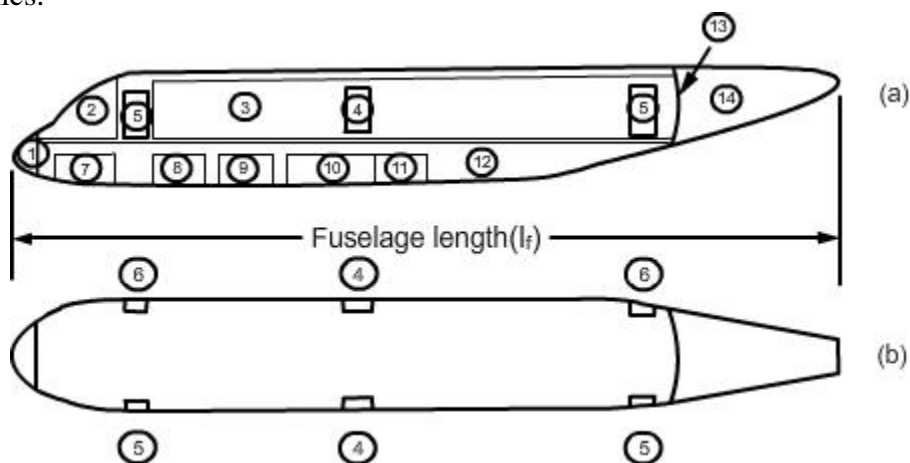
Features of the fuselage of a passenger airplane

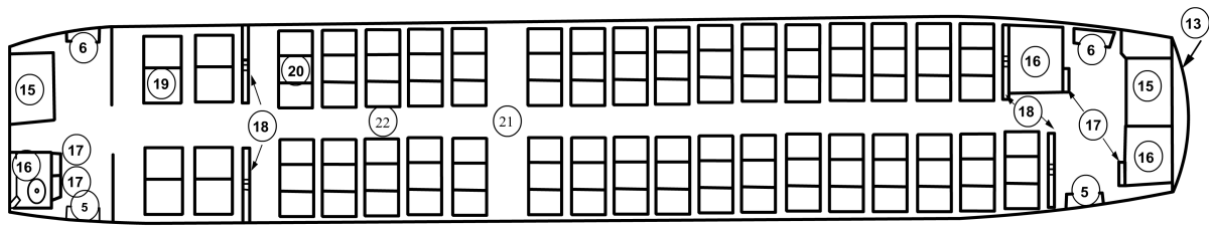
Figure below shows the side view, plan view and cabin layout of a medium range passenger jet airplane with low wing. A cross-section of fuselage with six abreast seating is shown in Fig b.

The portion of the fuselage ahead of the cockpit is referred to as nose. It generally houses the radar.

The cockpit houses the pilots and other flight crew. It is also called the flight deck or crew station. It has the flight instruments and controls. The considerations for the design of the cockpit are as follows.

- The pilots and the crew members should be able to reach all controls comfortably. They must be able to see all instruments and communicate by voice or touch between them without undue efforts.
- Visibility from cockpit should adhere to the standards during take-off, landing, and other phases of the flight. The shape of the wind shield should be in accordance with the fuselage aerodynamics.

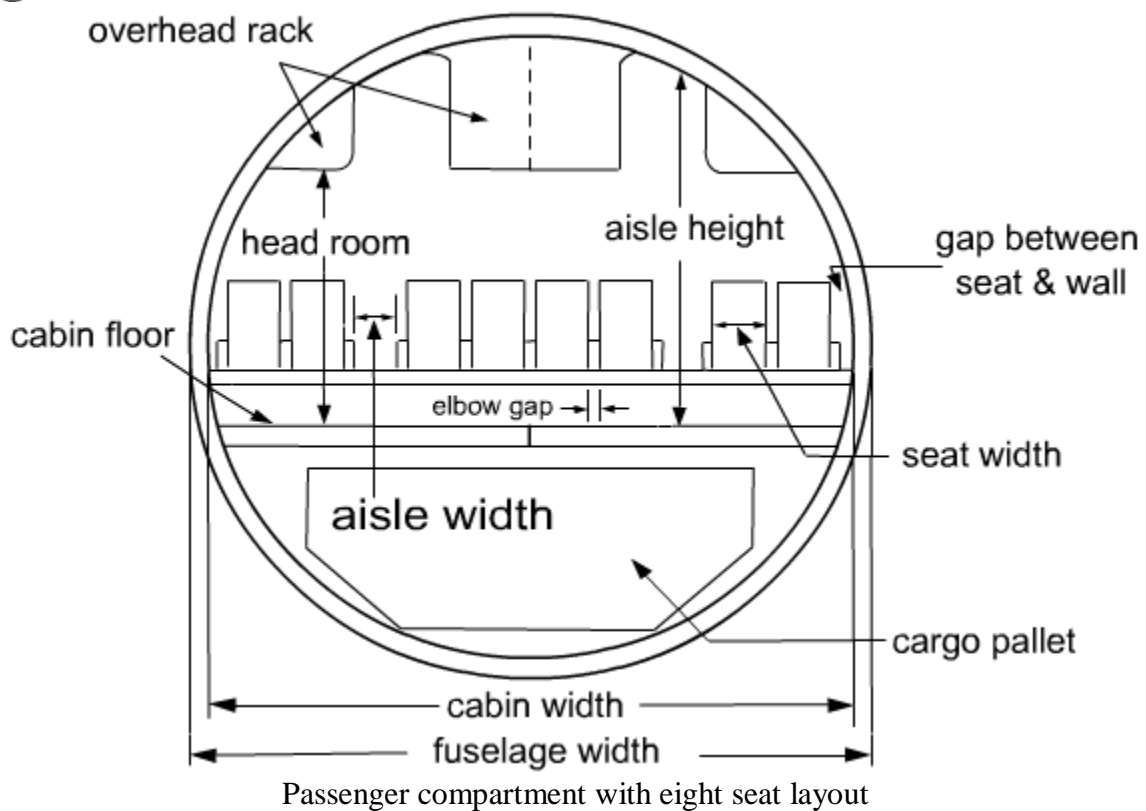


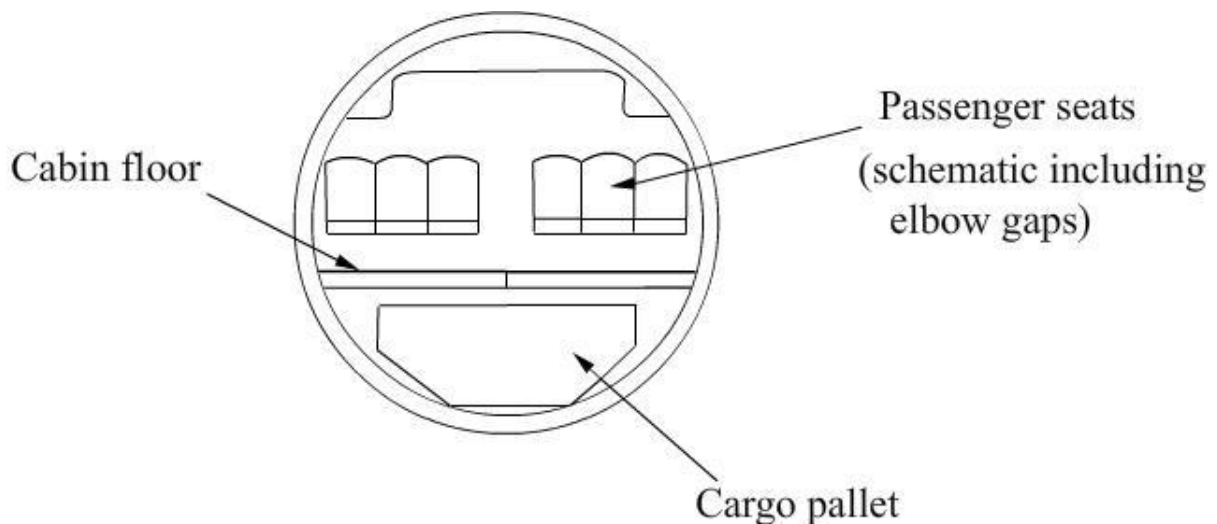


Schematic side view, plan view and cabin layout of a medium range passenger jet airplane with low wing

(a) Side view (b) Plan view (c) Layout of cabin

- ① Nose, ② Cockpit or flight deck, ③ Passanger cabin, ④ Emergency exit,
- ⑤ Passanger door, ⑥ Service door, ⑦ Nose wheel well, ⑧ Systems,
- ⑨ Front cargo compartment, ⑩ Wing box, ⑪ Main wheel well, ⑫ Aft cargo compartment, ⑬ Aft pressure bulk head, ⑭ Auxilliary power unit, ⑮ Galley,
- ⑯ Toilet, ⑰ Cabin attendant seat, ⑱ Screen, ⑲ First class seat,
- ⑳ Economy class seat, ㉑ Larger gap between seats near emergency exits,
- ㉒ Aisle





Another cabin layout with six seats and different type of cargo pallet

The types of seating arrangements are classified as first class, business class, economy class and tourist class. The dimensions of seat width, seat pitch and aisle width are the highest for the first class and are the lowest for the tourist class. Very important persons (VIP), like the President and Prime minister, generally have airplanes with special features.

WING AND FUSELAGE CONSTRUCTION

Fuselage

The fuselage is the main structure or body of the fixed-wing aircraft. It provides space for cargo, controls, accessories, passengers, and other equipment. In single-engine aircraft, the fuselage houses the power plant. In multiengine aircraft, the engines may be either in the fuselage, attached to the fuselage, or suspended from the wing structure. There are two general types of fuselage construction: truss and monocoque.

Truss Type

A truss is a rigid framework made up of members, such as beams, struts, and bars to resist deformation by applied loads.

The truss-framed fuselage is generally covered with fabric. The truss-type fuselage frame is usually constructed of steel tubing welded together in such a manner that all members of the truss can carry both tension and compression loads. In some aircraft, principally the light, single engine models, truss fuselage frames may be constructed of aluminum alloy and may be riveted or bolted into one piece, with cross-bracing achieved by using solid rods or tubes.

Most early aircraft used this technique with wood and wire trusses and this type of structure is still in use in many lightweight aircraft using welded steel tube trusses. The truss type fuselage frame is assembled with members forming a rigid frame e.g. beams, bar, tube etc... Primary members of the truss are 4 longerons.



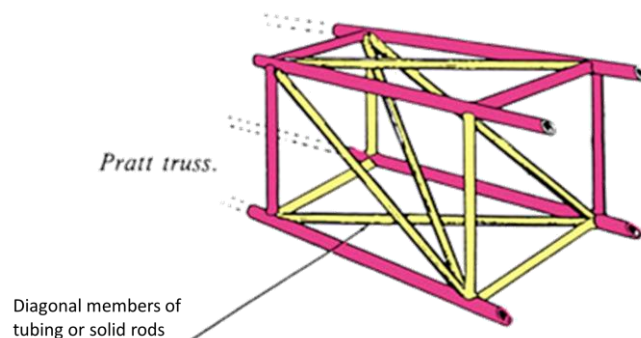
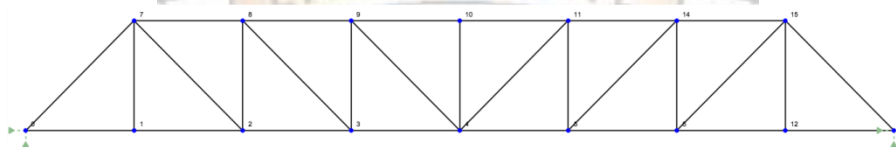
There are two types of truss structure.

- PRATT TRUSS
- WARREN TRUSS

PRATT TRUSS

A Pratt Truss has been used over the past two centuries as an effective truss method. The vertical members are in compression, whilst the diagonal members are in tension. This simplifies and produces a more efficient design since the steel in the diagonal members (in tension) can be reduced. This has a few effects - it reduces the cost of the structure due to more efficient members, reduces the self weight and eases the constructability of the structure. This type of truss is most appropriate for horizontal spans, where the force is predominantly in the vertical direction.

Below is an example of a Pratt Truss,



A truss-type fuselage with pratt truss.

Advantages

- Aware of member's behaviour - diagonal members are in tension, vertical members in compression
- The above can be used to design a cost effective structure
- Simple design
- Well accepted and used design

Disadvantages

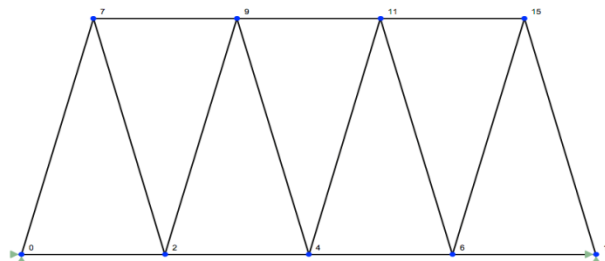
- Not as advantageous if the load is not vertical

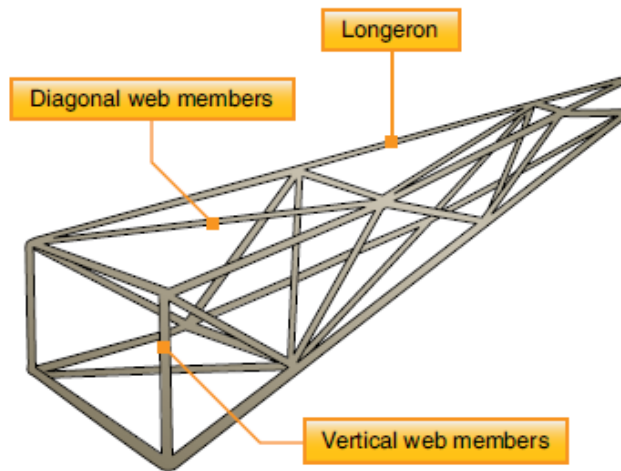
Best Used For:

- Where a cost effective design is required
- Where a mix of loads are applied
- Where a simple structure is required

WARREN TRUSS

The Warren Truss is another very popular truss structure system and is easily identified by its construction from equilateral triangles. One of the main advantages of a Warren Truss is its ability to spread the load evenly across a number of different members; this is however generally for cases when the structure is undergoing a spanned load (a distributed load). Its main advantage is also the cause of its disadvantage - the truss structure will undergo concentrated force under a point load. Under these concentrated load scenarios, the structure is not as good at distributing the load evenly across its members. Therefore the Warren truss type is more advantageous for spanned loads, but not suitable where the load is concentrated at a single point or node. An example of a Warren Truss and its axial forces under a distributed load is shown below.





A truss-type fuselage. A Warren truss uses mostly diagonal bracing.

Advantages

- Spreads load fairly evenly between members
- Fairly simple design

Disadvantages

- Poorer performance under concentrated loads
- Increased constructibility due to additional members

Best Used For:

- Long span structures
- Where an evenly distributed load is to be supported
- Where a simple structure is required

Monocoque Type

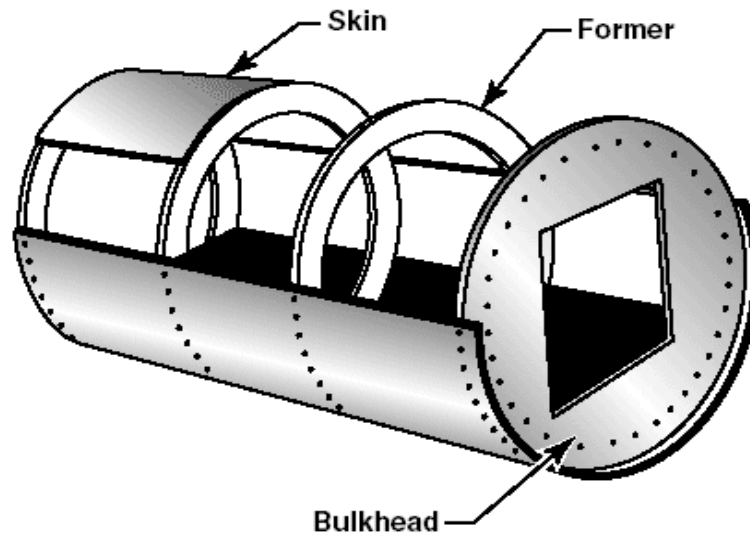
The monocoque (single shell) fuselage relies largely on the strength of the skin or covering to carry the primary loads.

The design may be divided into two classes:

1. Monocoque
2. Semimonocoque

Different portions of the same fuselage may belong to either of the two classes, but most modern aircraft are considered to be of semi-monocoque type construction.

The true monocoque construction uses formers, frame assemblies, and bulkheads to give shape to the fuselage. The heaviest of these structural members are located at intervals to carry concentrated loads and at points where fittings are used to attach other units such as wings, power plants, and stabilizers. Since no other bracing members are present, the skin must carry the primary stresses and keep the fuselage rigid. Thus, the biggest problem involved in monocoque construction is maintaining enough strength while keeping the weight within allowable limits.



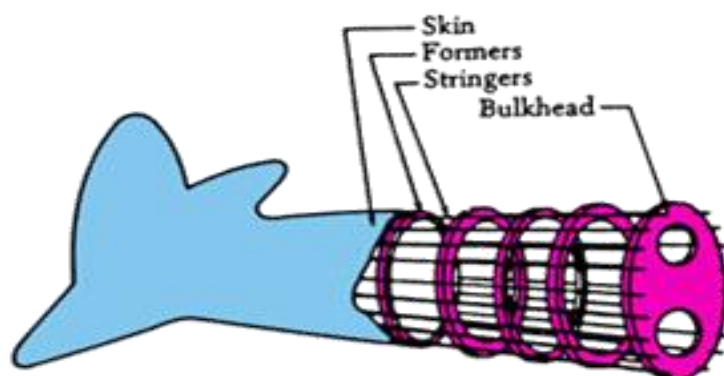
An airframe using monocoque construction.

Semi-monocoque Type

To overcome the strength/weight problem of monocoque construction, a modification called semi-monocoque construction was developed.

It also consists of frame assemblies, bulkheads, and formers as used in the monocoque design but, additionally, the skin is reinforced by longitudinal members called longerons. Longerons usually extend across several frame members and help the skin support primary bending loads. They are typically made of aluminum alloy either of a single piece or a built-up construction.

Stringers are also used in the semimonocoque fuselage. These longitudinal members are typically more numerous and lighter in weight than the longerons. They come in a variety of shapes and are usually made from single piece aluminum alloy extrusions or formed aluminum. Stringers have some rigidity but are chiefly used for giving shape and for attachment of the skin. Stringers and longerons together prevent tension and compression from bending the fuselage.



Semi-monocoque Structure of an airplane

Other bracing between the longerons and stringers can also be used. Often referred to as web members, these additional support pieces may be installed vertically or diagonally. It must be noted that manufacturers use different nomenclature to describe structural members. For example, there is often little difference between some rings, frames, and formers. One

manufacturer may call the same type of brace a ring or a frame. Manufacturer instructions and specifications for a specific aircraft are the best guides.

The semi-monocoque fuselage is constructed primarily of alloys of aluminum and magnesium, although steel and titanium are sometimes found in areas of high temperatures. Individually, no one of the aforementioned components is strong enough to carry the loads imposed during flight and landing. But, when combined, those components form a strong, rigid framework. This is accomplished with gussets, rivets, nuts and bolts, screws, and even friction stir welding.

A gusset is a type of connection bracket that adds strength.



Gussets are used to increase strength.

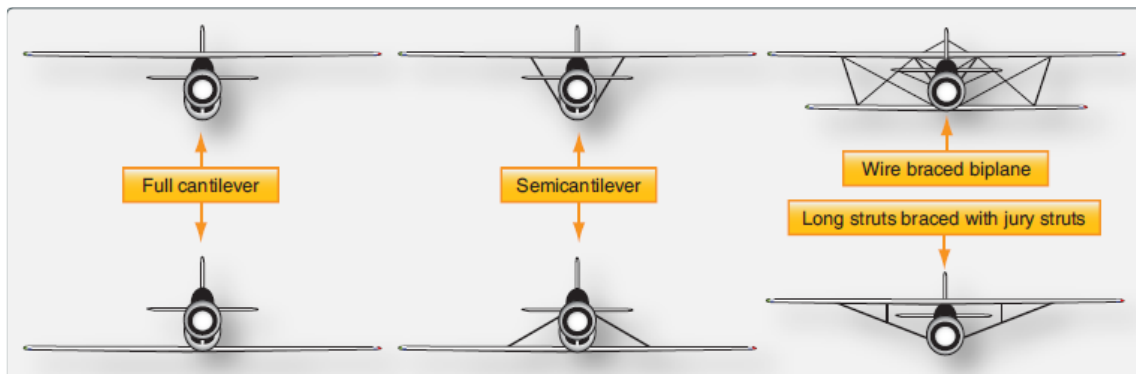
To summarize, in semi-monocoque fuselages, the strong, heavy longerons hold the bulkheads and formers, and these, in turn, hold the stringers, braces, web members, etc. All are designed to be attached together and to the skin to achieve the full strength benefits of semi-monocoque design. It is important to recognize that the metal or covering carries part of the load. The fuselage skin thickness can vary with the load carried and the stresses sustained at a particular location.

The advantages of the semi-monocoque fuselage are many. The bulkheads, frames, stringers, and longerons facilitate the design and construction of a streamlined fuselage that is both rigid and strong. Spreading loads among these structures and the skin means no single piece is failure critical. This means that a semi-monocoque fuselage, because of its stressed-skin construction, may withstand considerable damage and still be strong enough to hold together. Fuselages are generally constructed in two or more sections. On small aircraft, they are generally made in two or three sections, while larger aircraft may be made up of as many as six sections or more before being assembled.

Wing Structure

The wings of an aircraft are designed to lift it into the air. Their particular design for any given aircraft depends on a number of factors, such as size, weight, use of the aircraft, desired speed in flight and at landing, and desired rate of climb. The wings of aircraft are designated left and right, corresponding to the left and right sides of the operator when seated in the cockpit. Often wings are of full cantilever design. This means they are built so that no external bracing is needed. They are supported internally by structural members assisted by the skin of the aircraft. Other aircraft wings use external struts or wires to assist in supporting the wing and carrying the aerodynamic and landing loads. Wing support cables and struts are generally made from steel. Many struts and their attach fittings have fairings to reduce drag. Short, nearly vertical supports called jury struts are found on struts that attach to the wings a

great distance from the fuselage. This serves to subdue strut movement and oscillation caused by the air flowing around the strut in flight. Figure shows samples of wings using external bracing, also known as semicantilever wings. Cantilever wings built with no external bracing are also shown.

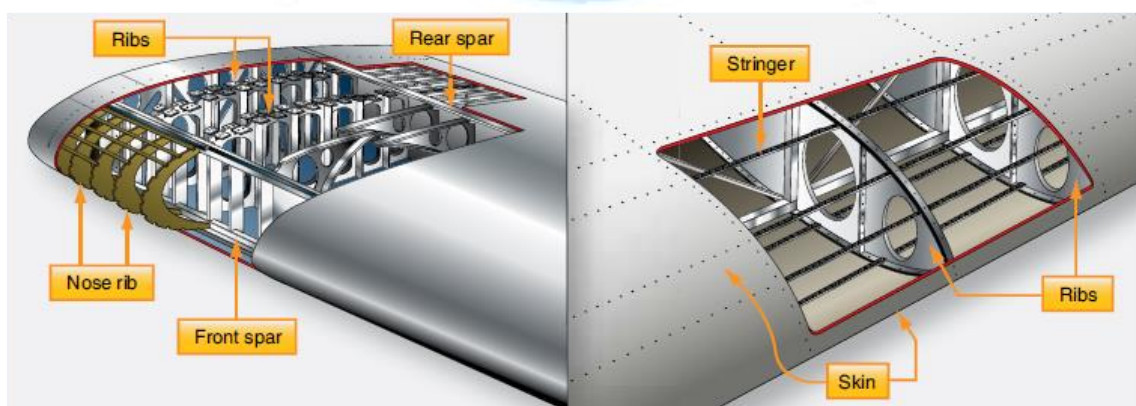


Externally braced wings, also called semicantilever wings, have wires or struts to support the wing. Full cantilever wings have no external bracing and are supported internally.

Aluminum is the most common material from which to construct wings, but they can be wood covered with fabric, and occasionally a magnesium alloy has been used. Moreover, modern aircraft are tending toward lighter and stronger materials throughout the airframe and in wing construction. Wings made entirely of carbon fiber or other composite materials exist, as well as wings made of a combination of materials for maximum strength to weight performance.

The internal structures of most wings are made up of spars and stringers running spanwise and ribs and formers or bulkheads running chordwise (leading edge to trailing edge).

The spars are the principle structural members of a wing. They support all distributed loads, as well as concentrated weights such as the fuselage, landing gear, and engines. The skin, which is attached to the wing structure, carries part of the loads imposed during flight. It also transfers the stresses to the wing ribs. The ribs, in turn, transfer the loads to the wing spars.

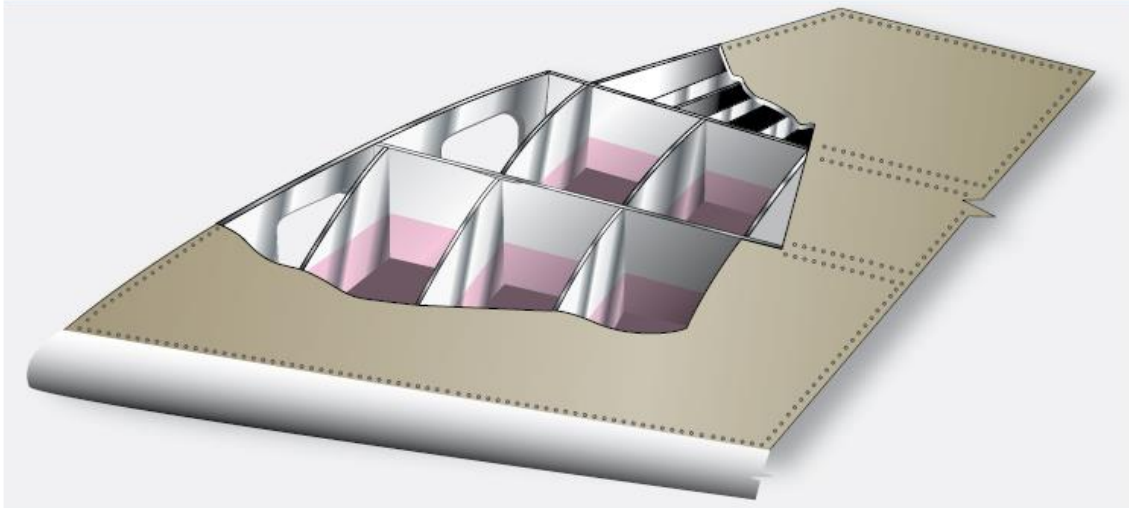


Wing structure nomenclature

In general, wing construction is based on one of three fundamental designs:

1. Monospar
2. Multispar
3. Box beam

Modification of these basic designs may be adopted by various manufacturers. The monospar wing incorporates only one main spanwise or longitudinal member in its construction. Ribs or bulkheads supply the necessary contour or shape to the airfoil. Although the strict monospar wing is not common, this type of design modified by the addition of false spars or light shear webs along the trailing edge for support of control surfaces is sometimes used. The multispar wing incorporates more than one main longitudinal member in its construction. To give the wing contour, ribs or bulkheads are often included.



Box beam construction.

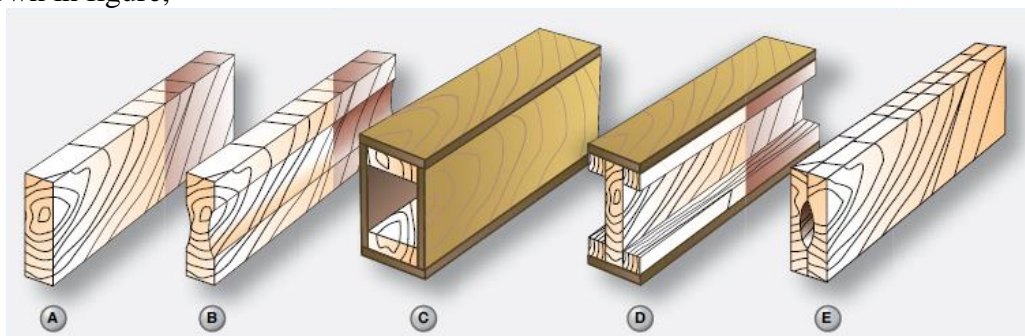
The box beam type of wing construction uses two main longitudinal members with connecting bulkheads to furnish additional strength and to give contour to the wing. A corrugated sheet may be placed between the bulkheads and the smooth outer skin so that the wing can better carry tension and compression loads. In some cases, heavy longitudinal stiffeners are substituted for the corrugated sheets. A combination of corrugated sheets on the upper surface of the wing and stiffeners on the lower surface is sometimes used. Air transport category aircraft often utilize box beam wing construction.

Wing Spars

Spars are the principal structural members of the wing. They correspond to the longerons of the fuselage. They run parallel to the lateral axis of the aircraft, from the fuselage toward the tip of the wing, and are usually attached to the fuselage by wing fittings, plain beams, or a truss. Spars may be made of metal, wood, or composite materials depending on the design criteria of a specific aircraft.

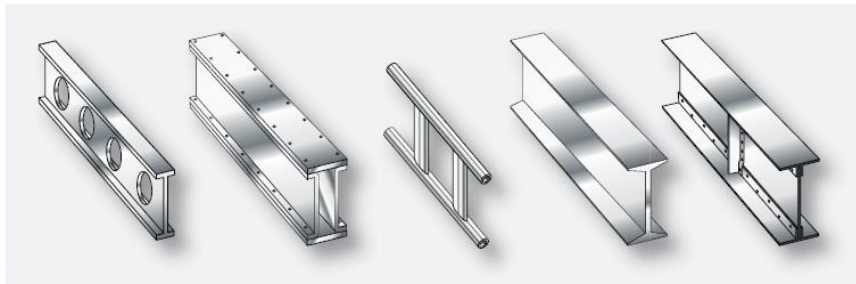
Wooden spars are usually made from spruce. They can be generally classified into four different types by their cross-sectional configuration.

As shown in figure,



They may be (A) solid, (B) box shaped, (C) partly hollow, or (D) in the form of an I-beam. Lamination of solid wood spars is often used to increase strength. Laminated wood can also be found in box shaped spars. The spar in *Figure 1-25E* has had material removed to reduce weight but retains the strength of a rectangular spar. As can be seen, most wing spars are basically rectangular in shape with the long dimension of the cross-section oriented up and down in the wing.

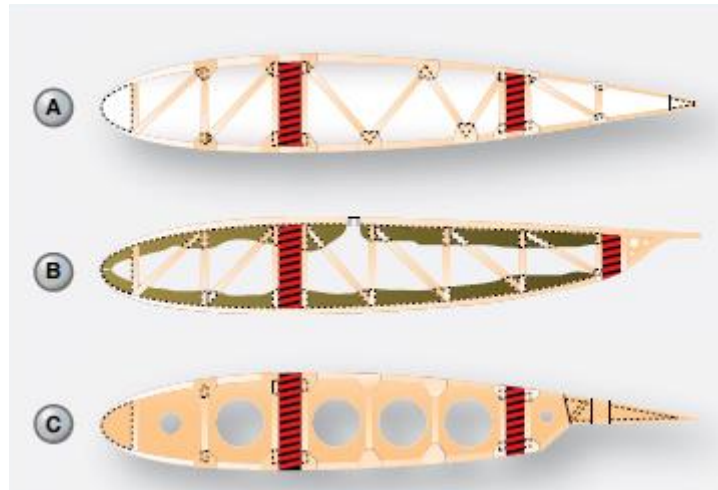
Currently, most manufactured aircraft have wing spars made of solid extruded aluminum or aluminum extrusions riveted together to form the spar. The increased use of composites and the combining of materials should make airmen vigilant for wings spars made from a variety of materials. Figure shows examples of metal wing spar cross-sections.



Wing Ribs

Ribs are the structural crosspieces that combine with spars and stringers to make up the framework of the wing. They usually extend from the wing leading edge to the rear spar or to the trailing edge of the wing. The ribs give the wing its cambered shape and transmit the load from the skin and stringers to the spars. Similar ribs are also used in ailerons, elevators, rudders, and stabilizers. Wing ribs are usually manufactured from either wood or metal. Aircraft with wood wing spars may have wood or metal ribs while most aircraft with metal spars have metal ribs. Wood ribs are usually manufactured from spruce. The three most common types of wooden ribs are the plywood web, the lightened plywood web, and the truss types. Of these three, the truss type is the most efficient because it is strong and lightweight, but it is also the most complex to construct.

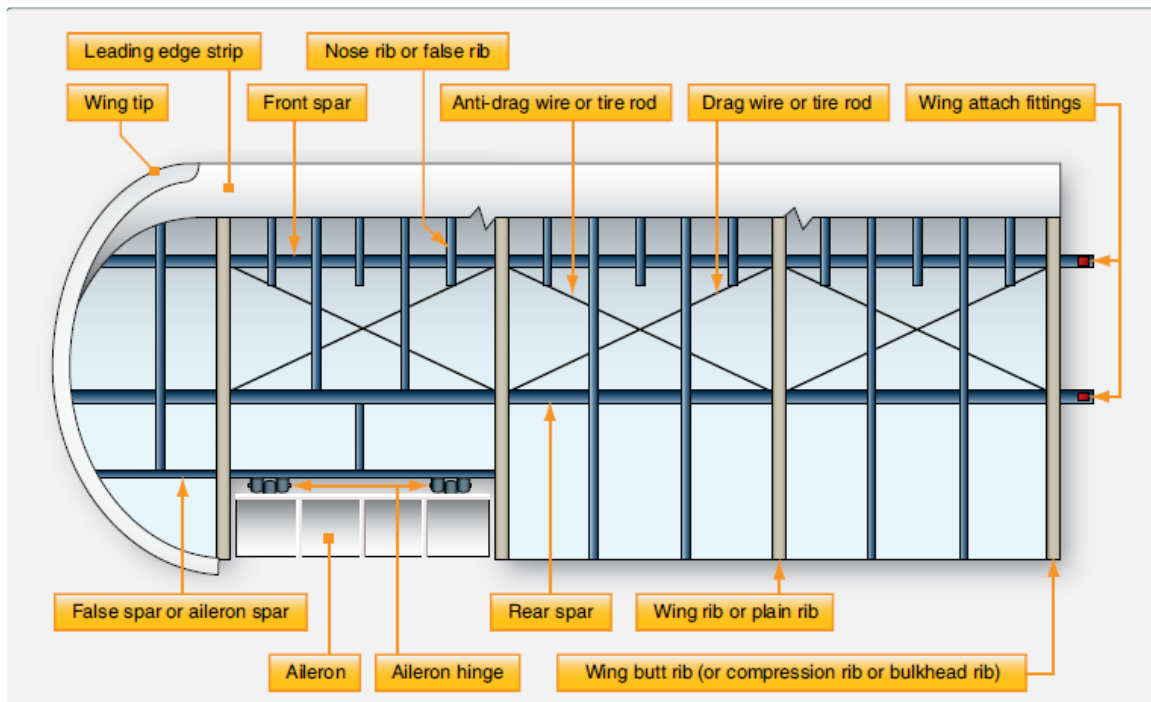
Figure shows wood truss web ribs and a lightened plywood web rib. Wood ribs have a rib cap or cap strip fastened around the entire perimeter of the rib. It is usually made of the same material as the rib itself. The rib cap stiffens and strengthens the rib and provides an attaching surface for the wing covering. In *Figure A*, the cross-section of a wing rib with a truss-type web is illustrated. The dark rectangular sections are the front and rear wing spars. Note that to reinforce the truss, gussets are used. In *Figure B*, a truss web rib is shown with a continuous gusset. It provides greater support throughout the entire rib with very little additional weight. A continuous gusset stiffens the cap strip in the plane of the rib. This aid in preventing buckling and helps to obtain better rib/skin joints where nail-gluing is used. Such a rib can resist the driving force of nails better than the other types.



Continuous gussets are also more easily handled than the many small separate gussets otherwise required. *Figure C* shows a rib with a lighten plywood web. It also contains gussets to support the web/cap strip interface. The cap strip is usually laminated to the web, especially at the leading edge.

A wing rib may also be referred to as a plain rib or a main rib. Wing ribs with specialized locations or functions are given names that reflect their uniqueness. For example, ribs that are located entirely forward of the front spar that are used to shape and strengthen the wing leading edge are called nose ribs or false ribs. False ribs are ribs that do not span the entire wing chord, which is the distance from the leading edge to the trailing edge of the wing. Wing butt ribs may be found at the inboard edge of the wing where the wing attaches to the fuselage. Depending on its location and method of attachment, a butt rib may also be called a bulkhead rib or a compression rib if it is designed to receive compression loads that tend to force the wing spars together. Since the ribs are laterally weak, they are strengthened in some wings by tapes that are woven above and below rib sections to prevent sidewise bending of the ribs. Drag and anti-drag wires may also be found in a wing. In *Figure*, they are shown crisscrossed between the spars to form a truss to resist forces acting on the wing in the direction of the wing chord. These tension wires are also referred to as tie rods. The wire designed to resist the backward forces is called a drag wire; the anti-drag wire resists the forward forces in the chord direction. *Figure illustrates* the structural components of a basic wood wing.

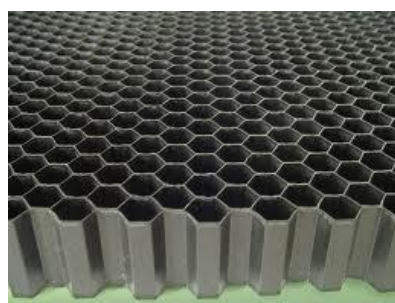
At the inboard end of the wing spars is some form of wing attach fitting as illustrated in *Figure*. These provide a strong and secure method for attaching the wing to the fuselage.



Basic wood wing structure and components.

Honeycomb construction

Honeycomb structures are natural or man-made structures that have the geometry of a honeycomb to allow the minimization of the amount of used material to reach minimal weight and minimal material cost. The geometry of honeycomb structures can vary widely but the common feature of all such structures is an array of hollow cells formed between thin vertical walls. The cells are often columnar and hexagonal in shape. A honeycomb shaped structure provides a material with minimal density and relative high out-of-plane compression properties and out-of-plane shear properties.



Honeycomb structure

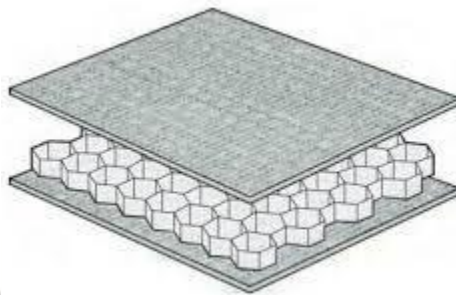
Man-made honeycomb structural materials are commonly made by layering a honeycomb material between two thin layers that provide strength in tension. This forms a plate-like assembly. Honeycomb materials are widely used where flat or slightly curved surfaces are needed and their high strength is valuable. They are widely used in the aerospace industry for this reason, and honeycomb materials in aluminium, fibreglass and advanced composite

materials have been featured in aircraft and rockets since the 1950s. They can also be found in many other fields, from packaging materials in the form of paper-based honeycomb cardboard, to sporting goods like skis and snowboards.

The main use of honeycomb is in structural applications. The standard hexagonal honeycomb is the basic and most common cellular honeycomb configuration.

Honeycomb composites

Natural honeycomb structures occur in many different environments, from beehives to honeycomb weathering in rocks. Based on these, man-made honeycomb structures have been built with similar geometry to allow the reduction of the quantity of material used, and thereby realizing minimal weight and material cost.



Honeycomb structure with panels

Man-made honeycomb structures have an array of hollow cells formed between thin vertical walls, so that the material has minimal density, strength in tension and high out-of-plane compression properties.

Geometric types of honeycomb structures

In geometry, a honeycomb is a space filling or close packing of polyhedral or higher-dimensional cells, so that there are no gaps. It is an example of the more general mathematical tiling or tessellation in any number of dimensions.

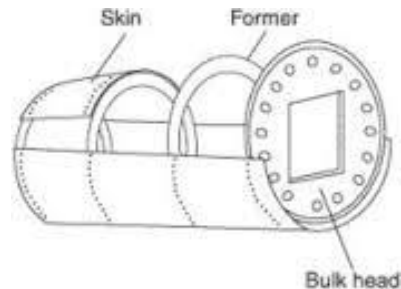
Honeycombs are usually constructed in ordinary Euclidean ("flat") space. They may also be constructed in non-Euclidean spaces, such as hyperbolic honeycombs. Any finite uniform polytope can be projected to its circumsphere to form a uniform honeycomb in spherical space.

Bulkheads

The bulkheads provide shape for the fuselage. The skin of the fuselage to bear the structural load with bulkheads at each end and forming rings at intervals to maintain the skin shape. A hybrid of truss and monocoque, in semi-monocoque construction panels of aerodynamically-curved skin are riveted on top of an internal structure consisting of bulkheads, stringers and followers to absorb the bending forces. The monocoque design uses stressed skin to support

almost all imposed loads. The true monocoque construction mainly consists of the skin, formers, and bulkheads. The formers and bulkheads provide shape for the fuselage.

The semi-monocoque system uses a substructure to which the airplane's skin is attached. The substructure, which consists of bulkheads and/or formers of various sizes and stringers, reinforces the stressed skin by taking some of the bending stress from the fuselage.



Bulkhead

Stringers

Stringer is a stiffening member which supports a section of the load carrying skin, to prevent buckling under compression or shear loads. Stringers keep the skin from bending. Longitudinal members are sometimes referred to as longitudinal, stringers, or stiffeners.

Role of Stringers in Aircraft Wings

In aircraft construction, a stringer is a thin strip of material to which the skin of the aircraft is fastened. In the fuselage, stringers are attached to formers (also called frames) and run in the longitudinal direction of the aircraft. They are primarily responsible for transferring the aerodynamic loads acting on the skin onto the frames and formers. In the wings or horizontal stabilizer, longerons run span wise and attach between the ribs. The primary function here also is to transfer the bending loads acting on the wings onto the ribs and spar.

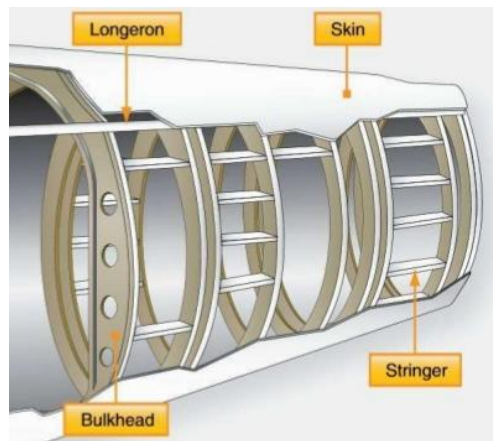
Different Shapes of Stringers

The stringers on an aluminum airplane are normally extruded or bent into shape, and can have a number of different cross sections.

Typically Shapes for stringers are

- i. HAT Stringer
- ii. I-Stringer
- iii. J-Stringer
- iv. Y-Stringer
- v. Z Stringer.

On wooden airplanes, they are usually spruce square or rectangular cross sections.

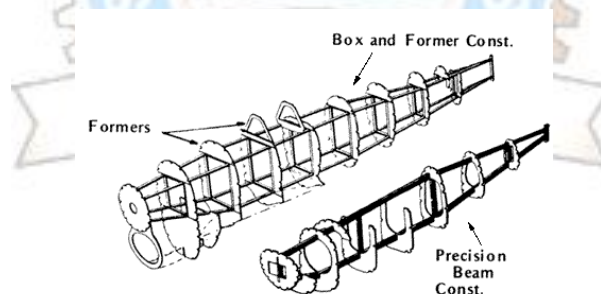


Stringers

Formers

A former is a structural member of an aircraft fuselage, of which a typical fuselage has a series from the nose to the empennage, typically perpendicular to the longitudinal axis of the aircraft. The primary purpose of formers is to establish the shape of the fuselage and reduce the column length of stringers to prevent instability. Formers are typically attached to longerons, which support the skin of the aircraft.

The Former-and-Longeron technique was adopted from boat construction (also called stations and stringers), and was typical of light aircraft built until the advent of structural skins, such as fibreglass and other composite materials.



Longerons

A longeron is part of the structure of an aircraft, designed to add rigidity and strength to the frame. It also creates a point of attachment for other structural supports, as well as the skin of the aircraft. They provide lengthwise support and the number of longerons present in an aircraft varies, depending on the size and how it is designed. Like other structural members, they need to be checked periodically for signs of damage that might compromise their function.

Materials like wood, carbon fiber, and metal can be used in longeron construction. Older aircraft were made almost entirely with wood, while it is a more rare construction material today because it does not provide as much strength and flexibility as other materials. The

materials are carefully tested before being installed to make sure there are no cracks or other flaws that might cause them to fail once in place or while the plane is in use.

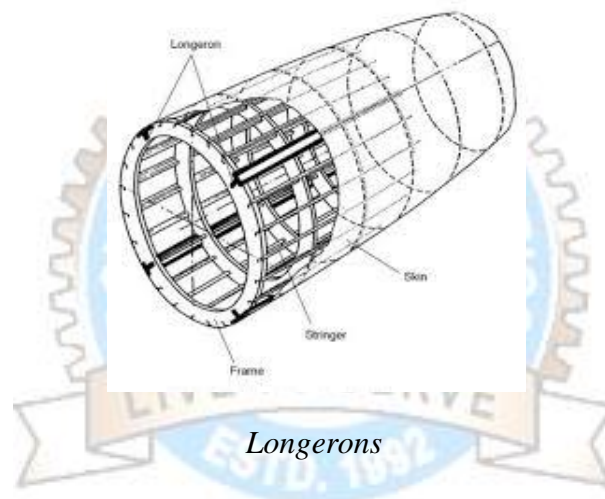
Each longeron attaches directly to the frame of the aircraft using bolts. In some planes, shorter longitudinal supports called stiffeners or stringers are fastened to the longerons. Confusingly, these terms are also sometimes used as alternate names for the longeron. The skin, whether made from metal, leather, canvas, or other materials, can be attached to the aircraft once the longerons are in place. Insulating material and lining may be installed on the other side, depending on how the plane is going to be used.

Longerons functions

They resist bending and axial loads along with the skin.

They divide the skin into small panels and thereby increase its buckling and failure stresses.

They act with the skin in resisting axial loads caused by pressurization.



SCHOOL OF AERONAUTICS (NEEMRANA)

UNIT-III NOTES

FACULTY NAME: D.SUKUMAR.

CLASS: B.Tech AERONAUTICAL

SUBJECT CODE: 6AN5

SEMESTER: VI

SUBJECT NAME: AIRCRAFT DESIGN

LANDING GEARS:

Different kinds of landing gears, and associated arrangement for civil and military airplanes. Preliminary calculations for locating main and nose landing gears.

INTRODUCTION:

Aircraft landing gear supports the entire weight of an aircraft during landing and ground operations. They are attached to primary structural members of the aircraft. The type of gear depends on the aircraft design and its intended use. Most landing gear has wheels to facilitate operation to and from hard surfaces, such as airport runways. Other gear feature skids for this purpose, such as those found on helicopters, balloon gondolas, and in the tail area of some tail dragger aircraft. Aircraft that operate to and from frozen lakes and snowy areas may be equipped with landing gear that have skis. Aircraft that operate to and from the surface of water have pontoon-type landing gear. Regardless of the type of landing gear utilized, shock absorbing equipment, brakes, retraction mechanisms, controls, warning devices, cowling, fairings, and structural members necessary to attach the gear to the aircraft are considered parts of the landing gear system.



Basic landing gear types include those with wheels (a), skids (b), skis (c), and floats or pontoons (d).

Numerous configurations of landing gear types can be found. Additionally, combinations of two types of gear are common. Amphibious aircraft are designed with gear that allows landings to be made on water or dry land. The gear features pontoons for water landing with extendable wheels for landings on hard surfaces. A similar system is used to allow the use of skis and wheels on aircraft that operate on both slippery, frozen surfaces and dry runways. Typically, the skis are retractable to allow use of the wheels when needed.



An amphibious aircraft with retractable wheels (left) and an aircraft with retractable skis (right).

Landing Gear Arrangement

Three basic arrangements of landing gear are used: tail wheel type landing gear (also known as conventional gear), tandem landing gear, and tricycle-type landing gear.

Tail Wheel-Type Landing Gear

Tail wheel-type landing gear is also known as conventional gear because many early aircraft use this type of arrangement. The main gear are located forward of the center of gravity, causing the tail to require support from a third wheel assembly. A few early aircraft designs use a skid rather than a tail wheel. This helps slow the aircraft upon landing and provides directional stability. The resulting angle of the aircraft fuselage, when fitted with conventional gear, allows the use of a long propeller that compensates for older, underpowered engine design. The increased clearance of the forward fuselage offered by tail wheel-type landing gear is also advantageous when operating in and out of non-paved runways. Today, aircraft are manufactured with conventional gear for this reason and for the weight savings accompanying the relatively light tail wheel assembly.



Tail wheel configuration landing gear on a DC-3 (left) and a STOL Maule MX-7-235 Super Rocket.

The proliferation of hard surface runways has rendered the tail skid obsolete in favor of the tail wheel. Directional control is maintained through differential braking until the speed of the aircraft enables control with the rudder. A steerable tail wheel, connected by cables to the rudder or rudder pedals, is also a common design. Springs are incorporated for dampening.



The steerable tail wheel of a Pitts Special.

Tandem Landing Gear

Few aircraft are designed with tandem landing gear. As the name implies, this type of landing gear has the main gear and tail gear aligned on the longitudinal axis of the aircraft. Sailplanes commonly use tandem gear, although many only have one actual gear forward on the fuselage with a skid under the tail. A few military bombers, such as the B-47 and the B-52, have tandem gear, as does the U2 spy plane. The VTOL Harrier has tandem gear but uses small outrigger gear under the wings for support. Generally, placing the gear only under the fuselage facilitates the use of very flexible wings.



Tandem landing gear along the longitudinal axis of the aircraft permits the use of flexible wings on sailplanes (left) and selects military aircraft like the B-52 (center). The VTOL Harrier (right) has tandem gear with outrigger-type gear.

Tricycle-Type Landing Gear

The most commonly used landing gear arrangement is the tricycle-type landing gear. It is comprised of main gear and nose gear.

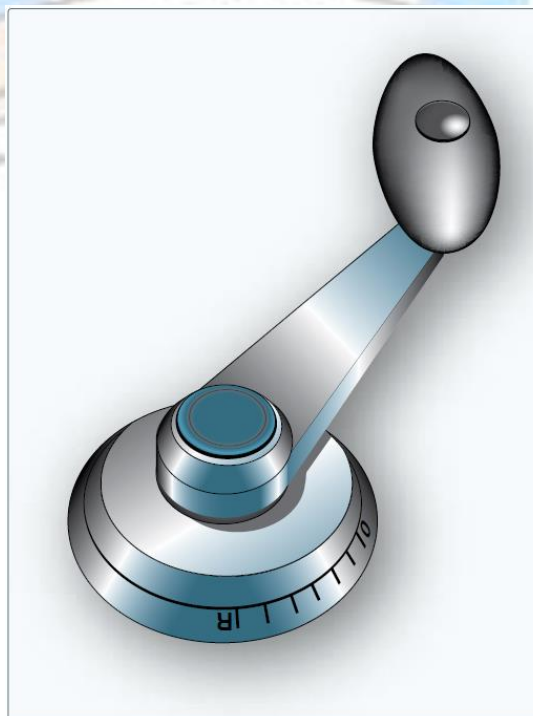


Tricycle-type landing gear with dual main wheels on a Learjet (left) and a Cessna 172, also with tricycle gear (right).

Tricycle-type landing gear is used on large and small aircraft with the following benefits:

1. Allows more forceful application of the brakes without nosing over when braking, which enables higher landing speeds.
2. Provides better visibility from the flight deck, especially during landing and ground maneuvering.
3. Prevents ground-looping of the aircraft. Since the aircraft center of gravity is forward of the main gear, forces acting on the center of gravity tend to keep the aircraft moving forward rather than looping, such as with a tail wheel-type landing gear.

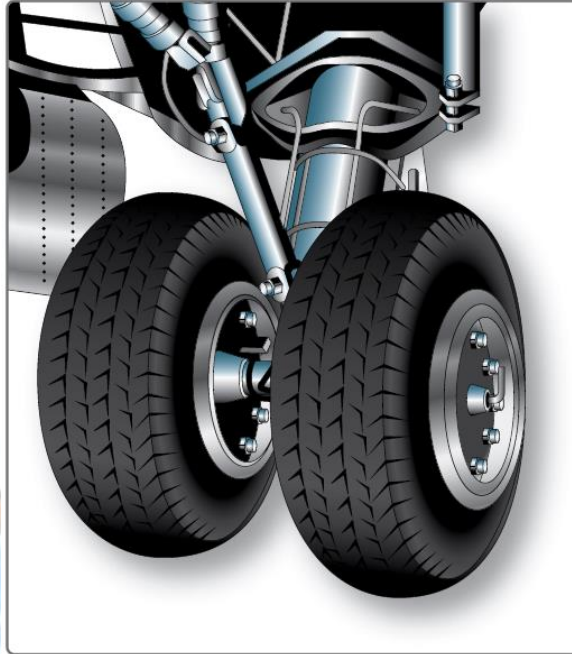
The nose gear of a few aircraft with tricycle-type landing gear is not controllable. It simply casters as steering is accomplished with differential braking during taxi. However, nearly all aircraft have steerable nose gear. On light aircraft, the nose gear is directed through mechanical linkage to the rudder pedals. Heavy aircraft typically utilize hydraulic power to steer the nose gear. Control is achieved through an independent tiller in the flight deck.



A nose wheel steering tiller located on the flight deck.

The main gear on a tricycle-type landing gear arrangement is attached to reinforced wing structure or fuselage structure.

The number and location of wheels on the main gear vary. Many main gears have two or more wheels.



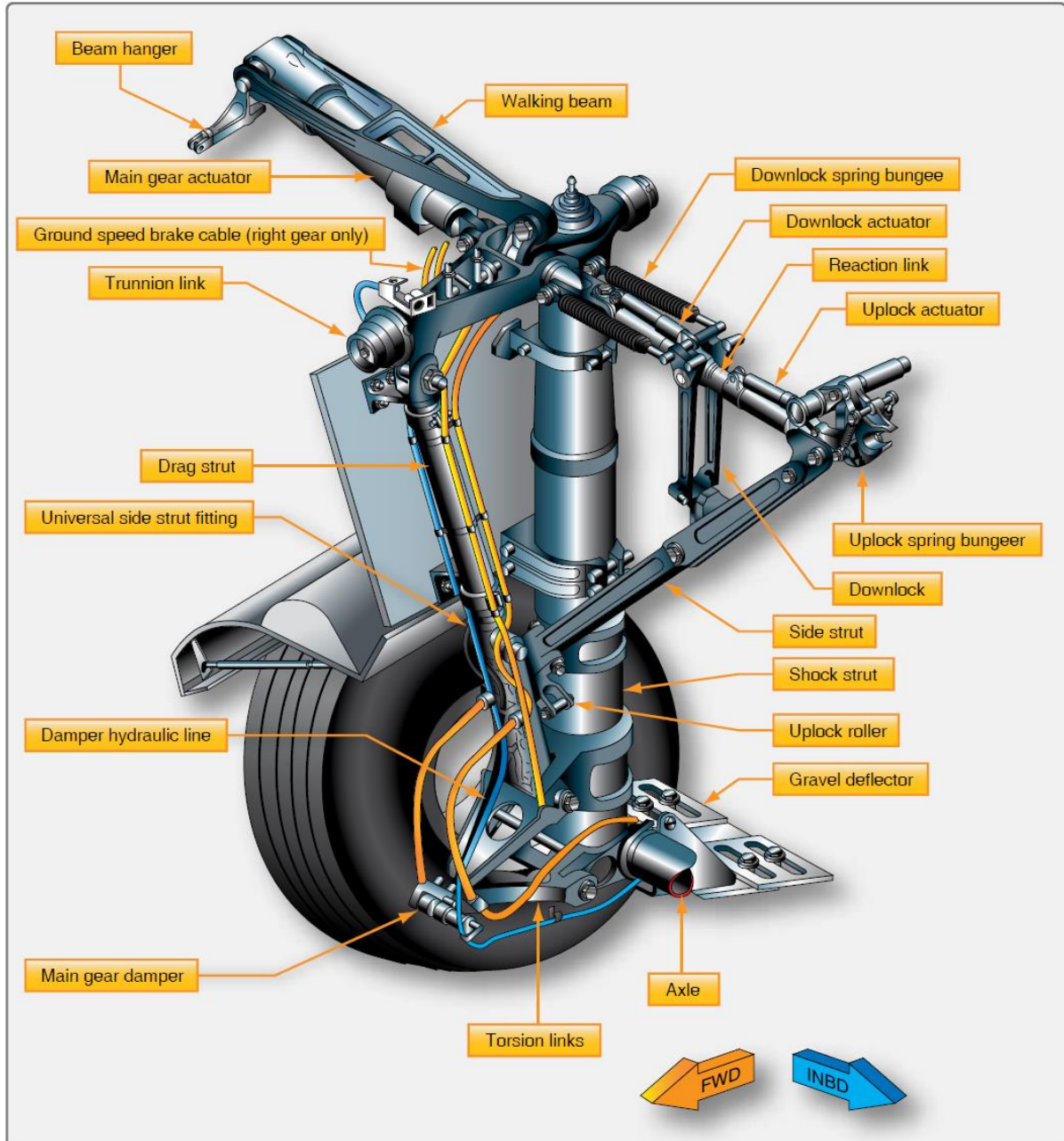
Dual main gear of a tricycle-type landing gear.

Multiple wheels spread the weight of the aircraft over a larger area. They also provide a safety margin should one tire fail. Heavy aircraft may use four or more wheel assemblies on each main gear. When more than two wheels are attached to a landing gear strut, the attaching mechanism is known as a bogie. The number of wheels included in the bogie is a function of the gross design weight of the aircraft and the surface type on which the loaded aircraft is required to land. *Figure below* illustrates the triple bogie main gear of a Boeing 777.



Triple bogie main landing gear assembly on a Boeing 777.

The tricycle-type landing gear arrangement consists of many parts and assemblies. These include air/oil shock struts, gear alignment units, support units, retraction and safety devices, steering systems, wheel and brake assemblies, etc. A main landing gear of a transport category aircraft is illustrated in *Figure below* with many of the parts identified as an introduction to landing gear nomenclature.



Nomenclature of a main landing gear bogie truck.

Fixed and Retractable Landing Gear

Further classification of aircraft landing gear can be made into two categories: fixed and retractable. Many small, single engine light aircraft have fixed landing gear, as do a few light twins. This means the gear is attached to the airframe and remains exposed to the slipstream as the aircraft is flown. Mechanisms to retract and stow the landing gear to eliminate parasite

drag add weight to the aircraft. On slow aircraft, the penalty of this added weight is not overcome by the reduction of drag, so fixed gear is used. As the speed of the aircraft increases, the drag caused by the landing gear becomes greater and a means to retract the gear to eliminate parasite drag is required, despite the weight of the mechanism.

A great deal of the parasite drag caused by light aircraft landing gear can be reduced by building gear as aerodynamically as possible and by adding fairings or wheel pants to streamline the airflow past the protruding assemblies. A small, smooth profile to the oncoming wind greatly reduces landing gear parasite drag. *Figure below* illustrates a Cessna aircraft landing gear used on many of the manufacturer's light planes.

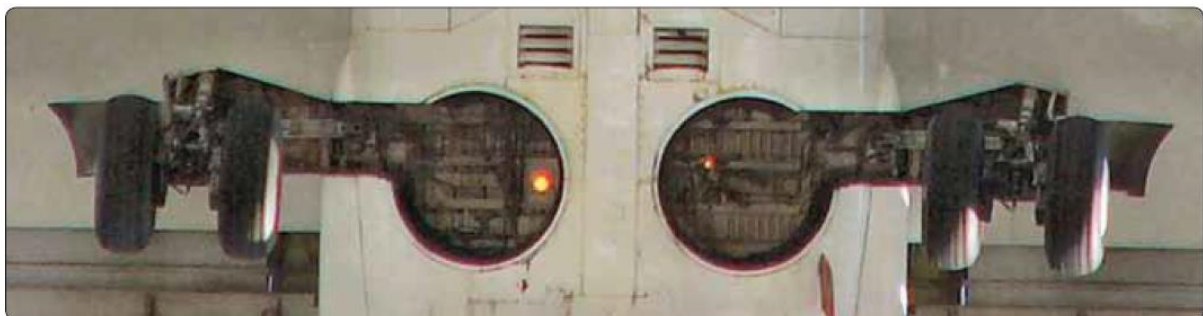


Wheel fairings, or pants, and low profile struts reduce parasite drag on fixed gear aircraft.

The thin cross section of the spring steel struts combine with the fairings over the wheel and brake assemblies to raise performance of the fixed landing gear by keeping parasite drag to a minimum.

Retractable landing gear stows in fuselage or wing compartments while in flight. Once in these wheel wells, gear is out of the slipstream and does not cause parasite drag.

Most retractable gear has a close fitting panel attached to them that fairs with the aircraft skin when the gear is fully retracted. *[Figure below]* Other aircraft have separate doors that open, allowing the gear to enter or leave, and then close again.



The retractable gear of a Boeing 737 fair into recesses in the fuselage. Panels attached to the landing gear provide smooth airflow over the struts. The wheel assemblies mate with seals to provide aerodynamic flow without doors.

Shock Absorbing and Non-Shock Absorbing Landing Gear

In addition to supporting the aircraft for taxi, the forces of impact on an aircraft during landing must be controlled by the landing gear.

This is done in two ways:

- 1) The shock energy is altered and transferred throughout the airframe at a different rate and time than the single strong pulse of impact, and
- 2) The shock is absorbed by converting the energy into heat energy.

Leaf-Type Spring Gear

Many aircraft utilize flexible spring steel, aluminum, or composite struts that receive the impact of landing and return it to the airframe to dissipate at a rate that is not harmful. The gear flexes initially and forces are transferred as it returns to its original position. *[Figure below]* The most common example of this type of non-shock absorbing landing gear is the thousands of single-engine Cessna aircraft that use it. Landing gear struts of this type made from composite materials are lighter in weight with greater flexibility and do not corrode.



Non-shock absorbing struts made from steel, aluminum, or composite material transfer the impact forces of landing to the airframe at a non-damaging rate.

Rigid

Before the development of curved spring steel landing struts, many early aircraft were designed with rigid, welded steel landing gear struts. Shock load transfer to the airframe is direct with this design. Use of pneumatic tires aids in softening the impact loads. *[Figure below]* Modern aircraft that use skid-type landing gear make use of rigid landing gear with no significant ill effects. Rotorcraft, for example, typically experience low impact landings that are able to be directly absorbed by the airframe through the rigid gear (skids).



Rigid steel landing gear is used on many early aircraft.

Bungee Cord

The use of bungee cords on non-shock absorbing landing gear is common. The geometry of the gear allows the strut assembly to flex upon landing impact. Bungee cords are positioned between the rigid airframe structure and the flexing gear assembly to take up the loads and return them to the airframe at a non-damaging rate. The bungees are made of many individual small strands of elastic rubber that must be inspected for condition. Solid, donut-type rubber cushions are also used on some aircraft landing gear. [Figure below]



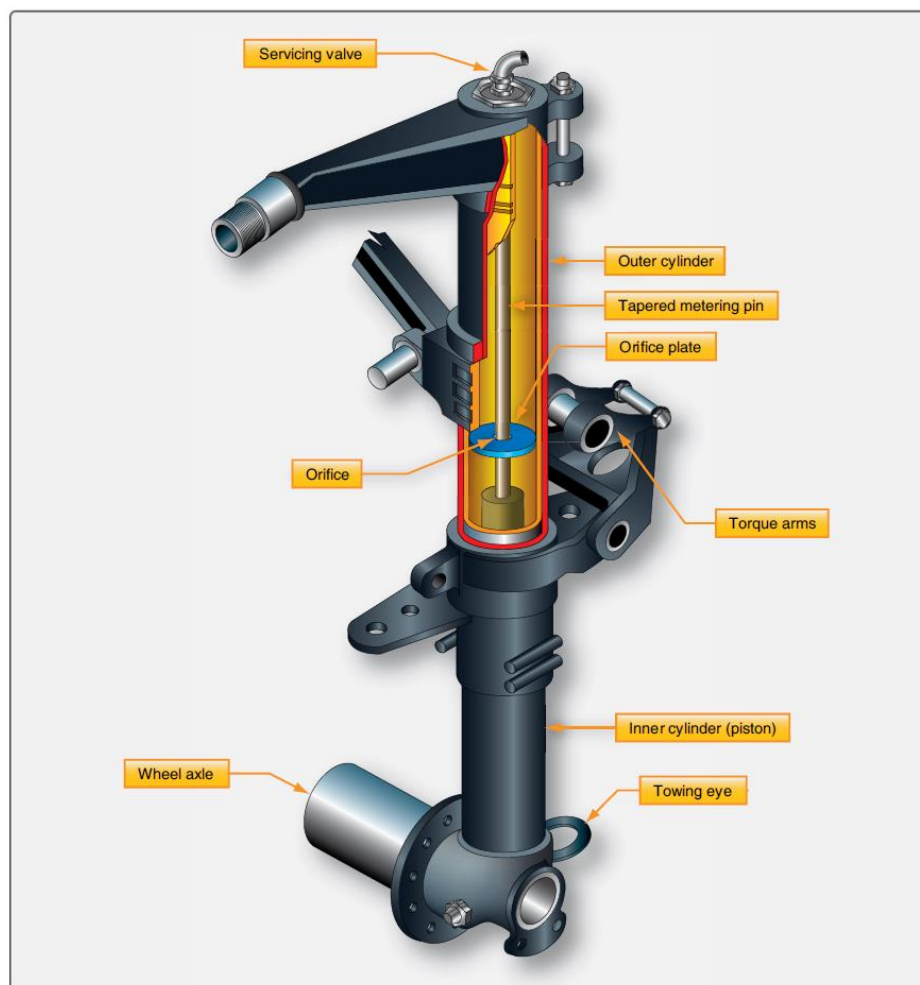
Piper Cub bungee cord landing gear transfer landing loads to the airframe (left and center). Rubber, donut-type shock transfer is used on some Mooney aircraft (right).

Shock Struts

True shock absorption occurs when the shock energy of landing impact is converted into heat energy, as in a shock strut landing gear. This is the most common method of landing shock dissipation in aviation. It is used on aircraft of all sizes. Shock struts are self-contained hydraulic units that support an aircraft while on the ground and protect the structure during landing. They must be inspected and serviced regularly to ensure proper operation.

There are many different designs of shock struts, but most operate in a similar manner. The following discussion is general in nature. For information on the construction, operation, and servicing of a specific aircraft shock, consult the manufacturer's maintenance instructions.

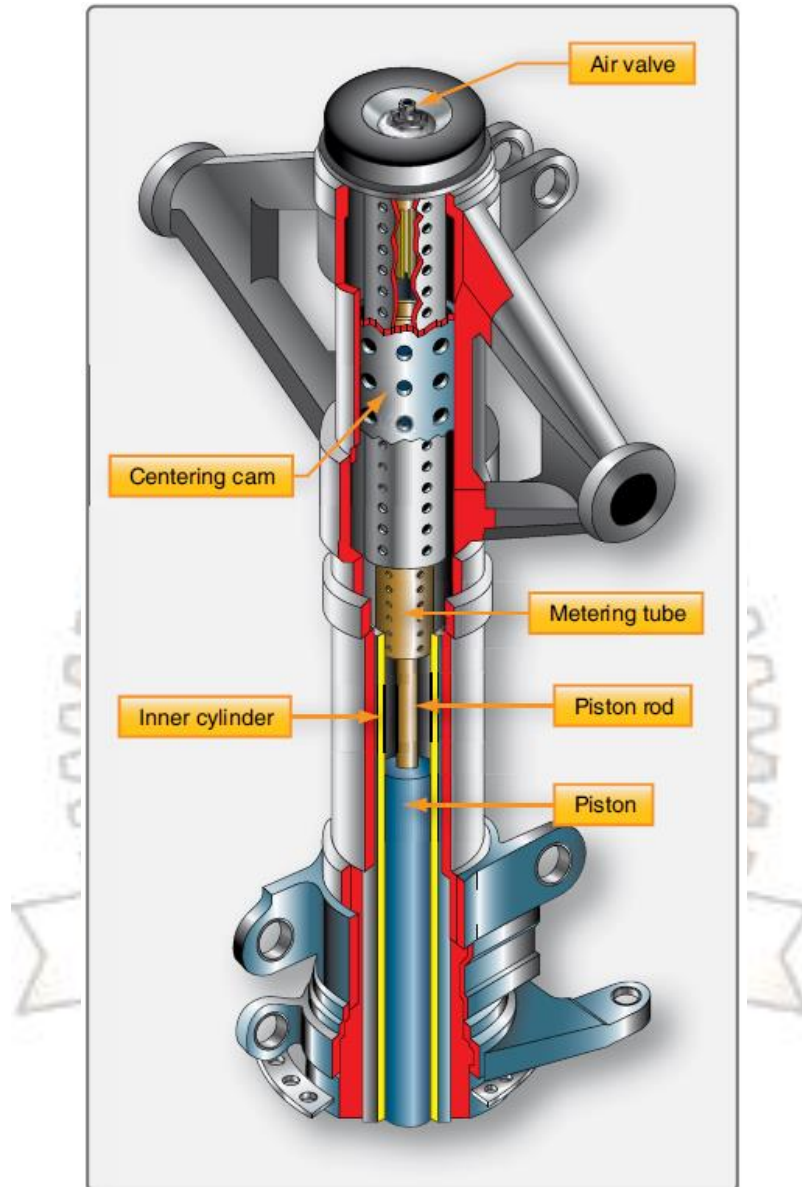
A typical pneumatic/hydraulic shock strut uses compressed air or nitrogen combined with hydraulic fluid to absorb and dissipate shock loads. It is sometimes referred to as an air/oil or oleo strut. A shock strut is constructed of two telescoping cylinders or tubes that are closed on the external ends. The upper cylinder is fixed to the aircraft and does not move. The lower cylinder is called the piston and is free to slide in and out of the upper cylinder. Two chambers are formed. The lower chamber is always filled with hydraulic fluid and the upper chamber is filled with compressed air or nitrogen. An orifice located between the two cylinders provides a passage for the fluid from the bottom chamber to enter the top cylinder chamber when the strut is compressed.



A landing gear shock strut with a metering pin to control the flow of hydraulic fluid from the lower chamber to the upper chamber during compression.

Most shock struts employ a metering pin similar to that shown in *Figure above* for controlling the rate of fluid flow from the lower chamber into the upper chamber. During the compression stroke, the rate of fluid flow is not constant. It is automatically controlled by the taper of the metering pin in the orifice. When a narrow portion of the pin is in the orifice, more fluid can pass to the upper chamber. As the diameter of the portion of the metering pin in the orifice increases, less fluid passes. Pressure build-up caused by strut compression and

the hydraulic fluid being forced through the metered orifice causes heat. This heat is converted impact energy. It is dissipated through the structure of the strut. On some types of shock struts, a metering tube is used. The operational concept is the same as that in shock struts with metering pins, except the holes in the metering tube control the flow of fluid from the bottom chamber to the top chamber. [Figure below]

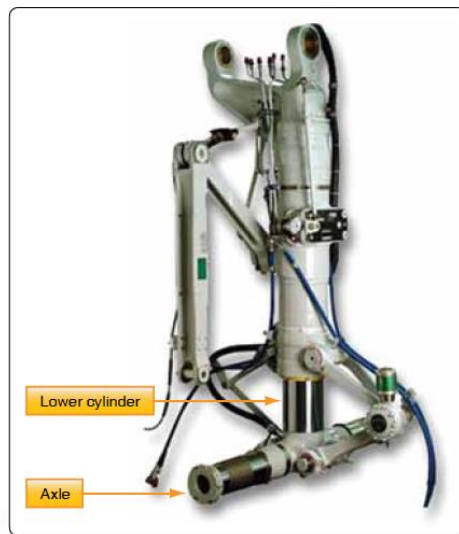


Some landing gear shock struts use an internal metering tube rather than a metering pin to control the flow of fluid from the bottom cylinder to the top cylinder.

Upon lift off or rebound from compression, the shock strut tends to extend rapidly. This could result in a sharp impact at the end of the stroke and damage to the strut. It is typical for shock struts to be equipped with a damping or snubbing device to prevent this. A recoil valve on the piston or a recoil tube restricts the flow of fluid during the extension stroke, which slows the motion and prevents damaging impact forces.

Most shock struts are equipped with an axle as part of the lower cylinder to provide installation of the aircraft wheels.

Shock struts without an integral axle have provisions on the end of the lower cylinder for installation of the axle assembly. Suitable connections are provided on all shock strut upper cylinders to attach the strut to the airframe. [Figure below]



Axles machined out of the same material as the landing gear lower cylinder.

The upper cylinder of a shock strut typically contains a valve fitting assembly. It is located at or near the top of the cylinder.

The valve provides a means of filling the strut with hydraulic fluid and inflating it with air or nitrogen as specified by the manufacturer. A packing gland is employed to seal the sliding joint between the upper and lower telescoping cylinders. It is installed in the open end of the outer cylinder. A packing gland wiper ring is also installed in a groove in the lower bearing or gland nut on most shock struts. It is designed to keep the sliding surface of the piston from carrying dirt, mud, ice, and snow into the packing gland and upper cylinder. Regular cleaning of the exposed portion of the strut piston helps the wiper do its job and decreases the possibility of damage to the packing gland, which could cause the strut to a leak.

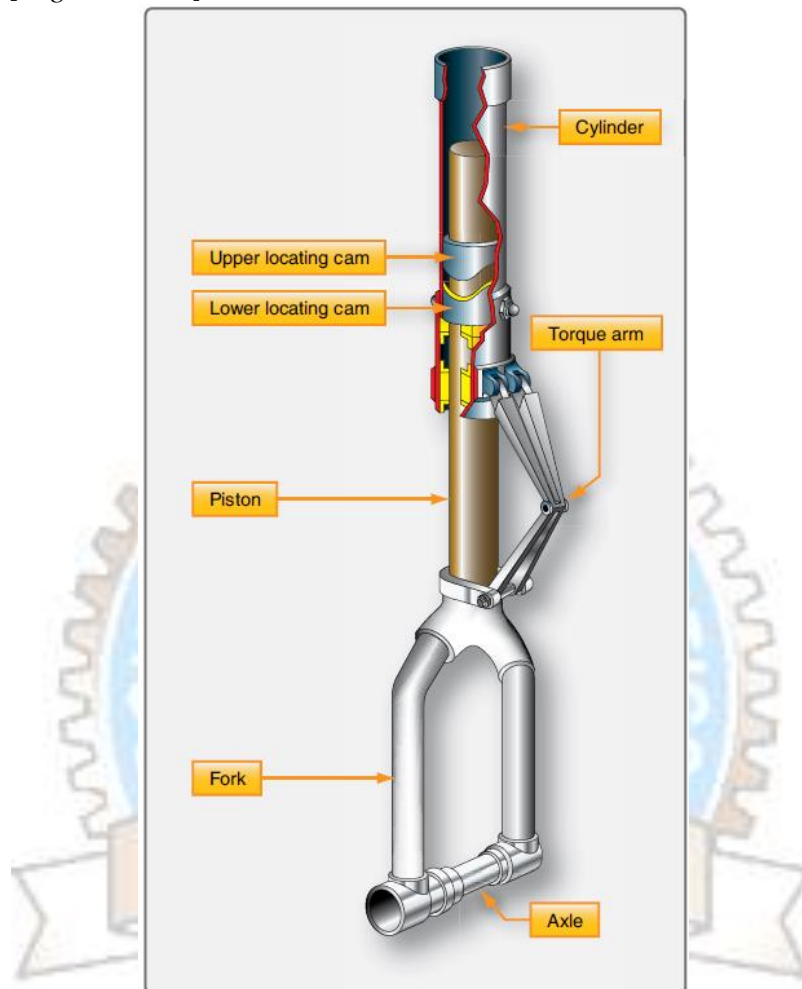
To keep the piston and wheels aligned, most shock struts are equipped with torque links or torque arms. One end of the links is attached to the fixed upper cylinder. The other end is attached to the lower cylinder (piston) so it cannot rotate.

This keeps the wheels aligned. The links also retain the piston in the end of the upper cylinder when the strut is extended, such as after takeoff. [Figure below]



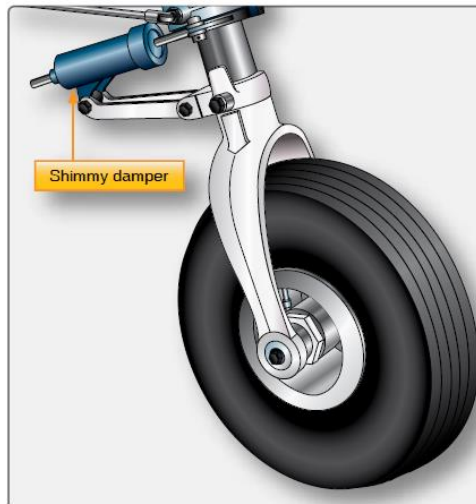
Torque links align the landing gear and retain the piston in the upper cylinder when the strut is extended.

Nose gear shock struts are provided with a locating cam assembly to keep the gear aligned. A cam protrusion is attached to the lower cylinder, and a mating lower cam recess is attached to the upper cylinder. These cams line up the wheel and axle assembly in the straight-ahead position when the shock strut is fully extended. This allows the nose wheel to enter the wheel well when the nose gear is retracted and prevents structural damage to the aircraft. It also aligns the wheels with the longitudinal axis of the aircraft prior to landing when the strut is fully extended. [Figure below]



An upper locating cam mates into a lower cam recess when the nose landing gear shock strut is extended before landing and before the gear is retracted into the wheel well.

Many nose gear shock struts also have attachments for the installation of an external shimmy damper. [Figure below]

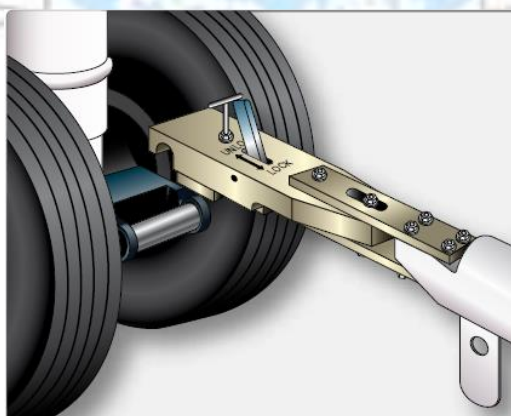


A shimmy damper helps control oscillations of the nose gear.

Nose gear struts are often equipped with a locking or disconnect pin to enable quick turning of the aircraft while towing or positioning the aircraft when on the ramp or in a hangar. Disengagement of this pin allows the wheel fork spindle on some aircraft to rotate 360°, thus enabling the aircraft to be turned in a tight radius. At no time should the nose wheel of any aircraft be rotated beyond limit lines marked on the airframe.

Nose and main gear shock struts on many aircraft are also equipped with jacking points and towing lugs. Jacks should always be placed under the prescribed points. When towing lugs are provided, the towing bar should be attached only to these lugs. *[Figure below]*

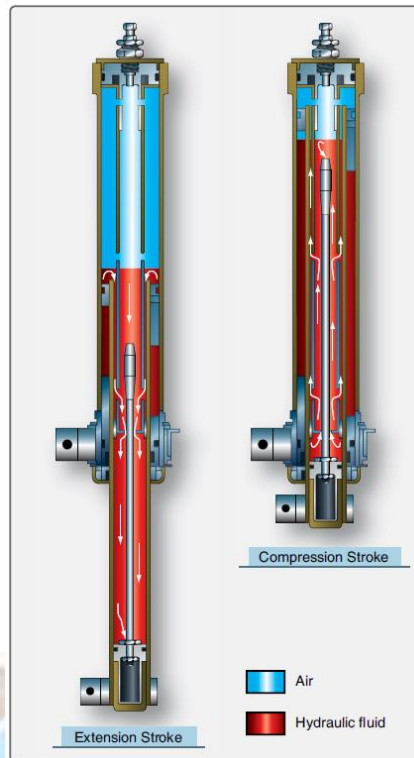
Shock struts contain an instruction plate that gives directions for filling the strut with fluid and for inflating the strut. The instruction plate is usually attached near filler inlet and air valve assembly. It specifies the correct type of hydraulic fluid to use in the strut and the pressure to which the strut should be inflated. It is of utmost importance to become familiar with these instructions prior to filling a shock strut with hydraulic fluid or inflating it with air or nitrogen.



A towing lug on a landing gear is the designed means for attaching a tow bar.

Shock Strut Operation

Figure below illustrates the inner construction of a shock strut.



Fluid flow during shock strut operation is controlled by the taper of the metering pin in the shock strut orifice.

Arrows show the movement of the fluid during compression and extension of the strut. The compression stroke of the shock strut begins as the aircraft wheels touch the ground. As the center of mass of the aircraft moves downward, the strut compresses, and the lower cylinder or piston is forced upward into the upper cylinder. The metering pin is therefore moved up through the orifice. The taper of the pin controls the rate of fluid flow from the bottom cylinder to the top cylinder at all points during the compression stroke. In this manner, the greatest amount of heat is dissipated through the walls of the strut. At the end of the downward stroke, the compressed air in the upper cylinder is further compressed which limits the compression stroke of the strut with minimal impact. During taxi operations, the air in the tires and the strut combine to smooth out bumps.

Insufficient fluids, or air in the strut, cause the compression stroke to not be properly limited. The strut could bottom out, resulting in impact forces to be transferred directly to the airframe through the metallic structure of the strut. In a properly serviced strut, the extension stroke of the shock strut operation occurs at the end of the compression stroke.

Energy stored in the compressed air in the upper cylinder causes the aircraft to start moving upward in relation to the ground and lower strut cylinder as the strut tries to rebound to its normal position. Fluid is forced back down into the lower cylinder through restrictions and snubbing orifices. The snubbing of fluid flow during the extension stroke dampens the strut rebound and reduces oscillation caused by the spring action of the compressed air. A sleeve, spacer, or bumper ring incorporated into the strut limits the extension stroke.

Efficient operation of the shock struts requires that proper fluid and air pressure be maintained. To check the fluid level, most struts need to be deflated and compressed into the fully compressed position. Deflating a shock strut can be a dangerous operation. The technician must be thoroughly familiar with the operation of the high-pressure service valve found at the top of the strut's upper cylinder. Refer to the manufacturer's instructions for proper deflating technique of the strut in question and follow all necessary safety precautions.

LANDING GEAR CONCEPT SELECTION:

Introduction:

The design and positioning of the landing gear are determined by the unique characteristics associated with each aircraft, *i.e.*, geometry, weight, and mission requirements. Given the weight and *cg* range of the aircraft, suitable configurations are identified and reviewed to determine how well they match the airframe structure, flotation, and operational requirements. The essential features, *e.g.*, the number and size of tires and wheels, brakes, and shock absorption mechanism, must be selected in accordance with industry and federal standards discussed in the following chapters before an aircraft design progresses past the concept formulation phase, after which it is often very difficult and expensive to change the design [19]. Three examples of significant changes made after the initial design include the DC-10-30, which added the third main gear to the fuselage, the Airbus A340, where the main gear centre bogie increased from two to four wheels in the -400 series, and the Airbus A-300, where the wheels were spread further apart on the bogie to meet LaGuardia Airport flotation limits for US operators.

Based on the design considerations as discussed in this chapter, algorithms were developed to establish constraint boundaries for use in positioning the landing gear, as well as to determine whether the design characteristics violate the specified requirements.

The considerations include stability at takeoff/touchdown and during taxiing, braking and steering qualities, gear length, attachment scheme, and ground maneuvers.

Configuration Selection:

The nose wheel tricycle undercarriage has long been the preferred configuration for passenger transports. It leads to a nearly level fuselage and consequently the cabin floor when the aircraft is on the ground. The most attractive feature of this type of undercarriages is the improved stability during braking and ground maneuvers. Under normal landing attitude, the relative location of the main assembly to the aircraft *cg* produces a nose-down pitching moment upon touchdown. This moment helps to reduce the angle of attack of the aircraft and thus the lift generated by the wing. In addition, the braking forces, which act behind the aircraft *cg*, have a stabilizing effect and thus enable the pilot to make full use of the brakes. These factors all contribute to a shorter landing field length requirement.

The primary drawback of the nose wheel tricycle configuration is the restriction placed upon the location where the main landing gear can be attached. With the steady increase in the aircraft takeoff weight, the number of main assembly struts has grown from two to four to accommodate the number of tires required to distribute the weight over a greater area.

Landing Gear Disposition:

The positioning of the landing gear is based primarily on stability considerations during taxiing, liftoff and touchdown, *i.e.*, the aircraft should be in no danger of turning over on its side once it is on the ground. Compliance with this requirement can be determined by examining the takeoff/landing performance characteristics and the relationships between the locations of the landing gear and the aircraft *cg*.

Angles of Pitch and Roll during Takeoff and Landing:

The available pitch angle (θ) at liftoff and touchdown must be equal, or preferably exceed, the requirements imposed by performance or flight characteristics. A geometric limitation to the pitch angle is detrimental to the liftoff speed and hence to the takeoff field length. Similarly, a geometric limitation to the roll angle (ϕ) could result in undesirable operational limit under cross-wind landing condition.

For a given aircraft geometry and gear height (hg), the limit for the takeoff/landing pitch angle follows directly from Fig. 1. The roll angle at which the tip of the wing just touches the ground is calculated using the expression

$$\tan \phi = \tan \Gamma + \frac{2hg}{s-t} - \tan \theta \tan \Lambda \quad (3.1)$$

In this case, Γ is taken as the dihedral angle, s is the wing span, t is the wheel track, and Λ is the wing sweep. Similar conditions may be deduced for other parts of the aircraft, except that Γ , Λ and s in Eq. (3.1) must be replaced with appropriate values. For example, the permissible roll angle associated with nacelle-to-ground clearance is determined with the following values: Γ measured from the horizon to the bottom of the nacelle in the front view, Λ measured from the chosen landing gear location to the engine in the top view, and s the distance between the engines.

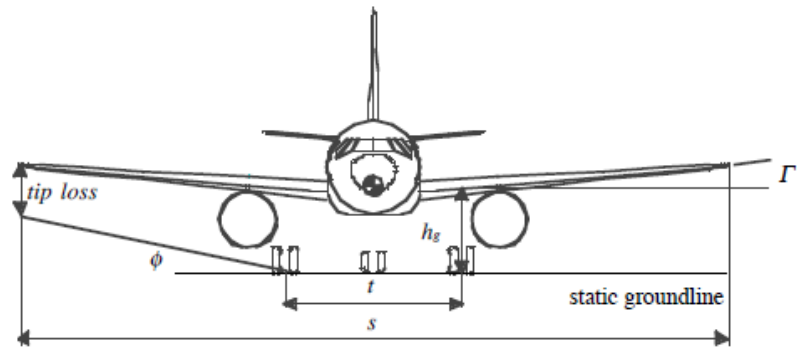
Pitch Angle Required for Liftoff

The takeoff rotation angle is prescribed in preliminary design, and then estimated.

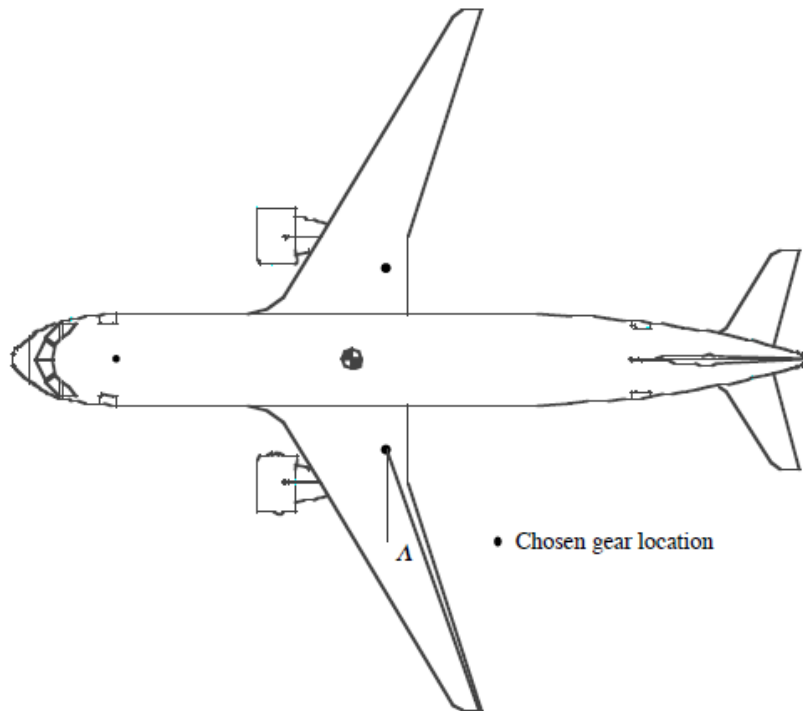
The final values for θ and ϕ are found as the detailed performance characteristics of the aircraft become available. The pitch angle at liftoff (θ_{LOF}) is calculated using the expression

$$\theta_{LOF} = \alpha_{LOF} + \frac{d\theta}{dt} \left(\frac{2l_1}{V_{LOF}} + \sqrt{\frac{l_2}{g} \frac{C_{L, LOF}}{dC_L/d\alpha}} \right) \quad (3.2)$$

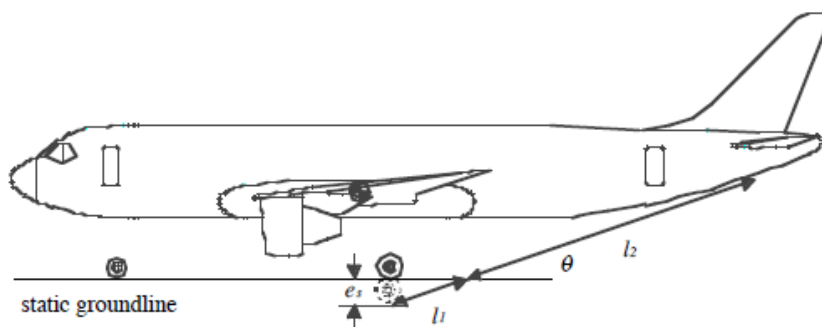
Where α_{LOF} is the highest angle of attack anticipated for normal operational use, V_{LOF} is the liftoff speed, g is the gravitational acceleration, $C_{L, LOF}$ is the lift coefficient, and $dC_L/d\alpha$ is the lift-curve slope. As shown in Fig. 1, the dimension of l_1 and l_2 are defined by the line connecting the tire-ground contact point upon touchdown and the location of the tail bumper, if one is present. For large transports, the typical value for the rate of rotation ($d\theta/dt$) is taken as four degrees per second



a) Front view



b) Top view



c) Side view

Figure 1 Geometric definition in relation to the pitch and roll angles

The detailed aerodynamic data required to use Eq. (3.2) is not always available at the conceptual design stage. In most aircraft the aft-body and/or tail bumper is designed such that the aircraft cannot rotate by more than a specified number of degrees at liftoff.

Typically, the value is between 12 and 15 degrees. In addition to the tail scrape problem, the aircraft cg cannot rotate over and aft of the location of the main assembly, a phenomenon known as tail tipping and is critical during landing.

Pitch and Roll Angles during Landing

With the flaps in the fully-deflected position, the critical angle of attack of the wing during landing is smaller than in takeoff. Consequently, the pitch angle during landing is generally less than that during takeoff. In the absence of detailed information, the pitch angle on touchdown (θ_{TD}) may be assumed equal to θ_{LOF} . As for the roll angle upon touchdown, an upper limit of between five and eight degrees is generally applied to large transport aircraft.

Stability at Touchdown and During Taxiing

Static stability of an aircraft at touchdown and during taxiing can be determined by examining the location of the applied forces and the triangle formed by connecting the attachment locations of the nose and main assemblies. Whenever the resultant of air and mass forces intersects the ground at a point outside this triangle, the ground will not be able to exert a reaction force which prevents the aircraft from falling over. As a result, the aircraft will cant over about the side of the triangle that is closest to the resultant force/ground intersect.

Assuming first that the location of the nose assembly is fixed, the lower limit of the track of the landing gear, identified as constraint I in Fig. 2, is defined by the line passing through the centre of the nose assembly and tangential to the circle with a radius of 0.54 times the height of the aircraft cg (h_{cg}) from the static ground line, centred at the fore-most cg location. The constant 0.54 is based on static and dynamic instability considerations at touchdown and during taxiing. Conversely, if the location of the main assembly is assumed to be fixed, the aft-most limit of the nose assembly mounting location, identified as constraint II in Fig. 2, is defined as the intersection of the aircraft centreline and the line that passes through the centre of the main assembly, tangential to the circle with a radius of 0.54 times of the height of aircraft cg .

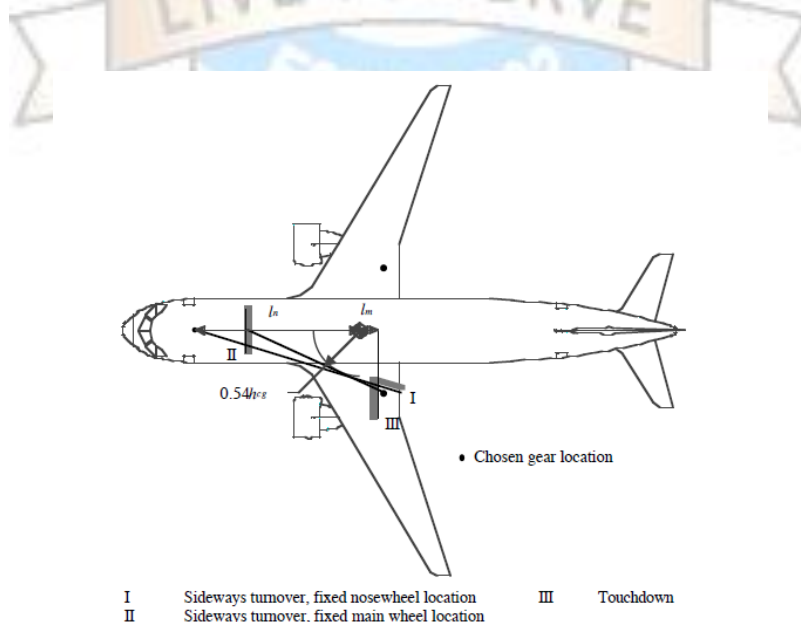


Figure 2: Limits for the undercarriage disposition based on stability

Condition at Touchdown

The most unfavourable condition at touchdown would be a landing with the aircraft cg at its aft-most and highest location, which can lead to the tail scrape and tail tipping phenomenon mentioned previously. Assuming there are no retarding forces, *i.e.*, spin-up load, a vertical force acting at a distance behind the aircraft cg is needed to produce a moment that will pitch the nose downward. Thus, the minimum allowable offset between the aft-most cg and the main assembly mounting locations, identified as constraint III in Fig. 2, is determined using the following expression

$$l_m \geq (h_{cg} + e_s) \tan \theta_{TD} \quad (3.3)$$

Where e_s is the total static deflection of the shock strut and tire, and θ_{TD} is the pitch angle at touchdown. Note that the offset distance is dependent on the value of the pitch angle, whose value is similar to the pitch angle at liftoff, *i.e.*, between 12 and 15 degrees. For a low-wing passenger aircraft, h_{cg} can be approximated assuming a full load of passengers and no wing fuel. This generally results in a vertical cg position at the main passenger-deck level.

Sideways Turnover Angle:

Forces acting sideways on the airplane in cross-wind landing condition or a high speed turn during taxiing could cause the aircraft to turnover on its side. It is thus desirable to keep the turnover angle (ψ) as small as possible. The angle is determined using the expression and δ is defined as the angle between the aircraft centreline and the line connecting the centre of the nose and main assembly.

$$\tan \psi = \frac{h_{cg}}{l_n \sin \delta} \quad (3.4)$$

$$\tan \delta = \frac{t}{2(l_m + l_n)} \quad (3.5)$$

The dimensions used in the above equations are given in Fig. 3. For land-based aircraft, either the maximum allowable overturn angle of 63 degrees or the stability considerations at takeoff and touchdown and during taxiing, whichever is the most critical, determines the lower limit for the track of the main assembly.

Braking and Steering Qualities

The nose assembly is located as far forward as possible to maximize the flotation and stability characteristics of the aircraft. However, a proper balance in terms of load distribution between the nose and main assembly must be maintained. When the load on the nose wheel is less than about eight percent of the maximum takeoff weight (MTOW), controllability on the ground will become marginal, particularly in cross-wind conditions.* This value also allows for fuselage length increase with aircraft growth. On the other hand, when the static load on the nose wheel exceeds about 15 percent of the MTOW, braking quality will suffer, the

dynamic braking load on the nose assembly may become excessive, and a greater effort may be required for steering. Note that these figures should be looked upon as recommendations instead of requirements.

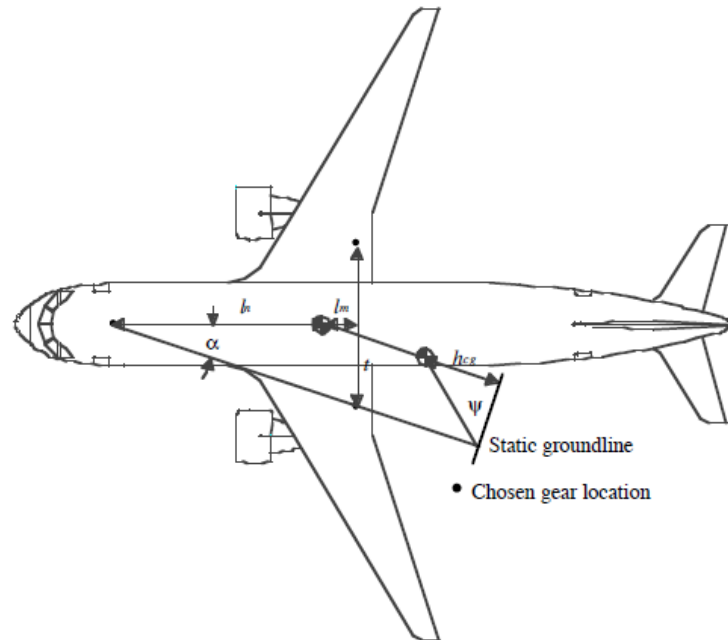


Figure 3 Turnover angle calculations

Gear Length:

Landing gear struts should be of sufficient length such that adequate clearance between the runway and all other parts of the aircraft, *e.g.*, the aft-body, wingtips, and engine nacelles, is maintained when the aircraft is on the ground. For a low-wing aircraft with wing-mounted engines, the above requirement proves to be one of the most challenging design issues in terms of permissible roll angle at touchdown. Although engine nacelle-to-ground clearance has not been explicitly defined, a similar requirement for propellers was specified in FAR Part 25 and can be used as an absolute minimum: seven-inch clearance between the propellers and the ground in level takeoff or taxiing attitude, whichever is most critical.

Landing Gear Attachment:

From considerations of surrounding structure, the nose and main assembly are located such that the landing and ground loads can be transmitted most effectively, while at the same time still comply with the stability and controllability considerations. For a wing mounted assembly, the trunnion is generally attached to the rear wing spar and the landing gear beam and the loads are transmitted directly to the primary wing-fuselage bulkheads. With the inclusion of fuselage-mounted assemblies in the multiple main-strut configurations, a secondary frame would then be added at a distance behind the rear wing-spar, where loads are transmitted forward to the primary wing-fuselage bulkhead through the keel and by shear in the fuselage skin. As for the nose assembly, structural considerations may be conclusive in deciding the mounting location, *i.e.*, at the proximity of forward cabin bulkhead to minimize weight penalty due to local structural reinforcement.

Ground Operation Characteristics:

Besides ground stability and controllability considerations, the high costs associated with airside infrastructure improvements, *e.g.*, runway and taxiway extensions and pavement reinforcements have made airfield compatibility issues one of the primary considerations in the design of the landing gear. In particular, the aircraft must be able to maneuver within a pre-defined space as it taxis between the runway and passenger terminal. For large aircraft, this requirement effectively places an upper limit on the dimension of the wheelbase and track.

Aircraft Turning Radii:

As shown in Fig.4, turning radii are defined as the distances between the center of rotation and various parts of the aircraft. The center of rotation is located at the intersection of the lines extending from the axes of the nose and main assemblies. For aircraft with more than two main struts, the line extending from the main assembly group is located midway between the fore and aft gears. The turning radii are a function of nose gear steering angle (β); the greater the angle, the smaller the radii. The upper limit for this angle is determined by the methods available to provide the steering action, which generally limits the angle to ± 60 degrees. The turning radius corresponding to a 180-degree turn ($r_{180^\circ \text{ turn}}$) as identified in Fig.4 is determined using the expression

$$r_{180^\circ \text{ turn}} = t \tan(90 - \beta) + \frac{b}{2} \quad (3.6)$$

Where b and t are the wheelbase and track, respectively.

Given the aircraft design group classification as listed in Table 1, the minimum turning diameter, *i.e.*, twice of the 180-degree turn radius, should be less than the corresponding runway pavement width.

Airplane design group	Wingspan, ft	Runway width, ft
III	79.0 < s < 118.0	100.0
IV	118.0 < s < 171.0	150.0
V	171.0 < s < 197.0	150.0
VI	197.0 < s < 262.0	200.0

Table: 1 FAA airplane design group classification for geometric design for airports

With the greater wheelbase and track dimensions as exhibited by large aircraft, the 180-degree turn maneuver can no longer be achieved with the conventional nose-steering scheme alone. As a result, combined nose and main assembly steering systems have been introduced on the newer large aircraft, *e.g.*, Boeing Models 747 and 777, to reduce the turning radii.* Other advantages provided by this feature include reduced tire wear and scuffing of the pavement surface in a sharp turn. Note that at the conceptual design phase of an aircraft, Eq. (3.6) is sufficient in producing a first-cut estimate. The resulting turning radii, which are based on nose-steering scheme, are slightly larger than the ones corresponding to combined nose and main assembly steering scheme, and thus provide a built-in safety margin.

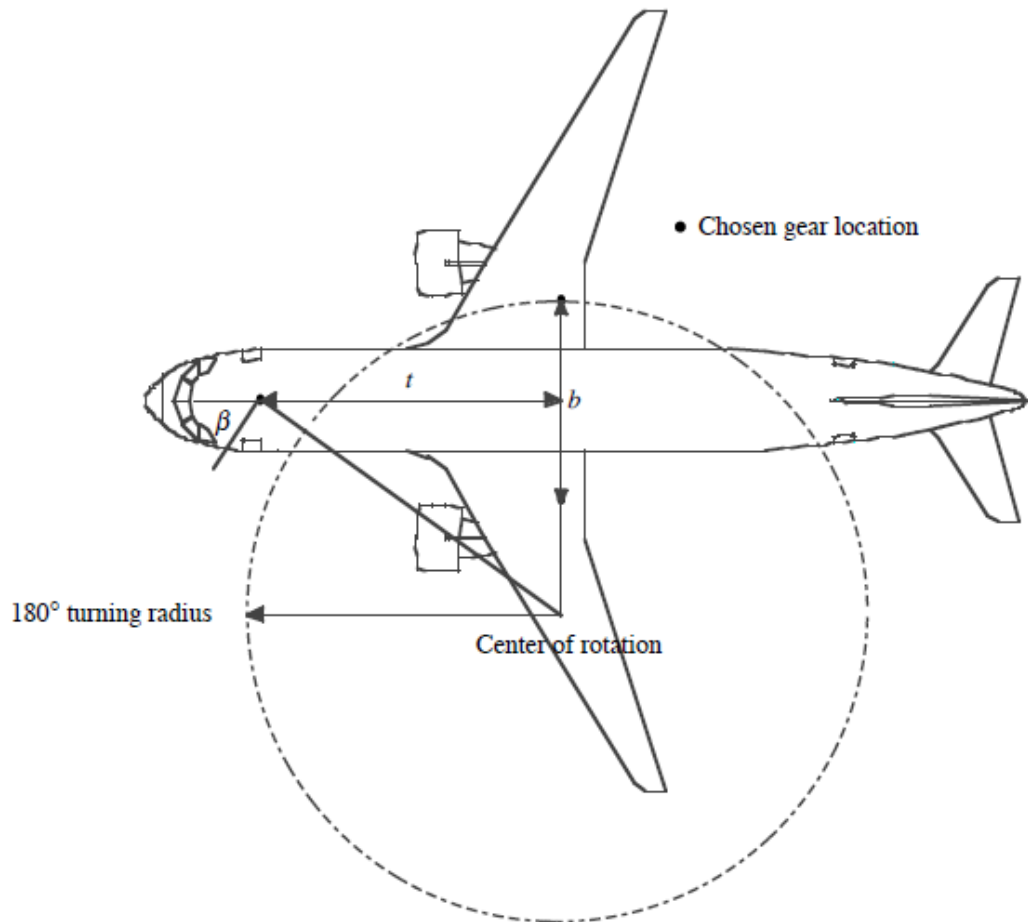


Figure 4 Aircraft turning radii

Centerline-guidance Taxiing

The size of the fillets at runway and taxiway intersections depend not only on wheelbase, radius of centerline curve, width of taxiway, and total change in direction, but also on the path that the aircraft follows. There are two options in which an aircraft can be maneuvered on a turn: one is to establish the centerline of the taxiway as the path of the nose gear; the other is to assume that the nose gear follows a path offset outward of the centerline during the turn. The former is selected as the critical design case since it is the most demanding of the two in terms of piloting skill, *i.e.*, difficult to keep the nose wheel, which is below and behind the pilot's field of view, on the centerline while taxiing, and thus requires a greater area of pavement during the maneuver as safety margin.

As shown in Fig-5, the maximum castor angle (ϕ), *i.e.*, the angle formed between the tangent to the centerline and the longitudinal axis of the aircraft, will occur at the end of the turn, where the nose wheel is at the point of tangency. The angle is approximated by

$$\sin \phi = \frac{b}{R} \quad (3.7)$$

Where R is the radius of centerline curve. A re-check should be made at this point to make sure that the design castor angle is within the permissible range of the steering angle. For a given wheelbase and track dimension, the required fillet radius (F) is calculated using the expression

$$F = \sqrt{R^2 + b^2 - 2Rb \sin\phi} - \frac{t}{2} - S \quad (3.8)$$

Where S is the minimum distance required between the edge of the outboard tire and the edge of the pavement. Given the aircraft design group classification number as determined from Table -1 and the corresponding FAA design values as presented in Table-2, the upper limit for the wheelbase and track of the aircraft can be determined using Eqs (3.7) and (3.8).

	Group III	Group IV	Group V	Group VI
Centerline radius, ft	100.0	150.0	150.0	170.0
Fillet radius, ft	55.0	80.0	85	85.0
Safety margin, ft	10.0	15.0	15.0	20.0

Table-2 FAA recommended taxiway exit geometry

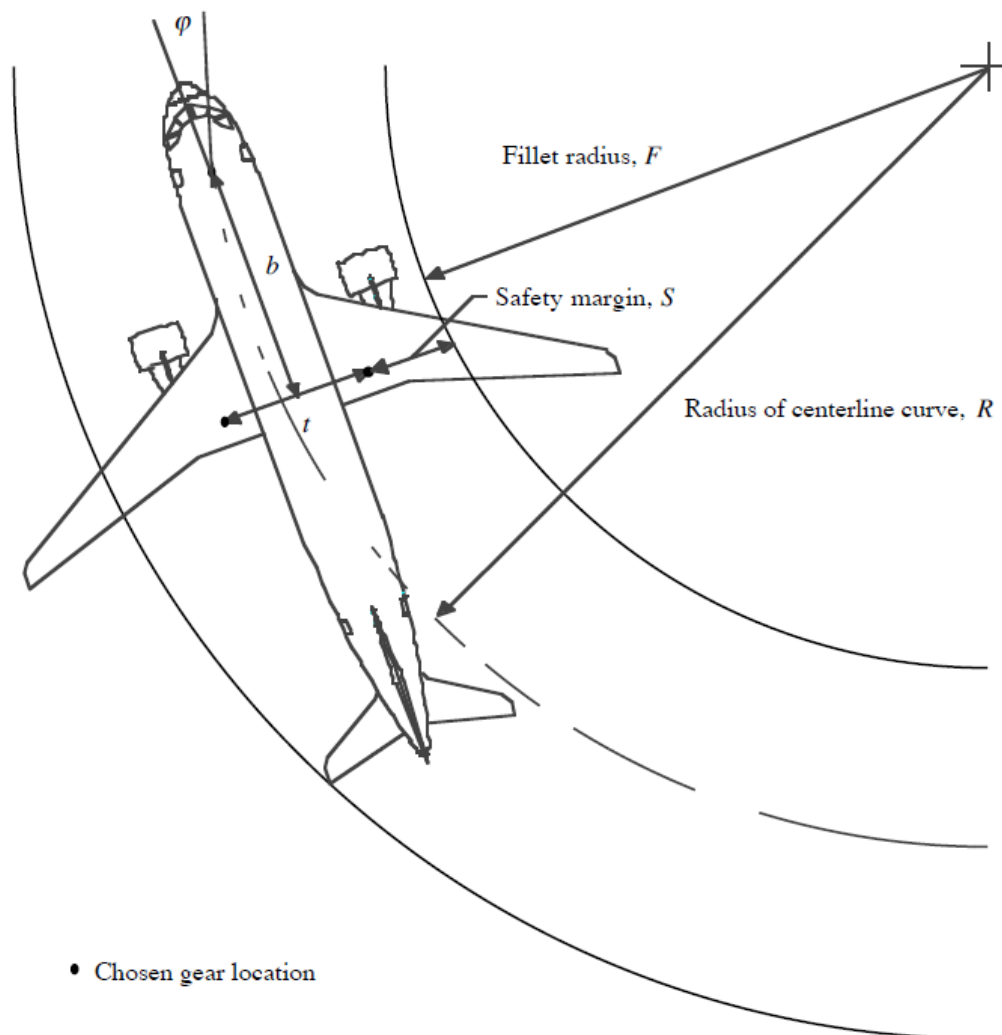
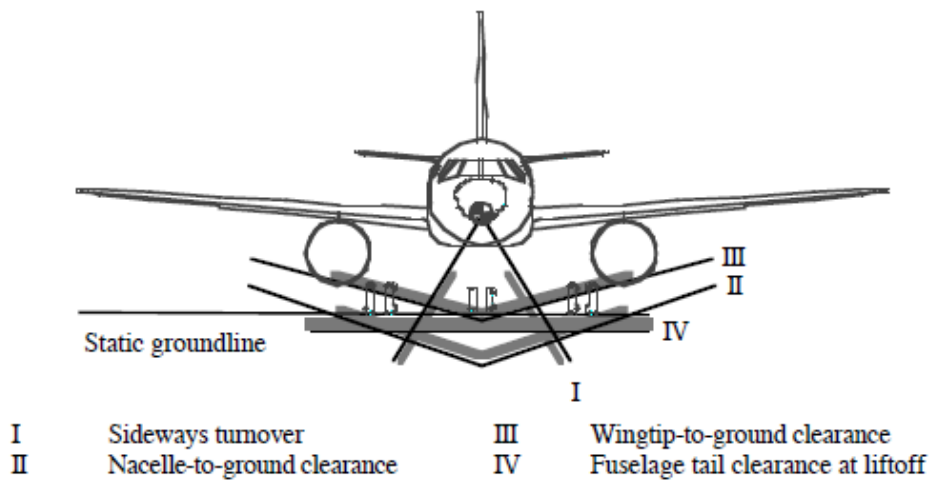


Figure-5 Taxiway fillet design

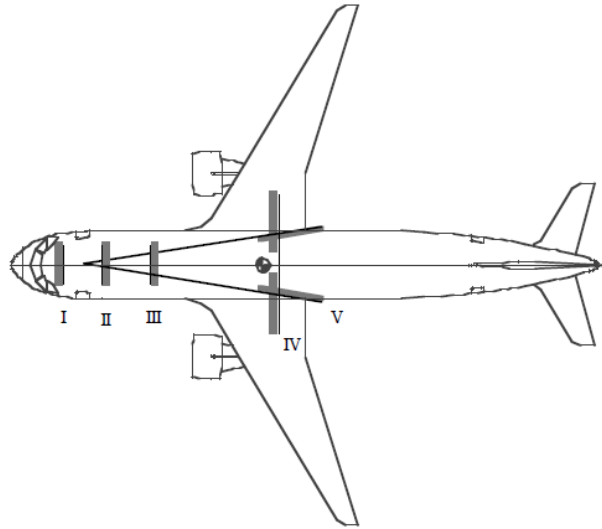
Landing Gear Disposition Constraints

Landing gear location constraints as discussed in the above sections are superimposed on the three-view of a notional aircraft for illustrative purposes. As shown in Fig. 6a, the main assembly must be located such that when the shock strut is at the fully-extended position, the tire-ground contact point is below constraints II and IV in the vertical direction and outboard of constraint I in the lateral direction. In the top view as shown in Fig. 6b, the main assembly must also be located aft of constraint IV in the longitudinal direction and outboard of constraint V in the lateral direction. As for the nose assembly, it must be located between constraints I and II in the longitudinal direction. And finally, as shown in Fig. 3.6c, the fully-extended tire-ground contact point is below constraint II in the vertical direction and aft of constraint II in the lateral direction.



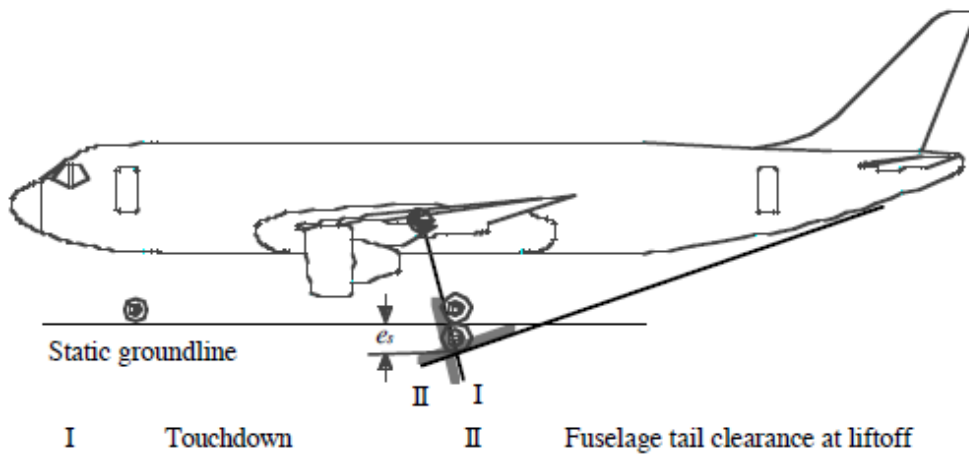
a) Front view





- | | | | |
|-----|--|----|---|
| I | Nosewheel load, 8% MTOW | IV | Touchdown |
| II | Nosewheel load, 15% MTOW | V | Sideways turnover, fixed nosewheel location |
| III | Sideways turnover, fixed main wheel location | | |

b) Top view



c) Side view

Figure-6 Landing gear attachment location constraints

SCHOOL OF AERONAUTICS (NEEMRANA)

UNIT-IV NOTES

FACULTY NAME: D.SUKUMAR.

CLASS: B.Tech AERONAUTICAL

SUBJECT CODE: 6AN5

SEMESTER: VI

SUBJECT NAME: AIRCRAFT DESIGN

INTEGRATION OF STRUCTURE AND POWER PLANT:

Estimation of Horizontal and Vertical tail volume ratios. Choice of power plant and various options of locations, considerations of appropriate air-intakes.

Integration of wing, fuselage, empennage and power plant. Estimation of centre of gravity.

EMPENNAGE GENERAL DESIGN

Functions of Empennages

Empennages create a force that acts upon a lever arm. Consequently a moment is created through empennages:

- The horizontal tail plane creates a moment around the lateral axis (pitch),
- The vertical tail plane (fin) principally creates a moment around the vertical axis (yaw). Ailerons and spoilers on the wing principally create a moment around the longitudinal axis (roll).

Control surfaces on empennages and on the wing are the customary way to create moments. However, there are other possibilities for creating moments:

- Moving the center of gravity (tail aft aircraft),
- Engine thrust (control jets on the VTOL aircraft).

Empennages ensure trim, stability and control.

Trim

The moment created by an empennage balances out moments occurring on the aircraft for another reason. The horizontal tailplane, for example, balances out the wing moment (Fig. 1). In the case of propeller aircraft, the rotating slipstream causes a moment at the rear of the fuselage and at the vertical tailplane. The vertical tailplane has to compensate for this moment. If an engine fails on a multi-engine aircraft, the vertical tailplane compensates for an asymmetrical moment distribution around the vertical axis.

CS 25.161 defines the term "trim":

- | |
|--|
| (a) Each aeroplane must meet the trim requirements of this paragraph after being trimmed , and without further pressure upon , or movement of, either the primary controls or their corresponding trim controls by the pilot or the automatic pilot. |
|--|

In simple terms: an aircraft is trimmed when the primary flight controls (pitch, roll, and yaw) are free of forces in controlled flight.

The trim has to be guaranteed for all prescribed center-of-gravity positions, airspeeds, flap and landing gear positions and in the event of engine failure (for details see: CS 25.161).

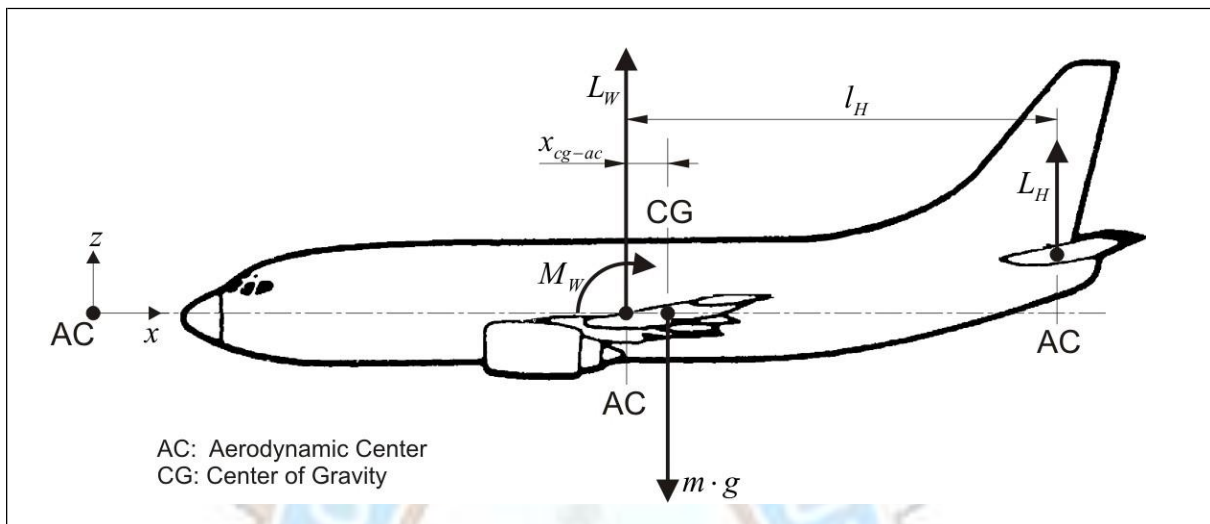


Fig.1 Forces and moments acting on an aircraft during trimmed horizontal flight.

Stability

Stability refers to the capacity of the aircraft to return to the original flying position after a disturbance from outside or after a brief control input. Details are contained in the certification regulations in CS 25.171 to CS 25.181. A distinction is made between static stability and dynamic stability.

- *Static stability.* Longitudinal static stability ensures that the airspeed remains stable.

The following is required according to CS 25.173:

- | | |
|-----|---|
| (a) | A pull must be required to obtain and maintain speeds below the specified trim speed, and a push must be required to obtain and maintain speeds above the specified trim speed. |
|-----|---|

The lateral static stability returns the aircraft to a slip-free flight. CS 25.177 requires the following:

- | | |
|-----|---|
| (b) | The static lateral stability (as shown by the tendency to raise the low wing in a sideslip with the aileron controls free) for any landing gear and wing-flap position and symmetric power condition, may not be negative at any airspeed |
|-----|---|

- *Dynamic stability* is contingent upon static stability. But an aircraft is not necessarily dynamically stable when it is statically stable, because if the aircraft returns to its original position after a disturbance, it can, of course, easily overshoot the original

position. If this oscillation ceases after a while (or an overshoot does not occur), this oscillation of the aircraft is dynamically stable. But if the amplitude of oscillation becomes greater and greater, this oscillation of the aircraft is dynamically unstable. Conventional aircraft exhibit the following "oscillation forms" or, to be more precise, modes (it does not always have to be an oscillation; it might also be a heavily damped movement):

- In a *longitudinal movement* (i.e. around the lateral axis): short period mode, phugoid.
- In a *lateral movement* (i.e. around the longitudinal and vertical axis): spiral mode, Dutch roll mode.

The modes can best be explained with a small model aircraft in the hand or in flight. Therefore, a further description is dispensed with at this point.

CS 25.181 requires that certification flights must demonstrate the following features:

- | | |
|-----|---|
| (a) | Any short period oscillation ... must be heavily damped with the primary controls - |
| (1) | Free; and |
| (b) | In a fixed position. |

Control

An aircraft must be sufficiently controllable in all critical flight states (CS 25.143 to CS 25.149). The control forces should not become too extreme (see CS 25.143(c)). In addition, the increase in control forces is dealt with using the limit load factor (CS 25.143):

- | | |
|-----|--|
| (f) | ... the stick forces and the gradient of the curve of stick force versus manoeuvring load factor must lie within satisfactory limits. The stick forces must not be so great as to make excessive demands on the pilot's strength ... and must not be so low that the aero- |
|-----|--|

Critical flight states for the empennage dimensioning from the point of view of control are:

- *Horizontal tailplane*: critical combination of center-of-gravity position, flap position and airspeed; rotation during take-off; flare when landing; control with trimmed horizontal stabilizer (CS 25.255).
- *Vertical tailplane (fin)*: Engine failure in cruise and during take-off and landing. Engine failure during take-off run, landing with crosswind (sideslip to compensate for crosswind component), spinning (CS 23.221).

An aircraft must possess sufficient **maneuverability** in accordance with its flight mission. It is scarcely possible to derive maneuverability criteria from the civil certification regulations. Instead the findings contained in military regulations – also for transport aircraft – are used in the design (see MIL-F-8785C and MIL-STD-1797). In the development phase a simulator model is created and the future aircraft is "flown" and

assessed by test pilots. The lever arm and aileron must be large enough for sufficient maneuverability. In addition, it must be possible to deflect the control surfaces quickly enough.

Shapes of the Empennage

Different empennage shapes are shown on selected aircraft in Fig. 2.

The **conventional tail** provides appropriate stability and control and also leads to the most lightweight construction in most cases. Approximately 70 % of aircraft are fitted with a conventional tail. Spin characteristics can be bad in the case of a conventional tail due to the blanketing of the vertical tailplane (Fig.3). The downwash of the wing is relatively large in the area of the horizontal tailplane. Rear engines cannot be teamed with conventional tails. Stabilizer trim is possible with comparatively low complexity. A larger vertical tailplane height is more appropriate for a conventional tail than a T-tail.

The **T-tail** is heavier than the conventional tail because the vertical tailplane has to support the horizontal tailplane. However, the T-tail has advantages that partly compensate for the described main disadvantage (weight). Owing to the end plate effect, the vertical tailplane can be smaller. The horizontal tailplane is more effective because it is positioned out of the airflow behind the wing and is subjected to less downwash. It can therefore be smaller. For the same reason the horizontal tailplane is also subject to less tail buffeting. The T-tail creates space for engines that are to be placed at the rear. The T-tail looks good, according to general opinion.

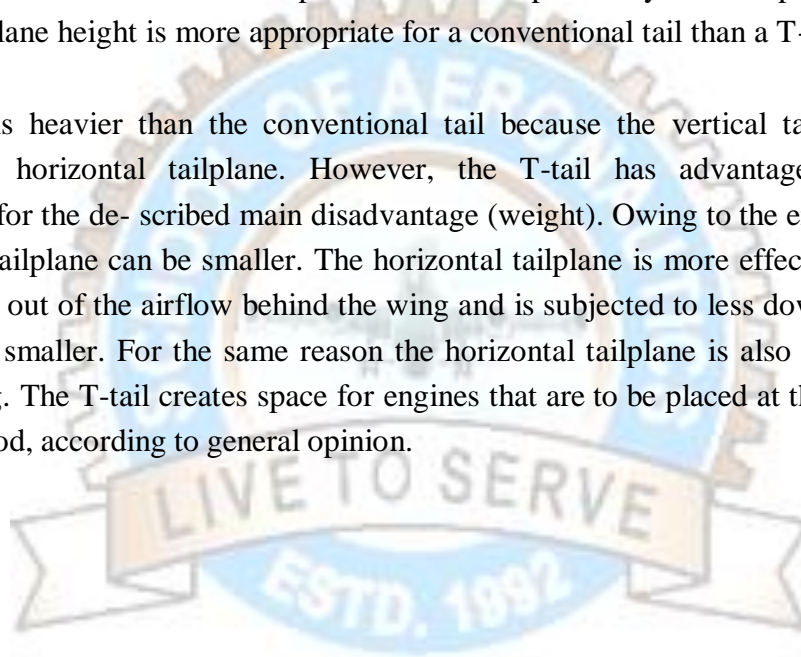




Fig. 2 Empennages of conventional aircraft configurations

1/3 of Rudder Area should be Un-Blanketed

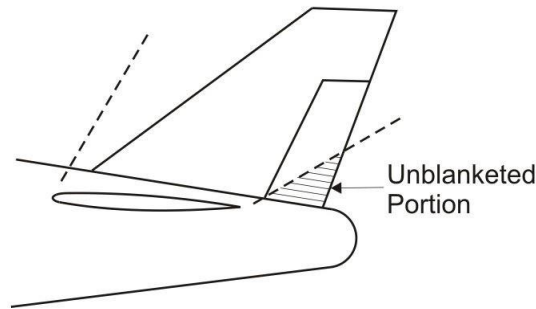


Fig 3. Influence of the empennage design on the spin recovery characteristics

With T-tails the problem of *deep stall* must be taken into account (Fig. 4). In the case of high angles of attack the horizontal tailplane can be caught up in the airflow behind the wing and be blanketed. If, in addition, the wing tends to make the aircraft pitch up at high angles of attack, a situation may arise in which the aircraft can no longer be recovered from the stall. Fig. 5 shows admissible positions of the horizontal tailplane.

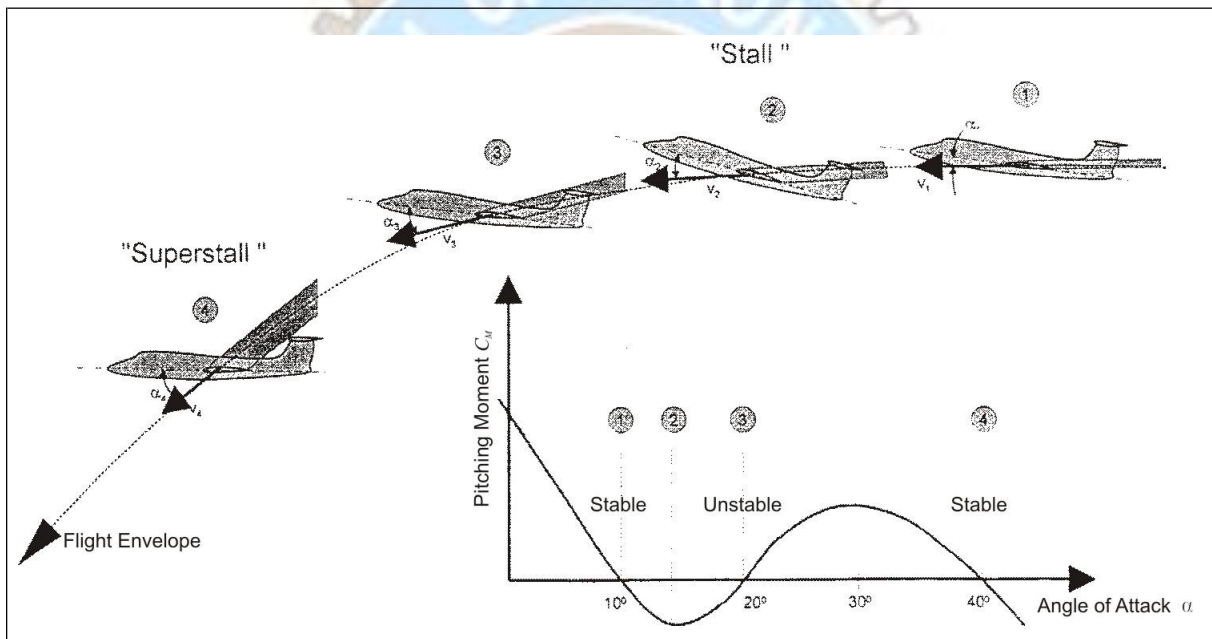


Fig. 4 Flight envelope, angle of attack and pitching moment during deep stall and super stall (Schmitt 1998)

The **cruciform tail** is a compromise between a conventional tail and a T-tail. The cruciform tail weighs less than the T-tail and allows the engines to be placed at the rear (e.g. Caravelle). However, the cruciform tail does not have a surface area advantage due to the end plate effect like the T-tail.

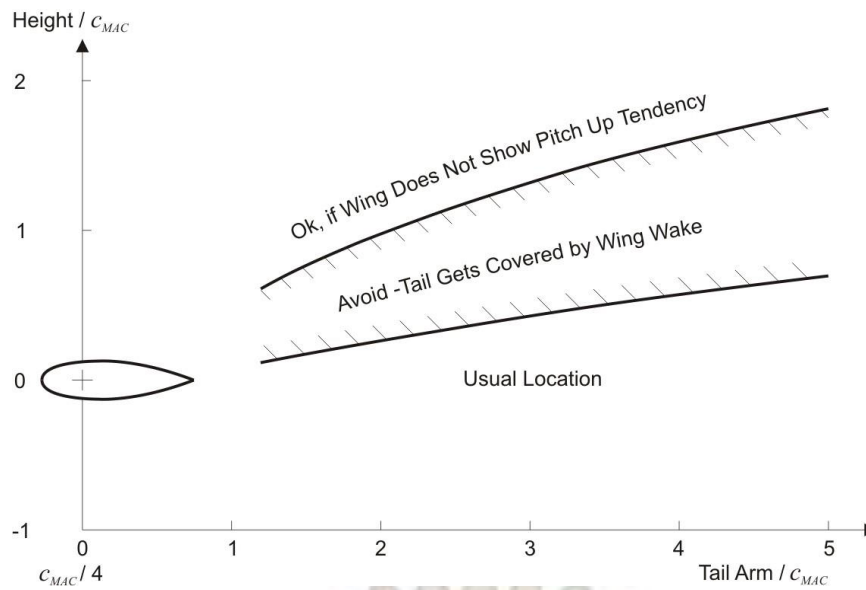


Fig. 5. Positioning of horizontal tailplanes

The aim of the **V-tail** is to achieve a smaller tail area than with horizontal and vertical tailplanes, for example in the form of the conventional tail. The V-tail is designed as follows: In the first step the required areas of a conventional horizontal tailplane S_H and vertical tailplane S_V are determined (see below). Theoretically the V-tail provides efficiency as a horizontal and vertical tailplane, corresponding to the projection of the V-tail in the horizontal and vertical. This theoretical approach gives the necessary V angle for the V-tail

$$v = \arctan \frac{S_V}{S_H} \quad (1)$$

And the necessary area

$$S_{V-Tail, theory} = \sqrt{S_H^2 + S_V^2} \quad (2)$$

On the basis of this theoretical analysis the V-tail only requires a tail area of $S_{V-tail} / (S_V + S_H) = 70.7\%$ compared to the conventional tail with $S_V / S_H = 1$. With other S_V / S_H Ratios the area saving is less. According to the **NACA 823** report, the V-tail must,

However, be larger in practice than the theory suggests for the same efficiency, so that the advantage of the smaller area is lost and a tail area

$$S_{V-Tail} = S_H + S_V \quad (3)$$

is necessary.

With a V-tail the control surfaces deflect in the same direction in the function of the elevator and in opposite directions in the function of the rudder. If the right rudder pedal is pressed, the right control surface of the V-tail moves down and the left control surface up. One of the disadvantages of the V-tail is the complicated mechanics required to combine the elevator and rudder inputs. Inconveniently a "rudder deflection" of the V-tail causes a roll moment against the desired turn. A roll moment in the direction of the desired turn is, on the other hand, achieved with the inverted V-tail. However, many aircraft configurations will not be able to accommodate an inverted V-tail due to the necessary ground clearance.

A **twin tail** can be used if a single vertical tailplane would be too big. Twin tails are covered less by the front fuselage in the case of high angles of attack than a vertical tail in the plane of symmetry. For the latter reason twin tails are seen on fighter aircraft that operate in the high angle of attack range. Fig. 2 shows additional tail configurations that might be advantageous under certain circumstances.

Other tail features:

- Through the **dorsal fin** (Fig. 6) the efficiency of the vertical tailplane where high angles of yaw exist is improved through vortex formation. The stall is thereby moved to higher angles of yaw.
- The **ventral fin** (Fig. 6) is not blanketed even with high angles of attack. The ventral fin also serves to prevent lateral instabilities in high-speed flight.

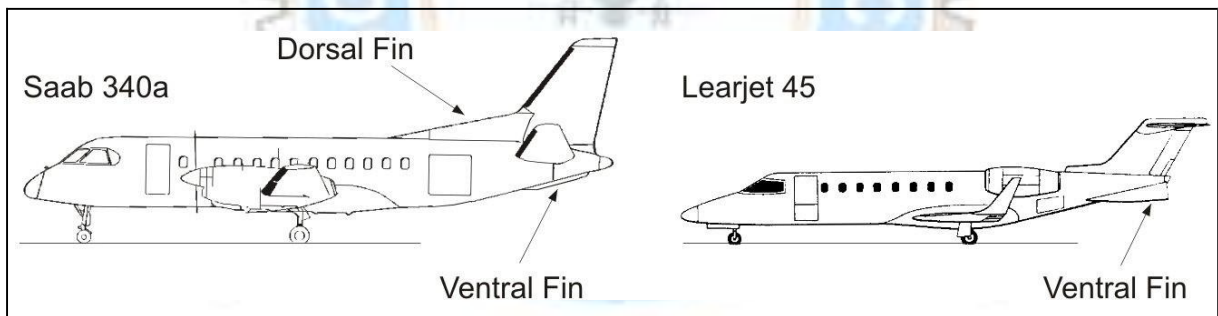


Fig. 6 Examples of aircrafts with dorsal fin and ventral fin

The **canard tails** (Fig. 7) are subdivided into *control canard* and *lifting canard*.

- In the case of a *control canard* the wing bears the aircraft's weight. Wings and fuselage alone show neutral stability; the canard is only used for control, but makes the system comprising fuselage, wing and tail instable. An electronic flight control system, EFCS, carries out the regulation and stabilization of the instable aircraft. An aircraft with canard must be designed in such a way that the wing can never be stalled. Instead the canard is first stalled. This necessitates that the wing's lift potential cannot be fully utilized.

- The *lifting canard* has less drag theoretically because the canard – in contrast to the horizontal tailplane of the tail aft configuration – creates lift (instead of negative lift) (compare with Fig. 1). By using the *lifting canard* the wing must be placed further to the rear. Through this placement the lifting canard is able to facilitate a center-of-gravity range that is normally required. However, the lifting canard displays various disadvantages that restrict its overall utility considerably: the placement of the wing further back on the fuselage increases the nose-heavy moment when using the landing flaps due to the larger lever arm. The wing of the canard must therefore have a greater area with less effective flaps than is customary with the tail aft configuration. Another way of solving this problem is to fit the canard with effective flaps or provide a variable sweep of the canard.

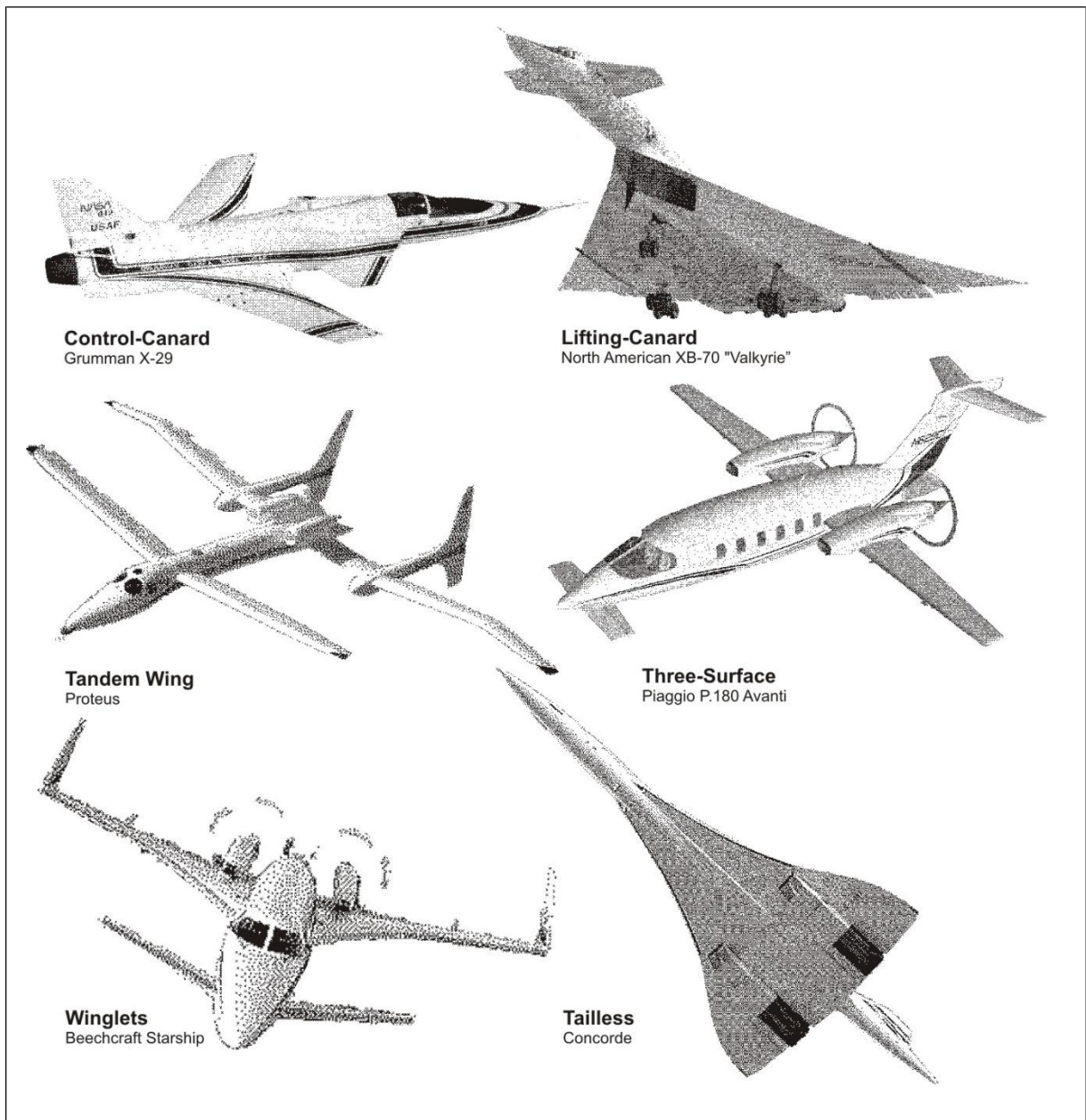


Fig. 7 Empennages of unconventional aircraft configurations

The **tandem wing** is a *lifting canard* where the lift forces are approximately evenly distributed between the wing and the canard.

The **three-surface configuration** makes it possible to create a pitching moment without influencing the lift on the wing. Therefore it is possible to better optimize the distribution of lift on the wing and thereby reduce the drag. One of the disadvantages is the additional complexity due to an additional area.

All configurations with canards have the disadvantage that the wing lies in a flow disturbed by the empennage placed at the front.

Design Rules

- The horizontal tailplane should be installed in a **position** so that it does not lie in the slipstream. If this rule is not observed, it may have the following effects:
 - structure fatigue due to tail buffeting;
 - increased noise in the cabin due to tail buffeting;
 - Considerable trim changes with differing choice of engine performance.

In some small single-engine aircraft the empennage is deliberately placed in the slipstream. Then one benefits from an increased efficiency of the tail assembly during take-off and landing, but may have to accept the disadvantages described above.

- The detailed **placement of the horizontal tailplane** can be determined from Fig. 5: low lying horizontal tailplanes are most suitable for getting an aircraft out of a stall. With subsonic aircraft the empennage can also be installed at the same height as the wing. A T-tail may only be used if the wing is uncritical and is not susceptible to excessive pitch-up.
- The **lever arm** of the empennage should be as large as possible, thereby making it possible to keep the tail areas small, which reduces weight and drag.
- The **aspect ratio** of the horizontal tailplane should be about half the aspect ratio of the wing. T-tails have a smaller aspect ratio of the vertical tailplane than conventional tails (Table 1). This allows weight disadvantages to be kept to a minimum.
- Tails with a taper ratio of $\lambda = 1$ are built in some cases as **rectangular tail** especially for general aviation aircraft. Rectangular tails reduce production costs.
- The **critical Mach number** of the empennage $M_{crit,H}$ And $M_{crit,V}$ Should be $\Delta M = 0.05$

Higher than the critical Mach number of the wing $M_{crit, W}$. Through this measure the efficiency of the tail assembly should also be guaranteed at high speed. Relative thickness, drag divergence Mach number, sweep, and the lift coefficient of the empennage must be chosen so as to ensure that a $\Delta M = 0.05$ can be achieved.

$$t / c = f(M_{DD}, \varphi_{25}, C_L, \text{airfoil})$$

These parameters can be chosen to approximately suit each other if the drag divergence Mach number M_{DD} of the tail is $\Delta M = 0.05$ higher than for the wing.

- The **sweep of the horizontal tailplane** should be approximately 5° larger than the sweep of the wing. Thus a higher critical Mach number of the horizontal tailplane can be achieved and a loss of efficiency due to shock waves is avoided. In addition, the lift gradient of the horizontal tailplane can be less than the lift gradient of the wing due to the increased sweep, so that the horizontal tailplane only reaches the stall state at larger angles of attack than the wing.
- The **sweep angle of the vertical tailplane** is 35° to 55° for aircraft with "high airspeeds" (flight with compressibility effects). The sweep angle of the vertical tailplane for aircraft with "low airspeeds" (flight without compressibility effects) should be less than 20° . A large sweep angle increases the lever arm and the angle where the vertical tailplane goes into stall, but reduces the maximum lift coefficient.
- The **horizontal tailplane** should have a **relative thickness** that is approximately 10 % less than the relative thickness in the outer wing. Thus, a higher critical Mach number of the horizontal tailplane can be achieved and a loss of efficiency due to shock waves is prevented.
- Symmetrical **airfoils** are chosen exclusively for vertical tailplanes. Symmetrical or virtually symmetrical airfoils with 9% to 12% relative thickness are chosen for horizontal tailplanes. For example, NACA 0009 or NACA 0012 (**Abbott 1959**) can be chosen. Asymmetrical horizontal tailplane airfoils are installed "upside-down" because the horizontal tailplane has to create negative lift.
- If the **left and right elevators** are to be **connected**, the sweep and the taper ratio must be selected so as to ensure that a hinge line is produced perpendicular to the aircraft's plane of symmetry. Reasons for connecting the elevators may be:
 - To reduce the elevators' tendency to flutter;
 - To facilitate joint actuation of the elevators.

- The **dihedral angle** can be chosen so that the empennage is positioned outside the engine slipstream. Dihedral of the horizontal tail is not used to modify roll stability as this is much more influenced by the wing.
- If the horizontal tailplane is fixed, an **incidence angle** of around 2° to 3° downwards should be chosen to create negative lift. A more flexible alternative is a movable, i.e. **trimmable horizontal stabilizer**, THS, which facilitates a larger center-of-gravity range.
- The horizontal tailplane can be designed as an **all moving tail**. An all moving tail only consists of one surface with an adjustable incidence angle. The all moving tail is more effective – especially at high Mach numbers – but also heavier than a fixed empennage with control surface. In the case of large aircraft high output may be required to move the all moving tail in flight with the necessary actuating speed. A compromise is the **trimmable horizontal stabilizer** mentioned above: the horizontal stabilizer is used to trim and is only adjusted gradually (with a low actuating power); the elevator is deflected correspondingly quicker for maneuvering. The trimmable horizontal stabilizer is the standard solution for transport aircraft.
- **Lifting canard** or **tandem wing** is designed like wings.

Tables 1, 2 and 3 contain parameters that can be referred to as guides for empennage design.

Table 1 Conventional aspect ratios A and taper ratios λ from empennages on transport category airplanes (**Raymer 1989**)

Type	Horizontal Tailplane		Vertical Tailplane	
	A	λ	A	λ
Conventional Tail	3.00 ... 5.00	0.3 ... 0.6	1.3 ... 2.0	0.3 ... 0.6
T-Tail	as Conventional Tail	as Conventional Tail	0.7 ... 1.2	0.6 ... 1.0

Table 2: Conventional design parameters for horizontal tails (**Roskam II**)

Type	Dihedral Angle ν [°]	Incidence Angle i_h [°]	Aspect Ratio A_h [-]	Sweep Angle ϕ [°]	Taper Ratio λ_h [-]
Business Jets	- 4 ... 9	-3.5 fixed	3.2 ... 6.3	0 ... 35	0.32 ... 0.57
Transport Jets	0 ... 11	variable	3.4 ... 6.1	18 ... 37	0.27 ... 0.62
Fighters	-23 ... 5	0 fixed or variable	2.3 ... 5.8	0 ... 55	0.16 ... 1.00
Supersonic Civil Transport	-15 ... 0	0 fixed or variable	1.8 ... 2.6	32 ... 60	0.14 ... 0.39

Table 3: Conventional design parameters for vertical tails (**Roskam II**)

Type	Dihedral Angle ν [°]	Incidence Angle i_h [°]	Aspect Ratio A_h [-]	Sweep Angle ϕ [°]	Taper Ratio λ_h [-]
Business Jets	90	0	0.8 ... 1.6	28 ... 55	0.30 ... 0.74
Transport Jets	90	0	0.7 ... 2.0	33 ... 53	0.26 ... 0.73
Fighters	75 ... 90	0	0.4 ... 2.0	9 ... 60	0.19 ... 0.57
Supersonic Cruise Airplanes	75 ... 90	0	0.5 ... 1.8	37 ... 65	0.20 ... 0.43

Design According to Tail Volume

The area of the horizontal tailplane S_H or the vertical tailplane S_V multiplied by the lever arm l_H or l_V is called tail volume. The tail volume coefficient is defined for the horizontal tailplane as

$$C_H = \frac{S_H \cdot l_H}{S_W \cdot c_{MAC}} \quad (4)$$

and for the vertical tailplane as

$$C_V = \frac{S_V \cdot l_V}{S_W \cdot b} \quad (5)$$

l_H the lever arm of the horizontal tailplane is the distance between the aerodynamic centers of wing and horizontal tailplane,

l_V the lever arm of the vertical tailplane is the distance between the aerodynamic centers of wing and vertical tailplane.

As a good approximation the 25 % - point on the mean aerodynamic chord can also be referred to instead of the distances between the aerodynamic centers.

Table 4 Conventional tail volume coefficients of horizontal and vertical tails (**Raymer 1989**)

type	horizontal C_H	vertical C_V
General Aviation - Twin Engine	0.80	0.07
Transport Jets	1.00	0.08
Jet - Trainer	0.70	0.06
Jet - Fighter	0.40	0.07

The tail size can be estimated from the tail volume coefficient if the tail lever arms l_H and l_V are known. The lever arms are not, however, fixed until the position of the wing has been established. However, this only takes place in Step 11 "Mass and Center of Gravity". For this reason the tail lever arms can only be estimated from the length of the fuselage in this case (Table 5).

Table 5: Conventional tail lever arms of horizontal and vertical tails (**Raymer 1998**)

aircraft configuration	average of l_H and l_V
propeller in front of fuselage	60% of fuselage length
engines on the wing	50 ... 55% of fuselage length
engines on the tail	45 ... 50% of fuselage length
control canard	30 ... 50% of fuselage length
sailplane	65% of fuselage length

- The tail volume coefficients can be reduced by 10% to 15% in the case of **trimmable horizontal stabilizers**.
- In the case of a **T-tail**, the tail volume coefficients can be reduced by 5% for horizontal and vertical tailplane due to the end plate effect and the improved flow.
- In the case of a control **canard** a tail volume coefficient of 0.1 can be set. In the case of a *lifting canard* the tail volume coefficient method cannot be applied. Instead a ratio of the areas of canard and wing is established.
- If the criteria for stability and control determine the dimensioning of an aircraft's tail design, the tail volume coefficients can be reduced by approximately 10% if the aircraft has an electronic flight control system, **EFCS**. However, for transport aircraft other criteria (such as engine failure for the rudder) often determine the dimensioning, so that tail area cannot necessarily be saved through an EFCS.

Elevator and Rudder

Elevator and rudder start on the fuselage and extend to approximately 90% of the (semi-) span of the tail, or up to the tip of the tail (Fig.8). They have a chord which accounts for approximately **25 % to 40 % of the chord of the tail**. Elevators are deflected downwards by a maximum of 15° to 25° and upwards by a maximum of 25° to 35°. Rudders are **deflected** by a **maximum** of 25° to 35°. **Torenbeek 1988** and **Roskam II** contain detailed tables with tail and control surface data.

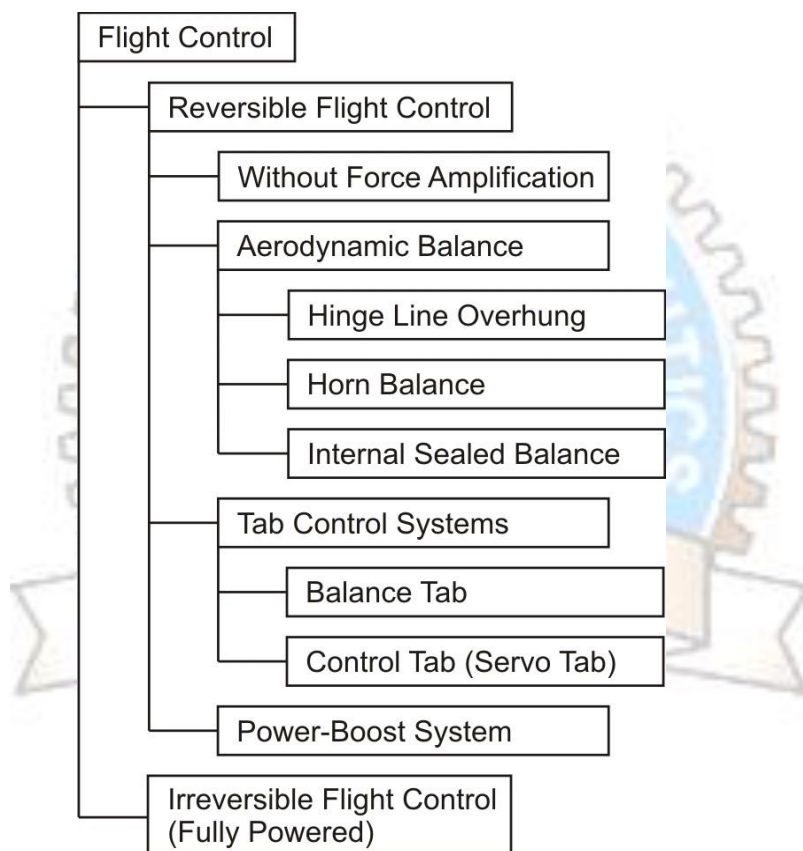
Particularly in the case of aircraft with a reversible flight control system (Fig.7) it is important to know the hinge moment required to deflect the rudder in the various flight states. The reason is that the hinge moment determines the hand and foot forces on the flight controls, which may not exceed specific maximum values according to CS 25.143(c). The hinge moment is calculated with

$$M_c = \frac{1}{2} \rho V^2 \cdot C_h \cdot S_F \cdot c_F \quad . \quad (6)$$

V is the airspeed, S_F is the control surface area, c_F is the rudder depth (measured from the hinge line to the trailing edge). The hinge moment coefficient C_h of a control surface is calculated from the hinge moment derivatives C_{h_α} and C_{h_δ} (See **DATCOM 1978** or **Roskam VI**).

It is important to bear in mind that asymmetrical airfoils already have a hinge moment coefficient C_{h_0} at $\alpha = \delta = 0$.

$$C_h = C_{h_0} + C_{h_\alpha} \cdot \alpha + C_{h_\delta} \cdot \delta \quad (7)$$



According to equation (6) the aerodynamic hinge moment increases with the size and speed of an aircraft. As the control forces may become too large even in small aircraft, measures must be taken to reduce them. The hinge moment is fully or partially carried by the pilot's muscular force on reversible flight controls. On irreversible flight controls the hinge moment is countered by the aircraft's onboard energy systems. Fig.8 shows the main options for reducing control forces.

The options are arranged according to increasing effectiveness but also complexity. Fig.9 shows two of these methods for hinge moment reduction. Horn and over-hang balance are often applied on small aircraft owing to their simple design.

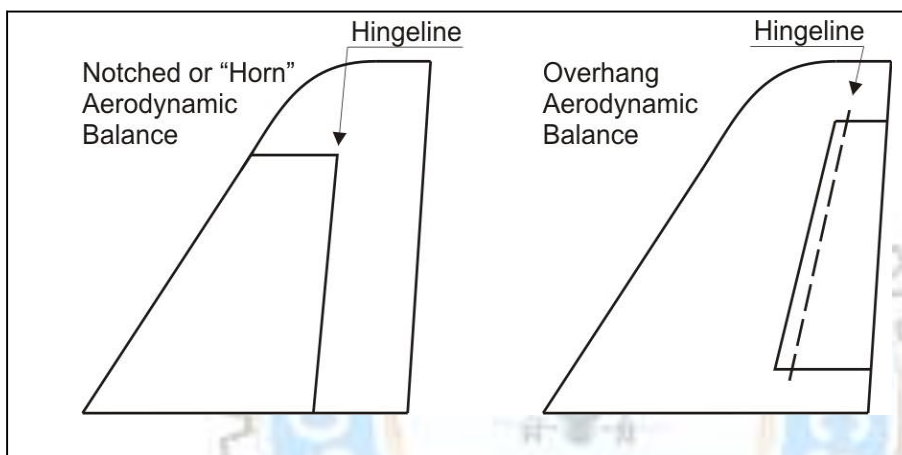
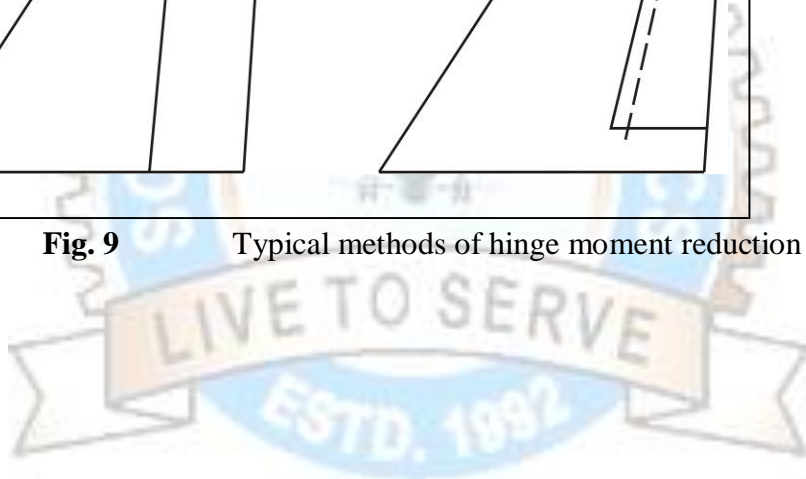


Fig. 9 Typical methods of hinge moment reduction



POWERPLANT

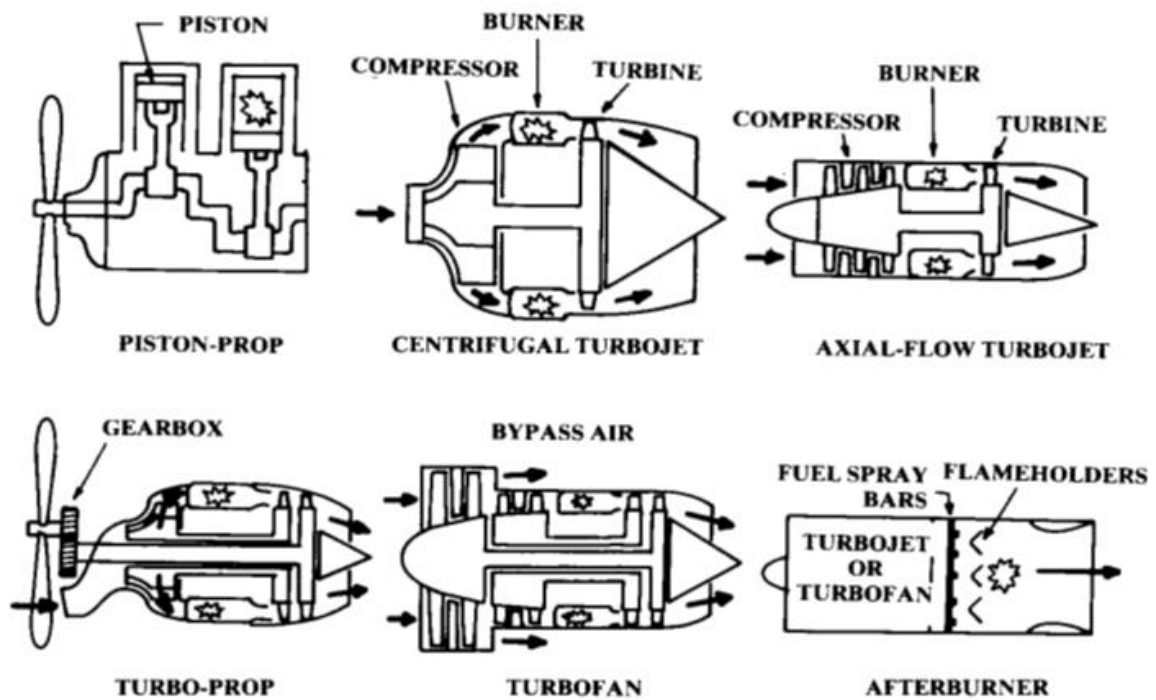


Fig. 10.1 Propulsion system options.

- Power plant characteristics
 - thrust, specific thrust, efficiency, specific fuel consumption
- Power plant types
 - Piston engines, gas turbines (turbojet, turbofan, turboprop, turbo shaft, prop fan)
 - Afterburning, thrust reversers, supersonic engines

Power plant Characteristics

Thrust (T)

- May be simply represented as:

$$T = \dot{m} (V_j - V_o)$$

Where: \dot{m} = mass flow rate through engine;

V_j = jet velocity; V_o = aircraft speed.

- Infinite number of combinations of mass flow and velocity increment possible, reflected in various Power plant types available.

Thrust varies with V_o and altitude, as depends upon air density (ρ).

Specific Thrust (T_{sp})

- Useful for comparing different types of engines:

$$T_{sp} = T / \dot{m} = (V_j - V_o)$$

For static condition ($V_o = 0$), $T_{sp} = V_j$

Overall Efficiency (η_o)

- Product of propulsive (or Froude) efficiency (η_p), thermal efficiency of gas generator (η_{th}) and mechanical transmission efficiency (η_{mech})

$$\text{i.e. } \eta_o = \eta_p \eta_{th} \eta_{mech} \quad (3)$$

Propulsive Efficiency (η_p)

Defined as:

$$\frac{\text{useful propulsive energy}}{\text{useful propulsive energy} + \text{unused jet kinetic energy}} \quad (4a)$$

Or

$$\eta_p = \frac{2}{\left(1 + \frac{V_j}{V_o}\right)} \quad (4b)$$

Note that maximum η_p (100%) occurs with no unused jet kinetic energy ($V_j = V_o$) but then no thrust developed - eq. (1)!

Propulsive Efficiency (η_p) Observations

- From eq. (4), high η_p obtained with low ($V_j - V_o$) term.
- From eq. (2), this also means a low value of T_{sp} .
- Also, for a given thrust, this equates to a high value for \dot{m} .
This is the operating principle behind *turbofan* (bypass ratio) *engines*.

- High \dot{m} , low T_{sp} high η_p
- Also reduced noise – varies with V_j
- But results in large engine diameter, increased weight & drag.

Powerplant Types

- Two main classes used on aircraft, both air-breathers:
 - Piston engines
 - Gas turbines
- Rockets only used for guided weapons (GW) and vehicles operating outside atmosphere (also possibly boost motors on aircraft).
- Similarly, ramjets not suitable for aircraft as develop no thrust at rest – only GW applications.

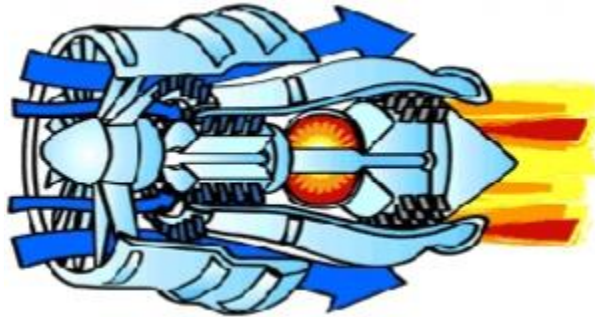
Piston Engines

- Combined with propeller (piston-prop) to provide propulsion for first 40+ years of flight.
- Individual units of up to 2 MW power output developed using large number of cylinders, arranged radially or in line of flight.
- Nowadays limited to small low-speed general a/c using engines up to about 400 kW.

Main disadvantages compared with gas turbines:

- Low power/weight ratio
- Power output does not increase with forward speed (unlike gas turbines).
- Piston engines are normally air-cooled (liquid-cooled if noise is a major design consideration but then heavier).
- Most use gasoline
- Very occasionally diesel.

GAS TURBINES



Used on vast majority of modern aircraft – only exception is small general aviation class, using piston-prop engines.

- Common features are:

- Air compressor
- Fuel injector
- Combustion chamber
- Turbine

- Power extracted by:

- Turbine mechanically driving shaft
- expanding exhaust nozzles in nozzle

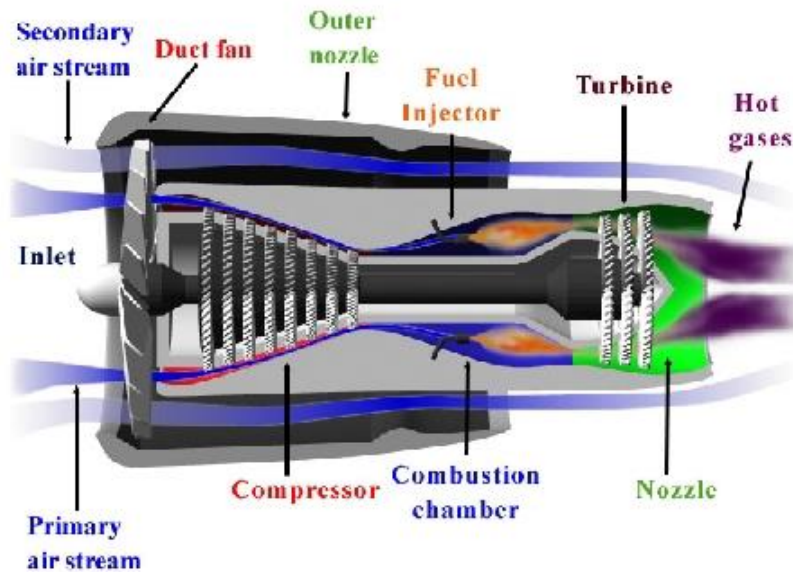
Turbojets - Basic Operating Features

- Five basic components:

- Intake: captures air and efficiently delivers it to compressor.
- Compressor: increases air pressure and temperature.
- Combustor: adds kerosene to the air and burns the mixture to increase the temperature and energy levels further.
- Turbine: extracts energy from the gases to drive the compressor via a shaft.
- Nozzle: accelerates the gases further.

Turbofans

- Compromise between turbojet and turboprop with propeller now a *fan* enclosed within the engine.
- Two air streams passing through engine, one of which *bypasses* internal core.



Turbofans - Basic Operating Features

Similar to turbojet but turbine split into two or more separate parts with low pressure turbine used to drive separate fan ahead of compressor via multiple shaft arrangement – hence more complex than turbojet.

- Bypass effect increases the available mass flow rate and thus reduces the jet velocity needed for a given amount of thrust (improves propulsive efficiency and also reduces noise).

Bypass Engine

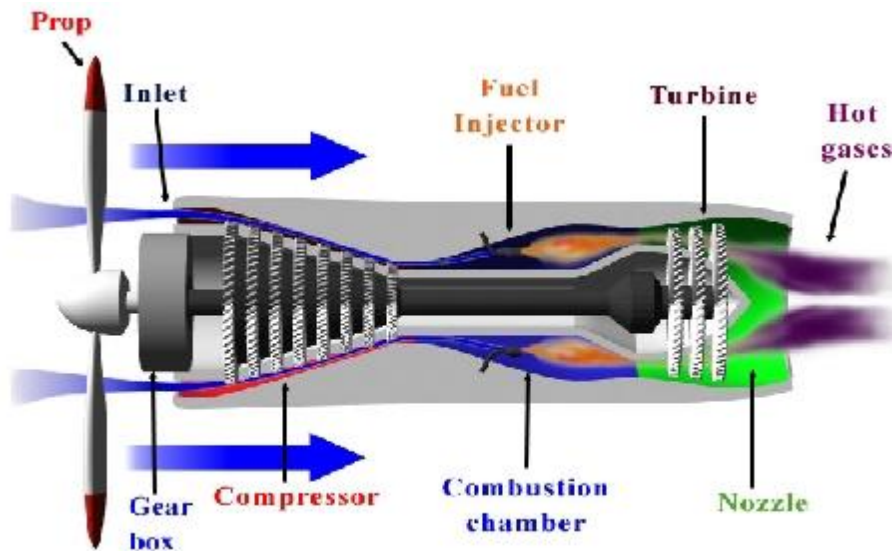
Bypass engine is engine with BPR of between 0.35 to 1.0 – used on most high performance combat a/c and guided weapons (GW).

Turbofans

- True turbofan is development of bypass engine, whereby first compressor stage is substantially increased in diameter to become a ducted fan.
- Most thrust is provided by fan – gas generator's primary function is to provide gases to drive fan through its separate shaft/turbine unit.
- Bypass ratio from 4 to 8 typically, or up to 10 with geared fan system.
- Overall pressure ratio of up to 35.
- High pressure turbine entry temperature of up to 1400°C – blade cooling issues.

Turboprop/Turbo shaft

- Turbine split into two stages:
- First (high pressure stage) drives compressor.
- Second (low pressure stage) drives:
 - Propeller (on turboprop)
 - Shaft (on turbo shaft)



- Low velocity exhaust gases also provide small residual thrust contribution.
- On turboprop, propellers rotate at between 1000 and 2000 rpm - since LP turbine rotates at over 10000 rpm, reduction gear required.
- On turbo shaft (e.g. helicopters), drive speed reduction achieved remotely.

Main advantages & disadvantages v turbofan:

- More fuel efficient at low speeds.
- speed limitation (about Mach 0.7)

Main advantages v piston-prop:

- high power/weight ratio
- power output increases with forward speed

Propfan (Unducted Fan Engine)

- Attempt to bridge gap between turbofan and turboprop.
- Uses advanced gas turbine to drive 8+ bladed propeller unit.
- Blades rotate very quickly (mostly supersonic) so are very thin, sharp-edged and swept at tips.
- Usually two sets of contra-rotating blades, e.g. GE/Snecma UDF (used on MD-80 testbed).
- Offers useful fuel efficiency up to Mach 0.8.

Problems include complexity, mass, structural integrity and noise

Afterburning/Reheat

- Exhaust gases are augmented by injecting and burning additional fuel between turbines and nozzle.
- Used on both basic turbojet and bypass engines.
- Thrust may be increased by up to 120% but at expense of up to 4x increase in sfc.
- used when performance requirements dictate need for short duration high thrust:
- Transonic acceleration
- Supersonic dash
- Requires use of variable geometry nozzle.
- Extra tailpipe length produces more weight & friction losses when not in use.

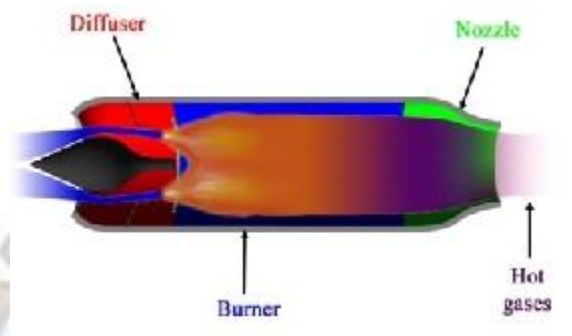
Thrust Reversers

- Act by deflecting gas flow.

- Several different types acting on hot or cold gases (mainly bucket, cascade or clam-shell variants).
- Used after touch-down to break a/c and reduce landing distance – also eases ground manoeuvres.
- Deactivated as speed falls to around 20 m/s to alleviate possible hot gas ingestion problems.

Ramjets

- Many applications for supersonic GW.
- Only three operating components:
 - Intake (diffuser);
 - Burner (combustion chamber);
 - Nozzle.



Ramjets - Basic Operating Features

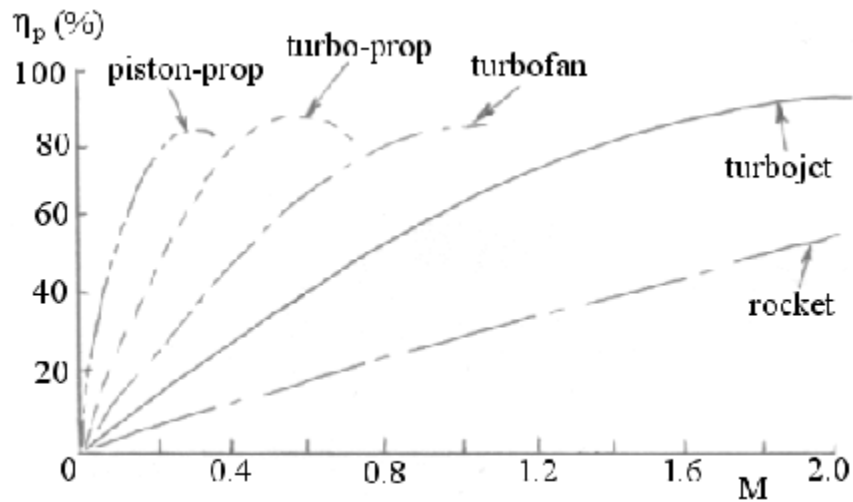
- Air decelerated in *intake (diffuser)* and pressure rises due to *ram effect*.
- Known as *ram pressure* and significant at supersonic speeds.
- A ramjet therefore needs neither a compressor nor a turbine, simplifying the design and reducing the cost.
- Greatest disadvantage is that it has to be accelerated up to typically $M = 2.0$ before it produces any useful thrust.
- Also complicated supersonic intake required to avoid shock losses - could be nose, side or ventral mounted.

Supersonic A/C Engines

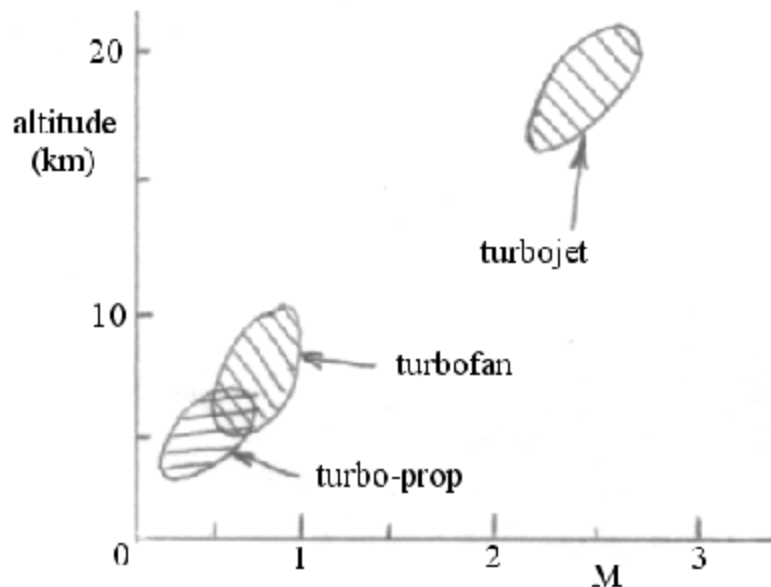
- Many design difficulties as completely different conditions for take-off and supersonic flight.
- Most engines therefore have variable geometry in inlet and nozzle
 - F-16's P&W F100-229 is exception with fixed geometry inlet.
- Most used to be basic turbojet, e.g. RR/Snecma Olympus (Concorde).
- Nowadays nearly all low bypass type, e.g. P&W F100-229 on F-15, F-16, etc with $BPR = 0.36$.

Powerplant Flight Regimes

- Internal thermal & mechanical efficiencies of all a/c air-breathing engines are similar, to a first degree.
- This means that a reasonable first order comparison of the use of various power plants can be determined through *propulsive efficiency* (η_p).



Choice primarily determined by operating Mach number (MN), though may also be influenced by operating altitude, rate of climb, range, noise, cost, politics, etc.



Flight Regimes – Propeller Engines

- Propeller thrust is derived by addition of small velocity change to large mass of air so that h_p increases rapidly with forward speed.
- At higher speeds h_p suffers due to compressibility effects on pressure distributions on the blades.
- Limit for modern wide-chord props with variable sweep and slow rotation is about $MN = 0.7$.
 - A400M has maximum MN of 0.72.
- For lower technology propellers, MN limit is about 0.65.
- Blade pitch adjustment enables high efficiencies over range of speeds.
- Usual preferred choice:
 - Piston-prop for up to $MN = 0.4$.
 - Turbo-prop for $0.4 < MN < 0.7$.

Flight Regimes – Turbofans

- Obvious choice when normal flight speed is high subsonic ($0.7 < M_N < 0.9$).
- Bypass ratio depends on application, compromise between:
 - engine diameter & mass (low bpr)
- Typical bpr of 4 to 8 on long-range transport a/c.
- Also used on a/c with $0.5 < M_N < 0.7$ – relatively small size enables more compact a/c design, e.g. on executive jet class.

Flight Regimes – Low Bypass Engines

- For $M_N > 0.9$, low bypass ratio (0.35 to 1.1) engines generally used.
- Mostly military applications (Concorde exception).
- Exhaust velocities up to 700 m/s (1100 m/s with afterburning).

Powerplant Performance Representation

- Require accurate representations of variations of
 - thrust (T) and specific fuel consumption (sfc) with
 - Flight speed, altitude & engine conditions.
- If available, if data and characteristics of known powerplant.

Thrust Representation – Turbojet & Bypass Engines

Flight Speed Effect

- Conveniently considered as one of three ranges:
 - Low subsonic ($M_N < 0.4$)
 - High subsonic ($0.4 < M_N < 0.9$)
 - Transonic & supersonic ($M_N > 0.9$)

Altitude Effect

- Up to 11 km altitude (i.e. in tropopause):

T as where

$$s = \rho / \rho_0 = \rho / 1.225$$

$$s = 0.6 \text{ (high bypass ratio) to } 0.85 \text{ (turbojet)}$$

- Above tropopause:

T as (i.e. $s = 1$)

Effect of Engine Operating Conditions

- Includes use of reheat (afterburning), operation at off-design conditions, non optimum intake and nozzle geometry, etc.
- Other ‘installation’ losses considered separately.
- All related to datum case (T_0)
 - Sea-level ISA, static, dry (i.e. without reheat).
- For any given condition, may use:

$$T = \tau T_0$$

where: τ = factor based on flight speed, operating conditions, bypass ratio.

- For $0 < M_N < 0.9$

$$\tau = F_T [K_{1T} + K_{2T} BPR + (K_{3T} + K_{4T} BPR) M_N] \sigma^*$$

- For $M_N > 0.9$

$$\tau = F_T [K_{1T} + K_{2T} BPR + (K_{3T} + K_{4T} BPR) (M_N - 0.9)] \sigma^*$$

- F_r is reheat factor
- For dry case (no reheat), $F_r = 1$
- For reheat:

$$F_r = \left(\frac{T_4}{T_3} \right)^{1.32 + 0.062 BPR}$$

where T_w/T_o = ratio of wet/dry sea-level ISA static thrust

sfc Representation Turbojet & Bypass Engines

- Same factors affect sfc as for thrust, i.e. speed, altitude, operating conditions and bypass ratio.
- Following representation may be used for dry cases:

$$sfc = sfc' (1 - 0.15 BPR^{0.45}) [1 + 0.28 (1 + 0.063 BPR^2) M_v] \sigma^{0.38}$$

where:

- sfc relates to particular design condition;
- sfc' is factor determined from known design condition.

Thrust/Weight Ratio

- Generally defined as: T/W_o or $T/(M_{og})$
 - Ratio of thrust (based on sea-level, static, dry value) to weight (design take-off value).
- Along with wing loading (W_o/S or M_{og}/S), it is the most important parameter affecting aircraft performance.
- Optimisation of T/W_o and W_o/S forms a major part of aircraft design synthesis procedure.
- True T/W is clearly not constant:
 - a/c weight varies during flight
 - Engine thrust varies with velocity, altitude and operating conditions.
- For prop-driven a/c, data is often presented as power/weight (P/W) ratio instead, Though may be converted to equivalent T/W since $P = T \times V$.
- T/W & W/S are interconnected for many performance calculations, e.g. take-off distance (frequently critical design driver)
- Short take-off distance possible with:
 - Large wing (low W/S), small engine (low T/W)
 - Small wing (high W/S), big engine (high T/W)
- Usual procedure is to estimate T/W from historical data and then calculate W/S from it for critical design requirements, e.g. stall speed during landing approach, engine-out rate of climb, etc.

Engine location

The type of engine mounting and its location play a major role in deciding the overall drag coefficient of the airplane. A conventional wing mounted engine is chosen as it facilitates periodic engine maintenance. This is important in airline industry where an unscheduled downtime could mean considerable loss to the company. The engines are attached to the lower side of the wing using pylons to reduce drag. The other reason for choosing a wing mounted engine is that the fuel is stored in the wing and this reduces the length of the fuel lines. From the data collection of similar airplanes, the engine location is fixed at 34% of the semi span.

C.G LOCATION AND c.g. TRAVEL

Wing location along length of fuselage

The longitudinal location of wing is decided based on the consideration that the c.g. of the entire airplane with full payload and fuel is around the quarter chord of the m.a.c of wing. For this purpose, the weights and the c.g locations of various components are tabulated. Then applying moment equilibrium about the nose of the airplane, the distance of the leading edge of root chord of the wing from the nose (X_{le}) is calculated to satisfy the aforesaid requirement. The steps to obtain X_{le} are given below.

As regards the c.g. locations of wing, horizontal tail and vertical tail it is assumed that the c.g. is at 40% of the respective m.a.c. The fuselage c.g. is taken to be at 42% of it's length. The engine c.g. location is taken to be at 40% of it's length. For this purpose the distance of the engine c.g. from the root chord is measured for various airplanes and a distance of 2 m is chosen. All other components (equipments, furnishings etc.) are assumed to have their combined c.g. location at 42% of the fuselage length. The tabulated values are given below. The weights of various components and the c.g. locations are given in table below.

Component	Weight (kgf)	c.g. location from nose (m)
Wing	5855.41	$X_{le}+5.34$
Fuselage	6606.60	13.86
Horizontal tail	1160.94	$X_{le}+20.05$
Vertical tail	746.22	$X_{le}+19.56$
Engine group	5659.19	$X_{le}+2$
Nose wheel	363.18	4.62
Main landing gear	1961.25	17.82
Fixed equipment total	7421.09	13.86
Fuel	12130.88	$X_{le}+4.76$
Payload	17270	14.13
Gross Weight	59175	$X_{le}+4.76$

C.G travel in critical cases

The movements of the c.g. under various loading conditions are examined below.

Full payload and no fuel

For the case of full payload and no fuel, the fuel contribution to the weight is not present. However, it has been assumed that the fuel tanks are located such that the c.g of the fuel is at the quarter chord of m.a.c. of wing. Since the c.g. of the entire airplane is also at the quarter chord of wing m.a.c., there is no shift in the c.g. when the fuel has been consumed. Hence, the C.G shift is 0%.

No payload and no fuel

For this case, the fuel as well as the payload contributions is not present. Since the c.g of payload is not at the c.g of the entire airplane, the c.g is bound to shift by a certain amount in this case. The moment calculations are performed and the new c.g location is obtained at 14.93 m from the nose. Therefore, the c.g shift: is $14.93 - 14.63 = 0.3$ m i.e. 7.28 % of m.a.c.

No payload and full fuel

For this case, since there is no payload, the c.g shifts. On performing calculations, the new c.g. location is obtained at 14.84 m. Therefore, the c.g. shift is : $14.84 - 14.63 = 0.21$ m i.e. + 5.7 % . Hence, the c.g shift is +5.17% of the m.a.c.

Payload distribution for 15% c.g travel

Sometimes the c.g. shift is calculated for hypothetical cases like (a) only half the pay load concentrated in the front half of the passenger cabin and (b) only half the pay load concentrated in the rear half of the passenger cabin. These cases result in large shift in c.g. Hence, an alternate strategy is suggested.

According to Ref.7, a total c.g shift of 15% is acceptable for commercial airplanes. To ensure this, as a first step the maximum payload that can be concentrated in the front portion of the passenger cabin is calculated such that a c.g shift of only 7.5% is obtained.

It is assumed that the percentage of payload is “x “and also the payload c.g of to be at x % of the passenger cabin length. Performing the c.g. calculations yields the value of x to be 90%.

As a second step, similar calculations are performed, such that the maximum payload that can be concentrated at the rear half of the passenger cabin resulting in a c.g shift of only 7.5 % . On performing the calculation, a value of 70% is obtained for x.

Hence, the c.g locations for various critical cases and payload distributions have been calculated.



SCHOOL OF AERONAUTICS (NEEMRANA)

UNIT-V NOTES

FACULTY NAME: D.SUKUMAR.

CLASS: B.Tech AERONAUTICAL

SUBJECT CODE: 6AN5

SEMESTER: VI

SUBJECT NAME: AIRCRAFT DESIGN

INTRODUCTION OF ADVANCED CONCEPTS:

Supercritical Wings, relaxed static Stability, controlled configured vehicles, V/STOL aircraft and rotary wing vehicles.

Design and layout of flying controls and engine controls.

SUPERCritical WINGS

The flow over a finite wing is different from that of flow over an airfoil. Transonic Jet aircrafts fly at speed of 0.8-0.9 Mach number. At these speeds speed of air reaches speed of sound somewhere over the wing and compressibility effects start to show up. The free stream Mach number at which local sonic velocities develop is called critical Mach number. It is always better to increase the critical Mach number so that formation of shockwaves can be delayed. This can be done either by sweeping the wings but high sweep is not recommended in passenger aircrafts as there is loss in lift in subsonic speed and difficulties during constructions. So engineers thought of developing an airfoil which can perform this task without loss in lift and increase in drag. They increased the thickness of the leading edge and made the upper surface flat so that there is no formation of strong shockwave and curved trailing edge lower surface which increases the pressure at lower surface and accounts for lift.

A concerted effort within the National Aeronautics and Space Administration (NASA) during the 1960's and 1970's was directed toward developing practical airfoils with two-dimensional transonic turbulent flow and improved drag divergence Mach numbers while retaining acceptable low-speed maximum lift and stall characteristics and focused on a concept referred to as the supercritical airfoil. This distinctive airfoil shape, based on the concept of local supersonic flow with isentropic recompression, was characterized by a large leading-edge radius, reduced curvature over the middle region of the upper surface, and substantial aft camber.

Effects of Trailing-Edge Thickness

The design philosophy of the supercritical airfoil required that the trailing-edge slopes of the upper and lower surfaces be equal. This requirement served to retard flow separation by reducing the pressure recovery gradient on the upper surface so that the pressure coefficients recovered to only slightly positive values at the trailing edge. For an airfoil with a sharp trailing edge, as was the case for early supercritical airfoils, such restrictions resulted in the airfoil being structurally thin over the aft region. Because of structural problems associated with sharp trailing edges and the potential aerodynamic advantages of thickened trailing edges for transonic airfoils, an exploratory investigation was made during the early development phases of the supercritical airfoil to determine the effects on the aerodynamic characteristics of thickening the

trailing edge shows that increasing the trailing-edge thickness of an interim ill-percent-thick supercritical airfoil from 0 to 1.0 percent of the chord resulted in a significant decrease in wave drag at transonic Mach numbers; however, this decrease was achieved at the expense of higher drag at subcritical Mach numbers.

Aerodynamic characteristics of an airfoil play a crucial role in the designing and performance of an aircraft. The changes in any of these parameters (Mach number, Lift & Drag coefficients, Pressure drag and the strength of the generated shock wave) will result in appreciable loss in stability of the aircraft. Several attempts have been made by researchers to obtain a better airfoil shape to enhance the aerodynamic efficiency. But, there were some early problems, as an airfoil approaches the speed of sound, the velocities on the upper surface become supersonic because of the accelerated flow over the upper surface, and there is a local field of supersonic flow extending vertically from the airfoil and immersed in the general subsonic field. The aircraft loses the stability when the flying speed reaches the speed of sound. This is because of the drag called Wave drag, which is caused by the formation of shock waves around the body, which radiate a considerable amount of energy. These shockwave causes the smooth flow of air hugging the wing's upper surface (the boundary layer) to separate from the wing and create turbulence. Separated boundary layers are like wakes behind a boat -- the air is unsteady and churning, and drag increases. This increases fuel consumption and it can also lead to a decrease in speed and cause vibrations. In rare cases, aircraft have also become uncontrollable due to boundary layer separation.

Although shock waves are typically associated with supersonic flow, they form at a lower speed at areas on the body where local airflow accelerates to sonic speed. The magnitude of the rise in drag is impressive, typically peaking at about four times the normal subsonic drag. The free stream Mach number at which local sonic velocities develop is called critical Mach number. It is always better to increase the critical Mach number so that formation of shockwaves can be delayed. This can be done either by sweeping the wings but high sweep is not recommended in passenger aircrafts as there is loss in lift in subsonic speed and difficulties during constructions. In order to overcome the situation, many numerical simulations have been carried out for each chosen profile to bring out the best possible stability characteristics so that they can be used in many aerodynamic applications. So it is always desirable for an airfoil to possess best stability characteristics which can further achieve good lifting performance at optimum and extreme flow conditions. Therefore, researchers developed an airfoil which can perform this task without loss in lift and increase in drag. They increased the thickness of the leading edge and made the upper surface flat so that there is no formation of strong shockwaves and curved trailing edge lower surface which increases the pressure at lower surface and accounts for lift. Two of the important technological advancements that arose out of attempts to conquer the sound barrier were the Whitcomb area rule and the Supercritical airfoils. A supercritical airfoil is shaped specifically to make the drag divergence Mach number as high as possible, allowing aircraft to fly with relatively lower drag at high subsonic and low transonic speeds. For a better performance aircraft needs to get the speed closer to Mach 1 without encountering large transonic drag and this can be achieved by delaying drag divergence phenomenon to higher Mach numbers by using the Supercritical airfoils as shown in Fig. 1a.

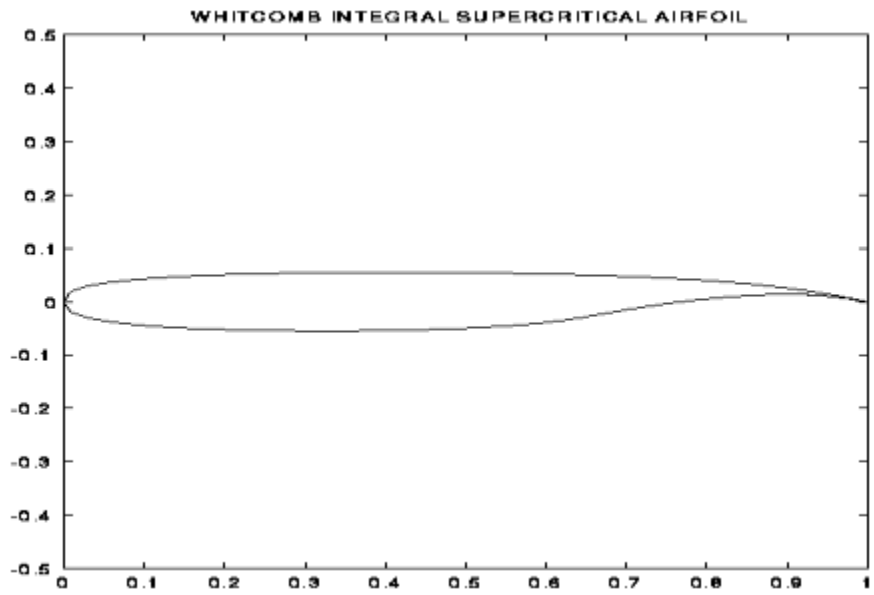


Fig -1a: Whitcomb supercritical airfoil

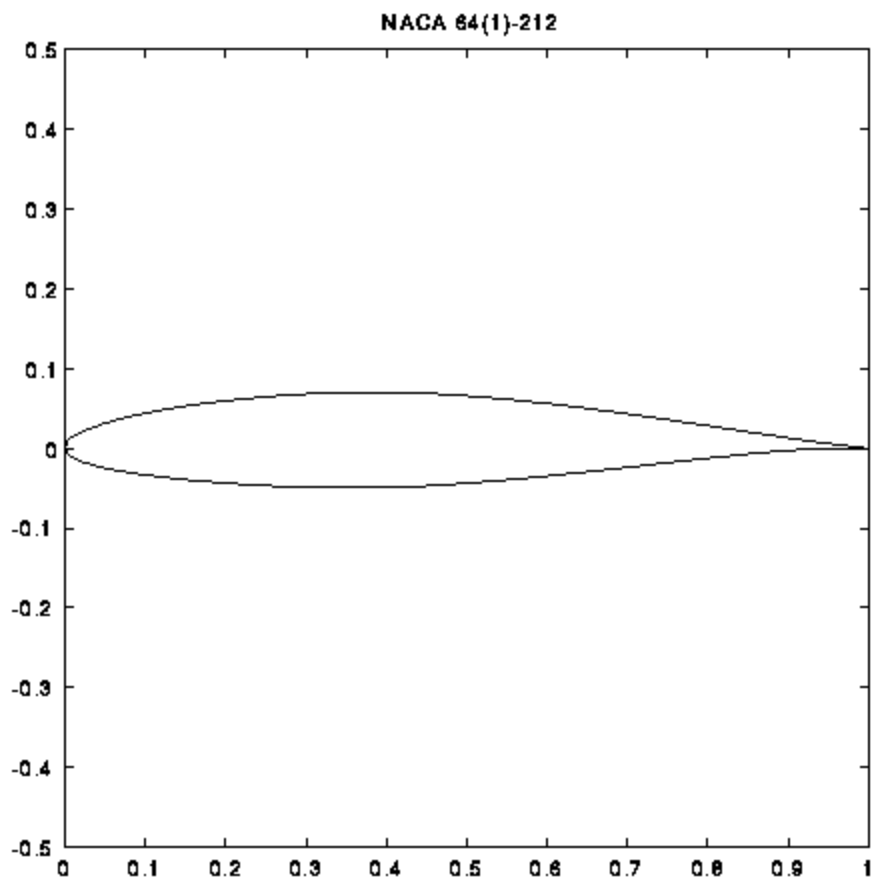


Fig -1b: NACA 64 series airfoil

DEVELOPMENT OF SUPERCRITICAL AIRFOIL

Supercritical airfoils are a class of transonic airfoils which operate with subsonic inlet and exit flow velocities and with embedded regions of supersonic flow adjacent to the airfoil surface. The term "supercritical" refers to the presence of velocities in the flow field which are above the "critical" or sonic speed. The supercritical airfoils were designed by NASA engineer Richard Whitcomb, and were first tested on the TF- 8A Crusader. While the design was initially developed as part of the Supersonic Transport (SST) project at NASA, it has since been mainly applied to increase the fuel efficiency of many high subsonic aircraft.

Slotted Supercritical Airfoil

In the early 1960's, Richard T. Whitcomb of the Langley Research Center proposed an airfoil with a slot between the upper and lower surfaces near the three-quarter chord to energize the boundary layer and delay separation on both surfaces (Fig. 2). It incorporated negative camber ahead of the slot with substantial positive camber rearward of the slot. Wind-tunnel results obtained for two-dimensional models of a 13.5-percent-thick airfoil of the slotted shape and a NACA 64A-series airfoil (Fig. 1b) of the same thickness ratio indicated that the slotted airfoil had a drag-rise Mach number of 0.79 compared with a drag-rise Mach number of 0.67 for the 64A-series airfoil. The drag at a Mach number just less than that of drag rise for the slotted airfoil was almost entirely due to skin friction losses and was approximately 10 percent greater than that for the 64A-series airfoil as shown in Fig. 3

Integral Supercritical Airfoil

The presence of a slot increased skin friction drag and structural complications. Furthermore, the shape of the lower surface just ahead of the slot itself was extremely critical and required very close dimensional tolerances. Because of these disadvantages an unslotted or integral supercritical airfoil (Fig. 2) was developed in the mid 1960's. Proper shaping of the pressure distributions was utilized to control boundary layer separation rather than a transfer of stream energy from the lower to upper surface through a slot. The maximum thickness-to-chord ratio for the integral Supercritical airfoil was 0.11 rather than 0.135 as used for the slotted airfoil. Theoretical boundary layer calculations indicated that the flow on the lower surface of an integral airfoil with the greater thickness ratio of the slotted airfoil would have separated because of the relatively high adverse pressure gradients at the point of curvature reversal.

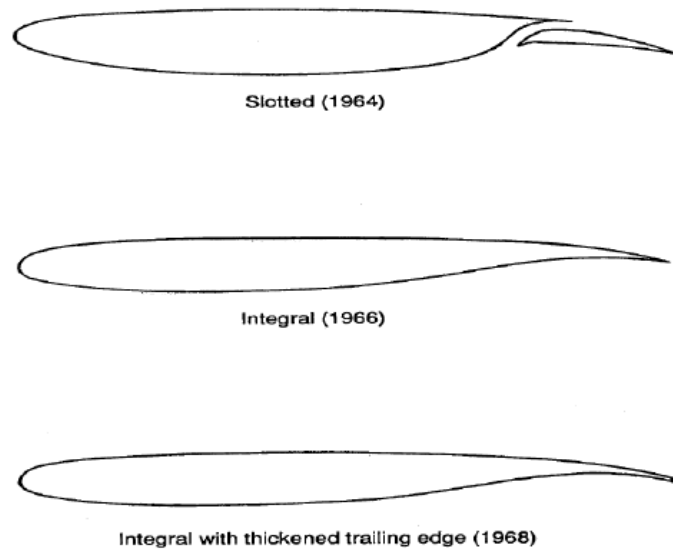


Fig- 2: Advancement in supercritical airfoil shape.

The experimental results shown in Fig. 3 indicated that the MDD for the integral airfoil was slightly higher than that for the slotted airfoil.

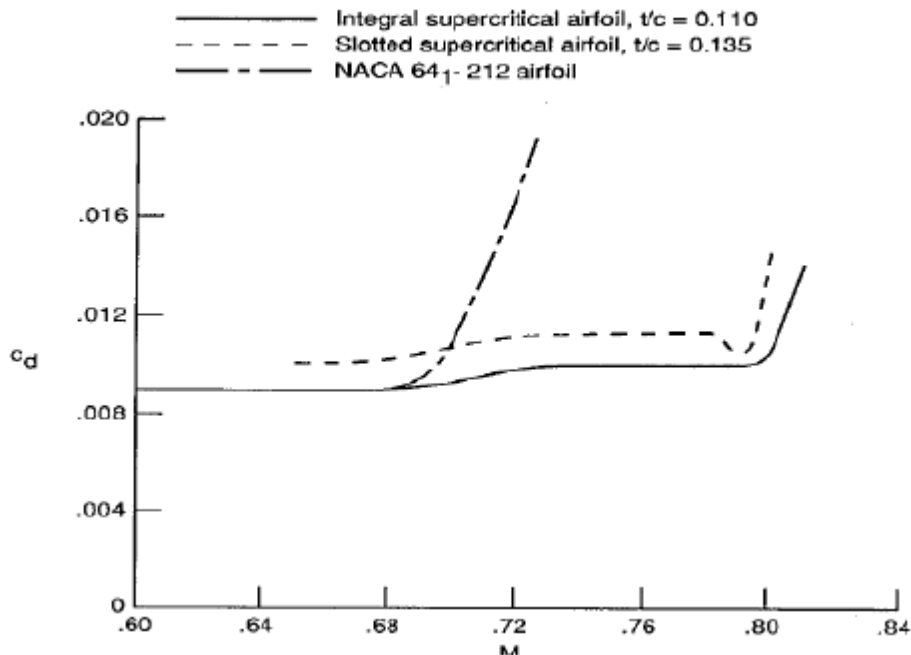


Fig- 3: Variation of drag coefficient with Mach number

GENERAL DESIGN PHILOSOPHY

Supercritical airfoils are a class of transonic airfoils which operate with subsonic inlet and exit flow velocities and with embedded regions of supersonic flow adjacent to the airfoil surface. The term "supercritical" refers to the presence of velocities in the flow field which are above the "critical" or sonic speed. The supercritical airfoils were designed by NASA engineer Richard Whitcomb, and were first tested on the TF- 8A Crusader. While the design was initially developed as part of the Supersonic Transport (SST) project at NASA, it has

since been mainly applied to increase the fuel efficiency of many high subsonic aircraft. The upper-surface pressure on NASA supercritical airfoils and related velocity distributions are characterized by a shock location significantly aft of the mid chord, results a rapid increase in pressure rearward of the mid chord to a substantially positive pressure forward of the trailing edge. The elimination of the flow acceleration on the upper surface ahead of the shock wave results primarily from reduced curvature over the mid chord region of the supercritical airfoil and provides a reduction of the Mach number ahead of the shock for a given lift coefficient with a resulting decrease of the shock strength as shown in Fig. 4. The strength and extent of the shock at the design condition could be reduced below that of the pressure distribution by shaping the airfoil to provide a gradual deceleration of the supersonic flow from near the leading edge to the shock wave.

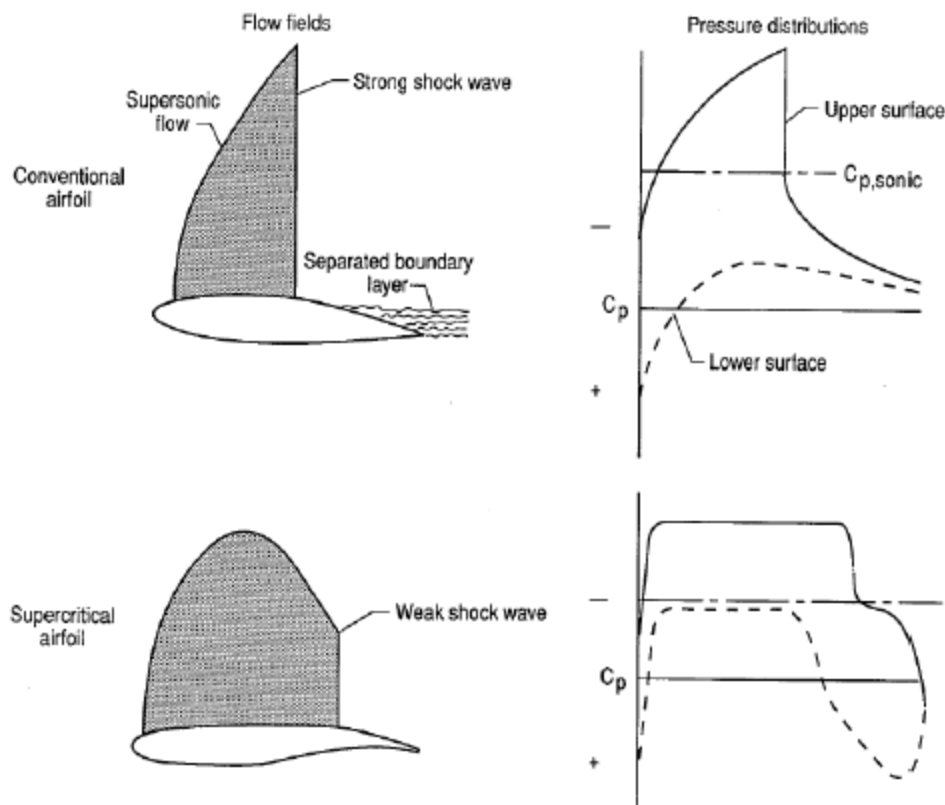


Fig-4: Comparison of transonic flow over a convention NACA 64 airfoil with transonic flow over a supercritical airfoil using CP variation

The airfoil produces expansion waves, or waves that tend to reduce pressure and increase velocity starting near the leading edge. If the flow field were a purely supersonic flow, there would be a continual expansion or acceleration of the flow from leading edge to trailing edge. There is actually an infinite series of expansions that move out of this supersonic field. When the flow is mixed, the expansion waves that emanate from the leading edge are reflected back from the sonic line as compression waves that propagate back through the supersonic field to the airfoil surface. Up to this point of contact, all the expansion waves have been accelerating the flow, but as soon as the compression waves get back to the surface, they start to decelerate the flow. These compression waves are then reflected off the solid airfoil surface as more compression waves. So, there are sets of competing waves working in the flow that are the key to obtaining good transonic characteristics for airfoils and those are need to be

balanced. Two primary factors influence the balancing of these expansion and compression waves: the leading edge and the surface over the mid chord regions. First, there need to be strong expansions from the leading-edge region so they can be reflected back as compression waves--thus the large leading radius characteristic of supercritical airfoils. The leading edge of supercritical airfoils should be substantially larger than the conventional previous airfoils and is more than twice that for a 6-series airfoil of the same thickness-to-chord ratio. Second, the curvature over the mid chord region must be kept fairly small so that there is not a very large amount of accelerations being emanated that must be overcome by the reflected compression waves--thus the flattened upper-surface characteristic of supercritical airfoils.

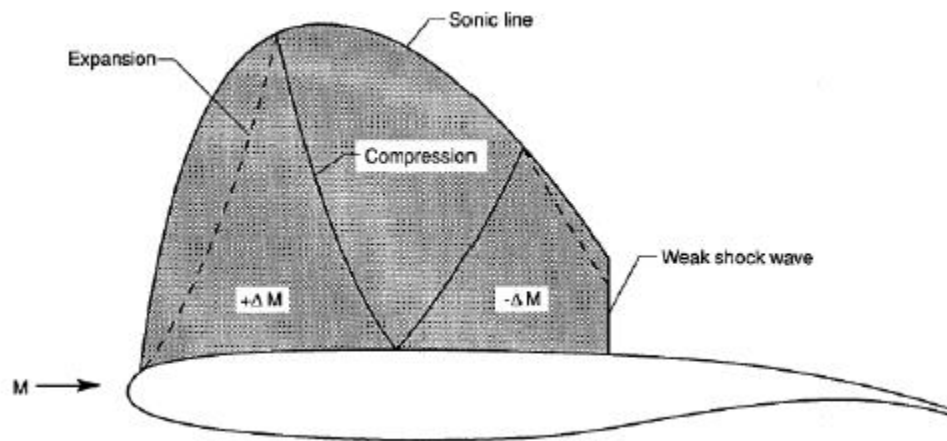


Fig-5: Schematic of the flow field over supercritical airfoil

Finally the critical Mach number (M_{Cr}) and drag divergence Mach number (M_{DD}) is increased by the shape of the supercritical airfoil. The pressure coefficient distribution over the top surface of a supercritical airfoil flying above M_{Cr} but below M_{DD} is sketched in Fig. 5. After a sharp decrease in pressure around the leading edge the pressure remains relatively constant over a substantial portion of the top surface. This is in contrast to the pressure coefficient distribution for a conventional airfoil flying above M_{Cr} . On a conventional airfoil, the sudden increase in pressure coefficient at mid-chord is due to the shock. At a certain point along the airfoil, a shock is generated, which increases the pressure coefficient to the critical value (C_{pCr}), where the local flow velocity will be Mach 1 (Fig. 4). The position of this shockwave is determined by the geometry of the airfoil; a supercritical foil is more efficient because the shockwave is minimized and is created as far aft as possible thus reducing drag. Compared to a typical airfoil section, the supercritical airfoil creates more of its lift at the aft end, due to its more even pressure distribution over the upper surface. Throughout the transonic range, the drag coefficient of the airplane is greater than in the supersonic range because of the erratic shock formation and general flow instabilities. Once a supersonic flow has been established, however, the flow stabilizes and the drag coefficient is reduced as shown in Fig. 6.

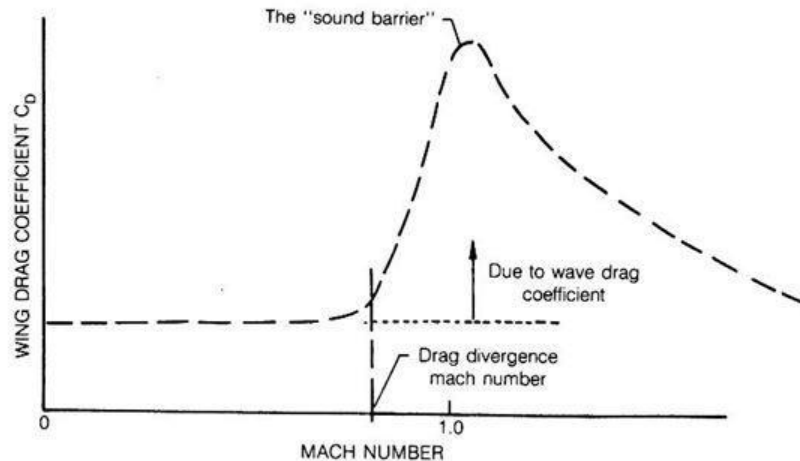


Fig-6: Reduction in drag with Mach number

Designation for Supercritical Airfoils

The airfoil designation is in the form SC(X)-ABCD, where SC(X) indicates Supercritical (Phase X). The next two digits, AB, designate the airfoil design lift coefficient in tenths (A.B), and the last two digits CD designate the airfoil maximum thickness in percent chord (CD percent).

Design guidelines

1. An off-design criterion is to have a well behaved sonic plateau at a Mach number below the design Mach number.
2. The gradient of the aft pressure recovery should be gradual enough to avoid separation (This may mean a thick trailing edge airfoil, typically 0.7% thick on a 10/11% thick airfoil.)
3. The airfoil has sufficient aft camber so that at design conditions the angle of attack is about zero. This prevents the location of the upper-surface crest (position of zero slopes) from being too far forward with the negative pressure coefficients over the mid chord acting over a rearward-facing surface.
4. Gradually decreasing supercritical velocity to obtain a weak shock.

FEATURES OF SUPERCRITICAL AIRFOIL

Trailing edge thickness

For an airfoil with a sharp trailing edge, as was the case for early supercritical airfoils, such restrictions resulted in the airfoil being structurally thin over the aft region. In order to investigate more comprehensively the effects of trailing-edge geometry, a refined 10-percent-thick supercritical airfoil was modified to permit variations in trailing-edge thickness from 0 to 1.5 percent of the chord and inclusion of a cavity in the trailing edge (Fig. 2). The results are (1) increasing trailing-edge thickness yielded reductions in transonic drag levels with no apparent penalty at subcritical Mach numbers upto a trailing Edge thickness of about 0.7 percent, (2) increases in both subsonic and transonic drag levels appeared with increases in trailing-edge thickness beyond approximately 0.7 percent, (3) small drag reductions through the Mach number range resulted when the 1.0-percent-thick trailing edge was modified to include a cavity in the trailing edge and (4) the general design criterion to realize the full aerodynamic advantage of trailing-edge thickness appeared to be such that the pressure coefficient over the upper surface of the airfoil recover to approximately zero at the trailing edge with the trailing-edge thickness equal to or slightly less than the local upper-surface boundary-layer displacement thickness.

Maximum thickness

In order to provide a source of systematic experimental data for the early supercritical airfoils, the 11-percent-thick airfoil and the 10-percent-thick airfoil were reported to compare the aerodynamic characteristics of two airfoils of different maximum thicknesses. For the thinner airfoil, the onset of trailing-edge separation began at an approximately 0.1 higher normal-force coefficient at the higher test Mach numbers, and the drag divergence Mach number at a normal-force coefficient of 0.7 was 0.01 higher. Both effects were associated with lower induced velocities over the thinner airfoil.

Aft Upper-Surface Curvature

The rear upper surface of the supercritical airfoil is shaped to accelerate the flow following the shock wave in order to produce a near-sonic plateau at design conditions. At intermediate supercritical conditions between the onset of supersonic flow and the design point, the upper-surface shock wave is forward and the rear upper-surface contour necessary to produce the near-sonic plateau at design conditions causes the flow to expand into a second region of supercritical flow in the vicinity of three-quarter chord. The modifications over the rear upper surface of supercritical airfoil were made to evaluate the effect of the magnitude of the off-design second velocity peak on the design point. The modification was accomplished by removing material over approximately the rear 60 percent of the upper surface without changing the trailing-edge thickness and resulted in an increase in surface curvature around mid chord and a decrease in surface curvature over approximately the rearmost 30 percent of the airfoil. The results indicated that attempts to reduce the magnitude of the second velocity peak at intermediate off-design conditions in that particular manner had an adverse effect on drag at design conditions. The results suggested, however, that in order to avoid drag penalties associated with the development of the second velocity peak into a second shock system on the upper surface at intermediate off-design conditions, the magnitude of the second peak should be less than that of the leading-edge peak.

The broad region of relatively low, nearly uniform, upper-surface curvature on the supercritical airfoil extends from slightly rearward of the leading edge to about 70 or 75 percent chord. The results of extending this region of low curvature nearer to the trailing edge in an attempt to achieve a more rearward location of the upper-surface shock wave without rapid increases in wave losses and associated separation, thus delaying the drag divergence Mach number at a particular normal-force coefficient or delaying the drag break for a particular Mach number to a higher normal-force coefficient. Extending this low curvature region too near the trailing edge, however, forces a region of relatively high curvature in the vicinity of the trailing edge with increased trailing-edge slope. This high curvature would be expected to produce a more adverse pressure gradient at the trailing edge, where the boundary layer is most sensitive, and would result in a greater tendency toward trailing-edge separation. The results indicated that although simply extending the region of low curvature farther than on earlier supercritical airfoils provided a modest improvement in drag divergence Mach number, it had an unacceptably adverse effect on drag at lower Mach numbers.

THE KORN EQUATION

Airfoil performance needs to be estimated before the actual airfoil design has been done. To estimate the capability of supercritical airfoils for the purposes of design studies without performing wind tunnel or detailed computational design work, several attempts have been made. The Korn equation was an empirical relation developed by Dave Korn at the NYU Courant Institute in the early 1970s. It appeared that airfoils could be designed for a variety of Mach numbers, thickness to chord ratios, and design lift coefficients. The Korn equation is

$$M_{DD} + \frac{C_L}{10} + \left(\frac{t}{c}\right) = \kappa_A,$$

Where, κ_A is an airfoil technology factor. The airfoil technology factor has a value of 0.87 for an NACA 6-series airfoil section, and a value of 0.95 for a supercritical section. M_{DD} is the drag divergence Mach number, C_L is the lift coefficient, and t/c is the airfoil thickness to chord ratio. This relation provides a simple means of estimating the possible combination of Mach, lift and thickness that can be obtained using modern airfoil design.

As air moves across the top of a supercritical airfoil it does not speed up nearly as much as over a curved upper surface. This delays the onset of the shock wave and also reduces aerodynamic drag associated with boundary layer separation. At a particular speed for a given airfoil section, the critical Mach number, flow over the upper surface of an airfoil can become locally supersonic, but slows down to match the pressure at the trailing edge of the lower surface without a shock. However, at a certain higher speed, the drag divergence Mach number, a shock is required to recover enough pressure to match the pressures at the trailing edge. This shock causes transonic wave drag, and can induce flow separation behind it; both have negative effects on the airfoils performance.

But Supercritical airfoil has a higher MDD, allowing the aircraft to fly at higher speeds without drag rise and shock waves are generating farther aft than traditional airfoils. Also shock induced boundary layer separation is reduced, this allows for more efficient wing design geometry (e.g., a thicker wing and/or reduced wing sweep, each of which may allow for a lighter wing). The structural design of a thicker wing is more straightforward and actually results in a more lightweight wing. Also, a thicker wing provides more volume for an increased fuel capacity. Clearly, the use of a supercritical airfoil provides a larger design space for transonic airplane. Lift that is lost with less curvature on the upper surface of the wing is regained by adding more curvature to the upper trailing edge. Now the aircraft can cruise at a higher subsonic speed and easily fly up into the supercritical range. Consequently, aircraft utilizing a supercritical wing have superior take-off and landing performance.

Higher subsonic cruise speeds and less drag translates into airliners and business jets getting to their destinations faster on less fuel, and they can fly farther and that help keep the cost of passenger tickets and air freight down. NASA's test program conducted at the Dryden Flight Research Centre from March 1971 to May 1973 and showed that the supercritical wing installed on an F-8 Crusader test aircraft increased transonic efficiency by as much as 15% and predicted that the net gain for air carriers worldwide would be nearly one-half billion dollars all due to fuel savings of the supercritical airfoil. Before the program ended, the U.S. Air Force teamed with NASA for a joint program to test a SCW designed for highly manoeuvrable military aircraft. An F-111, with a variable-geometry wing, was them testing aircraft and the basic supercritical research took place between 1973 and 1975. Results were extremely successful and showed the test wing generated up to 30% more lift than the conventional F-111 wing and performed as expected at all wing sweep angles. Several military aircraft in testing and development stages are being built with supercritical wing technology. Among them are the Lockheed-Martin F-22 advanced technology Fighter, and the two aircraft that will be considered for the U.S. military Joint Strike Fighter production contract, the Boeing X-32 and the Lockheed-Martin X-35.

Controlled Configured Vehicles

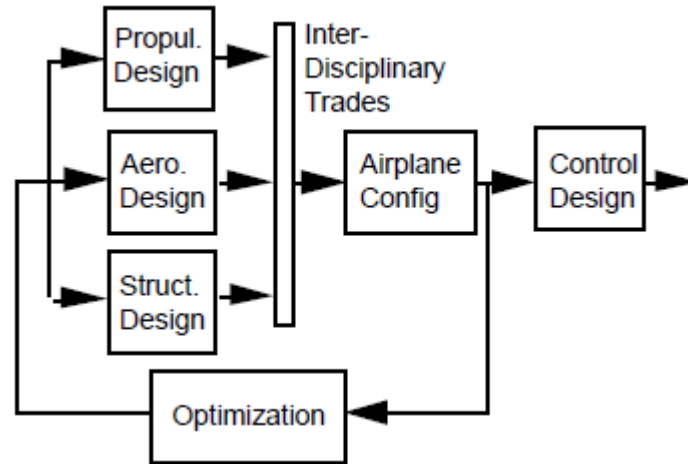
Introduction CCV

In the mid 1970s, flight control research was focused on the concept of a Control Configured Vehicle (CCV). The goal of CCV design was to improve aircraft performance through the use of active control. CCV concepts under study at the time included: improved handling qualities, flight envelope limiting, relaxed static stability, gust alleviation, maneuver load control, and active structural mode control. Many of the concepts were flight tested and, in some cases, the CCV design concept allowed for modifications of existing aircraft. For example, CCV concepts were used on the L-1011 aircraft to increase the gross take-off weight while minimizing wing structural changes. A design methodology is needed to find the optimum combination of control system development cost and total aircraft system performance and cost. Kehrer, for example, describes how use of stability augmentation methods during preliminary design led to a 150 inch reduction in fuselage length for the Boeing 2707-300 Supersonic Transport (SST).

The shortened fuselage also led to reduced vertical tail size and gear length, with a weight savings of 6,000 lbs and range increase of 225 nautical miles. The weight savings reported by the Boeing study came at the expense of an increase in control system development cost, however. The total cost of the Boeing SST flight and avionics systems were estimated to be double that of the Boeing 747. As a result, there was an assumption that the increased flight control system design complexity and cost (risk) was balanced by the performance improvements in the new design.

The first CCV aircraft was the YB-49 flying wing. The YB-49 was actually flight demonstrated at a 10% unstable static margin, using an automatic control system. The X-29 forward-swept wing aircraft represents one of the more recent aircraft where in the ability to use active control had a significant impact on the airframe configuration. To achieve the performance benefits of the forward swept wing-canard configuration, the X-29 airplane was required to have a 35% unstable static margin. Even more recently, the F-117 and B-2 aircraft undoubtedly have poor bare-airframe stability characteristics but have reached production status because of active control.

Each of these aircraft configurations would not be feasible had the impact of active control not been considered at the conceptual design stage. The CCV concept fostered research on the impact of active control on aircraft configurations. During this early development period, the realization that aircraft performance gains were achievable using active control was an important motivation for multivariable control research. Today, the use of a multivariable flight control system is accepted and even expected. However, to a large extent, a quantifiable impact of active control on the aircraft configuration design and layout has not been exploited. Design rules are certainly being used within airframe companies to include the benefit of active control on the configuration design. However, there appears to be no current systematic method through which the configuration can be optimized within the constraints of control system structure and control power.



(A) Traditional Aircraft Design Process

Figure (A) illustrates the traditional and CCV design processes as described. The “traditional” design process includes flight control design on the outside of the primary configuration selection and optimization loop. This process is represented by Figure (A). Basically, the airplane configuration is established through optimization amongst the aerodynamic, propulsion, and structures disciplines. The flight control design is not conducted until after the final aircraft configuration has been selected. Therefore, the design of the flight control system has no impact on the airplane configuration.

The CCV design process is illustrated by Figure (B). The CCV design concept includes active control system design in parallel with the other disciplines for configuration selection and optimization. Thus, flight control design directly affects configuration selection. However, the implication is that a complete control system design is carried out for each configuration iteration. One of the primary drawbacks of this approach, and others like it, is that a complete control system is designed at each iteration step.

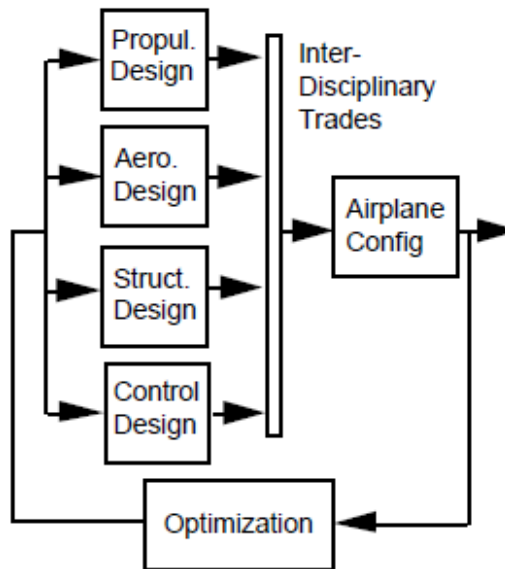


Figure (B) Control-Configured-Vehicle Design Process

If the flying qualities of the bare airframe are optimized, then it is reasoned that the control system of the aircraft will be inexpensive to develop and build. However, this approach ignores the benefits of active control completely and is contrary to the objectives of CCV design. This approach attempts to eliminate the control system rather than benefit from

it. As a result, statically unstable aircraft such as the F-16 and X-29 would not emerge from this approach.

The natural extension of CCV design is to link flight control considerations and configuration design such that the best configuration can be obtained through numerical optimization. This type of cross-disciplinary optimization is the basis for Multidisciplinary Design Optimization (MDO). An aircraft configuration MDO problem generally consists of separate modules which come from different traditional aeronautical disciplines such as structures, aerodynamics, and controls. The interaction between the structures and aerodynamics disciplines are at least clear conceptually - changes in geometric contours lead to lead changes in both fuel (drag) and structural weights.

V/STOL aircraft

Vertical takeoff and landing vehicles came into existence due to experiments carried out during the years 1950 – 1970 and almost all came out to be failures. Sometimes it used to have short run before the take off hence they were also called STOL, Shortrun Take Off and Landing vehicle. The flight control and stability of VTOL/STOL is very difficult and is of prime area of research presently in this field. This paper focuses on how the VTOL emerged gradually over the years and depicts the current advancement in the field of aerospace. VTOL has basically three configurations up till current development in this field, wing type configuration, helicopter type configuration and ducted type configuration. Wing type has fixed wings with vector thrust engine or moving wings with engine, ducted type has ducted rotor which helps to provide lift, helicopter type has rotor mounted above it to provide lift. Initially the VTOL developed were of wing type configuration, primarily for military purposes and were man operated but later their importance was know and more and more advanced designs of it came into existence. The Hover eye platform from Bertin Technologies was first major step in direction of unmanned VTOL. The Hover eye platform brought breakthrough in the field of ducted type configuration of VTOL. Recent trends for unmanned aerial vehicles in the field of aerospace and photography application is well known. Various helicopter type configurations used for UAV are explained along with their advantages over other configuration here. The latest ongoing research in this field is hover bike which is a hybrid machine. It uses ducted rotors to attain required lift in order achieve its objectives. It can be either manned or unmanned. Its concept emerged from the Hovercraft which has hybrid capability and used ducted fan to hover and maneuver. Design with single engine has problems of stability and the design with multi engine has problem of managing multi engines effectively. Engine with exposed rotors proves to be dangerous and so it should be very well considered. The need of the hour is to design a quite, low cost, low weight, high power to weight and effective control for VTOL and optimize its performance. Such VTOL can be used for anti terrorist activity, for complete surveillance purposes.

Most of the initial inventions of VTOL were of short run take off type or jump type vertical take off and landing vehicles some of example are Harrier, V-22 Osprey and Yak-38 Forger. They had wing type configuration. Lockheed manufactured XFV-1 in May 1951 and Convair manufactured XFV- pogo in 1951.both were experiments and completed their test flight.



FIGURE 7: Lockheed XFV-1 [2].

The Harrier was a jump style VTOL and was developed in Britain. It was also named as Harrier Jump Jet. Hawker Aircraft company came out with this design in 1957 [3]. It was mainly used for military purpose. It could take off vertically if it is under its maximum loading limit. It can also take short run take off for better fuel efficiency.

DESIGN AND LAYOUT OF FLYING CONTROLS AND ENGINE CONTROLS.

CONTROL SYSTEMS

Introduction

The architecture of the flight control system, essential for all flight operations, has significantly changed throughout the years. Soon after the first flights, articulated surfaces were introduced for basic control, operated by the pilot through a system of cables and pulleys. This technique survived for decades and is now still used for small airplanes.

The introduction of larger airplanes and the increase of flight envelopes made the muscular effort of the pilot, in many conditions, not sufficient to contrast the aerodynamic hinge moments consequent to the surface deflection; the first solution to this problem was the introduction of aerodynamic balances and tabs, but further growth of the aircraft sizes and flight envelopes brought to the need of powered systems to control the articulated aerodynamic surfaces.

Nowadays two great categories of flight control systems can be found: a full mechanical control on gliders and small general aviation, and a powered, or servo-assisted, control on large or combat aircraft.

One of the great additional effects after the introduction of servomechanisms is the possibility of using active control technology, working directly on the flight control actuators, for a series of benefits:

- Compensation for deficiencies in the aerodynamics of the basic airframe;
- Stabilisation and control of unstable airplanes, that have commonly higher performances;
- Flight at high angles of attack;
- Automatic stall and spinning protection;
- Gust alleviation.

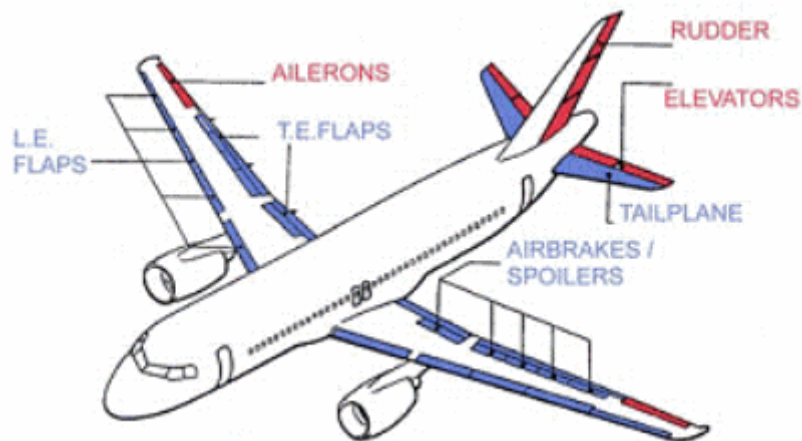


Fig. 8 – Flight control surfaces on airliner

A further evolution of the servo-assisted control is the fly-by-wire technique, based on signal processing of the pilot's demand before conversion into actuator control.

The number and type of aerodynamic surfaces to be controlled changes with aircraft category. Fig. 8 shows the classic layout for a conventional airliner. Aircraft have a number of different control surfaces:

Those indicated in red form the primary flight control, i.e. pitch, roll and yaw control, basically obtained by deflection of elevators, ailerons and rudder (and combinations of them); those indicated in blue form the secondary flight control: high-lift and lift-dump devices, airbrakes, tail trimming, etc.

Modern aircraft have often particular configurations, typically as follows:

- Elevons on delta wings, for pitch and roll control, if there is no horizontal tail;
- Flaperons, or trailing edge flaps-ailerons extended along the entire span;
- Ailerons, or stabilisers-ailerons (independently controlled);
- swing wings, with an articulation that allows sweep angle variation;
- Canards, with additional pitch control and stabilization

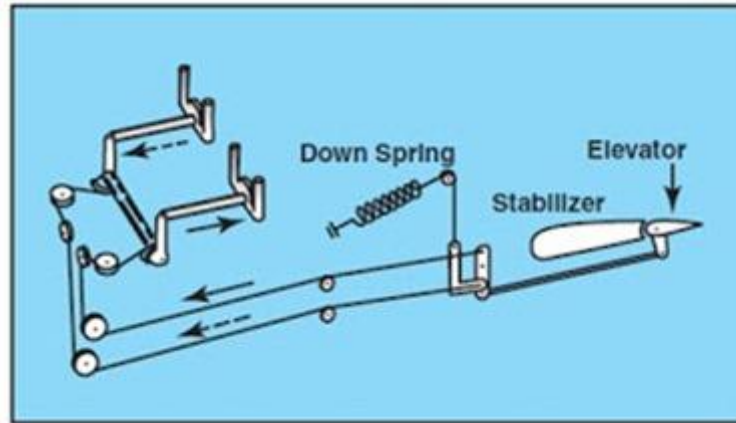
Primary flight control capability is essential for safety, and this aspect is dramatically emphasized in the modern unstable (military) airplanes, which could be not controlled without the continued operation of the primary flight control surfaces. For this reason the actuation system in charge of primary control has a high redundancy and reliability, and is capable of operating close to full performance after one or more failures.

Secondary actuation system failure can only introduce flight restriction, like a flap less landing or reduction in the max angle of attack; therefore it is not necessary to ensure full operation after failures.

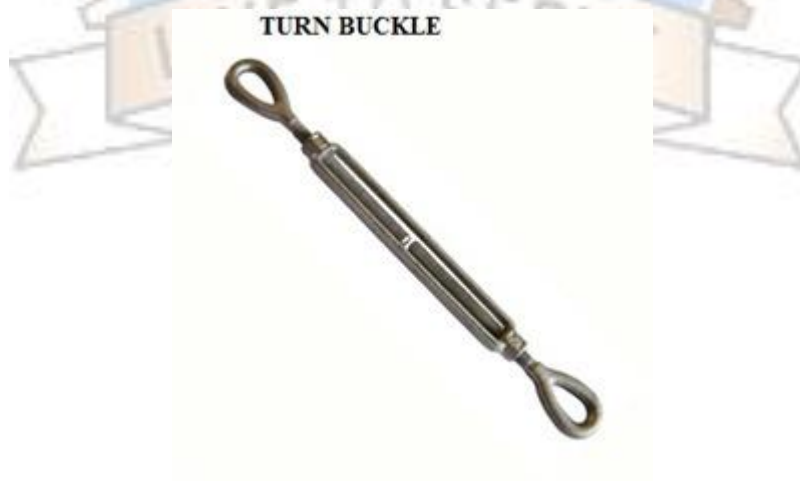
Fully powered Flight Controls

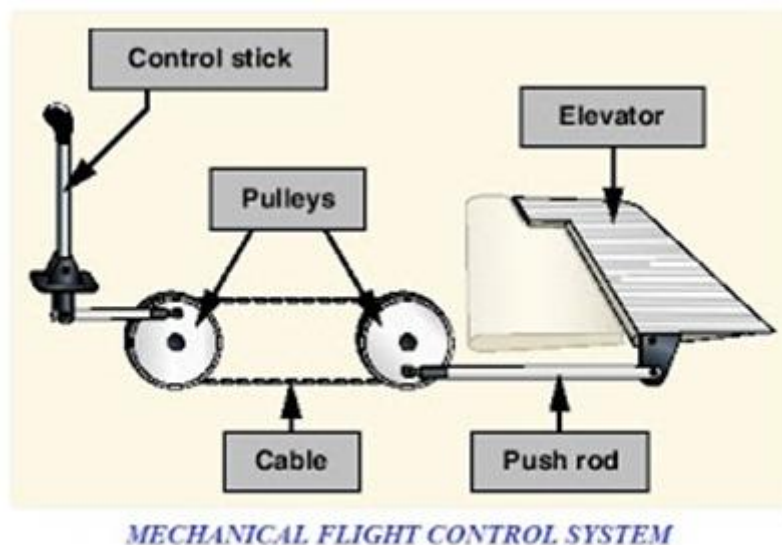
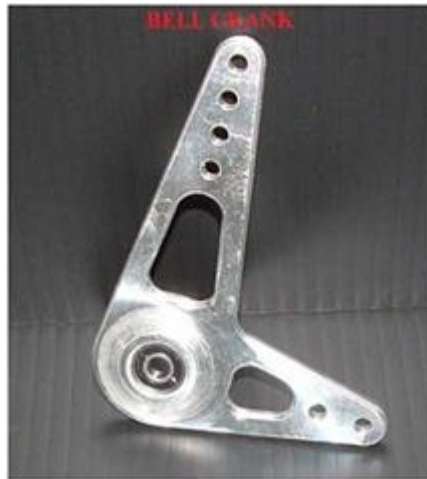
To actuate the control Surface the pilot has to give full effort. This is very tough to actuate the control surfaces through simple mechanical linkages. One can feel the equal toughness when raising the hand perpendicular to the airflow on riding a motorbike.

In this type of flight control system we will have



S.No	Item	Purpose
1	The cable	To transmit the power
2	Cable connector	To connect the cable
3	Turnbuckle	To adjust the Cable length
4	Fairlead	To guide the Cable
5	Pulley	To guide the in radial direction
6	Push pull rod	To go for and aft as per requirement
7	Control stick	To make orders for the remaining circuit





The most basic flight control system designs are mechanical and date back to early aircraft. They operate with a collection of mechanical parts such as rods, cables, pulleys, and sometimes chains to transmit the forces of the flight deck controls to the control surfaces. Mechanical flight control systems are still used today in small general and sport category aircraft where the aerodynamic forces are not excessive. When the pilot pushes the control stick forward/backward the cable is getting tensed through the linkages and it causes the Control surface to move respectively.

Power actuated systems

Hydraulic control

When the pilot's action is not directly sufficient for a control, the main option is a powered system that assists the pilot.

A few control surfaces on board are operated by electrical motors: as already discussed in a previous chapter, the hydraulic system has demonstrated to be a more suitable solution for actuation in terms of reliability, safety, weight per unit power and flexibility, with respect to the electrical system, then becoming the common tendency on most modern airplanes: the pilot, via the cabin components, sends a signal, or demand, to a valve that opens ports through which high pressure hydraulic fluid flows and operates one or more actuators.

The valve, that is located near the actuators, can be signalled in two different ways: mechanically or electrically; mechanical signalling is obtained by push-pull rods, or more

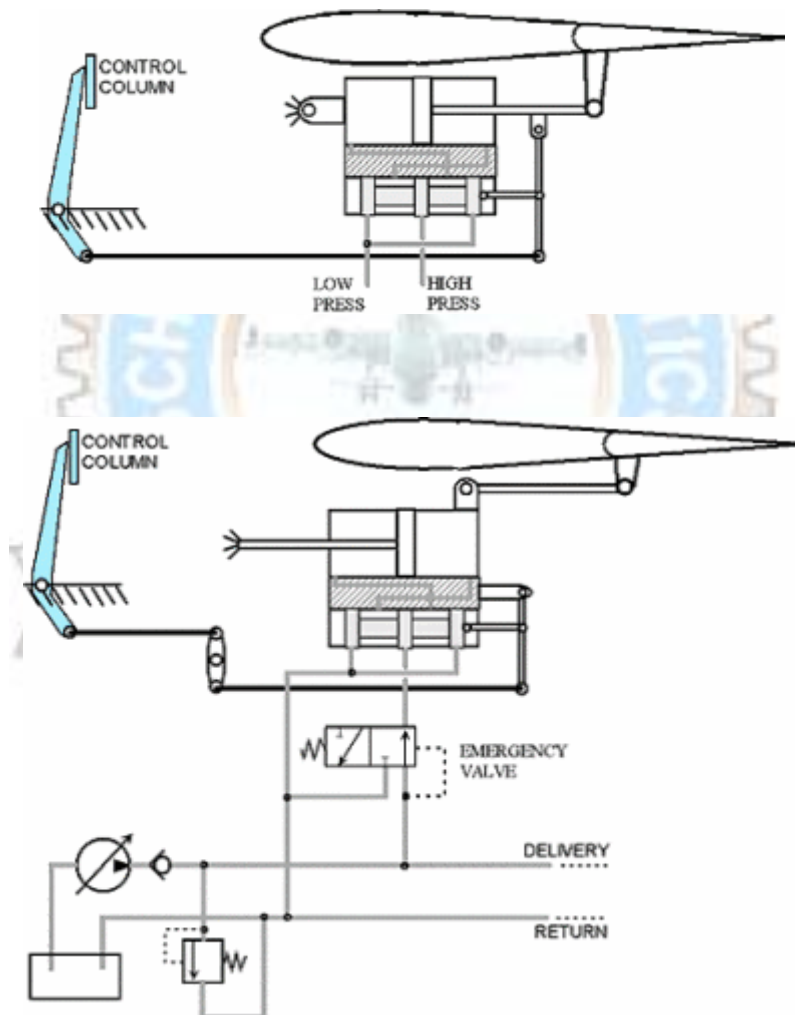
commonly by cables and pulleys; electrical signalling is a solution of more modern and sophisticated vehicles and will be later on discussed.

The basic principle of the hydraulic control is simple, but two aspects must be noticed when a powered control is introduced:

1. The system must control the surface in a proportional way, i.e. the surface response (deflection) must be function to the pilot's demand (stick deflection, for instance);
2. The pilot that with little effort acts on a control valve must have a feedback on the manoeuvre intensity.

The first problem is solved by using (hydraulic) servo-mechanisms, where the components are linked in such a way to introduce an actuator stroke proportional to the pilot's demand; many examples can be made, two of them are sketched, the second one including also the hydraulic circuit necessary for a correct operation.

In both cases the control valve housing is solid with the cylinder and the cabin column



Classic hydraulic servomechanisms

It has a mechanical linkage to drive the valve spool.

In the first case, the cylinder is hinged to the aircraft and, due to valve spool displacement and ports opening, the piston is moved in one direction or the other; the piston rod is also linked to the valve spool stick, in such a way that the piston movement brings the spool back

towards its neutral position; when this is reached, the actuator stops, then obtaining a deflection that is proportional to the demand.

In the second case the piston is constrained to the aircraft; the cabin column controls the valve spool stick; this will result in a movement of the cylinder, and this brings the valve housing again towards the valve neutral position, then resulting in a stroke proportional to the pilot's demand. The hydraulic circuit also includes an emergency valve on the delivery segment to the control valve; if the delivery pressure drops, due for instance to a pump or engine failure, the emergency valve switches to the other position and links all the control valve inlets to the tank; this operation hydraulically unlocks the system, allowing the pilot for manual actuation of the cylinder.

It is clear now that the pilot, in normal hydraulic operating conditions, is requested for a very low effort, necessary to contrast the mechanical frictions of the linkage and the movement of the control valve: the pilot is then no more aware of the load condition being imposed to the aircraft.

For this reason an artificial feel is introduced in powered systems, acting directly on the cabin control stick or pedals. The simplest solution is a spring system, then responding to the pilot's demand with a force proportional to the stick deflection; this solution has of course the limit to be not sensitive to the actual flight conditions. A more sophisticated artificial feel is the so-called Q feel. This system receives data from the pitot-static probes, reading the dynamic pressure, or the difference between total (p_t) and static (p_s) pressure, that is proportional to the aircraft speed v through the air density ρ :

$$p_t - p_s = \frac{1}{2} \rho v^2.$$

This signal is used to modulate a hydraulic cylinder that increases the stiffness in the artificial feel system, in such a way that the pilot is given a contrast force in the pedals or stick that is also proportional to the aircraft speed.

DIGITAL FLY BY WIRE SYSTEMS

Fly-By-Wire

In the 70's the fly-by-wire architecture was developed, starting as an analogue technique and later on, in most cases, transformed into digital. It was first developed for military aviation, where it is now a common solution; the supersonic Concorde can be considered a first and isolated civil aircraft equipped with a (analogue) fly-by-wire system, but in the 80's the digital technique was imported from military into civil aviation by Airbus, first with the A320, then followed by A319, A321, A330, A340, Boeing 777 and A380 (scheduled for 2005).

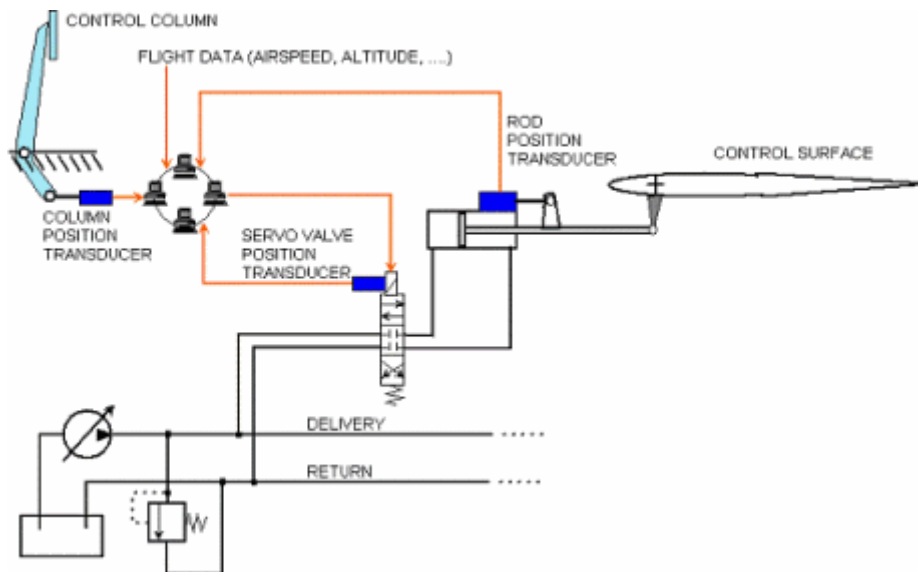
This architecture is based on computer signal processing and is schematically shown in fig. 6.5: the pilot's demand is first of all transduced into electrical signal in the cabin and sent to a group of independent computers (Airbus architecture substitute the cabin control column with a side stick); the computers sample also data concerning the flight conditions and servo-valves and actuators positions; the pilot's demand is then processed and sent to the actuator, properly tailored to the actual flight status.

The flight data used by the system mainly depend on the aircraft category; in general the following data are sampled and processed:

- Pitch, roll, yaw rate and linear accelerations

- Angle of attack and sideslip;
- Airspeed/mach number, pressure altitude and radio altimeter indications;
- Stick and pedal demands;
- Other cabin commands such as landing gear condition, thrust lever position, etc.

The full system has high redundancy to restore the level of reliability of a mechanical or hydraulic system, in the form of multiple (triplex or quadruplex) parallel and independent lanes to generate and transmit the signals, and independent computers that process them; in many cases both hardware and software are different, to make the generation of a common error extremely remote, increase fault tolerance and isolation; in some cases the multiplexing of the digital computing and signal transmission is supported with an analogue or mechanical back-up system, to achieve adequate system reliability.



Fly-by-wire system

Fly-by-wire system between military and civil aircraft; some of the most important benefits are as follows:

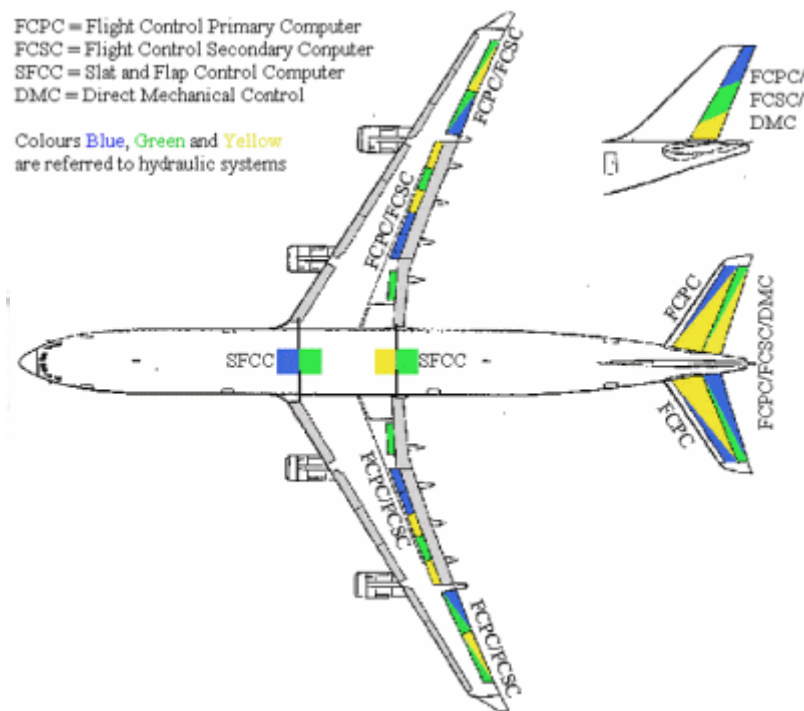
- flight envelope protection (the computers will reject and tune pilot's demands that might exceed the airframe load factors);
- increase of stability and handling qualities across the full flight envelope, including the possibility of flying unstable vehicles;
- turbulence suppression and consequent decrease of fatigue loads and increase of passenger comfort;
- use of thrust vectoring to augment or replace lift aerodynamic control, then extending the aircraft flight envelope;
- drag reduction by an optimised trim setting;
- higher stability during release of tanks and weapons;
- easier interfacing to auto-pilot and other automatic flight control systems;
- weight reduction (mechanical linkages are substituted by wirings);
- maintenance reduction;
- reduction of airlines' pilot training costs (flight handling becomes very similar in a whole aircraft family).

the flight mode: ground, take-off, flight and flare. Transition between modes is smooth and the pilot is not affected in its ability to control the aircraft: in ground mode the pilot has control on the nose wheel steering as a function of speed, after lift-off the envelope protection is gradually introduced and in flight mode the aircraft is fully protected by exceeding the maximum negative and positive load factors (with and without high lift devices extracted), angle of attack, stall, airspeed/Mach number, pitch attitude, roll rate, bank angle etc; finally, when the aircraft approaches to ground the control is gradually switched to flare mode, where automatic trim is deactivated and modified flight laws are used for pitch control.

The control software is one of the most critical aspects of fly-by-wire. It is developed in accordance to very strict rules, taking into account the flight control laws, and extensive testing is performed to reduce the probability of error. The risk of aircraft loss due to flight control failure is 2×10^{-6} per flight hour for a sophisticated military airplane, which anyway has the ejection seat as ultimate solution; the risk is reduced to 10^{-9} per flight hour for a civil airplane, were occupants cannot evacuate the airplane during flight.

Figure below shows, as example, the fly-by-wire layout for the Airbus 340. Three groups of personal computers are used on board: three for primary control (FCPC), two for secondary control (FCSC) and two for high lift devices control (SFCC). The primary and secondary computers are based on different hardware; computers belonging to the same group have different software.

Two additional personal computers are used to store flight data.



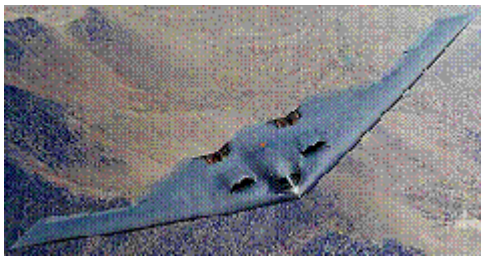
A340 fly-by-wire layout, including hydraulic system indications

In the drawing the computer group and hydraulic system that control each surface are indicated (there are three independent hydraulic systems on the A340, commonly indicated as Blue, Yellow and Green). The leading edge flaps are linked together, and so are the trailing edge flaps, and then they are controlled by hydraulic units in the fuselage.

The drawing shows a considerable redundancy of the flight control system: the inboard and outboard ailerons, elevators and rudder are controlled by both the primary and secondary

computers and operated by the three hydraulic sub-systems; the high lift devices are controlled by their specific computers and operated by the three hydraulic systems (Blue and Green for the leading edge, Yellow and Green for the trailing edge); the vertical stabiliser, having a secondary role, is controlled only by the secondary computers and operated by two hydraulic sub-systems. Thanks to this layout, first of all, in case of double hydraulic sub-system fault, the aircraft can be basically controlled with one hydraulic sub-system. Moreover, in case of total power black-out, the pilot can control the rudder and elevators by a mechanical back-up system, since the capability of this aircraft to land safely has been demonstrated with only limited pitch and yaw control.

Fly-by-wire architecture is inevitable for some aircraft categories: figure shows a typically unstable aircraft and a tilt rotor aircraft.



Northrop B-2



Bell-Boeing V-22

Fig – Need of fly-by-wire architecture for unstable (B-2) and thrust vectoring (V-22) airplanes

ENGINE CONTROL SYSTEMS

- It allow the engine to perform at maximum efficiency for a given condition
- Aids the pilot to control and monitor the operation of the aircraft's power plant
- Originally, engine control systems consisted of simple mechanical linkages controlled by the pilot then evolved and became the responsibility of the third pilot-certified crew member, the flight engineer
- By moving throttle levers directly connected to the engine, the pilot or the flight engineer could control fuel flow, power output, and many other engine parameters.
- Following mechanical means of engine control came the introduction of analog electronic engine control.
- Analog electronic control varies an electrical signal to communicate the desired engine settings
- It had its drawbacks including common electronic noise interference and reliability issues
- Full authority analogue control was used in the 1960s.
- It was introduced as a component of the Rolls Royce Olympus 593 engine of the supersonic transport aircraft Concorde. However the more critical inlet control was digital on the production aircraft.
- In the 1970s NASA and Pratt and Whitney experimented with the first experimental FADEC, first flown on an F-111 fitted with a highly modified Pratt & Whitney TF30 left engine.



Rolls Royce Olympus 593 engine

F-111C - Fighter – Bomber

Pratt & Whitney F100 – First Military Engine

Pratt & Whitney PW2000 - First Civil Engine fitted with FADEC

Pratt & Whitney PW4000 - First commercial "dual FADEC" engine.

The Harrier II Pegasus engine by Dowty & Smiths Industries Controls - The first FADEC in service.

Functions

- FADEC works by receiving multiple input variables of the current flight condition including air density, throttle lever position, engine temperatures, engine pressures, and many other parameters
- The inputs are received by the EEC and analyzed up to 70 times per second
- Engine operating parameters such as fuel flow, stator vane position, bleed valve position, and others are computed from this data and applied as appropriate.
- It controls engine starting and restarting.
- Its basic purpose is to provide optimum engine efficiency for a given flight condition.
- It also allows the manufacturer to program engine limitations and receive engine health and maintenance reports. For example, to avoid exceeding a certain engine temperature, the FADEC can be programmed to automatically take the necessary measures without pilot intervention.
- The flight crew first enters flight data such as wind conditions, runway length, or cruise altitude, into the flight management system (FMS). The FMS uses this data to calculate power settings for different phases of the flight.
- At takeoff, the flight crew advances the throttle to a predetermined setting, or opts for an auto-throttle takeoff if available.
- The FADECs now apply the calculated takeoff thrust setting by sending an electronic signal to the engines.
- There is no direct linkage to open fuel flow. This procedure can be repeated for any other phase of flight
- In flight, small changes in operation are constantly made to maintain efficiency.
- Maximum thrust is available for emergency situations if the throttle is advanced to full, but limitations can't be exceeded
- The flight crew has no means of manually overriding the FADEC.
- True full authority digital engine controls have no form of manual override available, placing full authority over the operating parameters of the engine in the hands of the computer
- If a total FADEC failure occurs, the engine fails
- If the engine is controlled digitally and electronically but allows for manual override, it is considered solely an EEC or ECU.

- An EEC, though a component of a FADEC, is not by itself FADEC. When standing alone, the EEC makes all of the decisions until the pilot wishes to intervene.

Safety

- With the operation of the engines so heavily relying on automation, safety is a great concern.
- Redundancy is provided in the form of two or more, separate identical digital channels.
- Each channel may provide all engine functions without restriction.
- FADEC also monitors a variety of analog, digital and discrete data coming from the engine subsystems and related aircraft systems, providing for fault tolerant engine control.

Applications

- FADECs are employed by almost all current generation jet engines, and increasingly in piston engines for fixed-wing aircraft and helicopters.
- The system replaces both magnetos in piston-engined aircraft, which makes costly magneto maintenance obsolete and eliminates carburetor heat, mixture controls and engine priming.
- Since, it controls each engine cylinder independently for optimum fuel injection and spark timing, the pilot no longer needs to monitor fuel mixture.
- More precise mixtures create less engine wear, which reduces operating costs and increases engine life for the average aircraft.
- Tests have also shown significant fuel savings

Advantages

- Better fuel efficiency
- Automatic engine protection against out-of-tolerance operations
- Safer as the multiple channel FADEC computer provides redundancy in case of failure
- Care-free engine handling, with guaranteed thrust settings
- Ability to use single engine type for wide thrust requirements by just reprogramming the FADECs.
- Provides semi-automatic engine starting
- Better systems integration with engine and aircraft systems
- Can provide engine long-term health monitoring and diagnostics
- Reduces the number of parameters to be monitored by flight crews
- Due to the high number of parameters monitored, the FADEC makes possible "Fault Tolerant Systems" (where a system can operate within required reliability and safety limitation with certain fault configurations)
- Can support automatic aircraft and engine emergency responses (e.g. in case of aircraft stall, engines increase thrust automatically).

Disadvantages

- No form of manual override available, placing full authority over the operating parameters of the engine in the hands of the computer.
- If a total FADEC failure occurs, the engine fails.
- In the event of a total FADEC failure, pilots have no way of manually controlling the engines for a restart, or to otherwise control the engine.
- With any single point of failure, the risk can be mitigated with redundant FADECs

- High system complexity compared to hydro mechanical, analogue or manual control systems
- High system development and validation effort due to the complexity

Auto pilot System

An autopilot is a mechanical, electrical, or hydraulic system used to guide a vehicle without assistance from a human being. An autopilot can refer specifically to aircraft, self-steering gear for boats, or auto guidance of space craft and missiles. The autopilot of an aircraft is sometimes referred to as “George”, after one of the key contributors to its development.

Today, autopilots are sophisticated systems that perform the same duties as a highly trained pilot. In fact, for some in-flight routines and procedures, autopilots are even better than a pair of human hands. They don’t just make flights smoother -they make them safer and more efficient. We’ll look at how autopilots work by examining their main components, how they work together — and what happens if they fail.

Autopilots and Avionics

In the world of aircraft, the autopilot is more accurately described as the automatic flight control system (AFCS). An AFCS is part of an aircraft’s avionics – the electronic systems, equipment and devices used to control key systems of the plane and its flight. In addition to flight control systems, avionics include electronics for communications, navigation, collision avoidance and weather. The original use of an AFCS was to provide pilot relief during tedious stages of flight, such as high-altitude cruising. Advanced autopilots can do much more, carrying out even highly precise maneuvers, such as landing an aircraft in conditions of zero visibility.

Although there is great diversity in autopilot systems, most can be classified according to the number of parts, or surfaces, they control. To understand this discussion, it helps to be familiar with the three basic control surfaces that affect an airplane’s attitude.

Autopilots can control any or all of these surfaces. A single-axis autopilot manages just one set of controls, usually the ailerons. This simple type of autopilot is known as a “wing leveler” because, by controlling roll, it keeps the aircraft wings on an even keel.

A two-axis autopilot manages elevators and ailerons. Finally, a three-axis autopilot manages all three basic control systems: ailerons, elevators and rudder.

The invention of autopilot

Famous inventor and engineer Elmer Sperry patented the gyrocompass in 1908, but it was his son, Lawrence Burst Sperry, who first flight-tested such a device in an aircraft. The younger Sperry’s autopilot used four gyroscopes to stabilize the airplane and led to many flying firsts, including the first night flight in the history of aviation. In 1932, the Sperry Gyroscope Company developed the automatic pilot that Wiley Post would use in his first solo flight around the world.

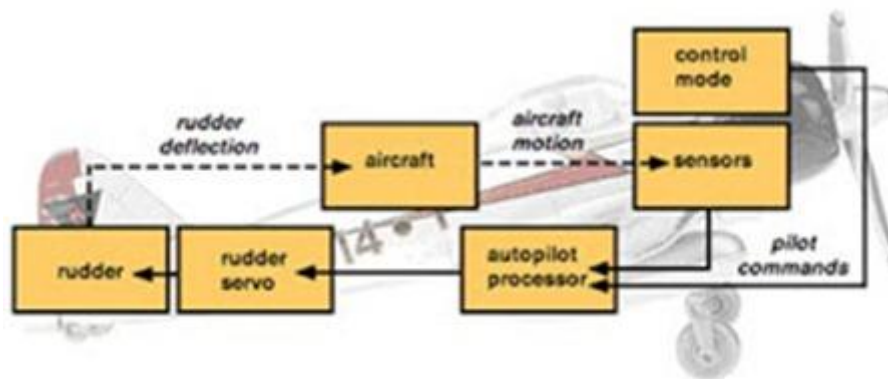
Autopilot Parts

The heart of a modern automatic flight control system is a computer with several high-speed processors. To gather the intelligence required to control the plane, the processors communicate with sensors located on the major control surfaces. They can also collect data from other airplane systems and equipment, including gyroscopes, accelerometers, altimeters, compasses and airspeed indicators.

The processors in the AFCS then take the input data and, using complex calculations, compare it to a set of control modes. A control mode is a setting entered by the pilot that defines a specific detail of the flight. For example, there is a control mode that defines how

an aircraft's altitude will be maintained. There are also control modes that maintain airspeed, heading and flight path.

These calculations determine if the plane is obeying the commands set up in the control modes. The processors then send signals to various servomechanism units. A servomechanism, or servo for short, is a device that provides mechanical control at a distance. One servo exists for each control surface included in the autopilot system. The servos take the computer's instructions and use motors or hydraulics to move the craft's control surfaces, making sure the plane maintains its proper course and attitude.



The above illustration shows how the basic elements of an autopilot system are related. For simplicity, only one control surface — the rudder — is shown, although each control surface would have a similar arrangement. Notice that the basic schematic of an autopilot looks like a loop, with sensors sending data to the autopilot computer, which processes the information and transmits signals to the servo, which moves the control surface, which changes the attitude of the plane, which creates a new data set in the sensors, which starts the whole process again. This type of feedback loop is central to the operation of autopilot systems.

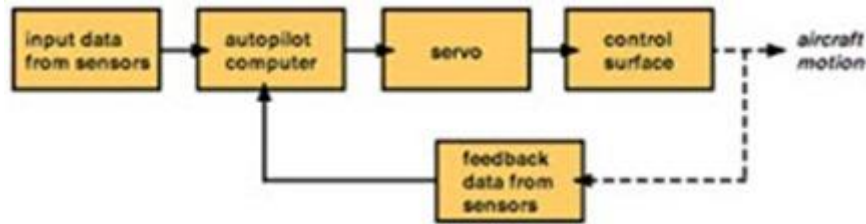
Autopilot Control Systems

An autopilot is an example of a control system. Control systems apply an action based on a measurement and almost always have an impact on the value they are measuring. A classic example of a control system is the negative feedback loop that controls the thermostat in your home. Such a loop works like this:

1. Its summertime and a homeowner set his thermostat to a desired room temperature say 78°F.
2. The thermostat measures the air temperature and compares it to the preset value.
3. Over time, the hot air outside the house will elevate the temperature inside the house. When the temperature inside exceeds 78°F, the thermostat sends a signal to the air conditioning unit.
4. The air conditioning unit clicks on and cools the room.
5. When the temperature in the room returns to 78°F, another signal is sent to the air conditioner, which shuts off.

It's called a negative feedback loop because the result of a certain action (the air conditioning unit clicking on) inhibits further performance of that action. All negative feedback loops require a receptor, a control center and an effector. In the example above, the receptor is the thermometer that measures air temperature. The control center is the processor inside the thermostat. And the effector is the air conditioning unit.

Automated flight control systems work the same way. Let's consider the example of a pilot who has activated a single-axis autopilot — the so-called wing leveler we mentioned earlier.



1. The pilot sets a control mode to maintain the wings in a level position.
2. However, even in the smoothest air, a wing will eventually dip.
3. Position sensors on the wing detect this deflection and send a signal to the autopilot computer.
4. The autopilot computer processes the input data and determines that the wings are no longer level.
5. The autopilot computer sends a signal to the servos that control the aircraft's ailerons. The signal is a very specific command telling the servo to make a precise adjustment.
 - a) Each servo has a small electric motor fitted with a slip clutch that, through a bridle cable, grips the aileron cable. When the cable moves, the control surfaces move accordingly.
 - b) As the ailerons are adjusted based on the input data, the wings move back toward level.
 - c) The autopilot computer removes the command when the position sensor on the wing detects that the wings are once again level.
 - d) The servos cease to apply pressure on the aileron cables.

This loop, shown above in the block diagram, works continuously, many times a second, much more quickly and smoothly than a human pilot could. Two- and three-axis autopilots obey the same principles, employing multiple processors that control multiple surfaces. Some airplanes even have auto thrust computers to control engine thrust. Autopilot and auto thrust systems can work together to perform very complex maneuvers.

Autopilot Failure

Autopilots can and do fail. A common problem is some kind of servo failure, either because of a bad motor or a bad connection. A position sensor can also fail, resulting in a loss of input data to the autopilot computer. Fortunately, autopilots for manned aircraft are designed as a failsafe — that is, no failure in the automatic pilot can prevent effective employment of manual override. To override the autopilot, a crew member simply has to disengage the system, either by flipping a power switch or, if that doesn't work, by pulling the autopilot circuit breaker.

Some airplane crashes have been blamed on situations where pilots have failed to disengage the automatic flight control system. The pilots end up fighting the settings that the autopilot is administering; unable to figure out why the plane won't do what they're asking it to do. This is why flight instruction programs stress practicing for just such a scenario. Pilots must know how to use every feature of an AFCS, but they must also know how to turn it off and fly without it. They also have to adhere to a rigorous maintenance schedule to make sure all sensors and servos are in good working order. Any adjustments or fixes in key systems may require that the autopilot be tweaked. For example, a change made to gyro instruments will require realignment of the settings in the autopilot's computer.

Modern Autopilot Systems

Many modern autopilots can receive data from a Global Positioning System (GPS) receiver installed on the aircraft. A GPS receiver can determine airplane's position in space by calculating its distance from three or more satellites in the GPS network. Armed with such positioning information, an autopilot can do more than keep a plane straight and level — it can execute a flight plan.

Most commercial jets have had such capabilities for a while, but even smaller planes are incorporating sophisticated autopilot systems. New Cessna 182s and 206s are leaving the factory with the Garmin G1000 integrated cockpit, which includes a digital electronic autopilot combined with a flight director. The Garmin G1000 delivers essentially all the capabilities and modes of a jet avionics system, bringing true automatic flight control to a new generation of general aviation planes. Wiley Post could have only dreamed of such technology back in 1933.

